GEMINI LAUNCH

GEMINI

LAUNCH VEHICLE NO. 4

FLIGHT EVALUATION (U)

Engineering Report 13227-4

Published as Supplemental Report 2
to the Gemini Program Mission Report-Gemini IV
MSC-G-R-65-3
by:
National Aeronautics and Space Administration
Manned Spacecraft Center
Houston, Texas

July 1965

MARTIN COMPANY

UNDER CONTRACT NUMBER
AF 04(695)-394
PRIORITY DX-A2

SPACE SYSTEMS DIVISION
AIR FORCE SYSTEMS COMMAND
UNITED STATES AIR FORCE . . . Los Angeles, California

[redacted]

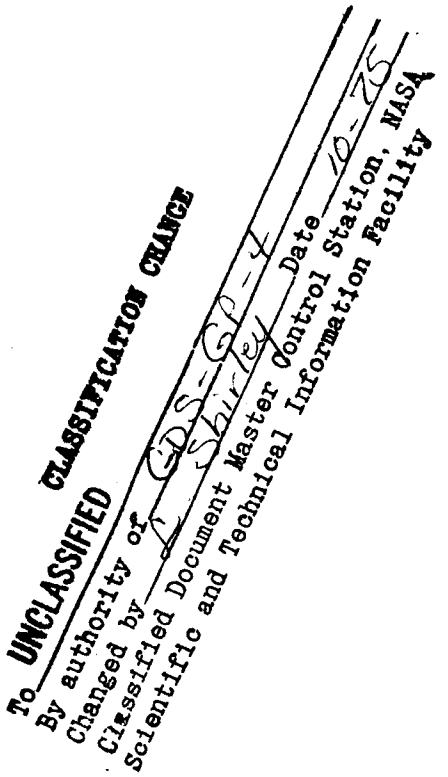

This document contains information affecting the National Defense of the United States within the meaning of the Espionage Laws, Title 18, U.S.C., Sections 793 and 794, the transmission or revelation of which in any manner to an unauthorized person is prohibited by law.

Group 4
Downgraded at 3-year intervals; declassified after 12 years. DOD DIR 5200.10

Copy No. _____

[redacted]

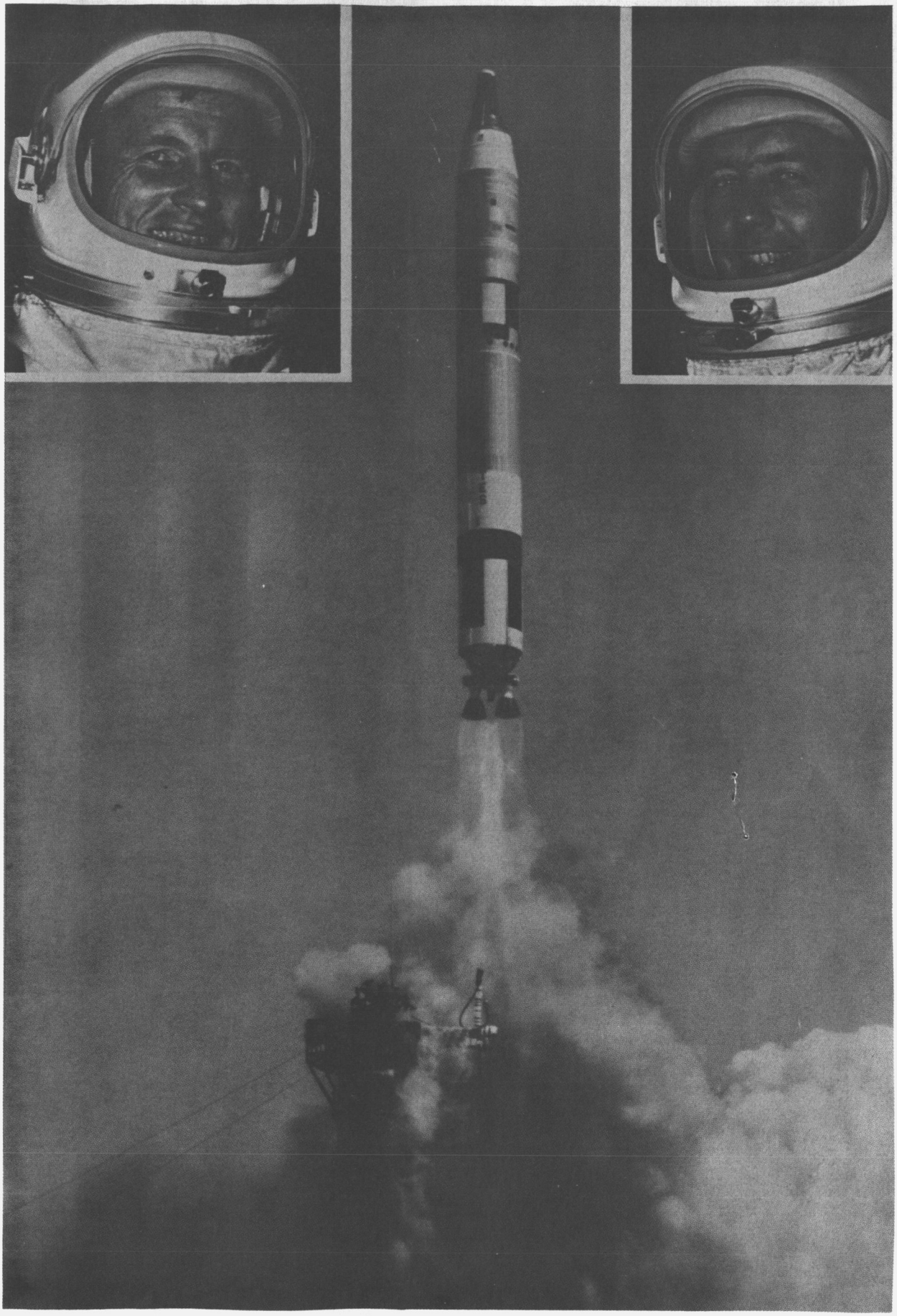

C68-3654

ER-13227-4

[redacted]

July 1965

GEMINI LAUNCH VEHICLE

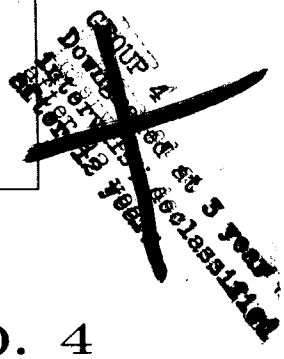

LAUNCH VEHICLE NO. 4 FLIGHT EVALUATION (U)

Approved by

L. J. Rose
Assistant Technical Director
Test Evaluation

J. C. Curlander
Technical Director

Published as Supplemental Report 2
to the Gemini Program Mission Report-Gemini IV
MSC-G-R-65-3
by:
National Aeronautics and Space Administration
Manned Spacecraft Center
Houston, Texas

Prepared by

MARTIN COMPANY, BALTIMORE DIVISION
Baltimore, Maryland 21203

Under CONTRACT AF 04(695)-394
PRIORITY DX-A2

For

SPACE SYSTEMS DIVISION
AIR FORCE SYSTEMS COMMAND

UNITED STATES AIR FORCE
Los Angeles, California

[redacted]

FOREWORD

This report has been prepared by the Gemini Launch Vehicle Program Test Evaluation Section of the Martin Company, Baltimore Division. It is submitted to the Space Systems Division, Air Force Systems Command, in compliance with Contract AF04(695)-394.

CONTENTS

CONTENTS (continued)

CONTENTS (continued)

SUMMARY

On 3 June 1965, Gemini-Titan No. 4 (GT-4) was launched successfully from Complex 19, Cape Kennedy, Florida. Launch vehicle/spacecraft separation was completed 365.24 seconds after liftoff. Spacecraft re-entry was successful after completion of 64 earth-fixed orbits.

The 240-minute countdown was picked up at 1000 hours, Greenwich Mean Time (GMT) and proceeded to T-35 minutes (1325 hours GMT), at which time a hold was initiated due to a malfunction in the electrical circuitry of the vehicle erector. After a 76-minute hold, the count was resumed at 1441 hours GMT and continued without incident through liftoff at 1515 hours GMT. The spacecraft was inserted into an orbit with perigee of 87 nautical miles and apogee of 152 nautical miles. All test objectives for the launch vehicle were achieved.

Stages I and II engines operated satisfactorily throughout powered flight. Stage I burning time was 155.702 seconds with shutdown initiated by fuel exhaustion. The Stage II engine was terminated by a guidance command after 181.320 seconds of operation. The second-stage redundant engine shutdown system (RESS) operated satisfactorily.

The flight control system (FCS) maintained satisfactory vehicle stability during Stages I and II flight. The roll and pitch programs were executed properly. During peak wind disturbances, vehicle rates never exceeded 1.7 deg/sec, and the maximum attitude error was 1.7 degrees. The maximum rate and attitude that occurred during staging did not exceed 2.9 deg/sec and 1.3 degrees, respectively.

The radio guidance system (RGS) performance was satisfactory. The rate and pulse beacons properly maintained lock throughout flight. Pitch and yaw commands were received by the decoder and properly transmitted to the FCS; the SECO signal also was properly transmitted by the decoder.

The hydraulic system operated satisfactorily during launch operations and flight.

The electrical system functioned as designed throughout the launch countdown and flight. Power transfer to vehicle batteries was smooth. The flashing beacon light assembly operated, as required, after SECO.

All channels of the PCM and FM instrumentation systems functioned properly throughout flight. The landline instrumentation system functioned satisfactorily prior to and up to liftoff. All airborne instrumentation hold functions monitored in the blockhouse remained within specification throughout the countdown.

The ordnance system umbilical dropweight release, propulsion system prevalves, explosive launch nuts and stage separation nuts operated as designed. The performances of the command control receivers and the MISTRAM transponder were satisfactory.

Malfunction detection system (MDS) performance during preflight checkout and flight was satisfactory. There were no switchover commands during the flight.

The flight environment encountered by GT-4 was within the launch vehicle design requirements. Flight loads were well within the structural capabilities of the launch vehicle.

The longitudinal oscillation (POGO) was noticed by one astronaut but caused no adverse effects. At Station 280, the peak value was 0.22 g zero-to-peak at a frequency of 11.0 cps.

Crew safety monitoring, which was conducted both at NASA-MSC (MCC-H) and at Cape Kennedy (MCC-C), worked efficiently. The activities at MCC-C were nearly identical with those conducted at MCC-H. Minor data transmission problems were encountered but did not hinder monitoring operations. There was no corrective action required during the flight.

The precount operation progressed without problems. The AGE and facilities operated without incident during the countdown. Launch propellant loading was completed within the scheduled time span and to the specified load and temperature limits.

The Stage I fuel vent topping umbilical (2DFVT) did not separate until approximately 20 feet of vehicle rise, instead of the planned 11 inches of rise. All electrical umbilicals disconnected properly and in the planned sequence. Engine blast and heat damage to the launch stand was minor and less than that from previous launches.

GLV-4 Test Objectives and Results

Objectives		Results	
Primary			
P-1	Evaluate launch vehicle system performance in placing a manned Gemini spacecraft into a prescribed orbit, and evaluate launch vehicle system operation for effect on crew safety.	P-1	Orbit insertion was within the predicted tolerance for V, h and γ; no launch vehicle system anomalies, which would have compromised crew safety, occurred.
Secondary			
S-1	Evaluate the Stage II redundant shutdown system (RESS) effect on SECO cutoff impulse.	S-1	The RESS operated as designed; post-SECO cutoff impulse was less than that resulting from shutdown without RESS.
S-2	Demonstrate ability to load propellants to the weight and temperature limits imposed by payload and vehicle requirements.	S-2	Achieved; tanks were loaded within the required tolerance of weight and temperature.
S-3	Evaluate launch countdown time and procedure for applicability in support of the rendezvous missions.	S-3	The four-hour countdown was accomplished as scheduled, except for the 76-minute hold for an erector lowering problem.
S-4	Evaluate launch vehicle subsystem performance during powered flight, including slow malfunction detection ground display systems at MCC.	S-4	All subsystems performed satisfactorily throughout the flight; slow malfunction monitoring operations at MCC (both Cape and Houston) were performed without incident.

I. INTRODUCTION

This report presents an evaluation of the systems performance of Gemini Launch Vehicle No. 4 (GLV-4) during the launch and flight of Gemini-Titan No. 4 (GT-4) from Complex 19, Cape Kennedy, Florida on 3 June 1965.

GT-4 was the second manned flight of the Gemini Program, with Astronauts J. A. McDivitt and E. H. White aboard the spacecraft. The GT-4 four-day mission was completed successfully.

The GT-4 vehicle was comprised of a two-stage GLV, essentially the same as GLV-3, and a spacecraft. The spacecraft was injected into an elliptical orbit of 87/152 nautical miles.

Significant events experienced by, and tests performed on, GLV-4 at Complex 19, ETR, are summarized in Fig. I-1.

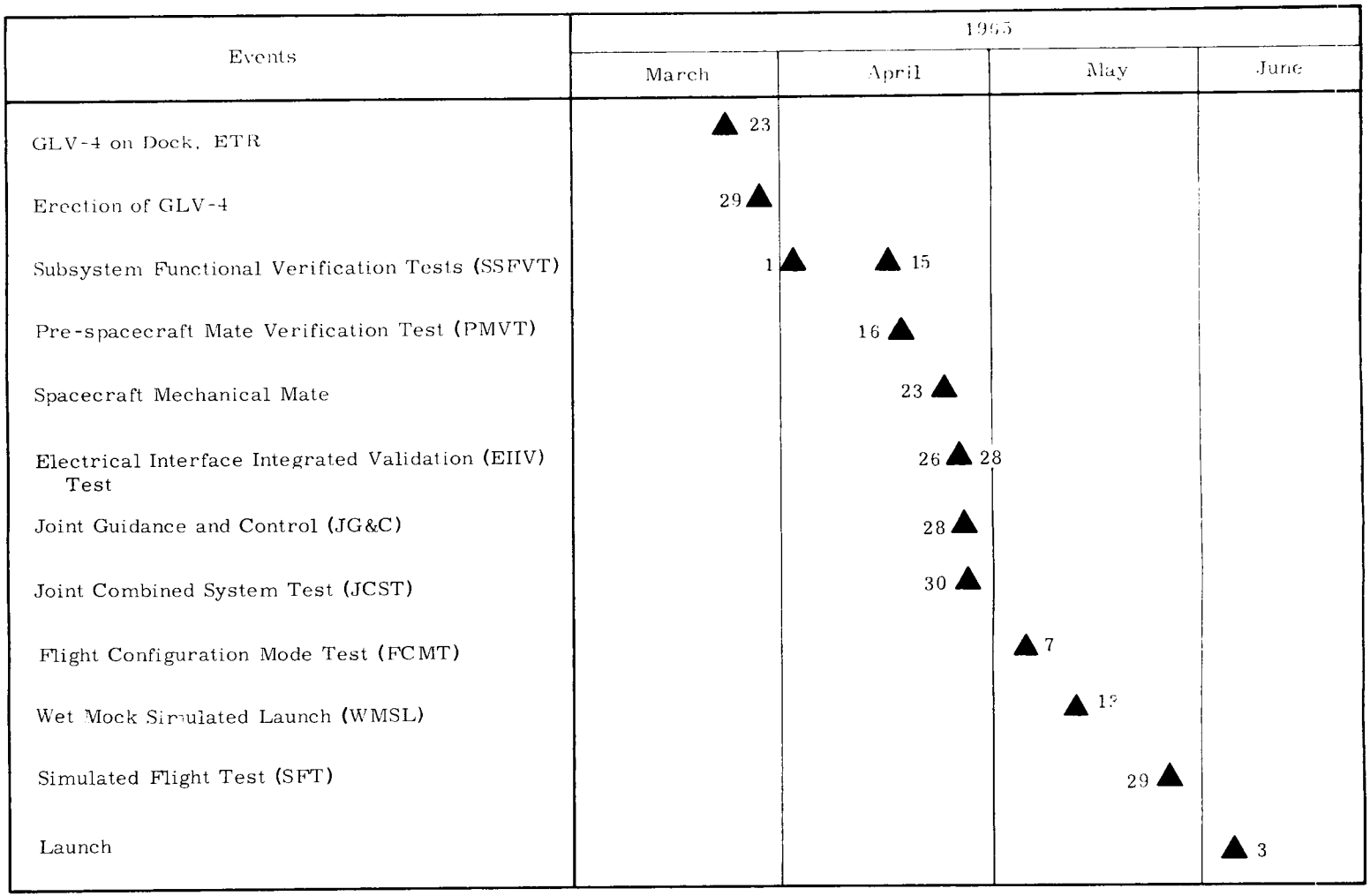

Fig. I-1. GT-4 Events at ETR

II. SYSTEM PERFORMANCE

A. TRAJECTORY ANALYSIS

1. Orbit Insertion

Gemini Launch Vehicle No. 4 (GLV-4) performed as predicted, and inserted the Gemini 4 spacecraft into earth orbit well within the allowable tolerance limits.

A comparison of the predicted and observed insertion conditions is given in Table II-1. In this table and in all succeeding references to a predicted (nominal) trajectory, the data were obtained from the GLV-4 45-day prelaunch report (Ref. 19). The observed trajectory parameters are those derived by the Martin Company from the Mod III-G final 10 PPS radar data. These data have been smoothed and are fully corrected for both refraction and systematic biases.

TABLE II-1

Comparison of Insertion Conditions at SECO+20 Seconds

Parameter	Planned Nominal	Observed	Observed Minus Planned	Preliminary Tolerance
Inertial velocity (fps)	25,756	25,745	-11	±30.3
Inertial flight path angle (deg)	0	0.059	0.059	±0.125
Altitude (naut mi)	87.456	87.703	+0.247	±0.346

2. Derivation of Trajectory Uncertainties

The preliminary tolerances for the prime insertion conditions are included in Table II-2. These tolerances have been computed in the following manner:

Total tolerance = preliminary tolerance plus 3σ data error

where:

Preliminary tolerance =

$$\sqrt{(\text{vehicle dispersions})^2 + (\text{RGS dispersions})^2}$$

TABLE II-2

Nominal Dispersions at BECO and at SECO+20 Seconds

Performance Parameter	Nominal Value (Ref. 19)	Nominal Dispersions		
		Vehicle Dispersion (Ref. 11)	RGS Dispersion (Ref. 12)	RSS of RGS and Vehicle Dispersions
BECO				
Time from liftoff (sec)	153.78	±4.44	N/A	±4.44
Geocentric radius (ft)	21,116,378	±13,734	↕	±13,734
Inertial velocity (fps)	9900	±196	↕	±196
Cross range (ft)	-833	±15,804	↕	±15,804
Cross-range velocity (fps)	-35	±394	↕	±394
Ground range (naut mi)	50.28	±3.40	↕	±3.40
Inertial flight path angle (deg)	18.66	±2.71	N/A	±2.71
SECO+20 seconds				
Time from liftoff (sec)	356.10	±7.45	±0.081	±7.45
Geocentric radius (ft) (Ref. 13)	21,438,813	±1554	±1410	±2100
Inertial velocity (fps) (Ref. 13)	25,756	±18.4	±24.09	±30.3
Cross range (ft)	-35,514	±73,592	±498	±73,597
Cross-range velocity (fps) (Ref. 13)	-401	±23.08	±9.90	±24.9
Ground range (naut mi)	538	±15.36	±0.1416	±15.36
Inertial flight path angle (deg)	0	±0.0540	±0.1125	±0.125

The vehicle dispersions and RGS dispersions are obtained from Refs. 9 and 12, respectively. In order to determine the total allowable tolerance, the data error must be computed and added arithmetically to the preliminary tolerance.

The insertion parameters in Table II-1 are well within the acceptable tolerance even without the addition of the Mod III-G data error (Ref. 7).

3. Geodetic and Weather Parameters

Significant geodetic parameters and surface weather conditions which existed at the time of launch are shown in Table II-3.

4. Flight Plan

The primary objective for GLV-4 was to place the Gemini 4 spacecraft into an elliptical earth orbit with an 87-nautical mile perigee* and a 161-nautical mile apogee. Having achieved orbital insertion at perigee altitude with a velocity of 25,766 fps,** the spacecraft will then coast to the desired apogee. The following flight plan was employed to attain these desired conditions.

A vertical rise is planned for the first 23.04 seconds following liftoff, during which time a programmed roll rate of 1.25 deg/sec is initiated to roll the vehicle from the pad orientation angle of 84.9 degrees to the planned flight azimuth of 72 degrees. At this time, an open-loop pitch program is begun (via a three-step rate command) which terminates at 162.56 seconds. The nominal commanded pitch rates and their times of application are as shown in Table II-4.

Guidance commands from the radio guidance system (RGS) are initiated at 168.35 seconds and continue until two seconds prior to SECO; however, velocity cutoff computations continue to SECO. A comparison of the planned and actual sequence of events is shown in Table II-5, and a profile of the GT-4 flight superimposed on the range planning map, appears in Fig. II-1.

5. Trajectory Results

Analysis of the fixed camera and radar data indicates a normal flight for Stages I and II. The resulting trajectory and aerodynamic

*Relative to Complex 19.
**Including 10 fps contributed by the spacecraft.

TABLE II-3

Geodetic and Weather Conditions at Launch

Location	
Site	Complex 19
Site coordinates (deg)	
Latitude	28.507 N
Longitude	80.554 W
Pad orientation (deg)	84.92 true azimuth
Weather	
Ambient pressure (psi)	14.77
Ambient temperature (° F)	81
Dew point (° F)	59
Relative humidity (%)	47
Surface wind	
Speed (fps)	12
Direction (deg)	60
Winds aloft	
Altitude (ft)	44,000
Speed (fps)	81
Direction (deg)	304 true azimuth
Cloud cover	Clear
Reference Coordinate System	
Type	AFMTC coordinate system No. 1
Origin	Center of launch ring, Complex 19
Positive X-axis	Downrange along flight azimuth tangent to ellipsoid
Positive Y-axis	To left of flight azimuth tangent to ellipsoid
Positive Z-axis	Forms a right-handed orthogonal system
Reference ellipsoid	Fischer
Launch	
Initial flight azimuth (deg)	72 true
Roll program (deg)	12.92 CW

TABLE II-4

Planned GLV Pitch Program

Program	Rate (deg/sec)	Time from Liftoff (sec)
Step 1	0.709	23.04 - 88.32
Step 2	0.516	88.32 - 119.04
Step 3	0.235	119.04 - 162.56

data are presented in tabular and graphical form in Table II-6 and in Figs. II-2 through II-24. Atmospheric conditions existing shortly after liftoff are presented in Figs. II-25 and II-26. Inspection of the trajectory data shows that a slightly high BECO condition was the only significant deviation from a nominal trajectory. Table II-7 contains a reconstruction of this condition based on dispersion studies obtained from Ref. 2.

Table II-7 is comprised of those items which can be measured to a fair degree of accuracy (Part A) and those items which can only be estimated due to the lack of suitable instrumentation (Part B).

The pitch program change which was effected after the GT-3 flight was instrumental in reducing the BECO altitude dispersion by approximately 50%. The remainder of the dispersion can be satisfactorily explained primarily by the slightly high thrust and specific impulse, pitch programmer error, and pitch engine misalignment. The amount of deviation for each perturbation used in the table was determined from postflight analysis of the engine and control system telemetry data wherever possible.

Prior to the flight of GT-4, it had been determined that the pitch programmer was slightly off-nominal and would tend to produce a lofted trajectory. Postflight analysis indicated a total error of -1.76%. As shown in Table II-7, this amount of programmer error would loft the trajectory by 4300 feet and decrease the velocity by 41 fps at BECO.

Postflight analysis indicated also that the roll programmer error resulted in a clockwise roll which was 0.25 degree less than planned.

Range Safety and Guidance Monitor displays both indicated a high and to-the-right trajectory compared to nominal until about LO + 100 seconds. At that time, a drift toward the left (northwest) began, and caused a maximum cross-range position dispersion (ΔY_f) of 3000 feet relative to nominal. This dispersion in Y_f was probably caused by the g-sensitive roll gyro drift.

TABLE II-5

GT-4 Flight Events Summary

Meas	Event	GMT (hr-min-sec)	Time from Liftoff	
			Actual	Planned
0800/0801	Power transfer	1514:30.7	-88.86	-89
FC B-10	MOCS T-0	1515:56.20	-3.36	-3.43
2104	$87FS_1$ (T-0)	1515:56.294	-3.268	-3.37
0356	Stage I S/A 1 MDTCPS make	1515:57.174	-2.388	-2.27
0357	Stage I S/A 2 MDTCPS make	1515:57.224	-2.338	-2.27
2101	TCPS S/A 1 and S/A 2	1515:57.286	-2.276	-2.2
1169	Launch nuts	1515:59.38	-0.18	-0.20
4421	First motion	1515:59.478	-0.084	-0.10
4422	Shutdown lockout (first motion)	1515:59.493	-0.069	-0.10
4423	Liftoff	1515:59.562	0	0
0734	Start roll program	1516:09.66	10.10	10.16
0734	End roll program	1516:19.96	20.40	20.48
0732	Start pitch program No. 1	1516:22.51	22.95	23.04
0732	Stop pitch program No. 1	1517:27.77	88.21	88.32
0732	Start pitch program No. 2	1517:27.77	88.21	88.32
0728	FCS gain change No. 1	1517:44.228	104.666	104.96
0732	Stop pitch program No. 2	1517:58.22	118.66	119.04
0732	Start pitch program No. 3	1517:58.22	118.66	119.04
--	Start tape recorder	1518:22.49	142.93	143.36
0735	Staging enable (TARS discrete)	1518:23.764	144.202	144.64
0741	IPS staging arm timer	1518:24.869	145.307	145.00

TABLE II-5 (continued)

Meas	Event	GMT (hr-min-sec)	Time from Liftoff	
			Actual	Planned
0356	Stage I S/A 1 MDTCPS break	1518:31.961	152.399	153.72
0357	Stage I S/A 2 MDTCPS break	1518:31.946	152.384	153.72
0032	$87FS_2/91FS_1$ (BECO)	1518:31.996	152.434	153.78
0502	Start P_{C_3} rise	1518:32.643	153.081	154.46
1085/1169	Stage separation	1518:32.705	153.143	154.51
0855	Stage II MDFJPS make	1518:32.676	153.114	154.68
--	Stop tape recorder	1518:34.74	155.18	156.78
--	Start tape recorder playback	1518:37.06	157.50	158.78
0732	Stop pitch program No. 3	1518:41.63	162.07	162.56
0740	RGS enable	1518:41.595	162.033	162.56
0755/0756	First guidance command	1518:48.057	168.495	168.35
0739	Stage II shutdown enable	1521:16.008	316.446	317.44
0777	Guidance SECO	1521:33.306	333.744	336.08
0519	$91FS_2$	1521:33.316	333.754	336.10
0522	Shutdown valve relay	1521:33.342	333.780	336.12
0521	Shutdown squib	1521:33.332	333.770	336.12
0799	ASCO	1521:33.399	333.837	336.13
0855	Stage II MDFJPS break	1521:33.476	333.914	336.40
AB-03	Spacecraft separation	1522:04.238	365.238	356.10

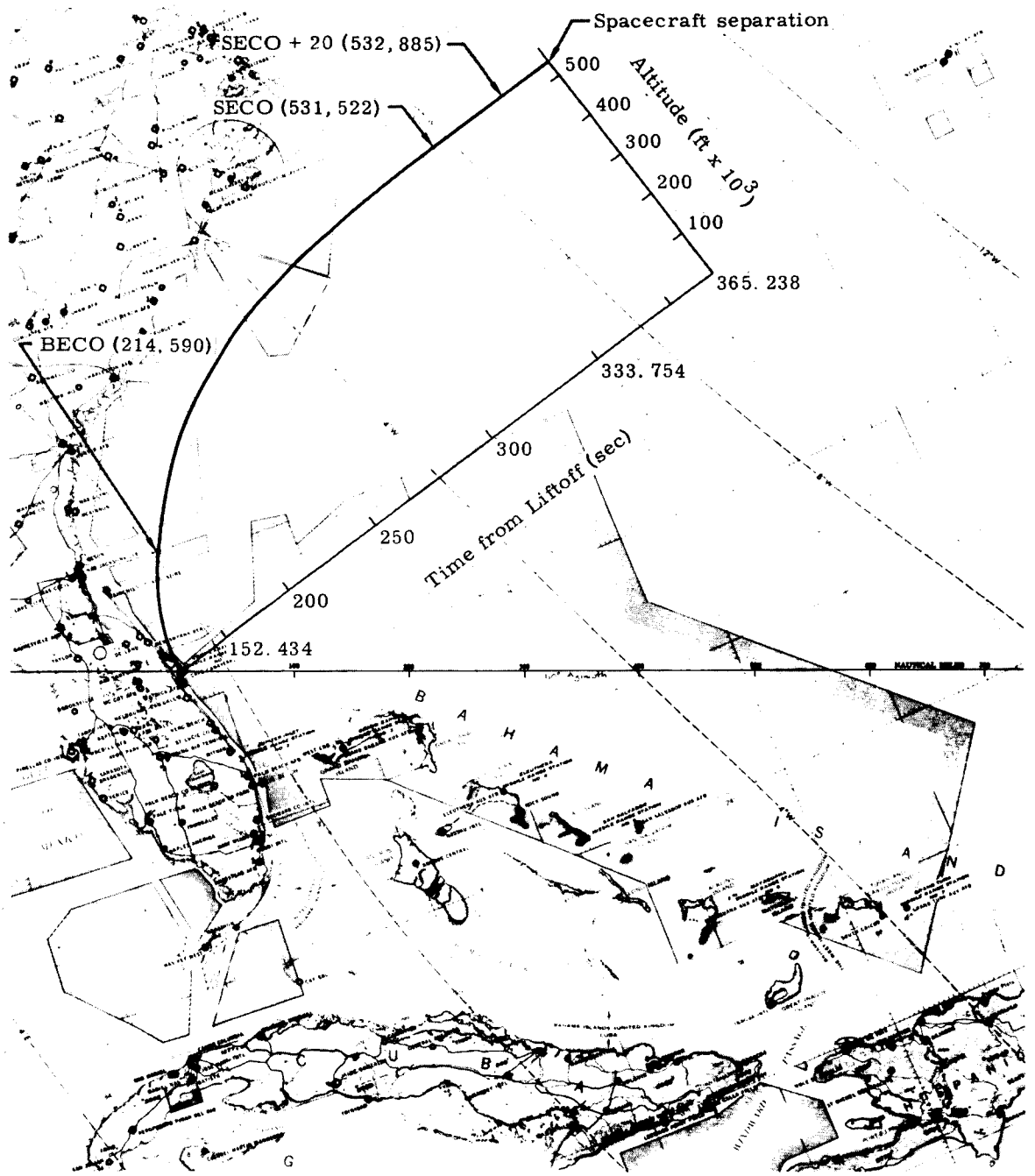

Fig. II-1. GT-4 Boost Flight Path Profile

TABLE II-6

Comparison of GT-4 Predicted and Observed Performance

	Nominal Trajectory (Ref. 19)	Tracking System					
		GE Mod III-G	MISTRAM I	FPQ-6 (19, 18)	FPQ-6 (0, 18)	FPQ-6 (3, 18)	FPQ-6 (7, 18)
BECO							
Time from liftoff (sec)	153.78	152.43	152.43	152.43	152.43	152.43	N/A
Inertial velocity (fps)	9,900	9,842	9,840	9,846	9,849	9,785	
Altitude (ft)	206,775	214,590	214,457	214,448	214,683	214,486	
Inertial flight path angle (deg)	18.66	20.36	20.34	20.27	20.32	20.28	
Ground range (naut mi)	50.28	48.75	48.76	48.77	48.74	48.74	
Geocentric radius (ft)	21,116,378	21,124,182	21,124,067	21,124,059	21,124,294	21,124,097	
Downrange position, X_f (ft)	308,431	299,165	299,236	299,298	299,105	299,116	
Cross-range position, Y_f (ft)	- 833	- 618	- 649	- 636	- 680	- 684	
Vertical position, Z_f (ft)	204,493	212,426	212,308	212,299	212,536	212,339	
Downrange velocity, $\dot{X}_f$ (fps)	8,123	7,975	7,974	7,984	7,983	7,926	
Cross-range velocity, $\dot{Y}_f$ (fps)	- 35	16	15.5	14	- 3	12	
Vertical velocity, $\dot{Z}_f$ (fps)	3,056	3,319	3,315	3,304	3,314	3,286	
Yaw steering velocity, V'_Y (fps)	--	205	--	206	224	210	
Biased yaw steering velocity, V_Y (fps)	228	--	--	--	--	--	
SECO + 20 Seconds							
Time from liftoff (sec)	356.10	353.75	353.75	353.75*	353.75	353.75	353.75*
Inertial velocity (fsp)	25,756	25,745	25,745	25,718	25,691	25,773	25,738
Altitude (ft)	531,383	532,885	531,465	529,120	533,191	532,610	533,971
Inertial flight path angle (deg)	0	0.059	0.033	0.268	0.348	0.569	0.7396
Ground range (naut mi)	538	531.5	531.7	531.6	531.4	531.49	531.45
Geocentric radius (ft)	21,438,813	21,440,331	21,438,866	21,436,559	21,440,632	21,440,055	21,441,415
Downrange position X_f (ft)	3,339,191	3,298,780	N/A	3,298,959	3,298,534	3,298,791	3,298,738
Cross-range position, Y_f (ft)	-35,514	-32,707	-31,458	-30,660	-31,055	-32,218	-32,005
Vertical position, Z_f (ft)	270,012	277,860	N/A	274,024	278,209	277,581	278,966
Downrange velocity, $\dot{X}_f$ (fps)	24,141	24,141	N/A	24,129	24,118	24,195	24,177
Cross-range velocity, $\dot{Y}_f$ (fps)	-401	-405	-394	-389	294*	-650	-468
Vertical velocity, $\dot{Z}_f$ (fps)	-3,780	-3,713	N/A	-3,617	-3,575	-3,490	-3,409
Yaw steering velocity, V'_Y (fps)	0	0	N/A	-16	-698	erratic	62
Biased yaw steering velocity, V_Y (fps)	-26	--	--	--	--	--	--

* unsmoothed data

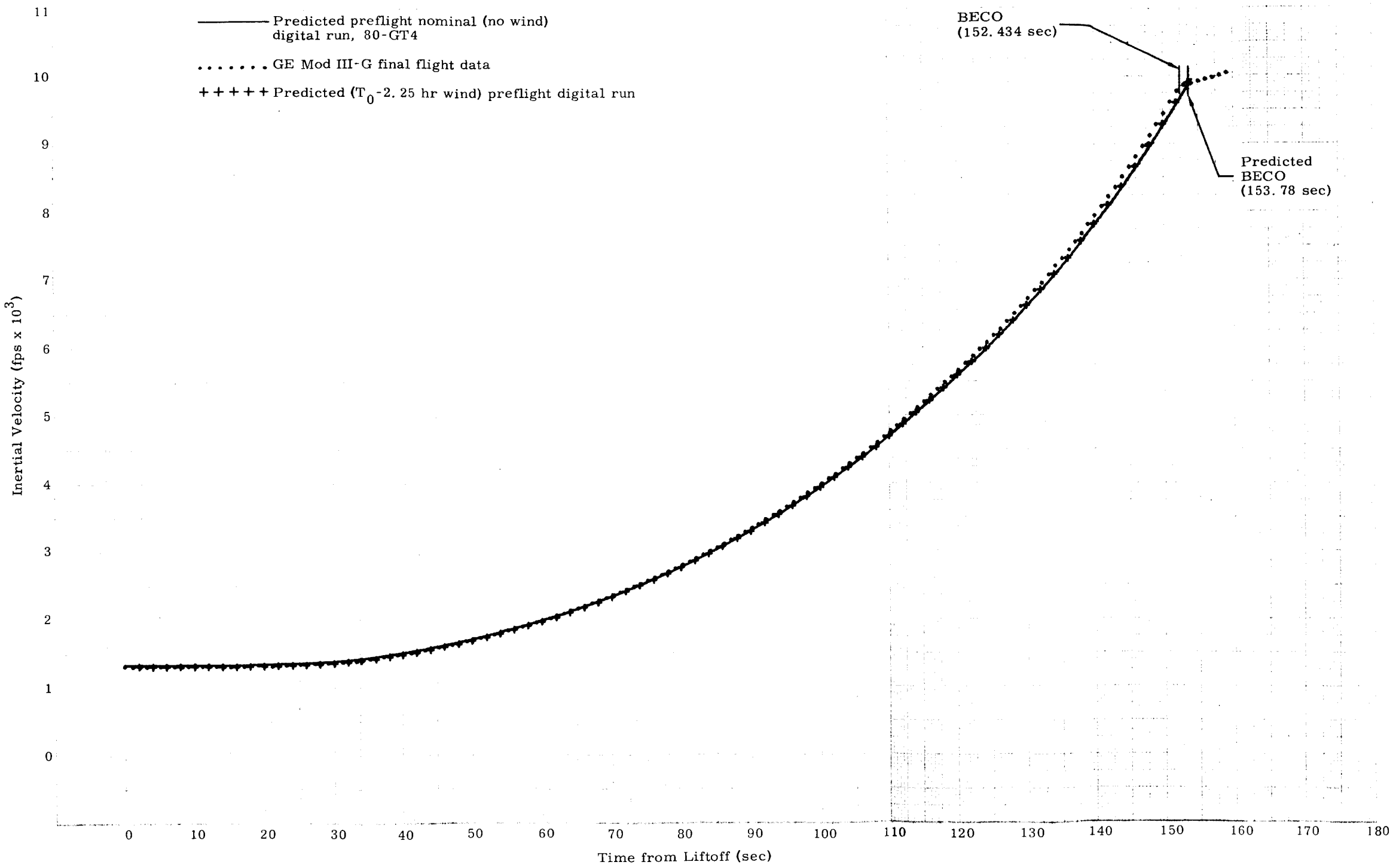

Fig. II-2. Inertial Velocity Versus Time: Stage I Flight

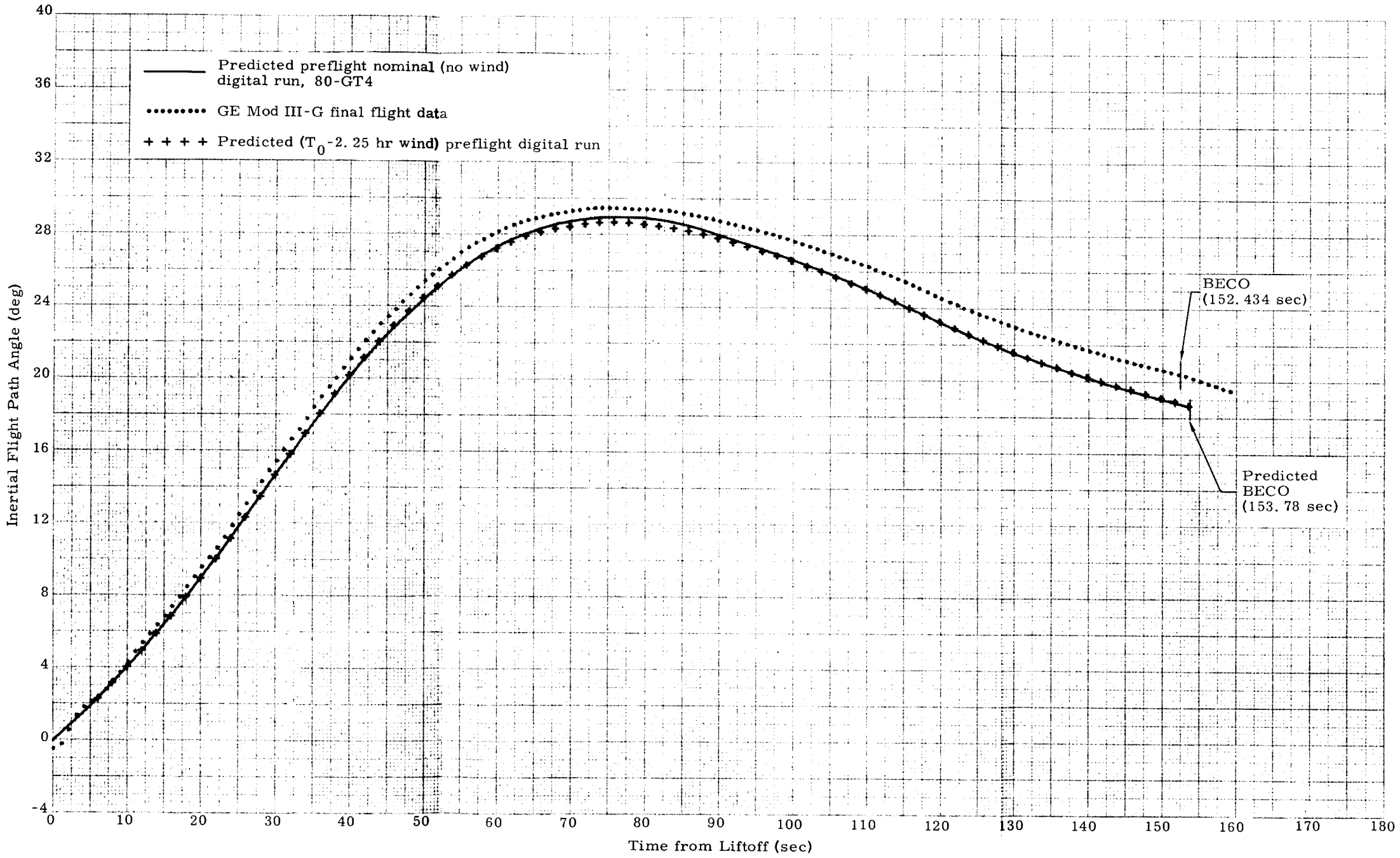

Fig. II-3. Inertial Flight Path Angle Versus Time: Stage I Flight

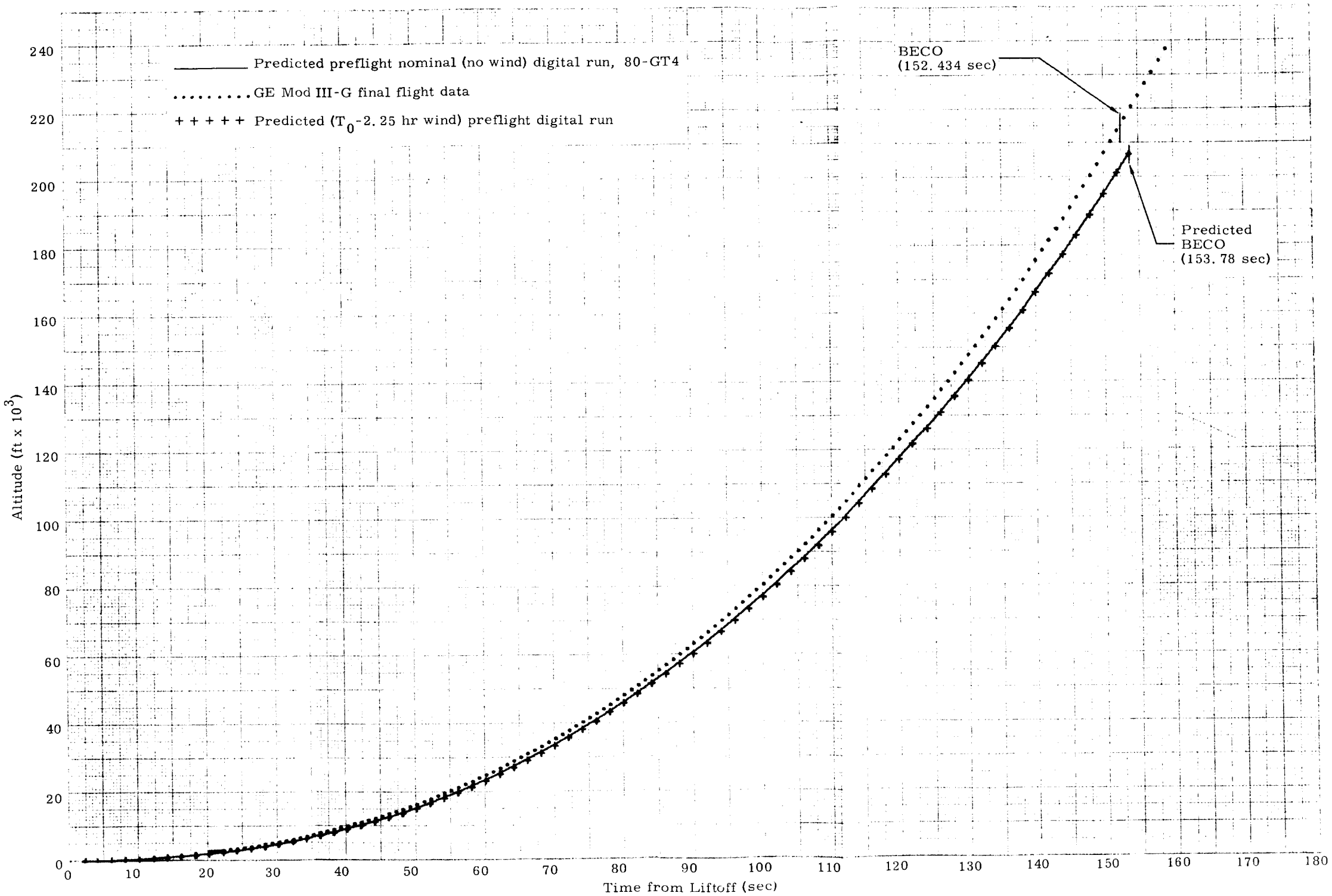

Fig. II-4. Altitude (h) Versus Time: Stage I Flight

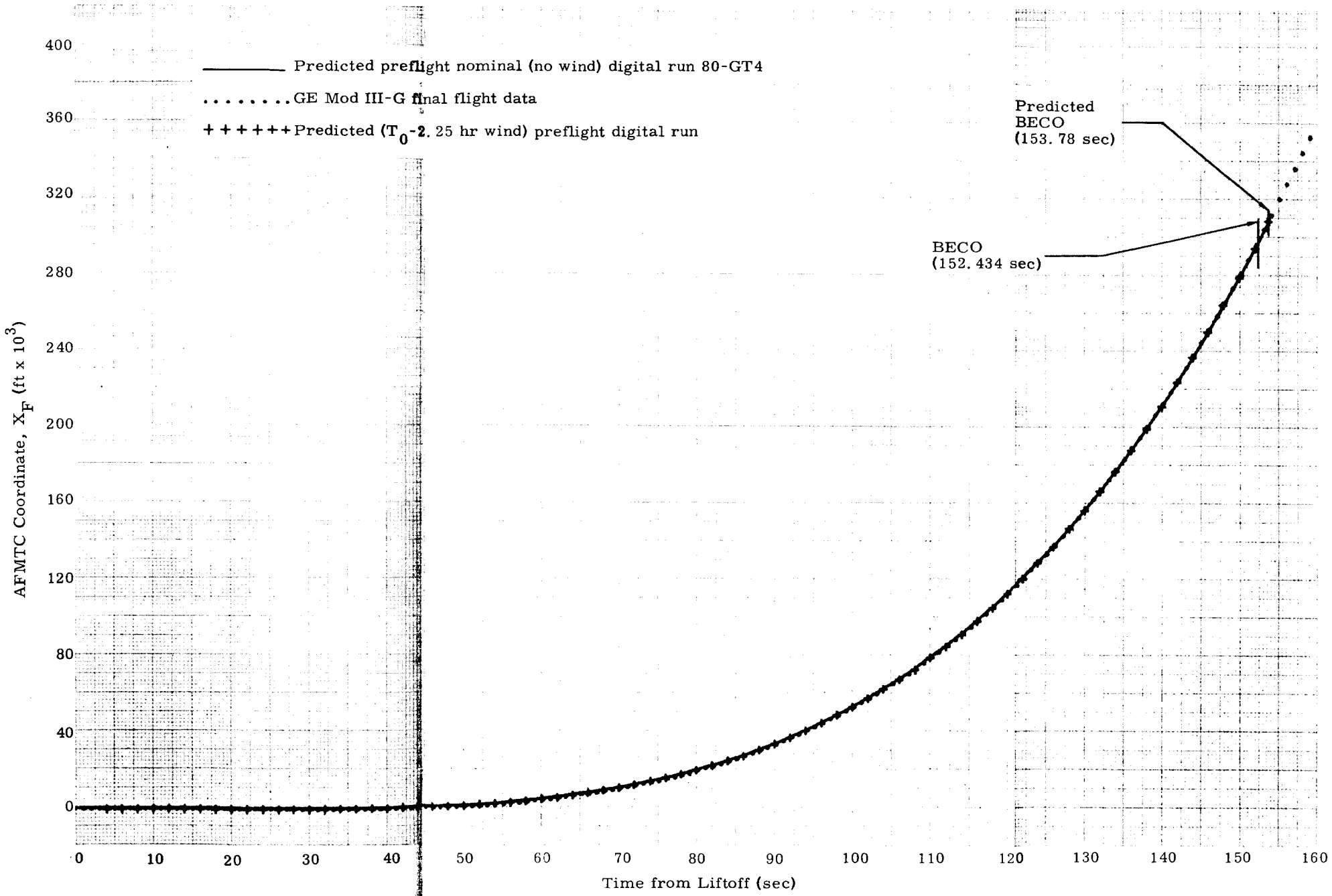

Fig. II-5. Downrange Position Coordinate (X_F) Versus Time: Stage I Flight

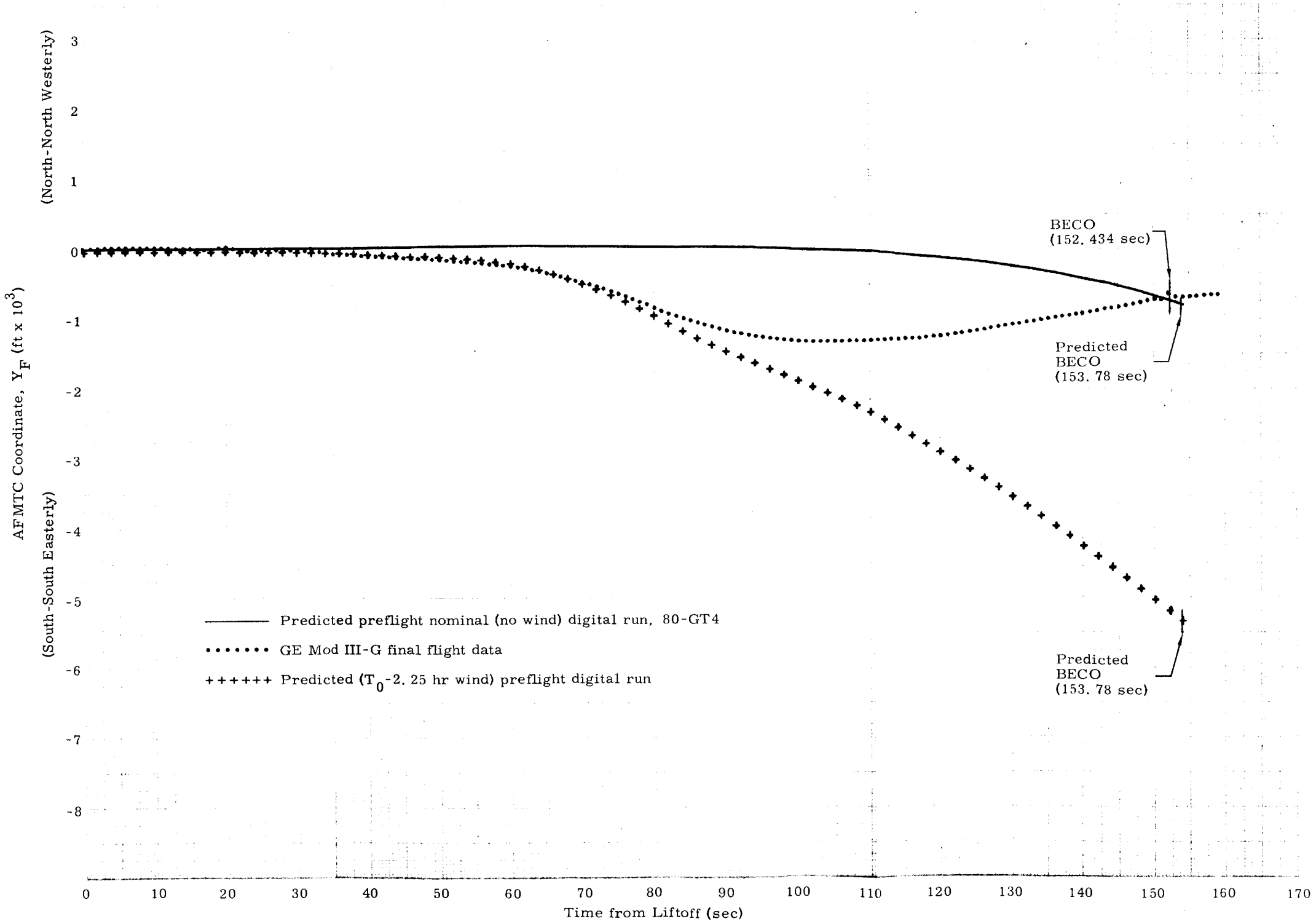

Fig. II-6. Cross-Range Position Coordinate (Y_F) Versus Time: Stage I Flight

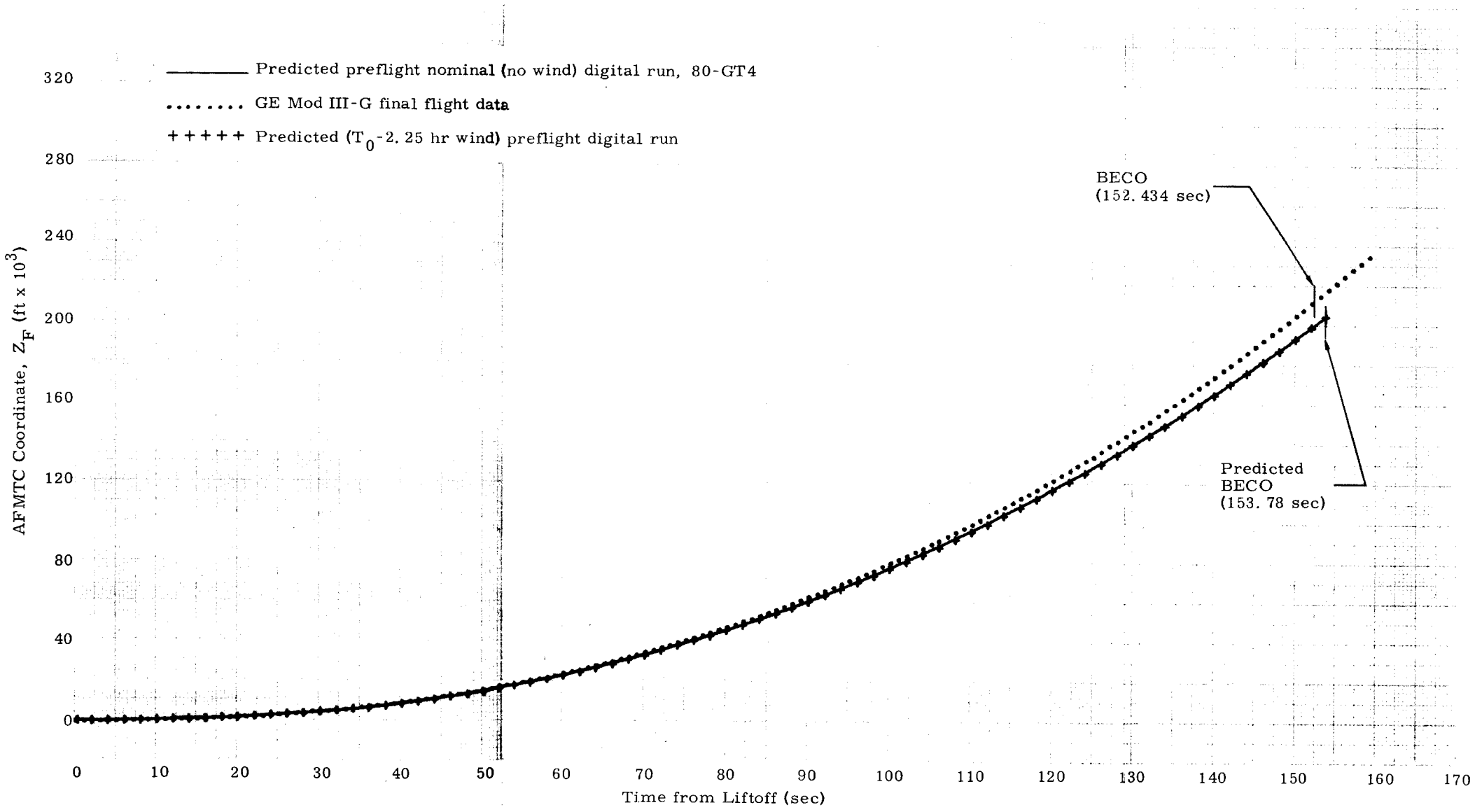

Fig. II-7. Vertical Position Coordinate (Z_F) Versus Time: Stage I Flight

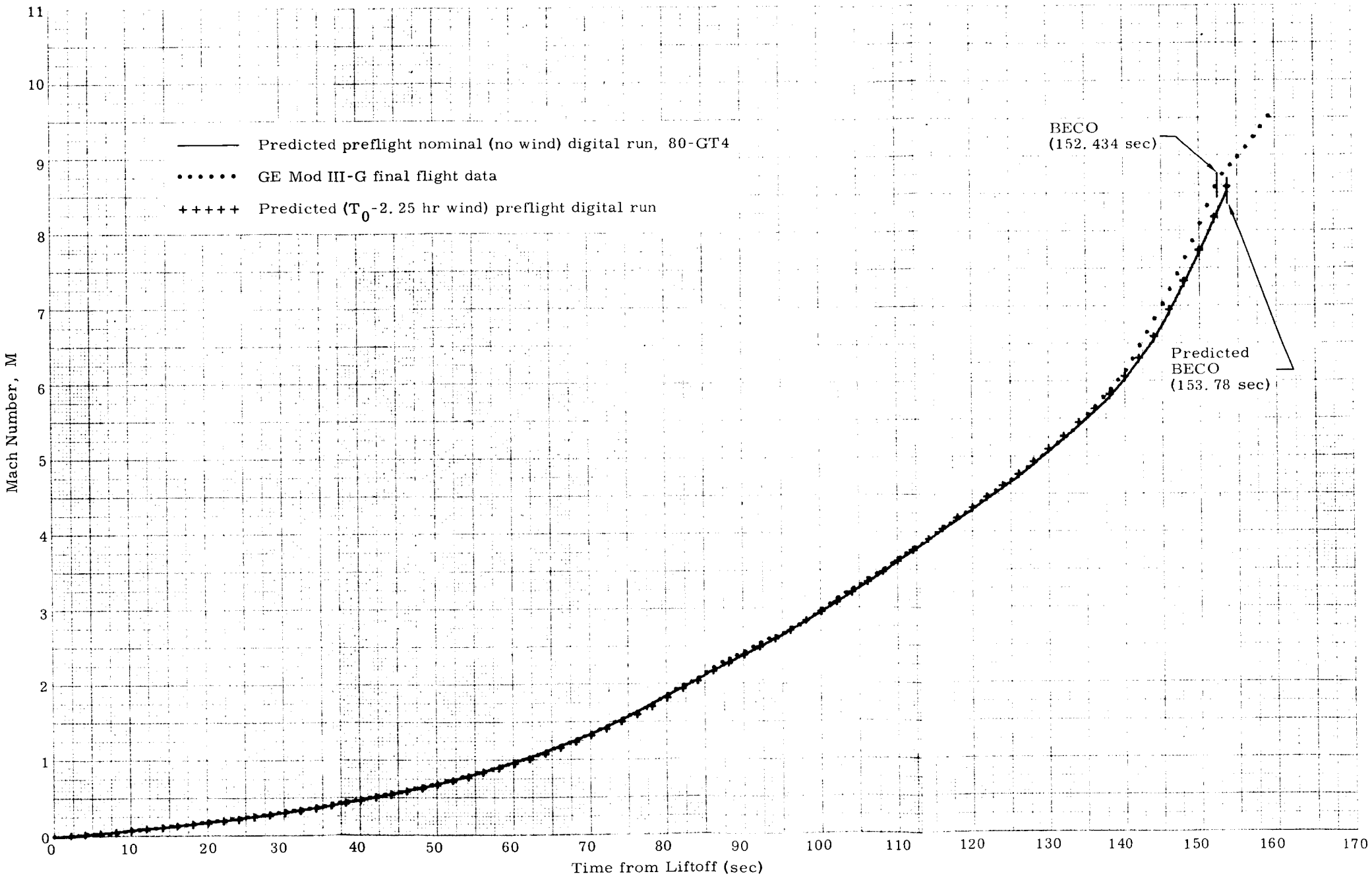

Fig. II-8. Mach Number (M) Versus Time: Stage I Flight

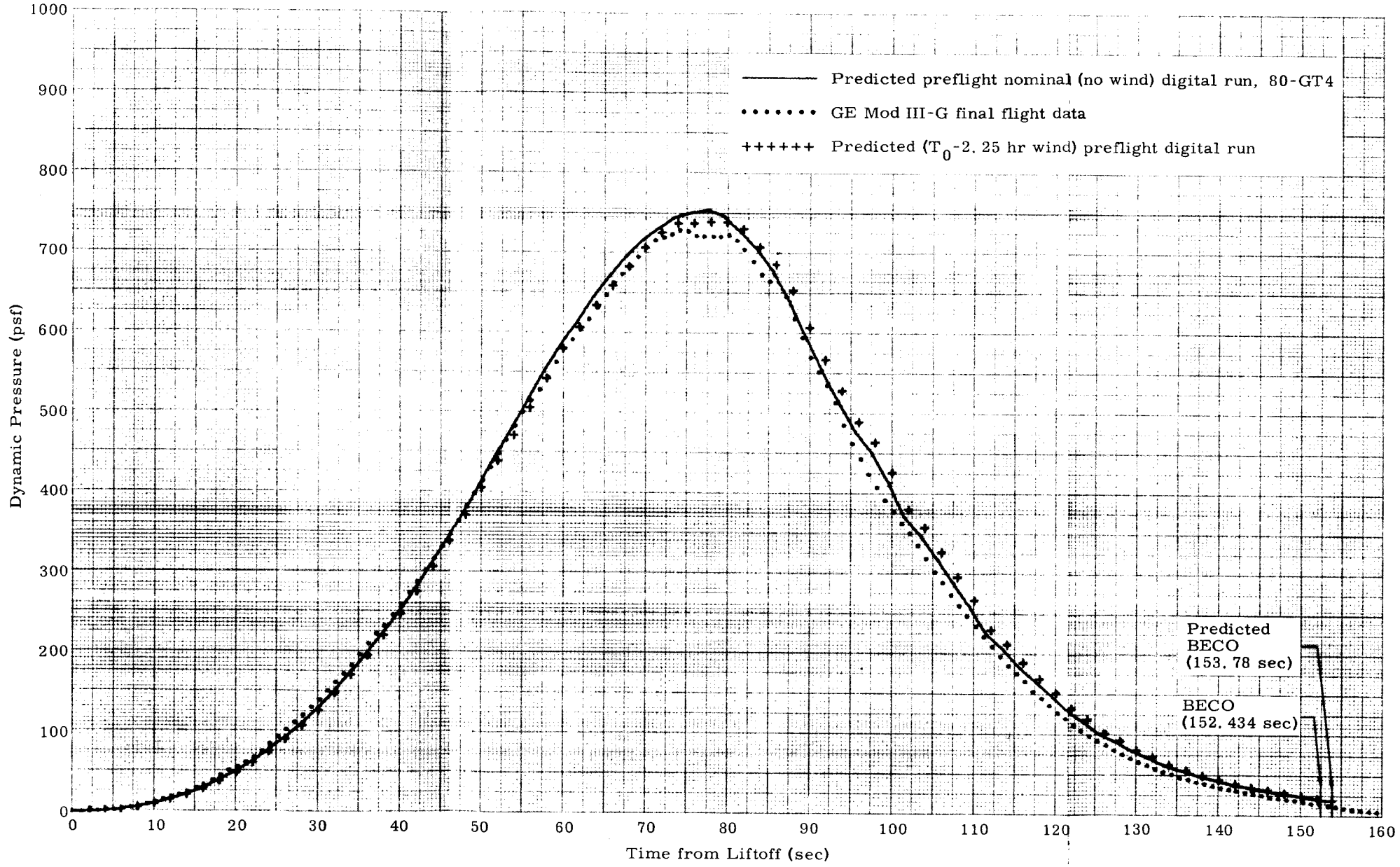

Fig. II-9. Dynamic Pressure (q) Versus Time: Stage I Flight

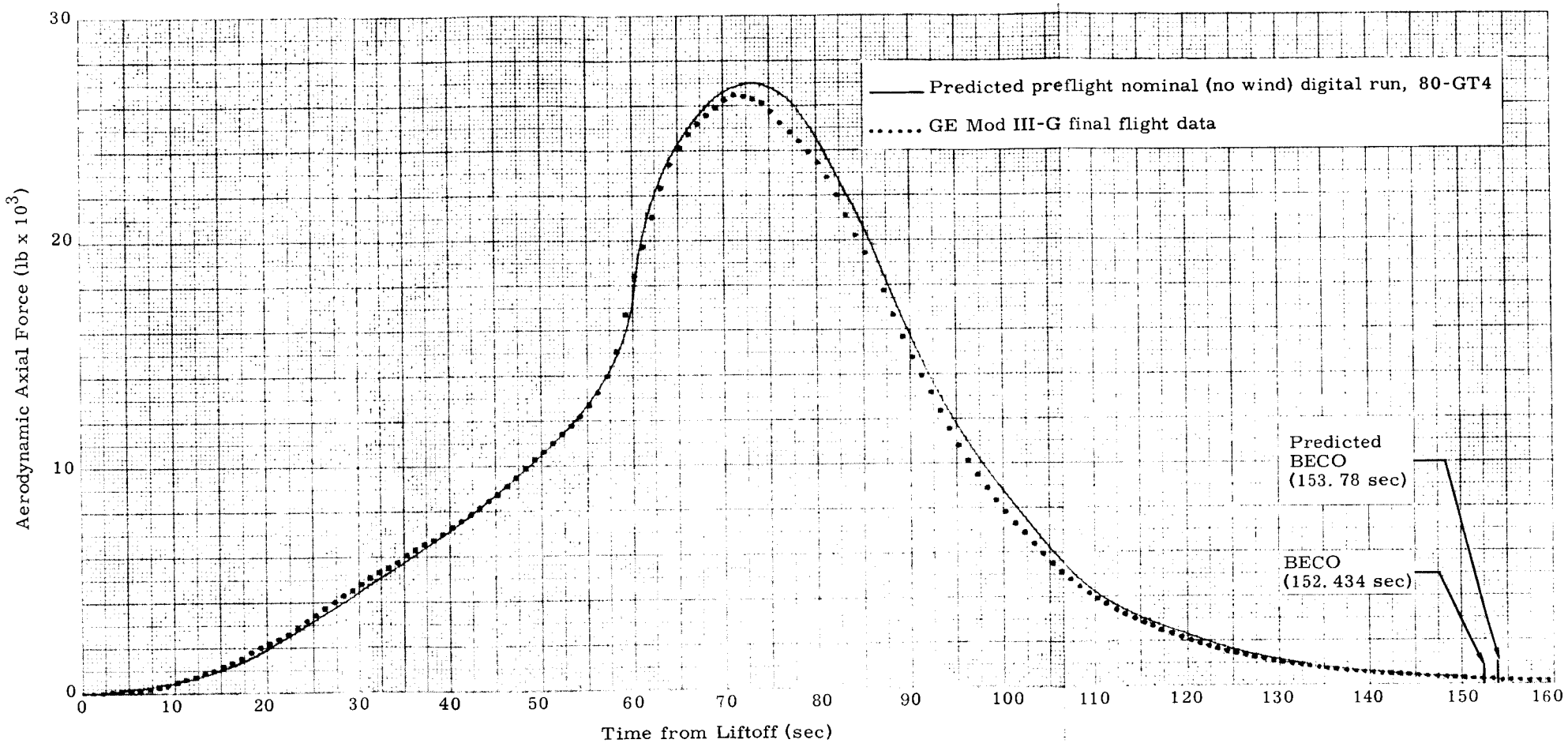

Fig. II-10. Axial Force Versus Time: Stage I Flight

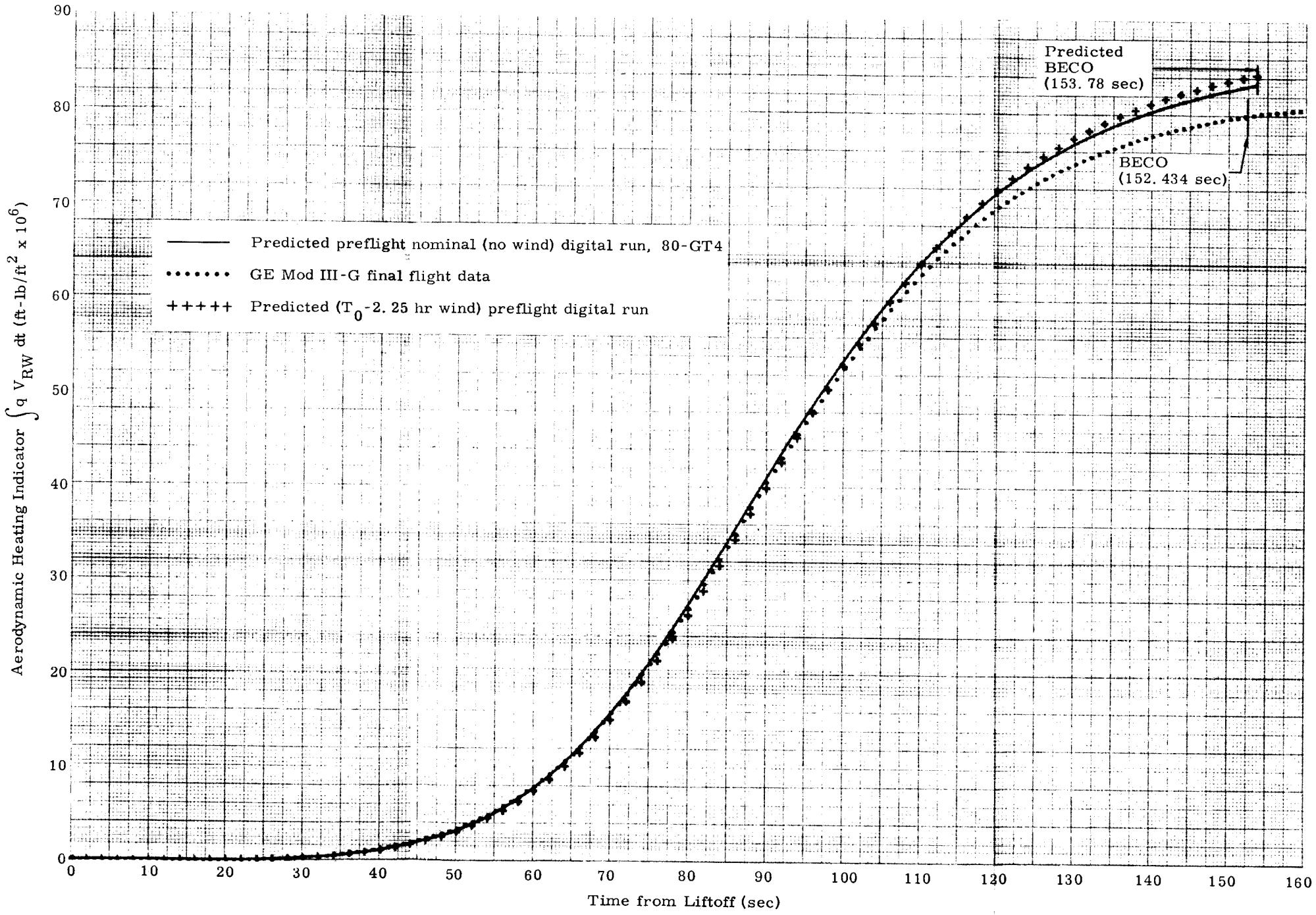

Fig. II-11. Aerodynamic Heating Indicator Versus Time: Stage I Flight

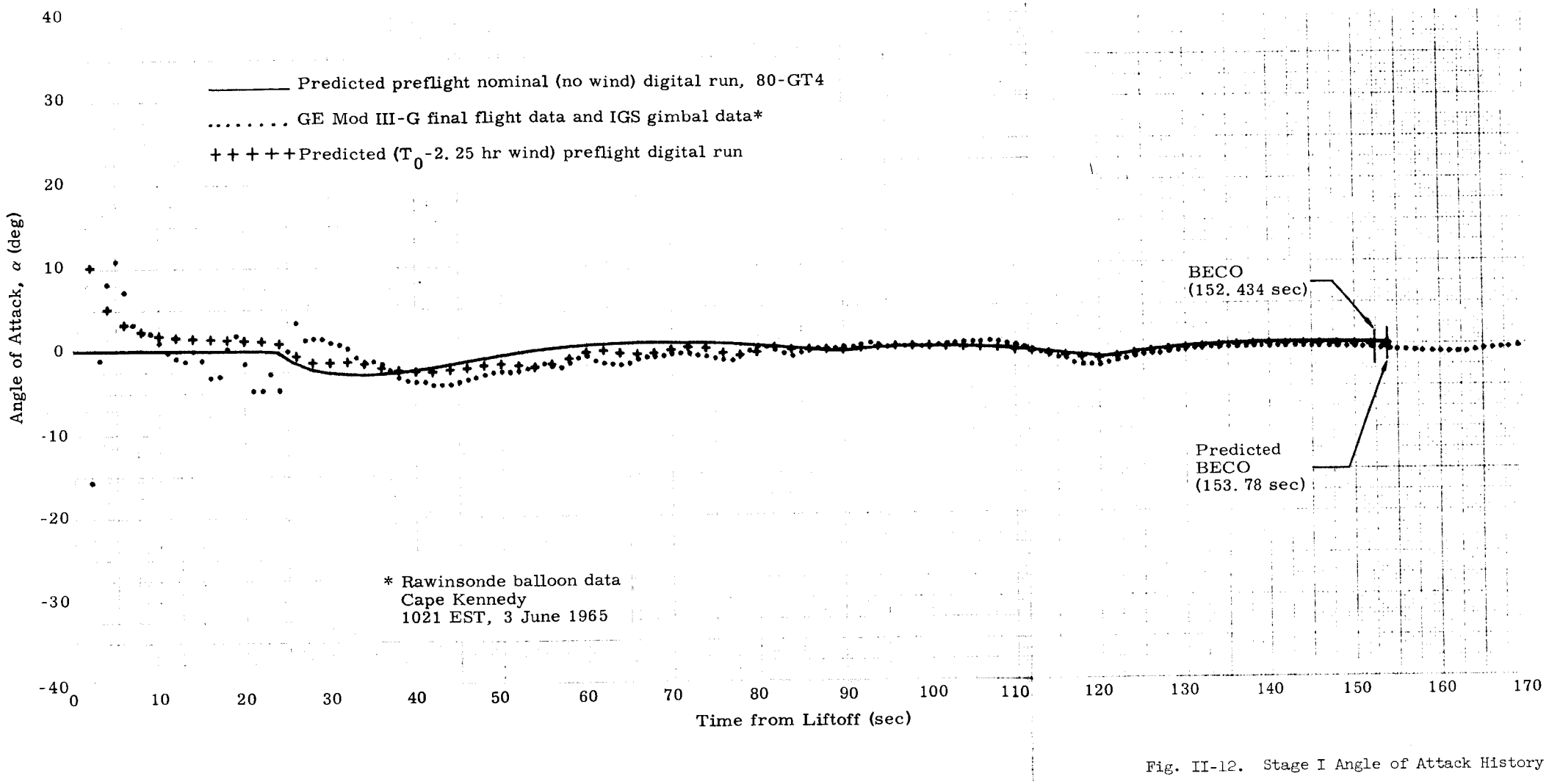

Fig. II-12. Stage I Angle of Attack History

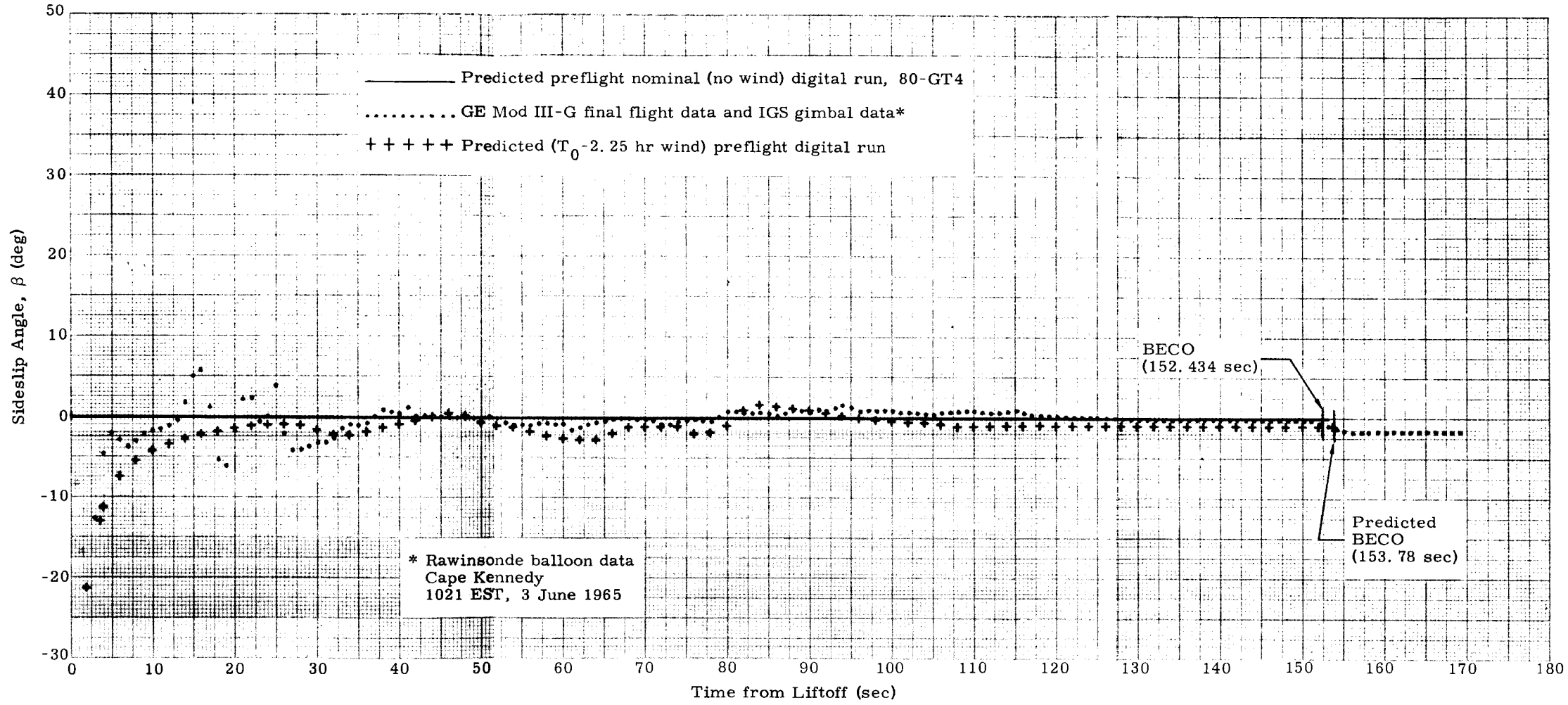

Fig. II-13. Stage I Angle of Sideslip History

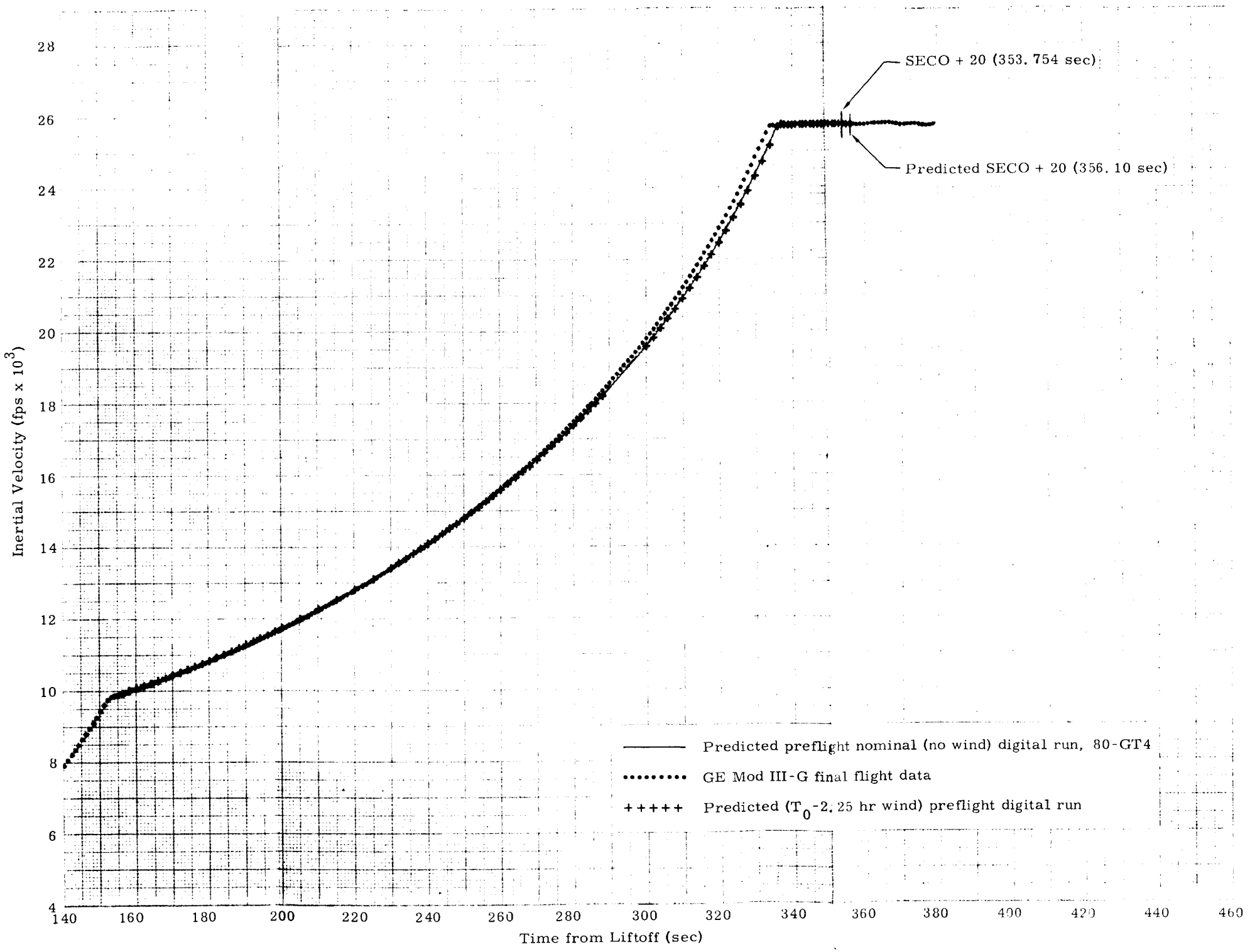

Fig. II-14. Resultant Inertial Velocity (V_I) Versus Time: Stage II Flight

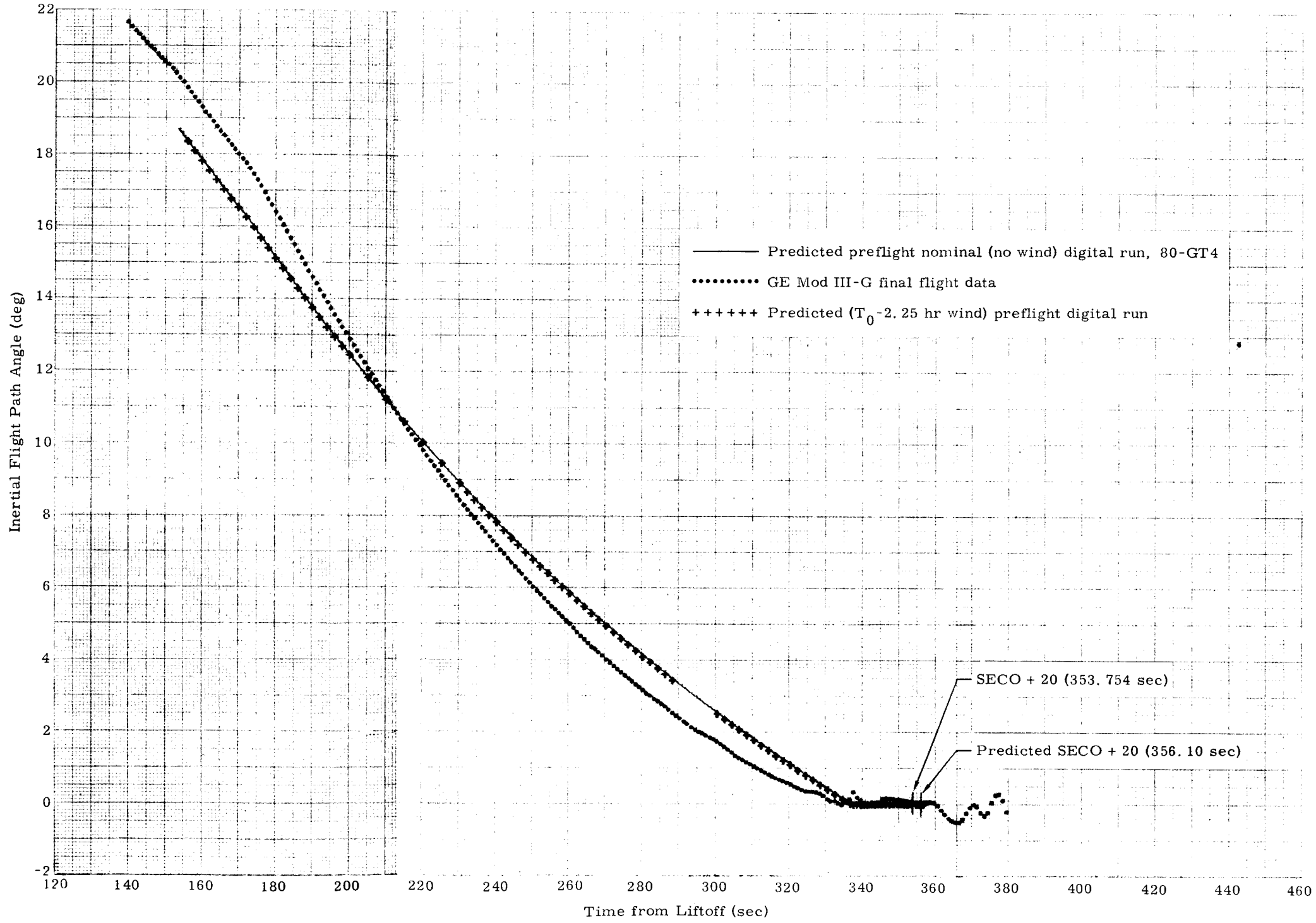

Fig. II-15. Inertial Flight Path Angle (γ_T) Versus Time: Stage II Flight

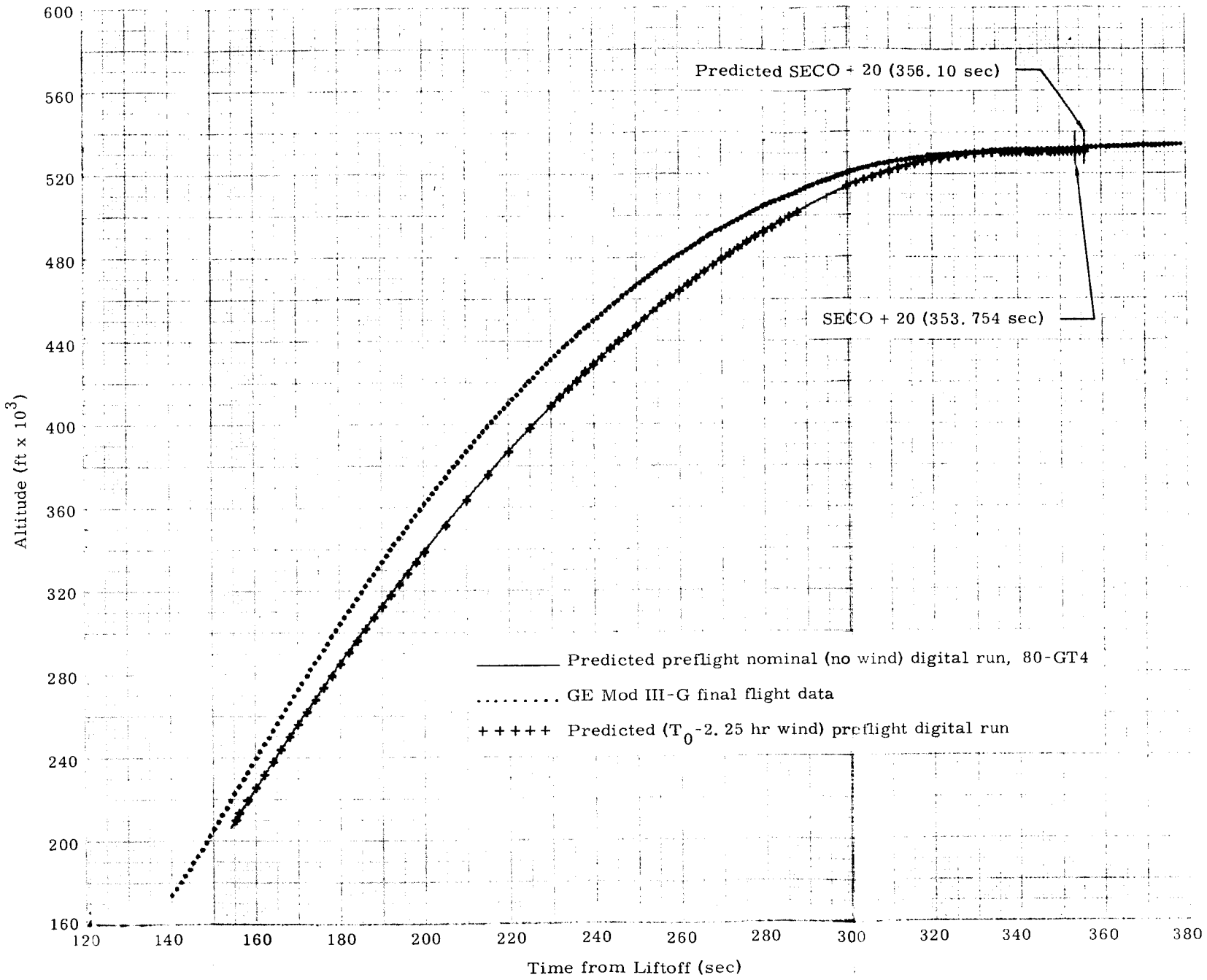

Fig. II-16. Altitude Versus Time: Stage II Flight

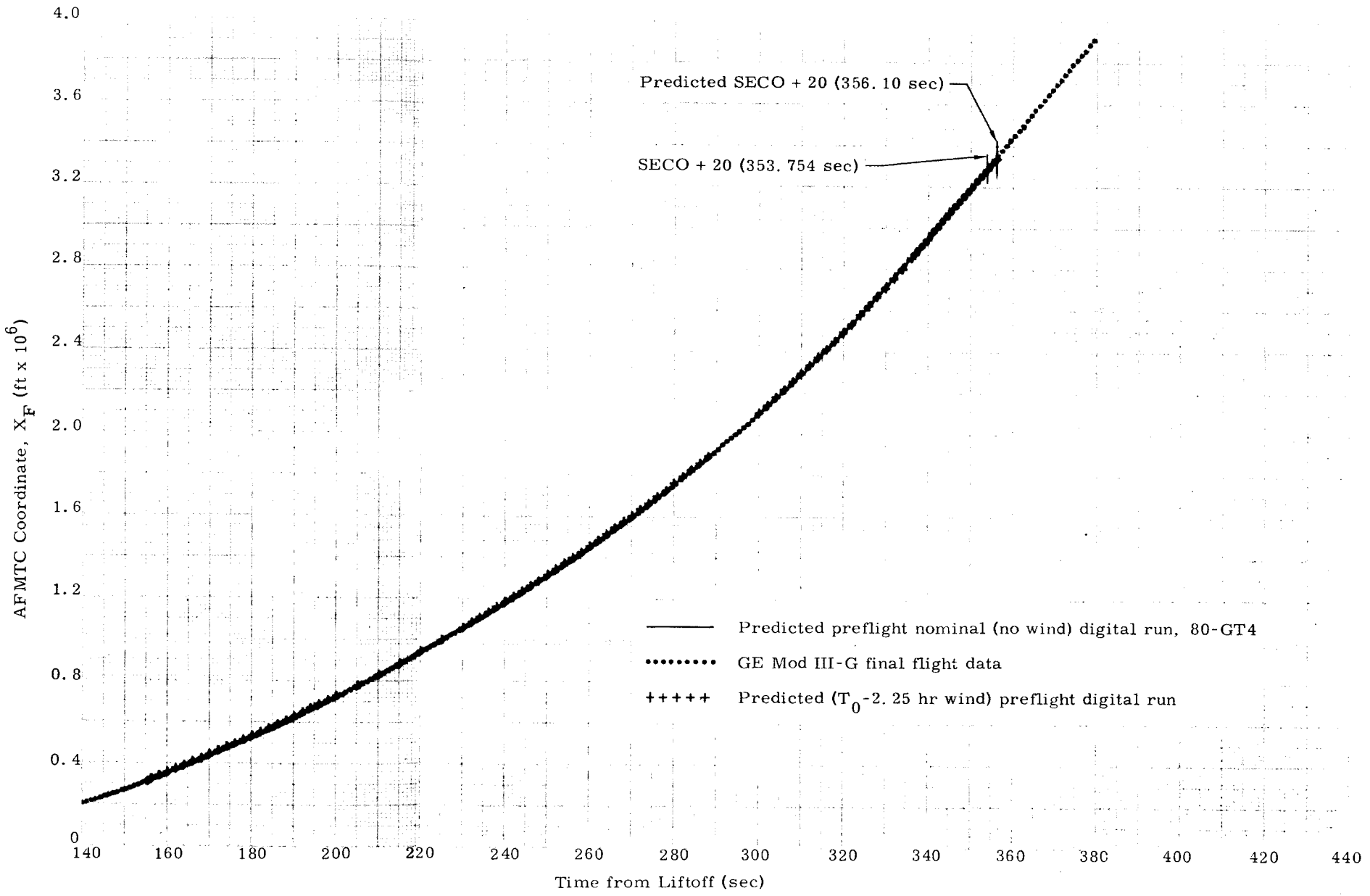

Fig. II-17. Downrange Position Coordinate (X_F) Versus Time: Stage II Flight

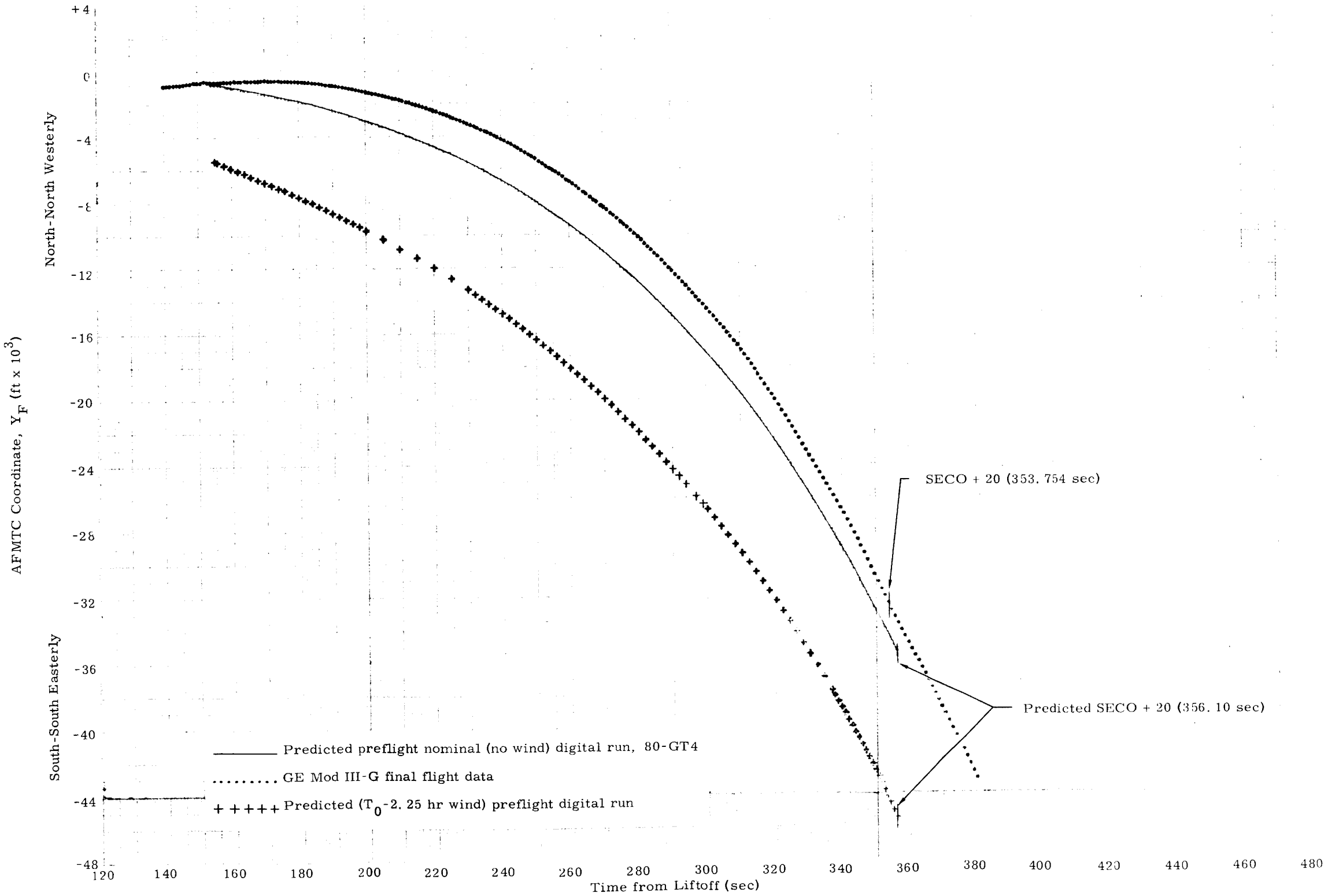

Fig. II-18. Cross-Range Position Coordinate (Y_F) Versus Time: Stage II Flight

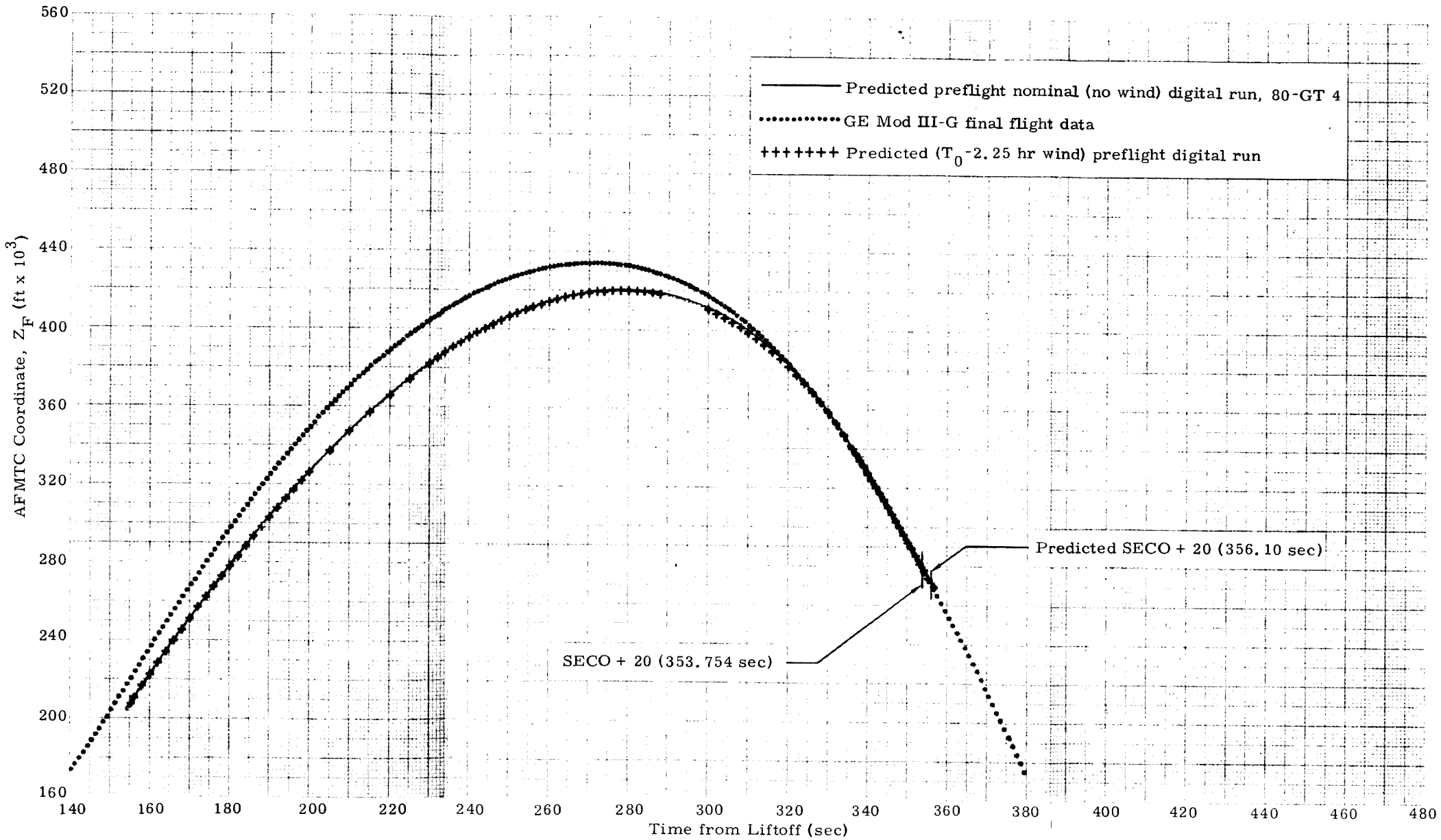

Fig. II-19. Vertical Position Coordinate (Z_F) Versus Time: Stage II Flight

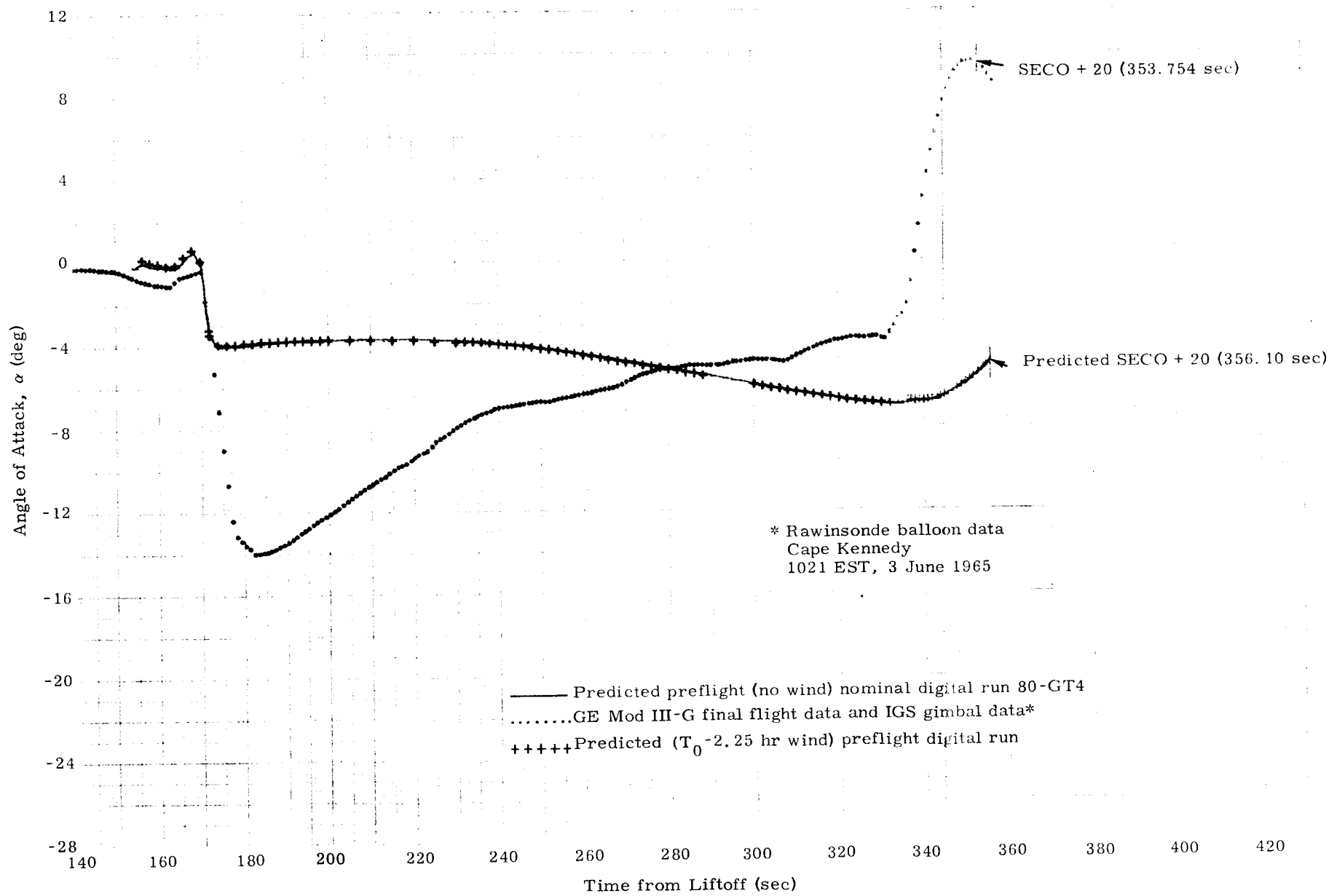

Fig. II-20. Stage II Angle of Attack History

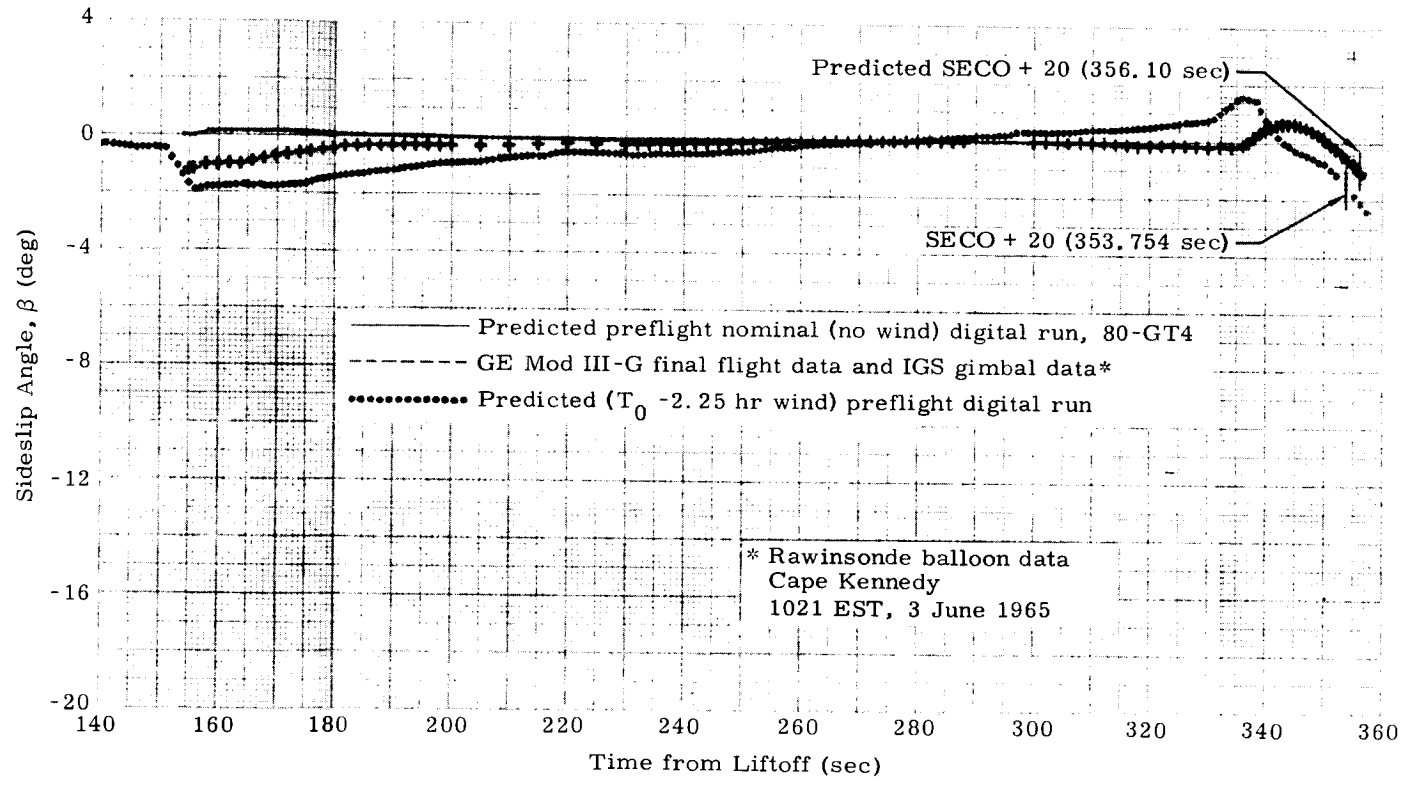

Fig. II-21. Angle of Sideslip Versus Time: Stage II Flight

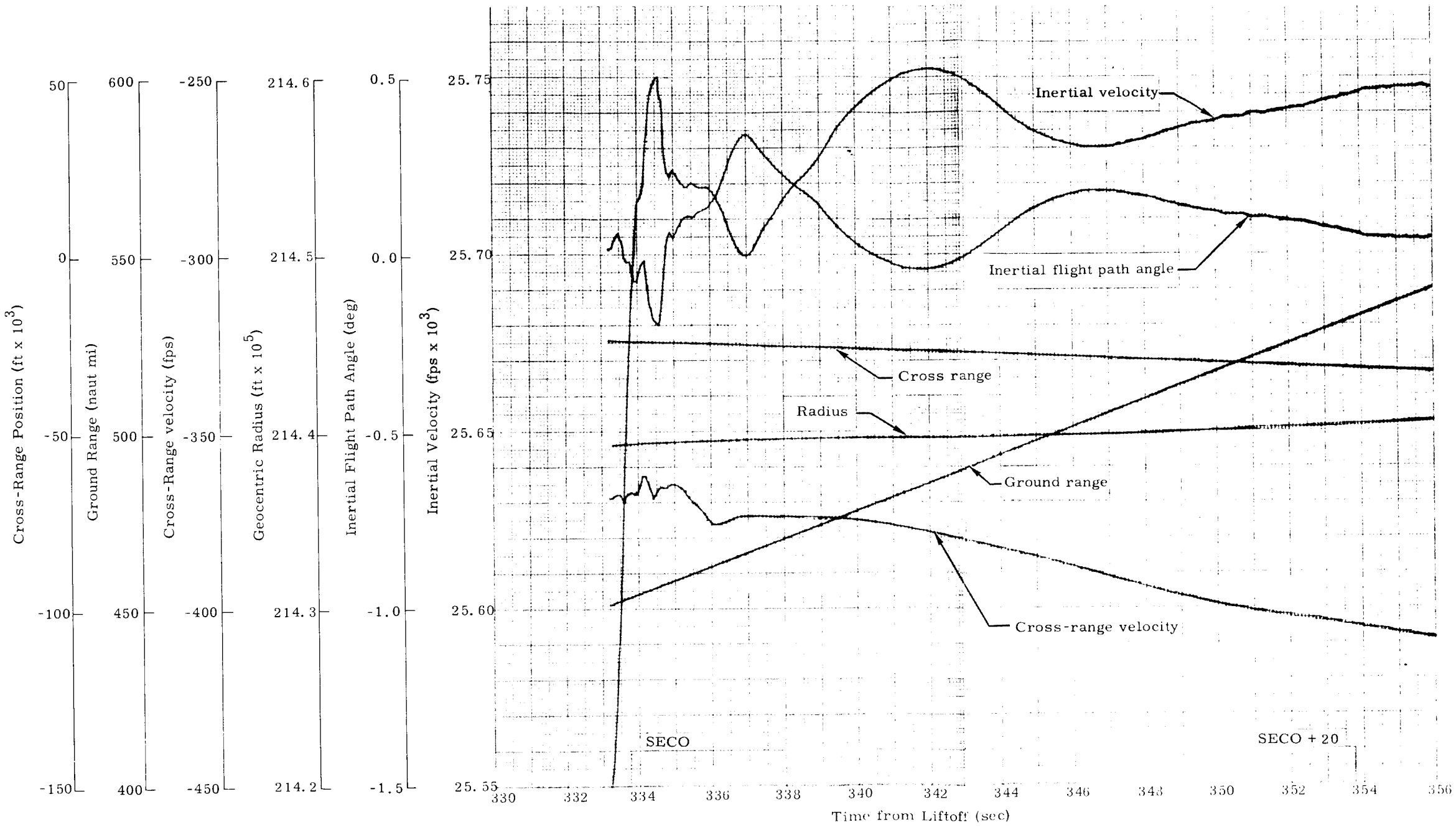

Fig. II-22. GE Mod III-G Flight Data from SECO to SECO + 20 Seconds

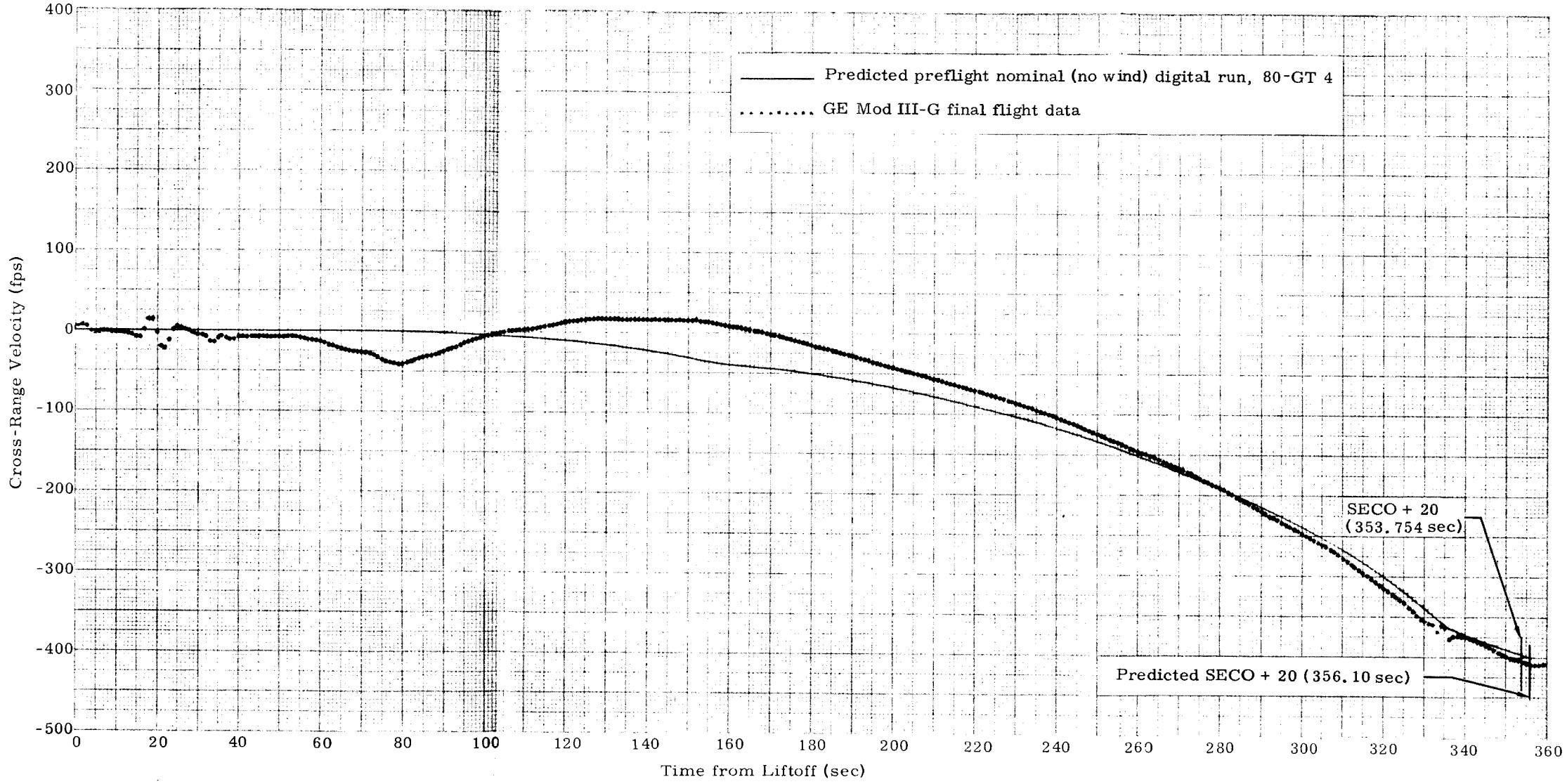

Fig. II-23. Cross-Range Velocity ($\dot{Y}_p$) Versus Time

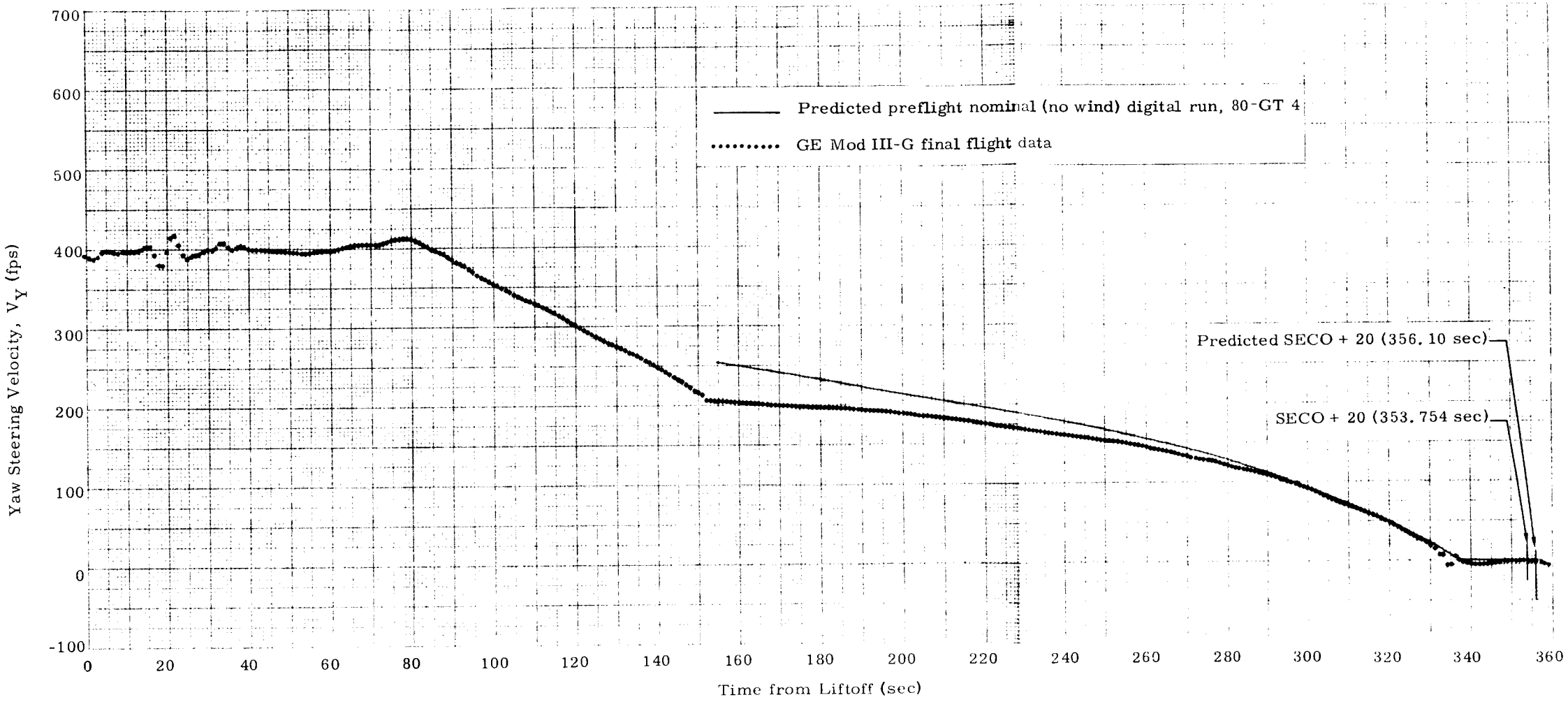

Fig. II-24. Yaw Steering Velocity (V_Y) Versus Time

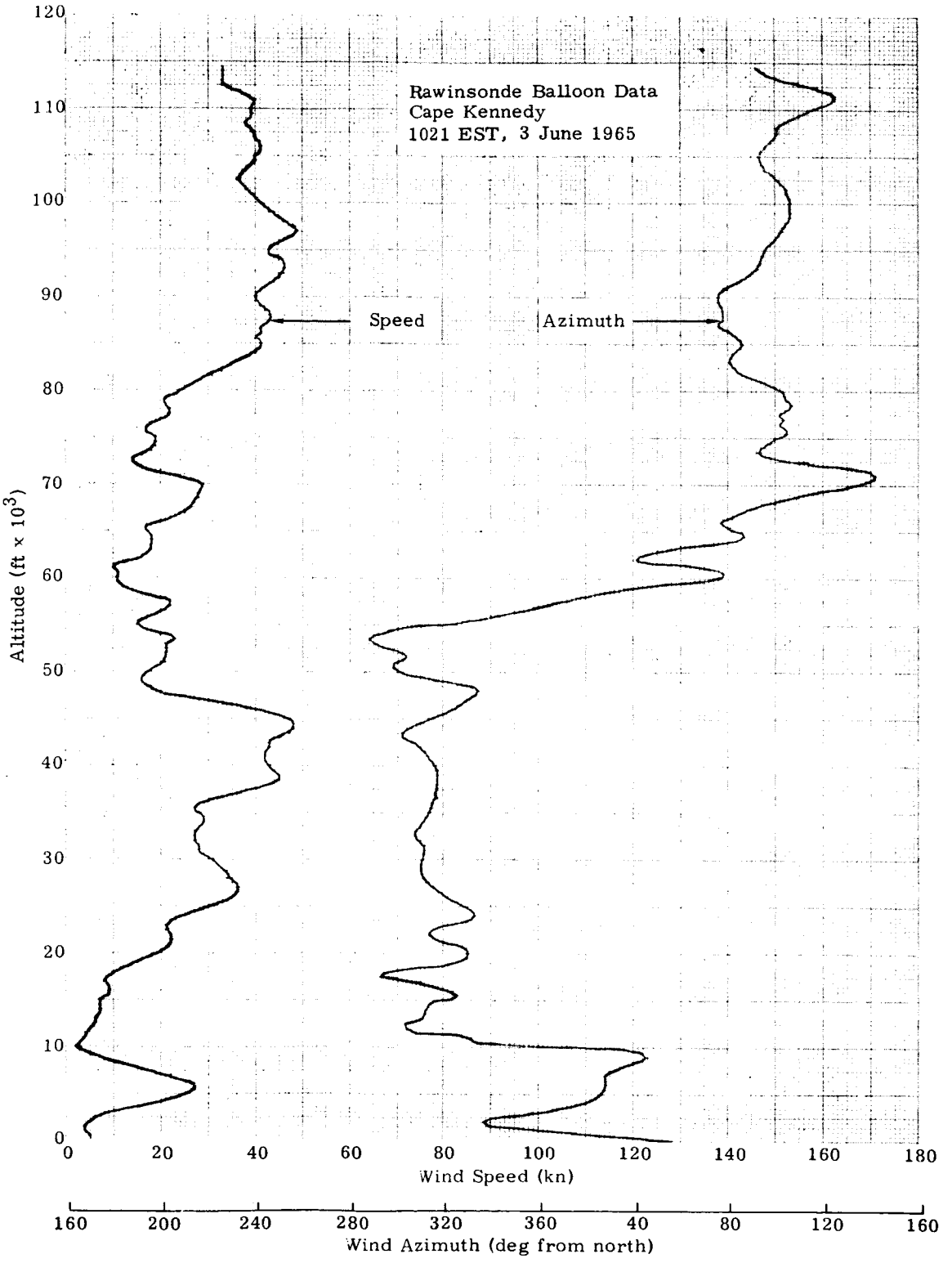

Fig. II-25. Wind Speed and Azimuth Versus Altitude

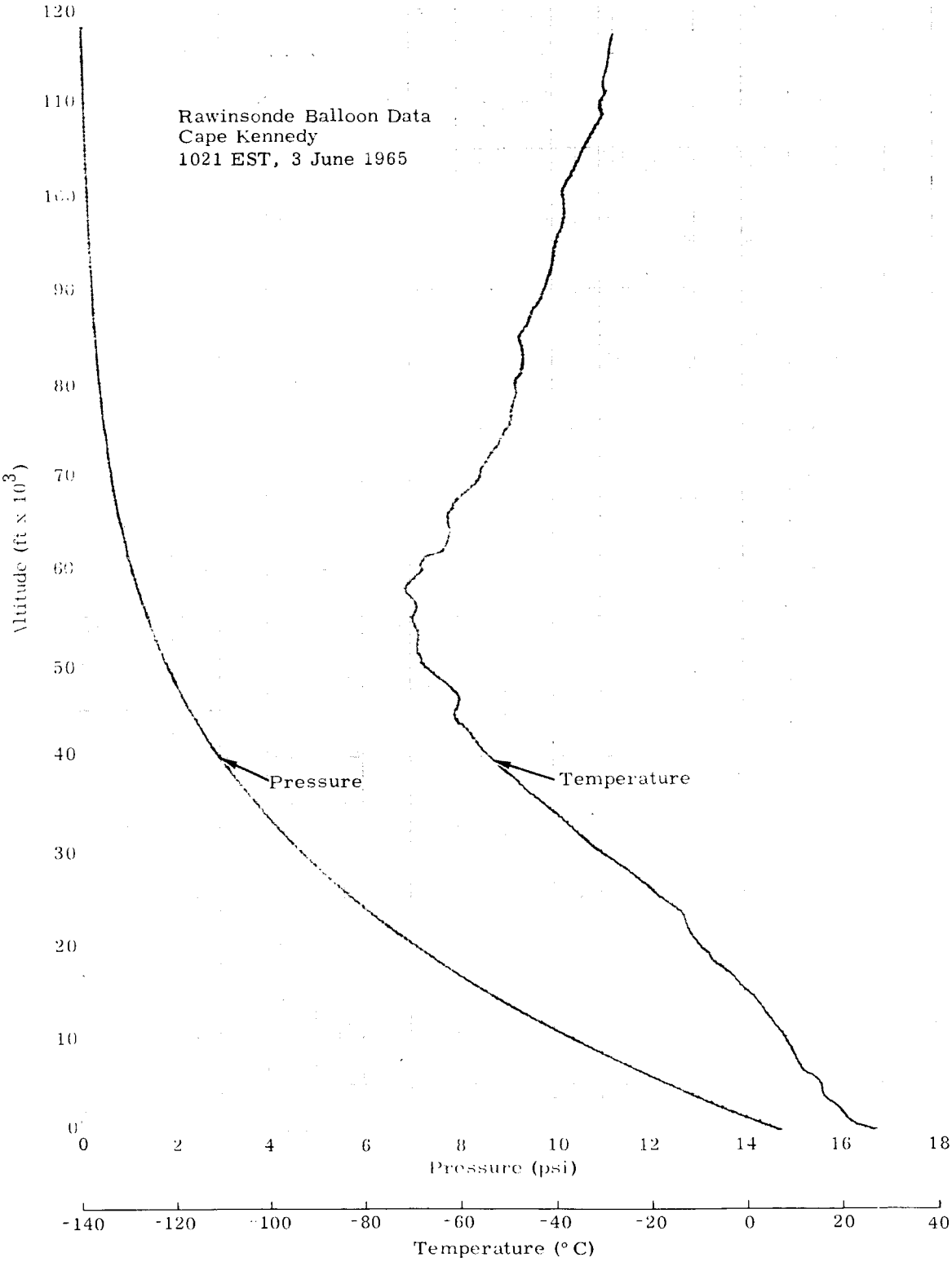

Fig. II-26. Ambient Temperature and Pressure Versus Altitude

TABLE II-7

Factors Contributing to GT-4 BECO Dispersions

	Δt (sec)	Δ Altitude (ft)	Δ Velocity (fps)	Δγ (deg)
A. Measured Parameters				
Thrust (+0.90% ≈ 4177 lb)	-1.17	+2510	--	+0.455
Wind (1521 GMT weather data)	--	-229	-6	+0.05
Outage (614 lb)*	-0.03	-88	-5	+0.01
Propellant loading (-438 lb)	-0.27	+80	-10	+0.08
Inert weight (+94 lb)	--	-220	-7	--
B. Trend Indications				
Pitch programmer error (-1.76%)	--	+4300	-41	+0.93
Pitch engine misalignment (0.10 deg)	--	+1440	-15	+0.36
Specific impulse (+0.23% ≈ 0.64 sec)	+0.35	+500	+26	-0.07
Apparent (A and B)	-1.12	+8293	-58	+1.815
Measured (Mod III-G data)	-1.35	+7815	-58	+1.70

*Mean outage = 567 lb.

Table II-8 contains a listing of the various tracking instrumentation sources and the corresponding trajectory time interval covered by each.

TABLE II-8

Data Available for Trajectory Analysis

Source	Type	Station	Flight Coverage (sec from liftoff)
AFETR	FPQ-6 radar Position, velocity and acceleration	Patrick 0.18 GBI 3.18 Grand Turk 7.18 MILA 19.18	+13 to +414 +63 to +382 +205 to +493 +14 to +425
	MISTRAM I		+47 to +387
	Fixed camera Position, velocity and acceleration		LO to + 24
	Theodolite Position, velocity, acceleration and attitude		LO to + 44
GE	Mod III radar Position, velocity and acceleration	Cape Kennedy	LO to + 396
NASA-MSC	Spacecraft IGS ascent parameters		LO to + 400

6. Look Angles

Upon initiation of closed-loop guidance at LO + 168.35 seconds, the RGS commanded the maximum 2 deg/sec nose-down pitching rate for an interval of approximately 7 seconds in order to correct for the slightly higher-than-nominal BECO position. This maneuver resulted in moderate negative angles of attack during this period as shown in Fig. II-20. The maximum look angle in pitch (LAP) occurred at approximately LO + 185 seconds where it reached + 25.4 degrees. This maximum value was well within the 40-degree boundary as shown in Fig. II-27 at a radar slant range of 6.75×10^5 feet.

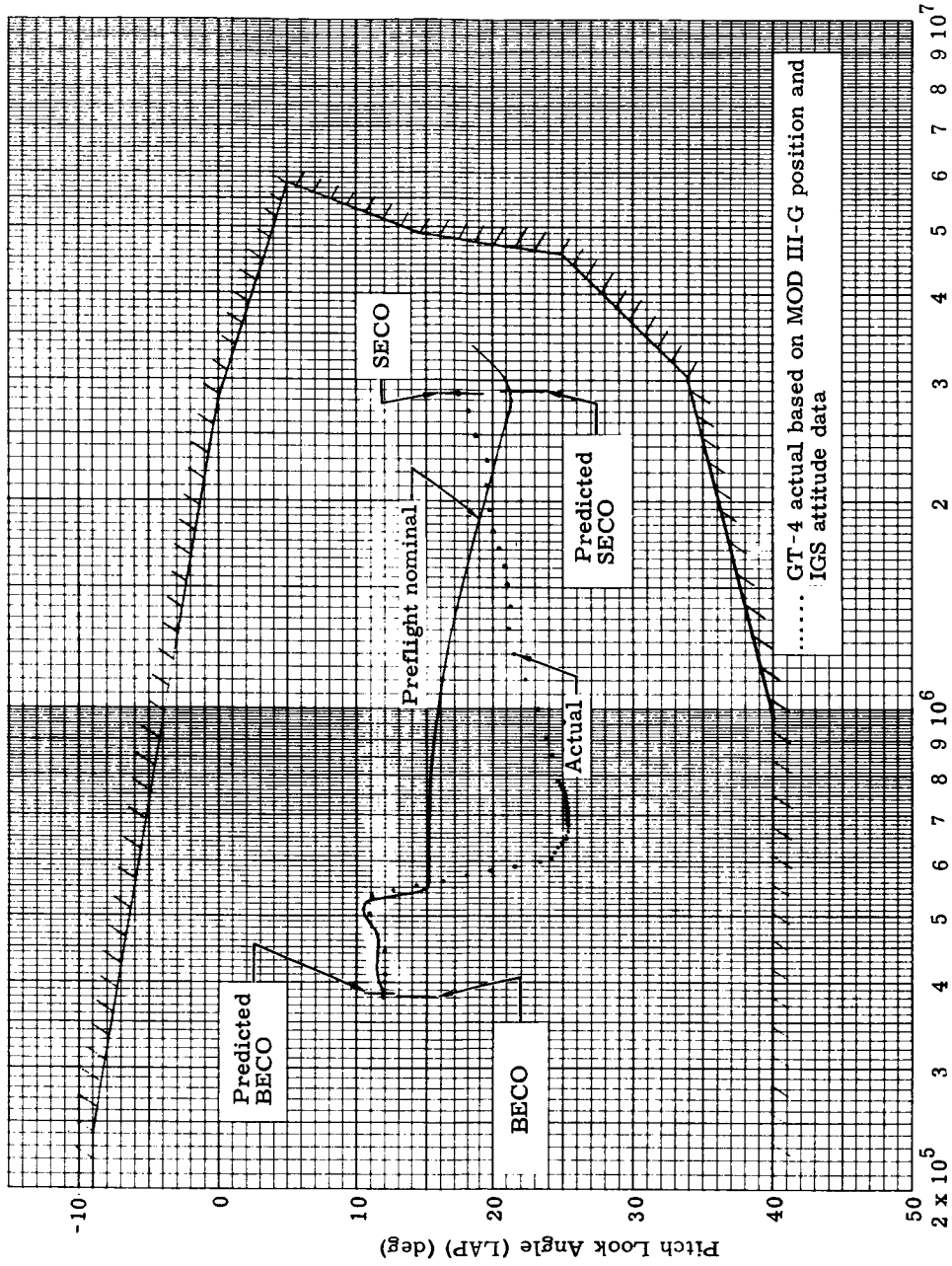

Fig. II-27. Permissible Pitch Look-Angle Envelope

Look angle in yaw (LAY) was also well within the established boundary (+7 degrees) as shown in Fig. II-28. The maximum value of LAY was 4.34 degrees occurring at a radar slant range distance of 4.09×10^5 feet at approximately 156 seconds after liftoff.

Reconstruction of the look angles in pitch and yaw verified the flight results within reasonable accuracy at LO + 180 seconds and LO + 160 seconds, respectively. These are the nearest convenient time slices to those for the maximum respective LAP and LAY measured values previously mentioned. Reconstructed look angles in pitch and yaw were obtained from LAP and LAY sensitivities derived from the GT-4 trajectory dispersion report (Ref. 9). The calculated individual dispersions, total reconstructed deviations, measured flight values, and preflight maximum dispersed values are shown in Tables II-9 and II-10. Both figures show that actual flight values were less than the preflight predicted maximums, which were calculated from the nominals in Ref. 19, in conjunction with the maximum RSS dispersions from Ref. 9.

TABLE II-9

Look Angle in Pitch (LAP) Reconstruction at Liftoff + 180 seconds

Parameter	Δ LAP (deg)
Stage I thrust (0.90% ≈ + 4177 lb)	2.94
Stage I specific impulse (0.23% ≈ 0.64 sec)	-0.14
Stage I outage (614 lb - 567 lb mean)	-0.03
Stage I pitch programmer error (TARS at -1.76%)	4.24
Stage I pitch engine misalignment (-0.1 deg)	1.79
Stage II pitch engine misalignment (+ 0.07 deg)	-0.08
Stage II thrust (0.64% ≈ + 649 lb)	0.06
Σ Δ (to be added to nominal)	8.78
Nominal trajectory value	15.10
Σ Total reconstructed deviation in LAP	23.88
Flight value	24.7[illegible]
Preflight maximum dispersed value	29.30

TABLE II-10

Yaw Look Angle (LAY) Reconstruction at Liftoff + 160 Seconds

Parameter	Δ LAY (deg)	ΔYaw Steering Velocity, V_Y (fps)
Winds (1021 EST, 6-3-65)	-0.27	+21
Stage I yaw engine misalignment (0.07 deg)	+0.28	-39
Stage I roll engine misalignment (-0.06 deg)	-0.06	-42
Stage II yaw engine misalignment (-0.26 deg)	+1.22	+3
Stage I thrust (+0.90% ≈ +4177 lb)	-0.05	-1
Stage I specific impulse (+0.23% +0.64 sec)	+0.02	-
Σ Δ (to be added to nominal)	+1.14	-58
Nominal trajectory value	+2.31	+251
Σ total reconstructed deviation in LAY	+3.45	+193
Flight value	+4.08	+203
Preflight maximum dispersed value	+5.08	-149 to +651

7. Maximum Dynamic Pressure

Due to the basically northwest winds aloft which prevailed at liftoff, the dynamic pressure environment through which the vehicle flew was slightly less than anticipated. The maximum value of 728 psf occurred at a somewhat lower altitude due to the slightly high trajectory. A list of atmospheric and aerodynamic parameters existing at the time of maximum dynamic pressure appears in Table II-11.

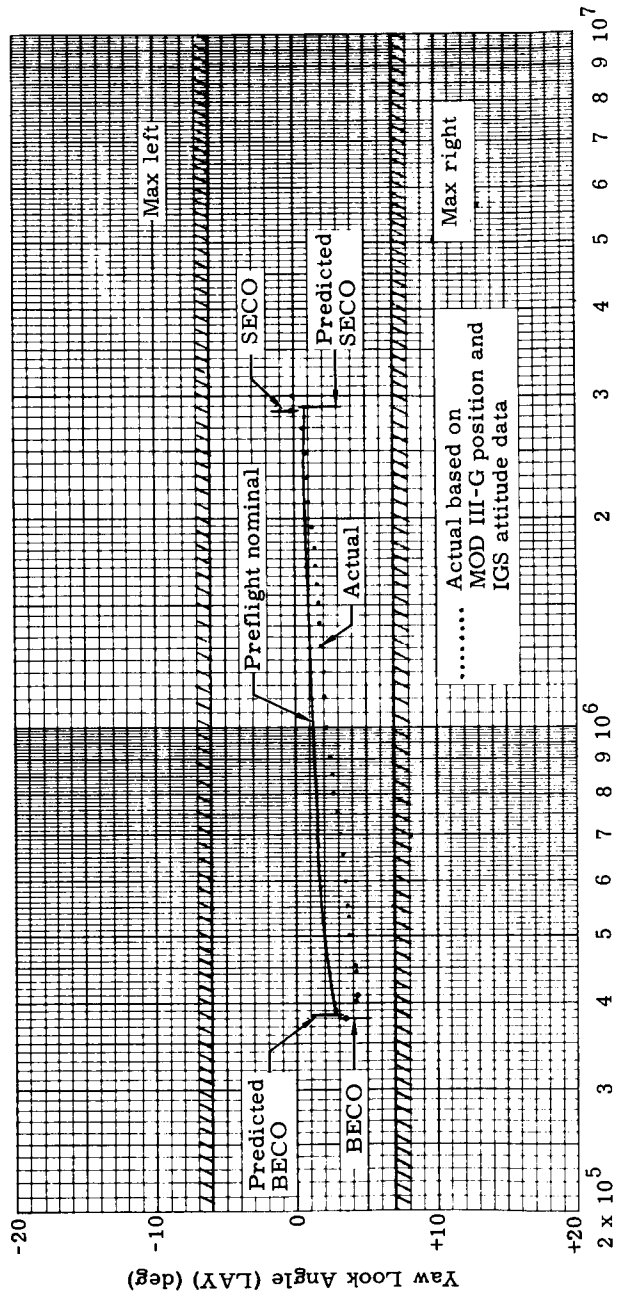

Fig. II-28. Permissible Yaw Look-Angle Envelope

TABLE II-11

Trajectory Parameters at Maximum Dynamic Pressure

Parameters	Planned nominal	Observed
Dynamic pressure (psf)	755	728
Time from liftoff (sec)	77.8	74.1
Mach number	1.72	1.56
Altitude (ft)	43,285	40,069
Relative flight path angle (deg)	51.74	54.54
Relative wind velocity (fps)	1,654	1,517
Wind velocity (fps)	0	72.5
Wind azimuth (deg from North)	--	317
Angle of attack (deg)	0.22	-0.86
Angle of sideslip (deg)	-0.03	-0.56

8. Angles of Attack and Sideslip

Predicted and actual histories of angle of attack and sideslip during the ascent are shown in Figs. II-12, II-13, II-20 and II-21. The predicted no-wind values were obtained from the GLV-4 45-day preflight report (Ref. 19), while the predicted values with wind were obtained from a prelaunch digital run utilizing the wind data obtained from the 0800 EST Rawinsonde sounding. Observed angles of attack and sideslip were derived using the Mod III-G radar position and velocity data, the IGS gimbal attitude data, and the wind speed and direction existing at the time of launch (Rawinsonde sounding 1777 at Cape Kennedy at 1021 EST).

The only significant deviation from the predicted nominal occurred shortly after start of closed-loop guidance when the RGS commanded a maximum 2 deg/sec nose-down pitching rate for 7 seconds to compensate for the off-nominal (high) BECO condition. A fairly large negative angle of attack logically resulted.

B. PAYLOAD CAPABILITY

Propellants remaining onboard after Stage II low level sensor uncover indicated that a burning time margin (BTM) of 2.017 seconds existed to a command shutdown. The total propellant weight margin was 673 pounds, and the corresponding GLV payload capability was

8598 pounds. These values and the predicted nominal and minimum values appear in Fig. II-19. The predicted payload capability curves were taken from the GLV-4 Preflight Report (Ref. 19); the predicted propellant weight and burning time margins are based on the difference between these curves and the 7868-pound spacecraft weight.

Final (real time) payload predictions differed from the predictions shown in Fig. II-29 due to (1) a 32-pound decrease in payload capability because jettisoning the spacecraft viewport and radar covers was delayed until SECO, and (2) extrapolated actual propellant temperatures were used instead of preflight predicted propellant temperatures. The last payload prediction indicated that the minimum payload capability was 62 pounds less than the spacecraft weight, and the nominal payload capability was 535 pounds greater than the spacecraft weight at the predicted launch time. The actual (postflight reconstructed) GLV payload capability was 730 pounds greater than the spacecraft weight. This can be attributed to the slightly off-nominal performance of a number of GLV components.

C. STAGING

Measured times of staging events (Table II-5) were within the times and tolerances predicted for this sequence with a Stage I fuel exhaustion shutdown. The time interval from staging signal ($87FS_2/91FS_1$) to start of Stage II engine chamber pressure (P_{c_3}) rise was 0.647 second. This compares favorably with the nominal expected time of 0.70 ± 0.08 second. Stage separation occurred 0.062 second following start of P_{c_3} rise; predicted time for this event with both the reconstructed P_{c_3} and the telemetered data was 0.055 and 0.065 second, respectively.

The time-distance relationship between the two stages during the staging process was established by using available telemetry data for engine thrusts and estimated values for vehicle weights, aerodynamic drag and the pressure force acting on Stage I. The thrust versus time histories used were derived from P_c data shown in Chapter III for Stage I shutdown and Stage II buildup (as recorded and as reconstructed with ignition transient spike from FM/FM telemetry data). Maximum stagnation pressure acting on the Stage I oxidizer tank dome was estimated to be 40 psia. Mass and aerodynamic drag values used were:

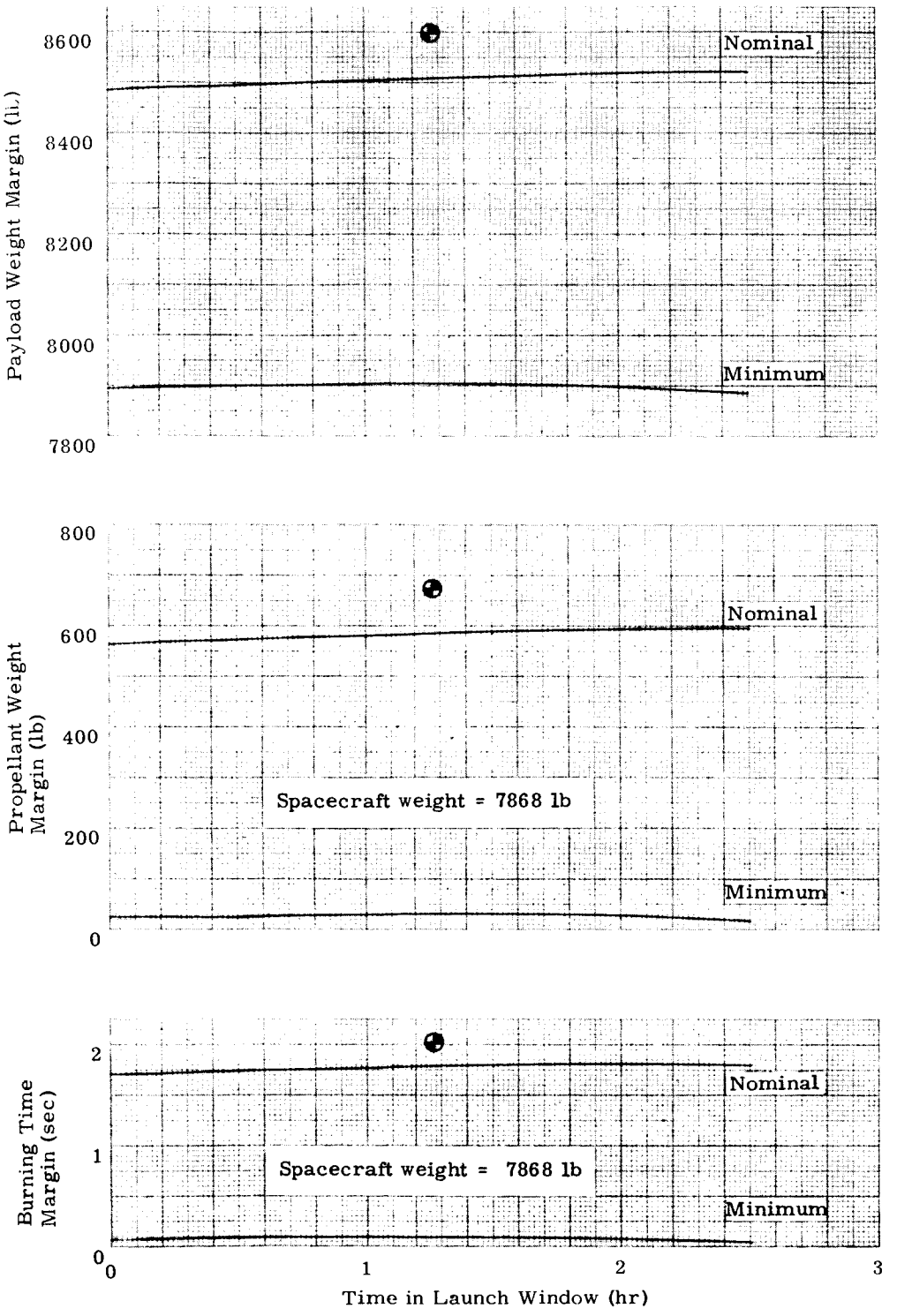

Fig. II-29. GLV-4 Payload Capability

Vehicle	Mass (slugs)	Aerodynamic Drag (lb_f)
Stage I	353	77
Stage II	2295	185

Results are shown in Fig. II-30, which is a plot of separation distance between the two stages as a function of time from P_{c_3} rise for the P_{c_3} obtained from telemetry data, and as reconstructed. This graph shows that eight feet of separation (distance required for Stage II engine nozzle to clear the Stage I ring frame at the separation plane) was reached in 0.420 second for the reconstructed P_{c_3} rise, and in 0.429 second for the measured P_{c_3} data. This time is approximately 0.170 second longer than that derived for GT-3. This difference is primarily due to the higher residual Stage I thrust on GT-4, typical of a fuel exhaustion shutdown.

As depicted in Fig. III-39, a shock overpressure of 69.5 psia was recorded by Meas 1085; to substantitate this pressure level, the reconstructed P_{c_3} rise rate $\left(\frac{(dp)}{dt}\right)$ was estimated to be approximately 66 psia/millisecond with a spike level of 770 psia.

Figure II-30 illustrates the occurrence times of the oxidizer lead, shock overpressure, ignition spike and step pressures as recorded by Meas 1085. Specific pressure values are noted in Fig. III-39.

D. WEIGHT STATEMENT

Table II-12 shows the GT-4 weight history from launch to orbital insertion.

The postflight weight report (Ref. 10) provides the background data for this summary. The report includes a list of dry weight empty changes at ETR and shows a derivation of weight empty from the actual vehicle weighing. Other items covered include the derivation of burnout, BECO, SECO and shutdown weights; weight comparisons with the BLH data; and the center-of-gravity travel envelope as a function of burn time for the horizontal, vertical and lateral planes.

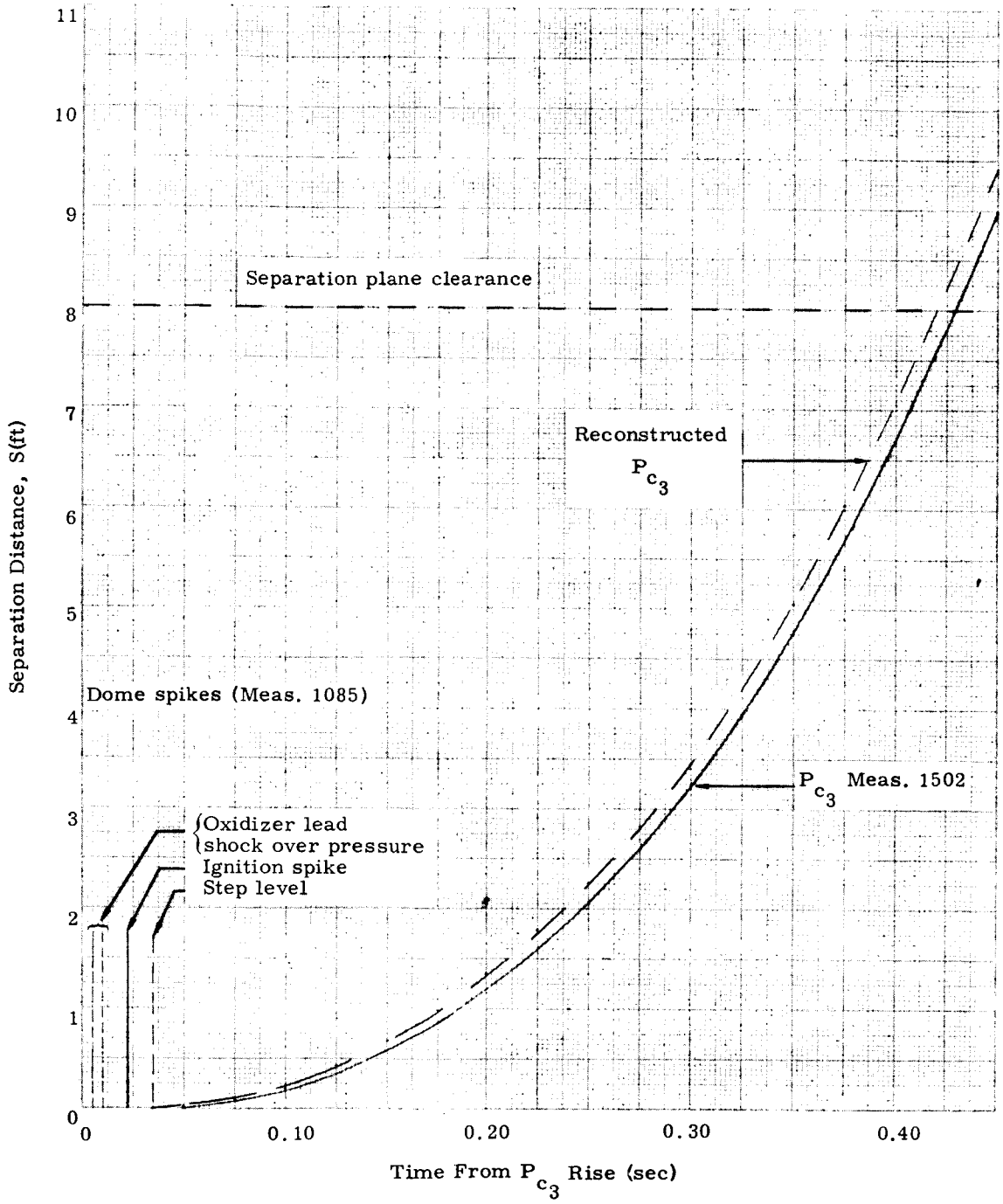

Fig. II-30. Estimated GT-4 Separation Distance Versus Time

TABLE II-12

GT-4 Weight Summary

	Step I	Step II	Step III	Stage Total
Loaded weight (lb)	271,803	66,068	7,868	345,749
Start and grain losses	-3,675			
Trajectory liftoff weight (lb)	268,128	66,068	7,868	342,064
Propellant consumed to BECO	256,235	11		
Coolant water			3	
Weight at BECO	11,893	66,057	7,865	85,815
Shutdown propellant	421			
Weight Stage I burnout	11,472	66,057	7,865	85,394
Stage II engine start	11,472	185		
Stage II liftoff		65,872	7,865	73,737
Propellant consumed to SECO		59,480		
Ablative and coolant water		20	4	
Stage II at SECO		6,372	7,861	14,233*
Shutdown propellant		142		
Weight at SECO +20 sec (lb)		6,230	7,861	14,091*

*Includes 673 lb usable propellant

III. PROPULSION SYSTEM

A. ENGINE SUBSYSTEM

The GLV-4 Stages I and II engines operated satisfactorily throughout the flight, and all test objectives were met. The Stage I burning time from $87FS_1$ was 155.702 seconds, and shutdown was initiated by fuel exhaustion. The Stage II engine operation was terminated by guidance command after 181.320 seconds of burning time.

Several minor anomalies occurred during the flight, none of which adversely affected engine or vehicle performance. These were as follows:

(1) The Stage II engine chamber pressure trace indicated double ignition spikes during the engine start transient.

(2) Measurement 0513 (Stage II engine fuel pressurant orifice inlet temperature) was unusually high after $91FS_1$ + 6 seconds. The probable cause for this abnormality was a leak or a restruction in the fuel coolant circuit of the autogenous gas cooler.

(3) Measurement 0520 (Stage II engine gas generator oxidizer injector pressure) decayed approximately 17.5 psi starting at $91FS_1$ + 160 seconds. The most probable cause of the pressure decay was an oxidizer leak in the gas generator feedline between the venturi and the injector.

(4) Two post-SECO perturbations were noted--one at SECO + 3.1 seconds and the other at SECO + 10.8 seconds. These disturbances were not reflected in engine parameters and were characteristic of the disturbances on previous Titan II and Gemini flights.

1. Stage I Engine (YLR87-AJ-7, S/N 1005)

a. Configuration and procedures

The GLV-4 Stage I engine incorporated one significant hardware change since GLV-3--the MDS/PMDS cable assemblies were modified to provide assemblies of small outside diameter dimensions. The gearboxes on engine S/N 1005 were hot fired with the engine during acceptance testing whereas the GLV-3 gearbox was a retrofit installation.

Additional procedures instituted for this launch were (1) to verify the torque values of engine "B" nut and bolted flange connections and (2) to recheck critical fittings for leaks.

b. Engine start transient

The S/A 1 and S/A 2 thrust chamber start transients were normal, as shown in Figs. III-1 and III-2. The ignition spikes reached 88% and 78% of rated thrust for S/A 1 and S/A 2, respectively, both above the engine model specification allowable of 75%. However, the GLV P_c instrumentation system has characteristically shown undamped oscillations which obscure the true transient performance indication and prevent the measured spike pressure from being representative of the actual pressure. Therefore, it is not possible to determine the exact values for the ignition spikes.

Significant engine start parameters are presented in Table III-1.

TABLE III-1

Stage I Engine Start Parameters

Parameter/Event	S/A 1	S/A 2
87FS$_1$ to initial P_c rise (sec)	0.74	0.77
P_c ignition spike (psia)	700	625
P_c step (psia)	440	420
P_c overshoot (psia)	None	None

c. Steady-state performance

Stage I engine flight performance agreed closely with the preflight predictions. Flight integrated average thrust and specific impulse were slightly higher than preflight predicted, and the mixture ratio shifted lower than predicted.

The engine performance was calculated from measured flight data using the Martin-Baltimore PRESTO program and the Stage I thrust coefficient relationship as modified by Martin. The latter modification increased thrust and specific impulse by approximately 3400 pounds and 2.0 seconds, respectively, above the values calculated with the Aerojet thrust coefficient relationship. The Martin modified thrust coefficient was also used in the preflight predictions.

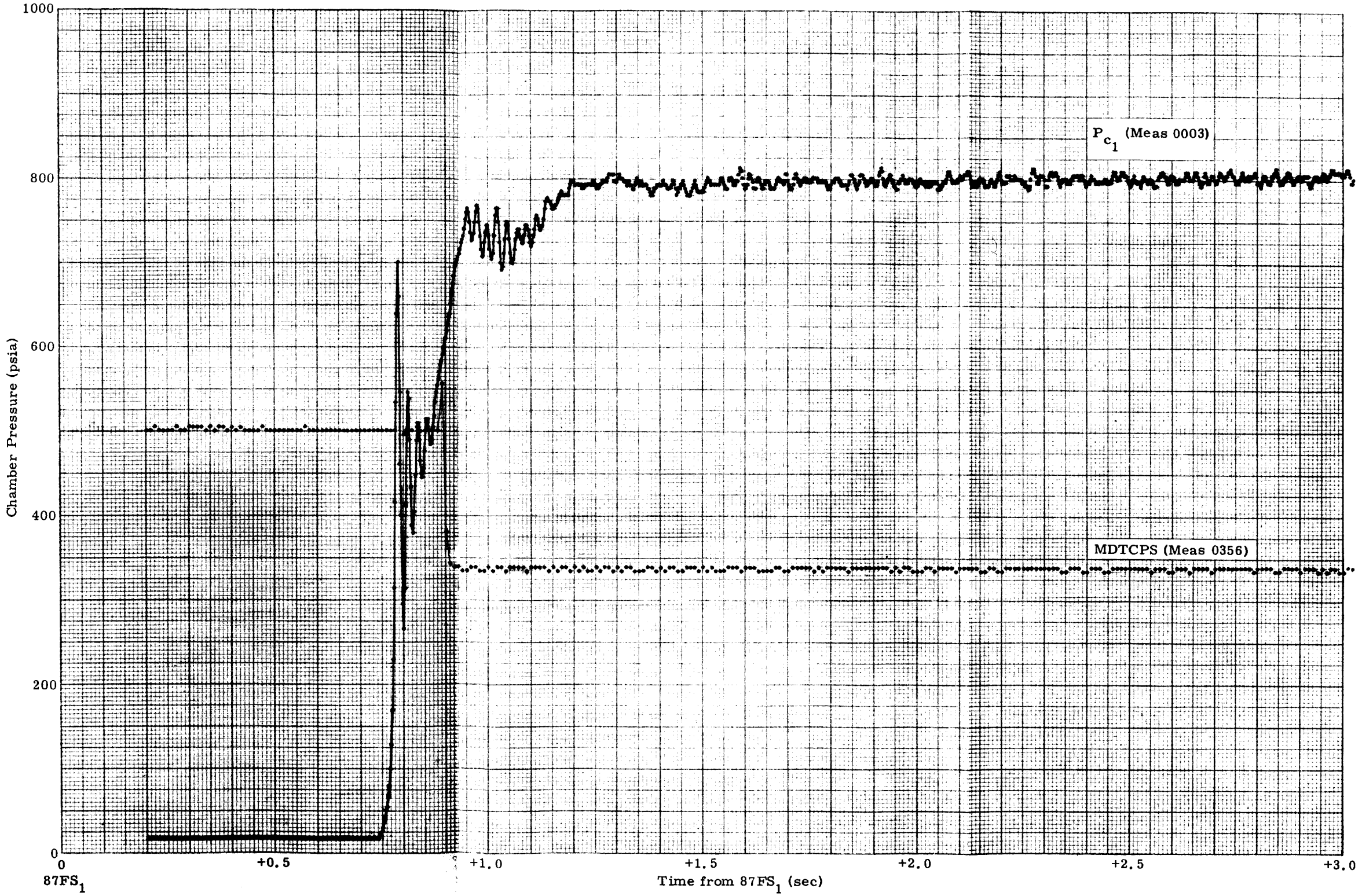

Fig. III-1. S/A 1 Start Transient

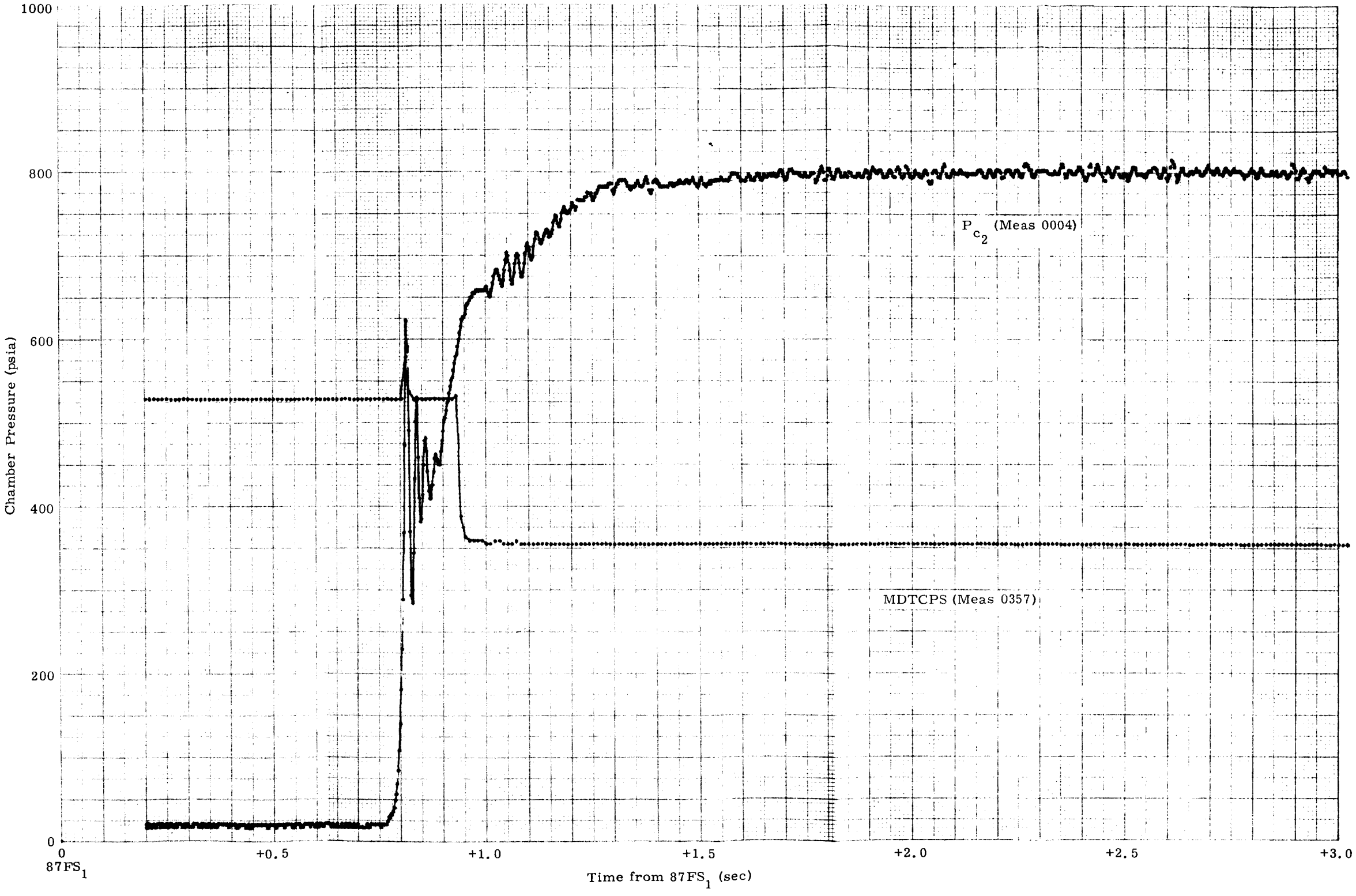

Fig. III-2. S/A 2 Start Transient

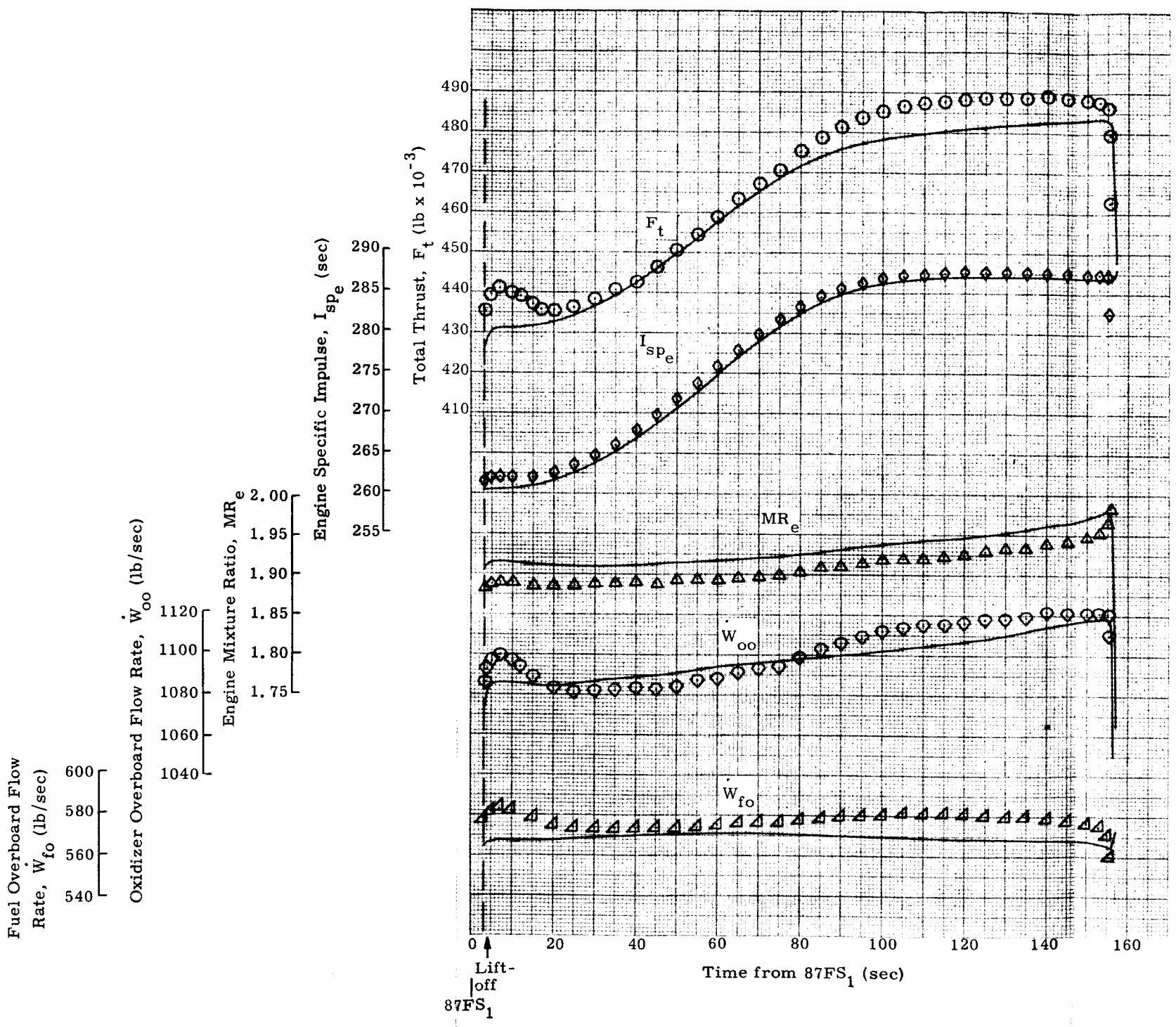

Average Engine Performance Integrated from Liftoff to $87FS_2$

Symbol	Preflight Prediction	Flight Average
F_t	463157.	467334.
I_{sp_e}	277.74	278.38
MR_e	1.9308	1.9097
$\dot{W}_{oo}$	1098.25	1101.49
$\dot{W}_{fo}$	569.32	577.30

——— Preflight prediction

Fig. III-3. Stage I Engine Flight Performance

The Stage I engine average flight performance, integrated from lift-off to $87FS_2$, is compared with the preflight prediction in Table III-2.

TABLE III-2

Predicted and Actual Stage I Engine Performance

Parameter	Preflight Predicted* (Average)	Flight* (Average)	Percent Difference
Thrust, engine (lb)	463,157	467,334	+ 0.90
Specific impulse, engine (sec)	277.74	278.38	+ 0.23
Mixture ratio, engine	1.9308	1.9097	- 1.09
Oxidizer flow rate, overboard (lb/sec)	1098.25	1101.49	+ 0.30
Fuel flow rate, overboard (lb/sec)	569.32	577.30	+ 1.40

*Based on Martin modified thrust coefficient relationship.

Calculated Stage I engine performance is presented in Fig. III-3. The preflight prediction is also shown for comparison.

Cyclic pressure oscillations, similar to those observed on GLV-1, GLV-2 and GLV-3, were present in the fuel discharge pressures (P_{fd}) of S/A 1 and S/A 2. The oscillations were not reflected in other measured parameters. The cause of these large P_{fd} oscillations has not been determined, although it is suspected that transducer vibration levels were amplified by the sensor mounting bracket.

Stage I engine flight performance calculated at the $87FS_1 + 57$ second time slice and corrected to standard inlet conditions appears in Table III-3. This is compared with acceptance test and the predicted flight performance at standard inlet conditions and the nominal time as used in the preflight prediction. The predicted flight performance at standard conditions was obtained by modifying the nominal acceptance test data for a 4850-pound acceptance-to-flight thrust growth, derived empirically from Titan II and GLV flight data.

TABLE III-3

Stage I Engine Performance Corrected to Standard Inlet Conditions at $87FS_1$ + 57 Seconds

Parameter	Acceptance Test*	Predicted Flight* (including 4850 pounds thrust growth)	Flight Performance*
Thrust, engine (lb)	437,331	442,181	440,937
Specific impulse, engine (sec)	261.05	261.05	261.53
Mixture ratio, engine	1.9495	1.9495	1.9246
Oxidizer flow rate, overboard (lb/sec)	1106.97	1119.25	1109.17
Fuel flow rate, overboard (lb/sec)	568.33	574.62	576.80

*Based on Martin modified thrust coefficient relationship.

The -1.28% shift in engine mixture ratio shown in Table III-3 was within the 3σ run-to-run repeatability of 1.38%.

d. Shutdown transient

Stage I engine shutdown was initiated by fuel exhaustion after a burn time of 155.702 seconds. Engine thrust at staging was approximately 57,800 pounds. The shutdown transient was normal for a fuel exhaustion. Significant parameters during shutdown are presented in Table III-4.

TABLE III-4

Stage I Engine Shutdown Parameters

Parameter/Event	S/A 1	S/A 2
Time from P_c decay to $87FS_2$ (sec)	0.22	0.21
P_c at $87FS_2$ (psia)	510	430
Time from $87FS_2$ to data dropout (sec)	0.71	0.71
P_c at data dropout (psia)	110	88

The Stage I engine shutdown characteristics (P_c) are presented in Figs. III-4 and III-5.

e. Engine malfunction detection system

The Stage I engine MDS operated satisfactorily throughout the flight. Engine MDS performance is shown graphically in Figs. III-1, III-2, III-4 and III-5; a discussion appears in Chapter X.

Table III-5 summarizes operation of the malfunction detection thrust chamber pressure switches (MDTCPS).

TABLE III-5

Stage I MDTCPS Operation

Switch	Actuation		Deactuation	
	Time (sec)	Pressure (psia)	Time (sec)	Pressure (psia)
$MDTCPS_1$	$87FS_1 + 0.88$	550	$87FS_2 - 0.04$	545
$MDTCPS_2$	$87FS_1 + 0.93$	580	$87FS_2 - 0.05$	530

f. Engine prelaunch malfunction detection system (PMDS)

All PMDS switches actuated within the specified actuation times and pressures as shown in Table III-6.

TABLE III-6

Stage I PMDS Switch Operation

	TCPS	OPPS	FPDPS
Actuation time			
Measured (sec)	$87FS_1 + 0.992$	$87FS_1 + 1.722$	$87FS_1 + 0.921$
Required (sec)*	$T_0 + 2.2$	$T_0 + 2.2$	$T_0 + 2.2$
Actuation pressure			
Measured (psia)	**	430	**
Required (psia)	600 to 640	360 to 445	46 to 79 (psid)

*Engine shutdown timers start from T-0; $87FS_1$ is 70 to 100 milliseconds after T-0.
**Not instrumented.

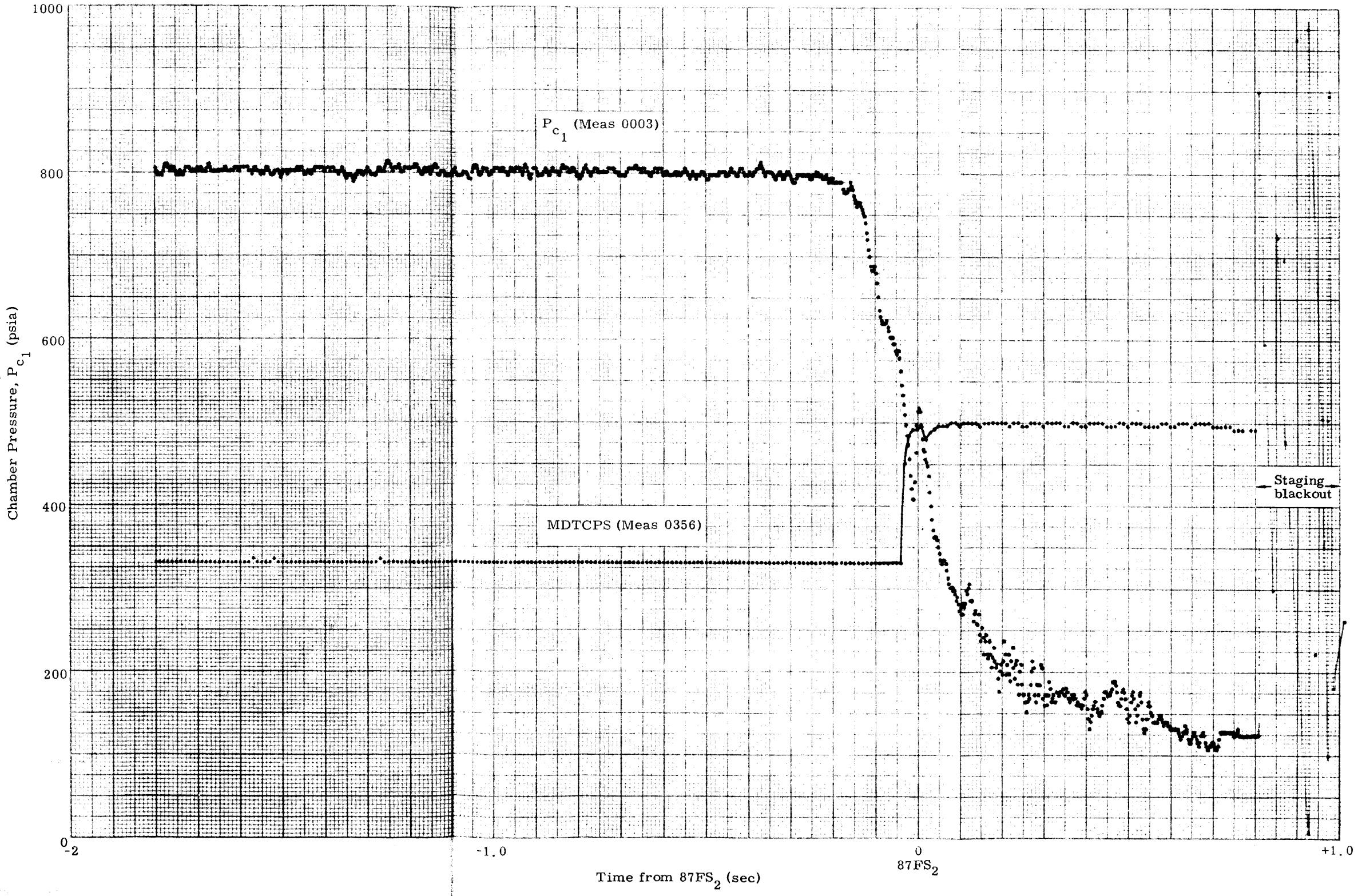

Fig. III-4. S/A 1 Shutdown Transient

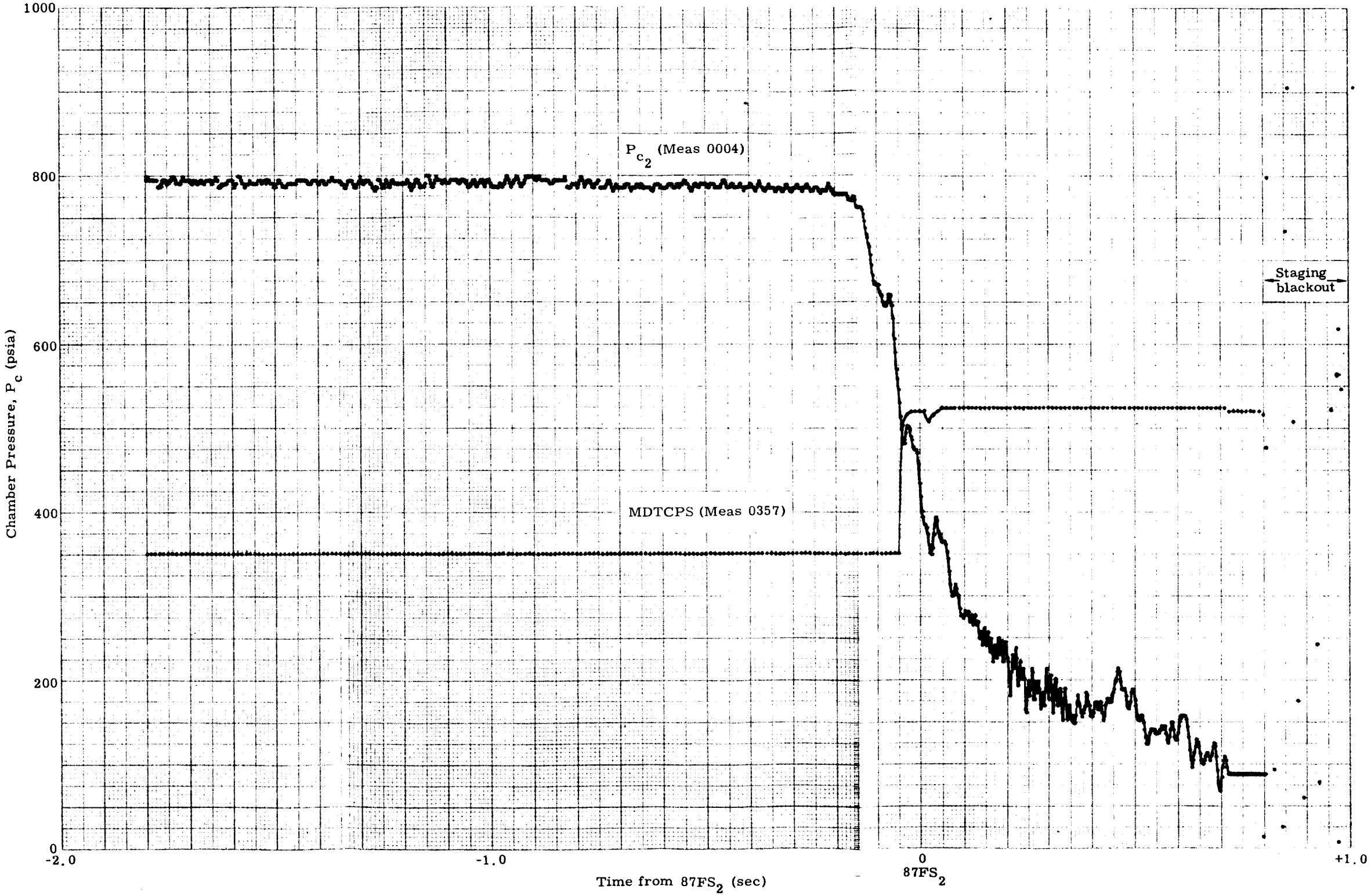

Fig. III-5. S/A 2 Shutdown Transient

2. Stage II Engine (YLR91-AJ-7, S/N 2003)

a. Configuration and procedures

The GLV-4 Stage II engine configuration was identical to that of GLV-3, and incorporated the redundant engine shutdown system (RESS), first employed on GLV-3.

Additional procedures instituted were (1) to verify the torque values of engine "B" nut and bolted flange connections and (2) to recheck critical fittings for leaks.

A special inspection was made of the turbine rotor to assure that weld repairs at the fir tree joints were proper.

b. Engine start transient

The start transient was normal except for a thrust chamber pressure double ignition spike (Fig. III-6). This phenomenon was never observed on Titan II or Gemini flights, although it has been noted in ground tests with no adverse effect on performance. The most probable cause of the double ignition spike indication was a localized detonation near the sensing port. The measured chamber pressure at this time was not representative of the thrust during the start transient. No problems were encountered on GLV-4 because of the double ignition spike.

Significant start events are summarized in Table III-7.

TABLE III-7

Stage II Engine Start Parameters

$91FS_1$ to P_c initial rise (sec)	0.65
P_c spike pressure, first spike (psia)	250
P_c ignition spike, second spike (psia)	805
P_c step pressure (psia)	500
P_c overshoot pressure (psia)	865

The gas generator oxidizer injector resistance (R_{OJGG}), as determined using the gas generator injector and turbine inlet pressures at $91FS_1$ + 5 seconds, was approximately 1170 units. This level is normal during flight, indicating a clean injector.

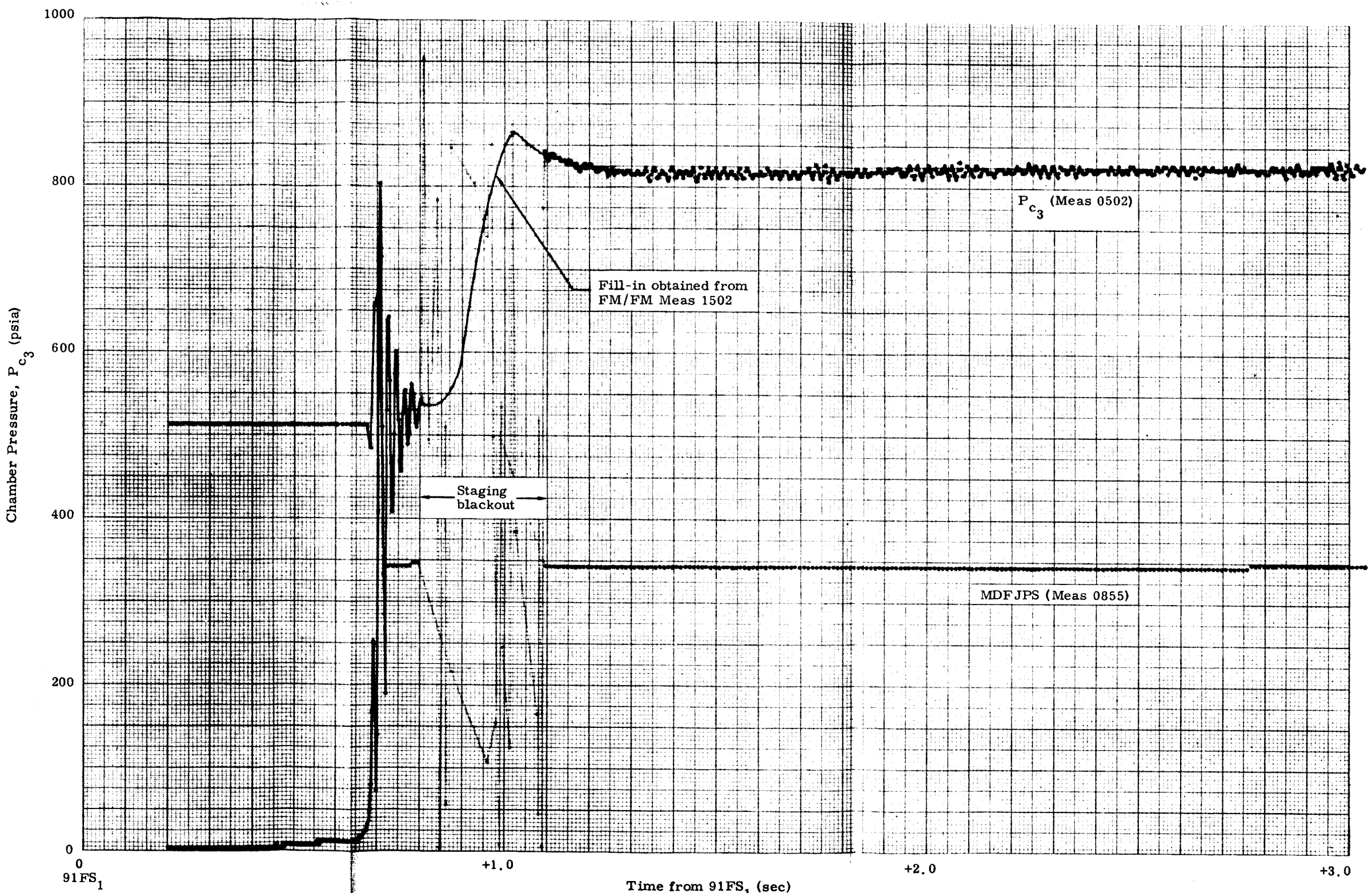

Fig. III-6. S/A 3 Start Transient

c. Steady-state performance

All Stage II engine flight performance parameters, integrated over steady-state operation, were within 1.0% of the preflight predicted performance. The average engine performance integrated from first steady-state to $91FS_2$ is compared to the preflight prediction in Table III-8.

TABLE III-8

Predicted and Actual Stage II Engine Performance

Parameter	Preflight Predicted Average	Flight Average	Percent Difference
Thrust, chamber (lb)	101,833	102,482	+0.64
Specific impulse, engine (sec)	311.32	310.37	-0.31
Mixture ratio, engine	1.7577	1.7595	+0.10
Oxidizer flow rate, overboard (lb/sec)	208.65	210.70	+0.98
Fuel flow rate, overboard (lb/sec)	118.44	119.50	+0.89

The engine steady-state flight performance, calculated using the Martin PRESTO program, is shown in Fig. III-7 for Stage II flight. The preflight prediction is also presented for comparison.

Two anomalies which were noted during steady-state operation of the Stage II engine are as follows:

(1) The gas generator oxidizer injector pressure (P_{OJGG}) began to decay at approximately $91FS_1$ + 160 seconds, and continued to decay throughout steady-state operation. The pressure decayed 13 psi in the first 7 seconds, and 4.5 psi in the final 14 seconds for a total pressure decrease of 17.5 psi. This decrease in P_{OJGG} had negligible effect on the overall engine operation. A reaction to the decreased pressure was not recorded on any other measured engine parameter. The most probable cause of the P_{OJGG} decay is that a leak developed in the oxidizer bootstrap circuit between the venturi and the

injector. The resultant effect was an estimated loss of approximately 6.5% (0.03 lb/sec) of the oxidizer flow to the gas generator.

(2) The fuel pressurant orifice inlet temperature (T_{FPOI}) increased abnormally high after approximately $91FS_1$ + 6 seconds. A low frequency oscillation existed throughout flight and the amplitude increased approximately 15 seconds before $91FS_2$. (Refer to Section C of this chapter for further discussion.)

Engine flight performance at the $91FS_1$ + 57 second time slice corrected to standard inlet conditions is shown in Table III-9. This is compared to the acceptance test and the predicted flight performance at standard inlet conditions, and the nominal time as used in the preflight prediction. The predicted flight performance at standard inlet conditions was obtained by adjusting the nominal acceptance test data for a 900-pound acceptance-to-flight thrust growth obtained from analysis of previous Titan II and GLV flights.

TABLE III-9

Stage II Engine Performance Corrected to Standard Inlet Conditions at $91FS_1$ + 57 Seconds

Parameter	Acceptance Test	Predicted Flight (including 900-lb thrust growth)	Flight Performance
Thrust, chamber (lb)	101,043	101,943	102,324
Specific impulse, engine (sec)	310.53	310.53	310.08
Mixture ratio, engine	1.7970	1.7970	1.7729
Oxidizer flow rate, overboard (lb/sec)	209.22	211.08	211.15
Fuel flow rate overboard (lb/sec)	116.17	117.21	118.84

d. Shutdown transient

Stage II engine shutdown was initiated by a guidance command after 181.32 seconds of burn time. The shutdown sequence included both

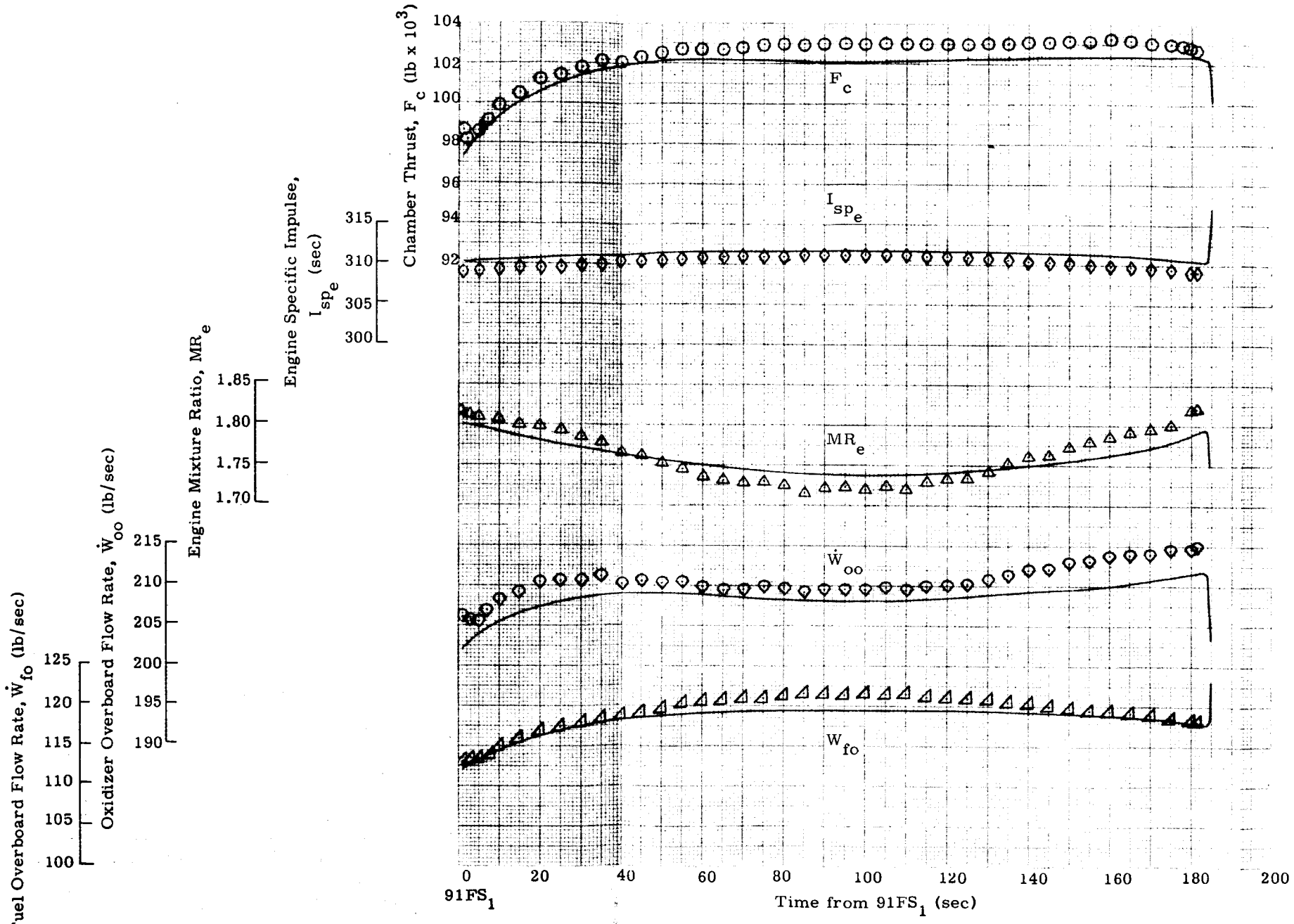

Average Engine Performance Integrated from First Steady-State to $91FS_2$		
Symbol	Preflight Prediction	Flight Average
F_c	101833.	102482.
I_{sp_e}	311.32	310.37
MR_e	1.7577	1.7595
$\dot{W}_{oo}$	208.65	210.70
$\dot{W}_{fo}$	118.44	119.50

——— Preflight prediction

Fig. III-7. Stage II Engine Flight Performance

the thrust chamber valve (TCV) and the redundant system as was used on GLV-3. The shutdown pressure transient is presented in Fig. III-8. The calculated engine shutdown impulse (including roll nozzle) from $91FS_2$ to $91FS_2$ + 20 seconds was 37,150 lb-sec as compared to the predicted value of 39,300 ± 7000 lb-sec. Calculations of the shutdown impulse utilized the ±10 g accelerometer data from $91FS_2$ to $91FS_2$ +0.685 second, and ±0.5 g accelerometer data from $91FS_2$ + 0.685 to $91FS_2$ + 20 seconds. The impulse determined from the ±10 g accelerometer was 26,800 lb-sec, and the impulse from the ±0.5 g accelerometer data was 10,350 lb-sec. Thrust tailoff is shown in Fig. III-9; an average vehicle weight of 14,092 pounds was used to construct this curve.

Perturbations were noted at $91FS_2$ + 3.1 seconds and $91FS_2$ + 10.8 seconds in the low level accelerometer data. Similar phenomena were observed during the Stage II thrust decay on GT-1, GT-2 and on numerous Titan II flights. The GT-4 disturbance was not observed in any of the measured engine parameters.

e. Engine malfunction detection system

The Stage II engine MDS operated satisfactorily throughout flight. Figures III-6 and III-8 illustrate the response times and engine chamber pressure correlation during the start and shutdown transients, respectively, of the malfunction detection fuel injector pressure switches (MDFJPS). The fuel injector pressure was not instrumented; therefore, actuation pressures are not available. A summary of the significant switch parameters is presented in Table III-10.

TABLE III-10

Stage II MDFJPS Operation

Actuation time (sec)	$91FS_1$ + 0.68
P_c at actuation (psia)	*
Deactuation time (sec)	$91FS_2$ + 0.16
P_c at deactuation (psia)	475

*P_c data invalid during chamber ignition.

[redacted]

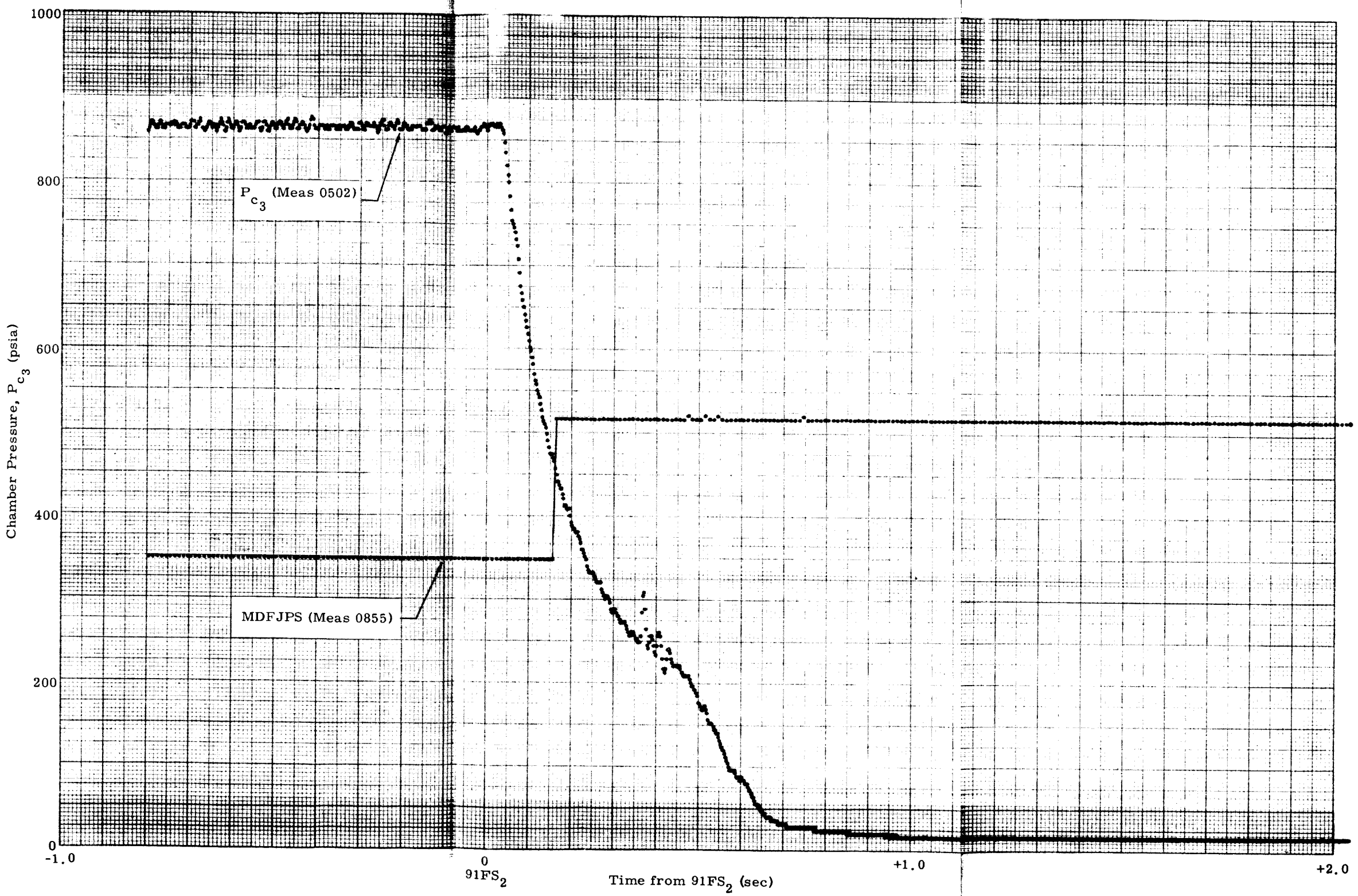

Fig. III-8. S/A 3 Shutdown Transient

ER 13227-4

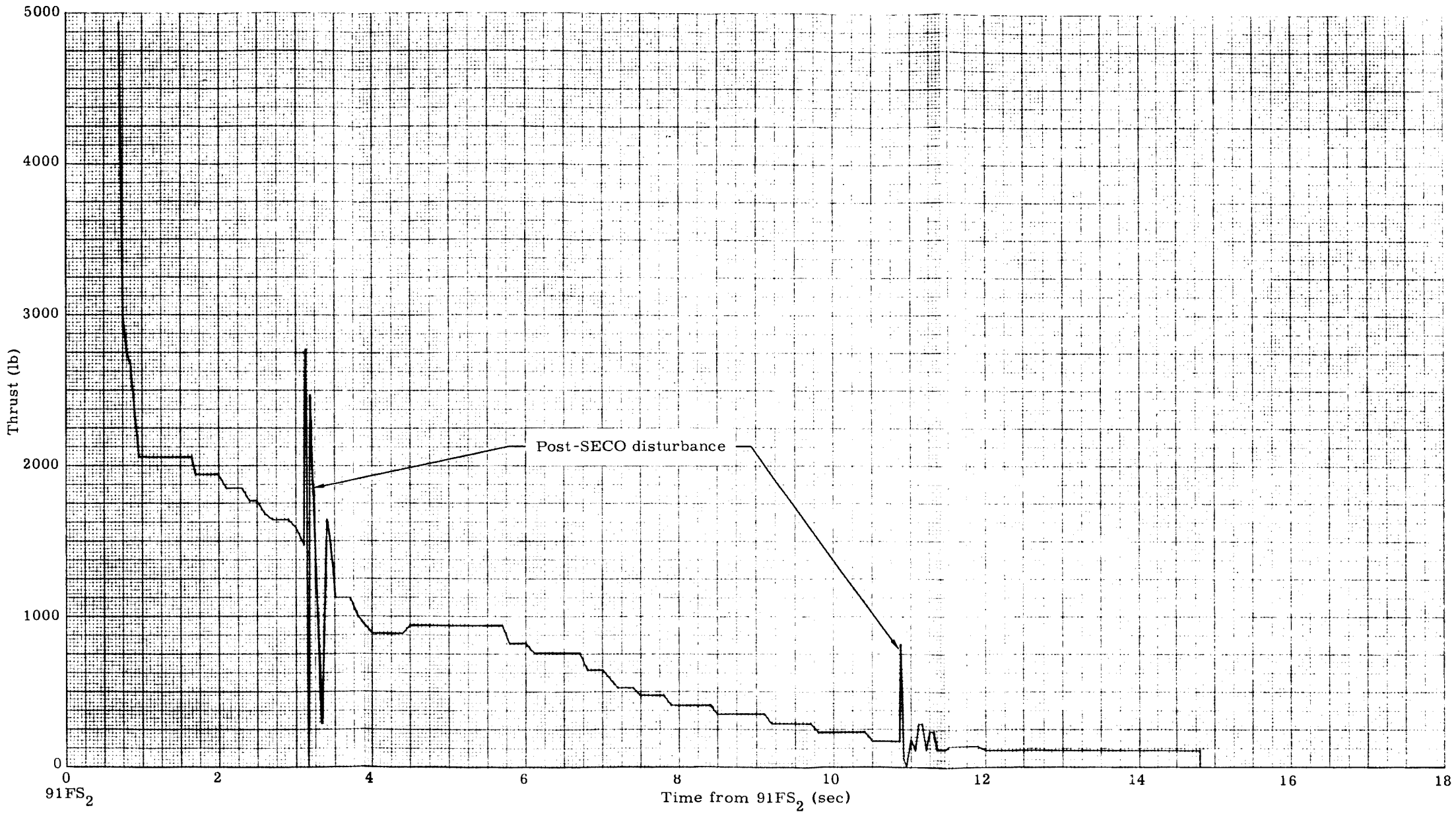

Fig. III-9. Stage II Engine Thrust Tail-Off

B. PROPELLANT SUBSYSTEM

1. Propellant Loading

a. Loading procedure

A number of problems were encountered during GT-4 propellant loading. These problems necessitated the performance of four loading operations (including that for launch). These operations were as follows:

Loading Operations	Description	Date
WMSL	Dual loading without prechill	5-12-65
First special loading	Separate loading with and without prechill on the Stage II fuel tank, with prechill on other three tanks	5-19-65
Second special loading	Separate loading of Stage II tanks using Stages I and II flowmeters	5-27-65
Launch	Dual loading similar to GLV-3 procedure	6-3-65

Propellant loading for the WMSL utilized two significant procedural revisions from the GLV-3 loading. Prechill was not used; nitrogen gas pressurization, rather than pumps, was used to move propellants from the RSV to the distribution unit level sensors. Important WMSL problems encountered are as follows:

(1) The fuel flowmeters were cross wired and caused incorrect totalizer operation.

(2) The difference between the flowmeter load and Hi-lite nominal (tab run) load was out of tolerance for each tank.

(3) Automatic pump shutoff did not occur when the Stage I oxidizer reached mission load.

(4) Normal fill procedures for Stage II fuel resulted in a flow back into the RSV when the pump was stopped.

(5) The Stage II fuel blanket pressure was 3 psi over nominal regulator setting.

The first problem resulted in an aborted fuel loading, but was corrected in time to continue the WMSL. A wiring installation change will be incorporated, effective for GLV-6 and up, so that cross wiring of either flowmeter set will be impossible.

The details of the second problem are reflected in Table III-13. All differences were negative (i. e., flowmeter less than tab run) and outside the 0.30% tolerance. Mission load was established in each case by using the "K" factor/ratio method. The four flowmeters used in the GT-4 WMSL were those used for the GT-3 launch loading, where all four read within the allowable tab run limits.

The third and fourth WMSL problems were the result of a misaligned digit on the primary totalizer and an inoperative check valve (CV 171), respectively. Both malfunctions were verified by failure analysis. A new check valve was installed after the WMSL; however, the totalizer remained in the system for all GLV-4 loading operations. All totalizers will be refurbished prior to loading GLV-5 to preclude further occurrence of the pump shutdown problem. In addition, the procedure now calls for manually stopping the pumps when the preset load is reached.

The fifth WMSL problem was due to an improper setting of hand loader No. 247. The correct pressure of 6 psig was obtained by a readjustment.

As a result of the WMSL problems, a special loading test was performed. The results of this test are shown in Table III-13. Prechill was reinstated in the procedures for all tanks because of its unknown effect on flowmeter automatic temperature compensator (ATC) response. In addition, Stage II fuel was first loaded without a prechill procedure in order to assess prechill effect. Loading without a prechill evidently contributes an error of approximately -0.1%. Other than the indicated discrepancy between flowmeter and Hi-lite loadings, no problems were experienced during the first special loading exercise. On the basis of the WMSL and first special loading, it was concluded that no major problem existed with the Stage I tanks, and that the Stage II flowmeters should be check-calibrated before a further plan was established. The Stage II oxidizer flowmeter (S/N 199173) was check-calibrated at Wyle Laboratories and found to have an error of -0.02%. The Stage II fuel flowmeter (S/N 199170) was check-calibrated at Martin-Denver and found to have an error of -1.4%. On the basis of these check calibrations and the first two loading operations, it was apparent that Stage II oxidizer tanking represented an unresolved problem.

A second special loading exercise was conducted on 27 May with new Stage II flowmeters installed. The results of this loading are shown in Table III-13. Other than the discrepancy indicated between the Hi-lite versus flowmeter data accumulated for the Stage II oxidizer tank on the three loading operations, no problems occurred. To resolve the problem in preparation for launch, the Stage I oxidizer flowmeter (S/N 199168) and Stage II oxidizer flowmeter (S/N 199167) were sent to Wyle Laboratories for calibration checks. The Stage I flowmeter had an error of -0.1366%; this meter was always in the system. The Stage II

flowmeter had an error of +0.4715%. Evidently, the Stage II flowmeter (S/N 199167) was not in calibration when installed after the first special loading exercise.

On the basis of results accumulated to this time, the plan for launch was made by postulating that the Hi-lite volumes and original tab runs were correct for both Stage I tanks and for the Stage II fuel tank. The calibration data for the Stage II oxidizer tank were concluded to be in error and a new tab run was prepared for this tank. The Stage II oxidizer Hi-lite volume for launch was constructed 0.74% less than the value used for WMSL. The Hi-lite/flowmeter problems of the three loadings prior to launch were attributed to the flowmeters and an incorrect Stage II oxidizer tank calibration.

The launch loading results are presented in Table III-13. The Stages I and II oxidizer systems had new flowmeters installed. The Stage II fuel loading was out of tolerance at Hi-lite, and mission load was accomplished by using the "K" factor/ratio method. The out-of-tolerance condition has been attributed to the flowmeter ATC assembly, because the validity of the Hi-lite volume had been established with considerable confidence.

The launch loading operation involved one other problem; it was identical to Problem No. 4 of the WMSL loading. The normal fill procedure for Stage II fuel resulted in a flow back out of the propellant tank into the RSV when the pump was stopped for the 4000-pound leak check. The problem was attributed to a faulty check valve (CV 171) as in the WMSL, and loading of Stage II fuel was successfully continued by using an alternate procedure. The check valve used in the launch was subjected to failure analysis and a piece of metal was found on the sealing surface.

The launch propellant loading events are presented in Table III-11.

TABLE III-11

GT-4 Propellant Loading Schedule

	Stage I Oxidizer	Stage I Fuel	Stage II Oxidizer	Stage II Fuel
Start (hr EST)	2058*	2333*	2058*	2333*
Hi-lite (hr EST)	2228*	0032**	2144*	0051**
Load complete (hr EST)	2237*	0050**	2158*	0106**

*2 June 1965.
**3 June 1965.

The discrepancies between Hi-lite and flowmeter readings, which appeared throughout the GT-4 loadings, have resulted in the following suggestions:

(1) Steps be taken to assure more confidence in tank calibration data

(2) More engineering controls be applied to the flowmeters, including additional and expanded calibrations of the flowmeter and ATCs

(3) The first propellant loading operation be conducted as soon as possible after the erection of the launch vehicle.

The flowmeters used in the GT-4 launch loading were check-calibrated after the mission, with the results shown in Table III-12.

TABLE III-12

Flowmeter Calibrations--Postlaunch

System	Flowmeter S/N	Check Calibration Facility	Apparent Error of Flowmeter Assembly at Launch (%)
Stage I oxidizer	202164	Wyle Laboratories	+0.104
Stage I fuel	199169	Martin-Denver	-0.180
Stage II oxidizer	204277	Wyle Laboratories	+0.169
Stage II fuel	199171	Martin-Denver	-0.036

b. Propellant load verification

Data from the four propellant loading operations are presented in Table III-13. The data compare indicated flowmeter loads at Hi-lite with tab run Hi-lite values obtained from tank calibrations. In the second special loading, flowmeter readings were corrected wherever flow rates were at off-nominal conditions. Stage II oxidizer Hi-lite value (tab run value) was revised for the launch loading on the basis of information gained during the first three loading exercises.

TABLE III-13

Summary of Propellant Load Verification

Loading Event	Tank	Flowmeter Serial	Flowmeter Stage	Prechill	Hi-Lite Temperature (° F)	Indicated Flowmeter Load (lb)	Hi-Lite Nominal Load (lb)	Difference Between Flowmeter and Hi-Lite Loaded (%)	Allowable Difference (%)
WMSL	Stage I oxidizer	199168	I	No	33.8	158,730	159,234	-0.317	0.30
	Stage I fuel	199169	I	No	32.8	80,430	80,750	-0.396	0.30
	Stage II oxidizer ③	199173	II	No	36.0	26,500	26,771	-1.012	0.30
	Stage II fuel	199170	II	No	36.1	19,850	20,187	-1.670	0.30
First special loading	Stage I oxidizer	199168	I	Yes	33.5	158,930	159,297	-0.230	0.30
	Stage I fuel	199169	I	Yes	34.3	80,460	80,687	-0.281	0.30
	Stage II oxidizer ③	199173	II	Yes	35.6	26,540	26,782	-0.904	0.30
	Stage II fuel	199170	II	No	36.1	19,900	20,187	-1.422	0.30
	Stage II fuel	199170	II	Yes	36.4	19,900	20,182	-1.397	0.30
Second special loading	Stage II oxidizer ③	199167	II	Yes	36.3	26,710	26,761	-0.191	0.30
	Stage II ozidizer ③	199168	I	Yes	36.9	26,538 ②	26,750	-0.793	0.30
	Stage II fuel	199171	II	Yes	36.1	20,150	20,187	-0.183	0.30
	Stage II fuel	199169	I	Yes	38.0	20,110 ②	20,166	-0.278	0.30
Launch	Stage I oxidizer	202164	I	Yes	32.1	159,360	159,487	-0.0797	0.30
	Stage I fuel	199169	I	Yes	32.6	80,540	80,770	-0.285	0.30
	Stage II oxidizer ①	204277	II	Yes	33.1	26,640	26,637 ①	+0.0113	0.30
	Stage II fuel	199171	II	Yes	34.7	20,120	20,202	-0.406	0.30

NOTES:

① Revised tab run.

② Adjusted for flow rate.

③ Calibration at Martin-Denver (12-30-64).

c. Total propellant load

Total mission loads for the launch, as determined by the flowmeters, are shown in Table III-14. All flowmeter totalizer readings were corrected by subtracting propellant vaporized, and that remaining in the fill lines. The flight operation afforded additional data for comparison because the flowmeters were check-calibrated following launch. Corrected flowmeter loads were obtained by applying the check calibration results with the flowmeter indicated readings.

TABLE III-14

Summary of Mission Loads

Tank	Flowmeter Indicated (lb)	Corrected Flowmeter (lb)	Requested (lb)
Stage I oxidizer	172,072	171,893	172,084
Stage I fuel	89,721	89,882	89,732
Stage II oxidizer	38,515	38,450	38,515
Stage II fuel	22,025*	22,026*	22,043

*Load out of tolerance at Hi-lite; data calculated by adding Hi-lite volume equivalent load and flowmeter topping load.

d. Flight verification of propellant loads

The total propellant loads as determined by flight verification are shown in Table III-15. The flight verification loads were calculated from a propellant inventory, using actual level sensor uncover times and tank calibration data to determine flow rates. Total, integrated, inflight, overboard propellant consumption was found using the engine analytical model. All transient propellant consumptions and pressurization gas weights were calculated from flight data (Tables III-16 and III-17).

The differences presented in Table III-15 represent the best estimate of how reconstruction from flight data compares with preflight information. Excellent agreement was obtained for both Stage I tanks; however, the Stage II results were unsatisfactory since Stage II differences were considerably greater than the loading tolerance of 0.35%. The corrected flowmeter values for Stage II are believed to be representative of the actual load to within 0.2% since flowmeter loads can be correlated with Hi-lite tank volumes based on the five loadings of the Stage II tanks.

The discrepancies for Stage II are believed to be due to the errors associated with calculating postflight out-of-tank flow rates. Several areas of investigation are being pursued, including flow rate errors in the time period from $91FS_1$ to high-level sensor uncover, volume between outage and high-level sensor, and flow rates from outage sensor uncover time to $91FS_2$. Tracking data will be used as a check on the reconstructed flow rates.

TABLE III-15

Flight Verification of Total Propellant Load

a. Comparison of Flight Verification Load with Requested Load			
Tank	Flight Verification Load (lb)	Requested Load (lb)	Difference (%)
Stage I oxidizer	172,085	172,084	0
Stage I fuel	89,926	89,732	+0.113
Stage II oxidizer	38,656	38,515	+0.366
Stage II fuel	22,100	22,043	+0.259
b. Comparison of Flight Verification Load with Corrected Flowmeter Loads			
Tank	Flight Verification Load (lb)	Corrected Flowmeter Load (lb)	Difference (%)
Stage I oxidizer	172,085	171,893	+0.112
Stage I fuel	89,926	89,882	+0.049
Stage II oxidizer	38,656	38,450	+0.535
Stage II fuel	22,100	21,986*	+0.520

*Actual flowmeter corrected reading irrespective of Hi-lite volume out-of-tolerance condition.

TABLE III-16

Stage I Constructed Propellant Loading

Predicted inflight engine mixture ratio		1.931	±1.17%
Average inflight mixture ratio (engine)		1.9097	±1.71%
Outage (percent of total usable propellants)		0.239% oxidizer	
	Oxidizer (lb)	Fuel (lb)	Total (lb)
Nonusable propellants			
A. Fuel bleed	0	11	11
B. Start consumption ($87FS_1$ to TCPS)	204	40	244
C. Holddown (TCPS to blow bolts (2 sec))	2,210	1,201	3,411
D. Trapped above interface at shutdown	0	95	95
E. Trapped below interface at shutdown	235	309	544
F. Vapor retained at shutdown			
1. For pressurization			
a. Oxidizer tank	324	0	324
b. Fuel tank	7	97	104
2. Vaporized	8	0	8
G. Total nonusable	2,988	1,753	4,741
Usable propellants			
A. Steady-state overboard (blow bolts to $87FS_2$)	168,122	88,113	256,235
B. Shutdown transient ($87FS_2$ to 0% thrust)	361	60	421
C. Outage	614		614
D. Total usable	169,097	88,173	257,270
Total propellant loaded	172,085	89,926	262,011
Propellant load at liftoff	169,675	88,685	258,360
Weight of initial pressurizing gas			
A. Fuel tank (N_2)			9
B. Oxidizer tank			
1. N_2			8
2. NO_2			9

TABLE III-17

Stage II Constructed Propellant Loading

Predicted inflight engine mixture ratio		1.758	±2.52%
Average inflight mixture ratio (engine)		1.7536	±1.55%
Outage (percent of total usable propellants)		±0.264% fuel	
Burning time margin		2.016 seconds	
	Oxidizer (lb)	Fuel (lb)	Total (lb)
Nonusable propellants			
A. Fuel bleed		11	11
B. Trapped above interface at $91FS_2$+20 sec (0% thrust)	0	0	0
C. Trapped below interface at $91FS_2$+20 sec (0% thrust)	20	14	34
D. Vapor retained after $91FS_2$			
1. Pressurization (fuel tank)	4	49	53
2. Vaporization (oxidizer tank)	21	0	21
E. Total nonusable	45	74	119
Usable propellants			
A. Start consumption ($91FS_1$ to 90% thrust)	131	51	182
B. Steady-state overboard (90% thrust to $91FS_2$)	37,967	21,513	59,480
C. Shutdown consumption ($91FS_2$ to 0% thrust)	79	63	142
D. Steady-state residuals (after $91FS_2$)			
1. Burning time margin	434	239	673
2. Outage		160	160
E. Total usable	38,611	22,026	60,637
Total propellants loaded	38,656	22,100	60,756
Weight of initial pressurizing gas			
A. Fuel tank (N_2)			5
B. Oxidizer tank			
1. N_2			20
2. NO_2			11

2. Propellant Temperature

a. Weather

A comparison of the F-45 day prediction, the F-1 day prediction, and the actual weather for the 3 June launch of GT-4 appears in Table III-20. The F-45 day prediction was based on weather for a June through September hot day. The F-1 day prediction was not in good agreement with the actual F-day weather. Predicted average dew point was 15% high and predicted average windspeed was 67% high.

b. Ready storage vessel temperature

The requested and actual ready storage vessel (RSV) temperatures are shown in Table III-18.

TABLE III-18

RSV Temperature

Propellant System	Meas	Requested Temperature (° F)	Actual Temperature (° F)
Fuel	4425	30.1	30.3
Oxidizer	4426	28.0	27.6

c. Flowmeter temperature

The propellant heating program predicts the temperature rise from the RSV to the flowmeter at the end of the precooling cycle. For GLV-4, the temperature rise was 1.8° F for oxidizer and 1.6° F for fuel.

The predicted and the actual flowmeter temperatures that occurred at the end of the precooling cycle are shown in Table III-19.

TABLE III-19

Propellant Temperature at Flowmeter

System	Meas	Predicted Temperature (° F)*	Actual Temperature (° F)	ΔTemperature (° F)
Stage I fuel	4431	31.9	31.3	0.6
Stage II fuel	4432	31.9	31.1	0.8
Stage I oxidizer	4433	29.4	29.7	+0.3
Stage II oxidizer	4434	29.4	29.2	-0.2

*Predicted temperature = RSV temperature actual plus predicted temperature rise between RSV and flowmeter.

TABLE III-20

Predicted and Actual Weather Conditions for GT-4 Launch

Time (hr EST)	Dry Bulb Temperature (° F)			Dew Point Temperature (° F)			Wind Speed (kn)			Cloud Cover		
	F-45 Day	F-1 Day	Actual	F-45 Day	F-1 Day	Actual	F-45 Day	F-1 Day	Actual	F-45 Day	F-1 Day	Actual
6-2-65												
1800	86.2			78.9			10			0.5		
1900	84.8			78.3			8			0.5		
2000	83.4			77.7			6			0.5		
2100	82.4	79	77.2	77.3	65	60	6	12	5	0.5	0.4	0.1
2200	81.4		77.0	76.7		59	7		9	0.5		0.1
2300	80.6		77.1	76.4		57	7		7	0.4		0.3
2400	80.0	78	77.3	76.0	66	56	7	10	5	0.2	0.2	0.2
6-3-65												
0100	79.6		76.5	75.8		55	7		2	0.2		0.1
0200	79.2		75.7	75.6		56	7		3	0.2		0.1
0300	78.8	78	74.1	75.4	67	56	7	6	0	0.4	0.2	0.3
0400	78.4		75.2	75.2		57	7		5	0.4		0.2
0500	78.0		75.7	75.0		56	6		8	0.4		0.3
0600	80.0	77	70.6	76.1	67	61	6	5	8	0.4	0.3	0.2
0700	82.4		73.7	77.5		62	7.5		4	0.4		0.1
0800	84.2		76.6	78.3		58	9		5	0.4		0
0900	85.9	80	76.0	78.9	68	58	10	8	4	0.4	0.5	0.1
1000	87.5		76.6	79.6		59	10		4	0.6		0.2
1100	88.6		76.6	80.1		60	10		6	0.6		0.3
1200	89.2	82	75.7	80.5	69	61	10	10	6	0.6	0.5	

The correlation of predicted and actual temperatures was good, the difference being partly attributable to weather changes.

The propellant temperature rise during the loading operation caused by the heat input from pump work is the difference between the flowmeter and RSV temperatures at the time that Hi-lite is achieved. The temperature rise that occurred during the GT-4 loading operation is shown in Table III-21.

TABLE III-21

Propellant Temperature Rise During Loading

System	Flowmeter Temperature (° F)	RSV Temperature (° F)	Temperature Rise (° F)
Stage I fuel	32.1	31.2	0.9
Stage II fuel	32.8	31.4	1.4
Stage I oxidizer	32.6	30.5	2.1
Stage II oxidizer	32.2	29.2	3.0

The RSV and flowmeter temperatures recorded during loading are shown in Figs. III-10 and III-11.

d. Hi-lite temperature

The requested and actual propellant temperatures at the time of high-level sensor covering are presented in Table III-22.

TABLE III-22

Propellant Temperature at Hi-Lite

System	Meas	Requested Temperature (° F)	Actual Temperature (° F)	Δ Temperature (° F)
Stage I fuel	4124	32.1	32.7	+0.6
Stage II fuel	4601	33.3	34.7	+1.4
Stage I oxidizer	4128	30.8	32.2	+1.4
Stage II oxidizer	4604	32.7	33.1	+0.4

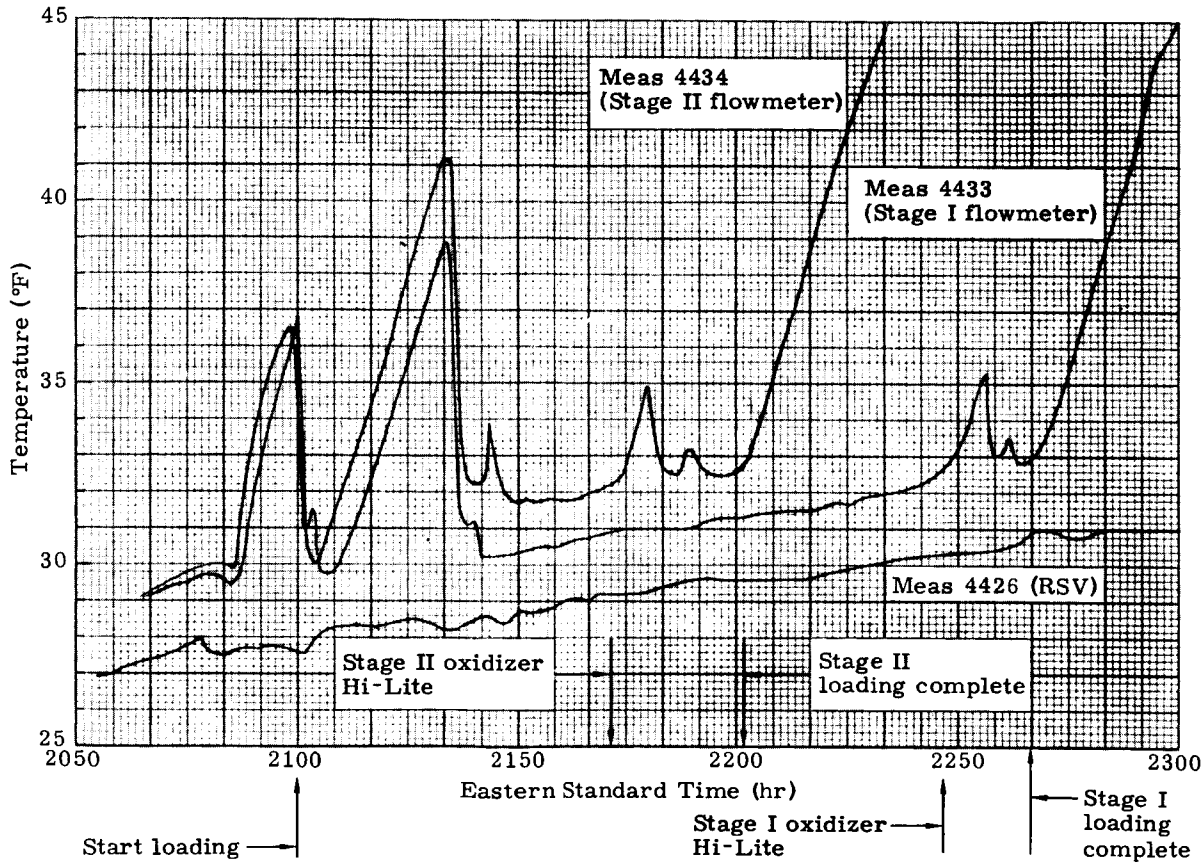

Fig. III-10. Oxidizer Temperatures During Loading

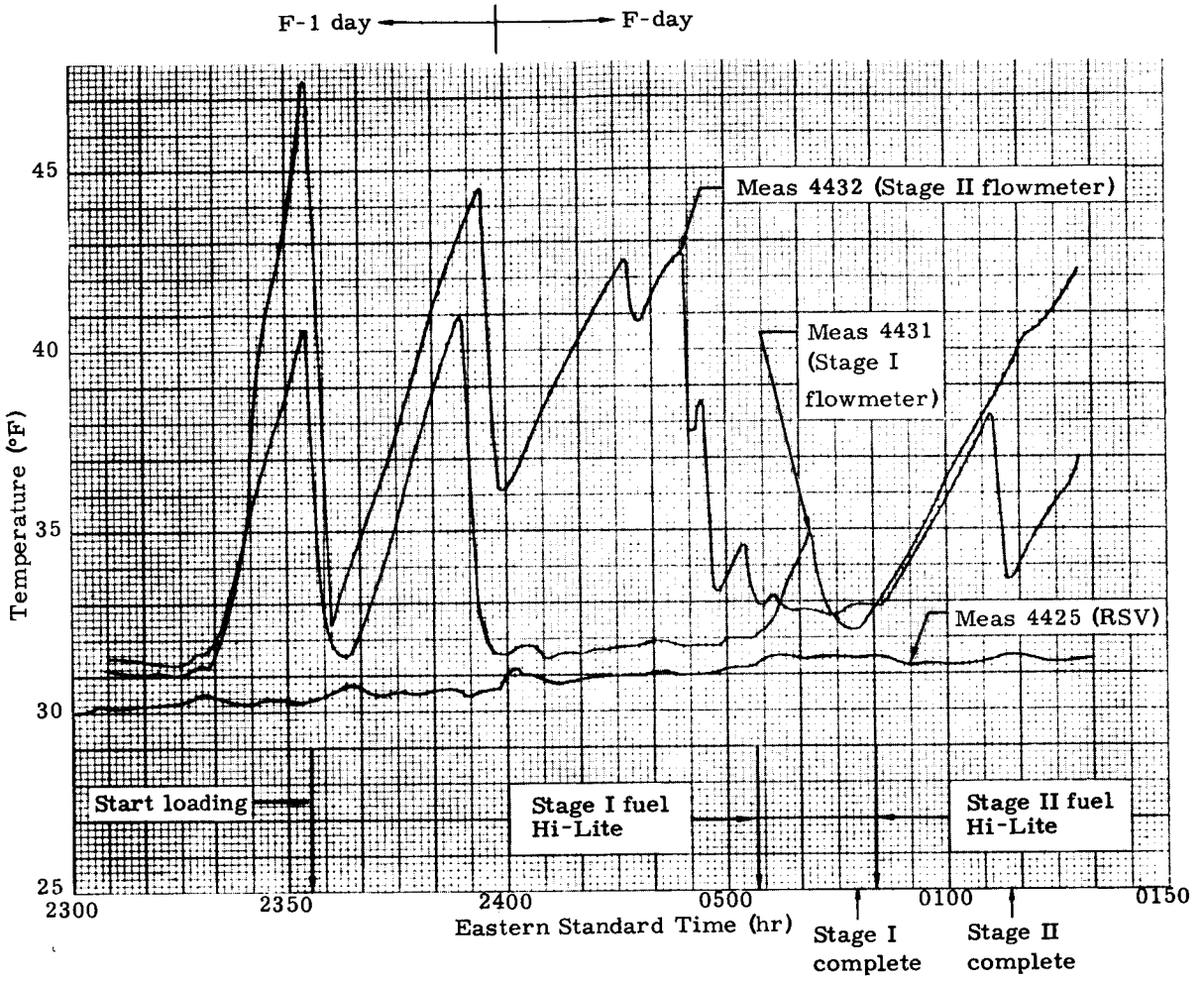

Fig. III-11. Fuel Temperature During Loading

The actual Hi-lite temperatures were within the ±2° F tolerance placed on the requested values.

e. Liftoff temperature

The propellant bulk temperatures at liftoff are shown in Table III-23. Predicted temperatures are also included.

TABLE III-23

Propellant Bulk Temperatures at Liftoff

Tank	F-45 Day Temperature Prediction (°F)	F-1 Day Temperature Prediction (°F)	Actual Temperature (°F)	Reconstructed Temperature (°F)
Stage I fuel	44.3	45.4	44.1	41.9
Stage II fuel	42.4	43.6	42.8	42.4
Stage I oxidizer	47.1	49.0	45.5	45.9
Stage II oxidizer	48.4	49.8	45.9	46.9

The reconstructed temperatures were obtained by factoring the actual weather and Hi-lite temperatures into the propellant heating program. The position of these temperatures in the mixture ratio band is shown in Figs. III-12 and III-13. The slightly lower actual temperatures were partially caused by the average actual ambient temperature being 7° F cooler than the average temperature in the F-45 day predictions.

Figures III-14, III-15, III-16 and III-17 present a comparison of the F-1 day prediction, and the reconstructed and the actual propellant temperatures during the countdown for each propellant tank. Correlation of actual and reconstructed temperatures is relatively good, while that of actual and F-1 prediction is quite poor. The importance of an accurate weather prediction is obvious.

A polyethylene curtain was placed around the Stage II fuel tank at 0400 hours EST, and removed between 0600 and 0700 hours EST. Prior to installation of the curtain, the temperature rise heating rate for this tank averaged approximately 0.59° F/hr; this was reduced to approximately 0.28° F/hr after installation, a reduction of slightly better than 50%.

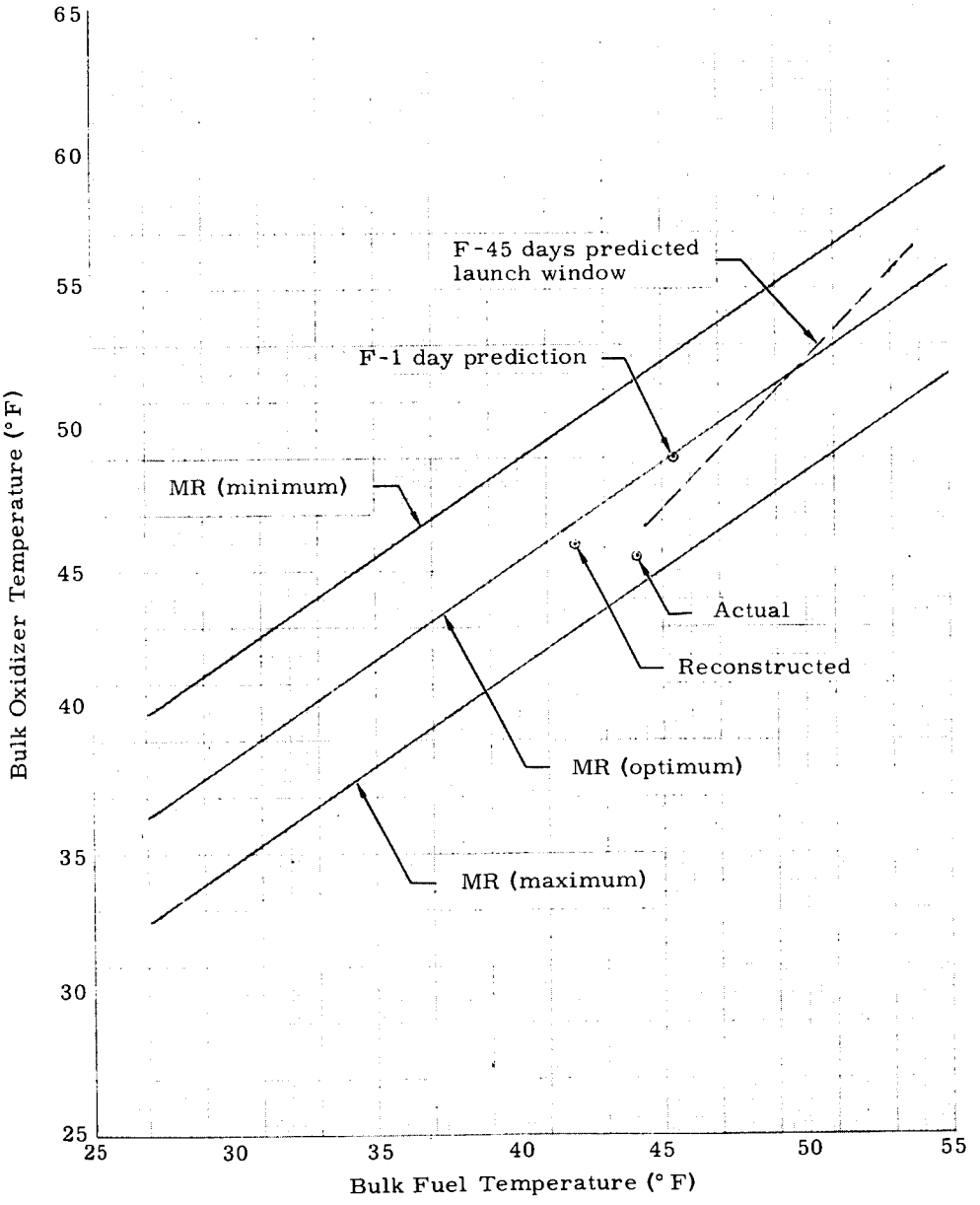

Fig. III-12. Propellant Bulk Temperatures at Liftoff, Stage I

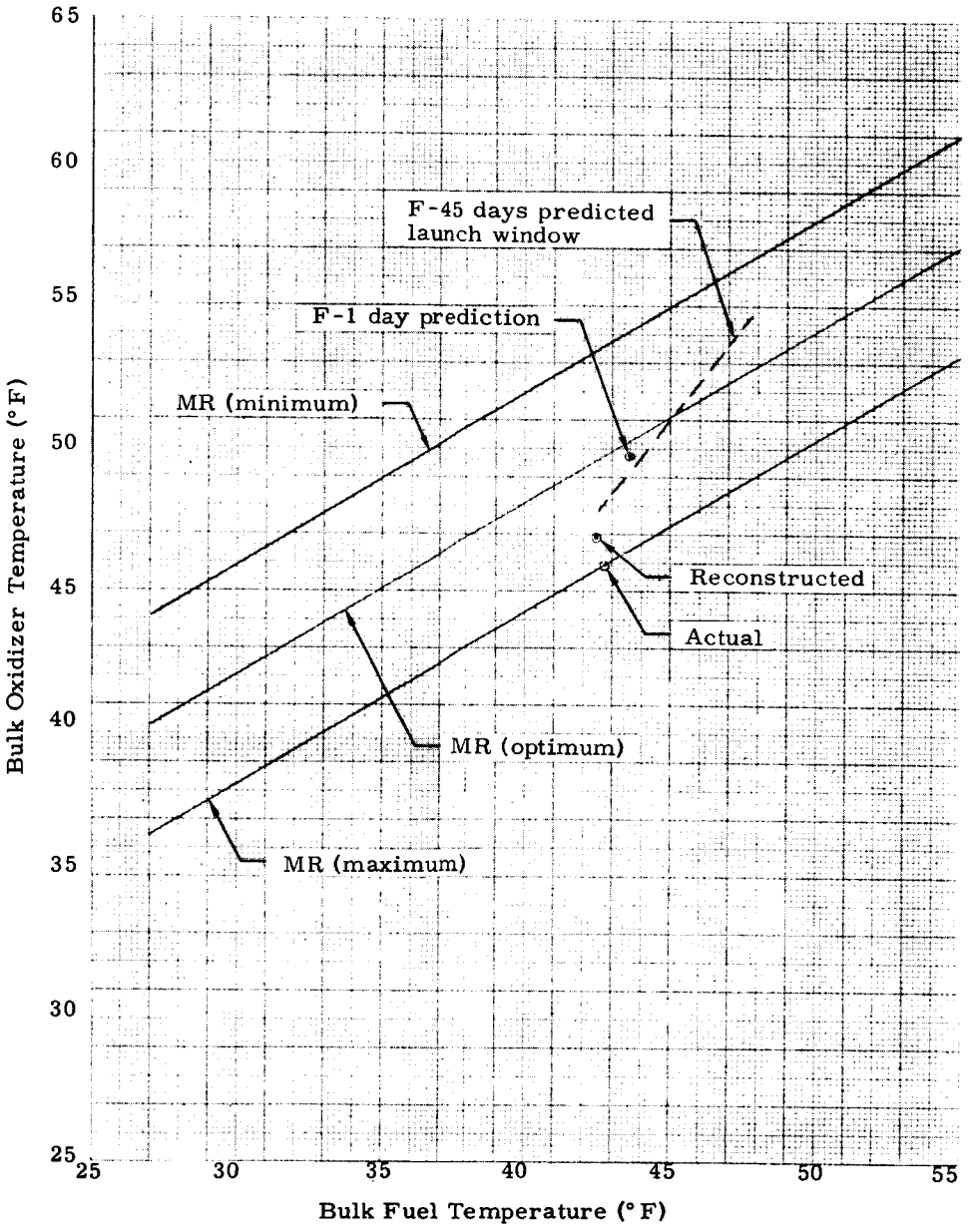

Fig. III-13. Propellant Bulk Temperatures at Liftoff, Stage II

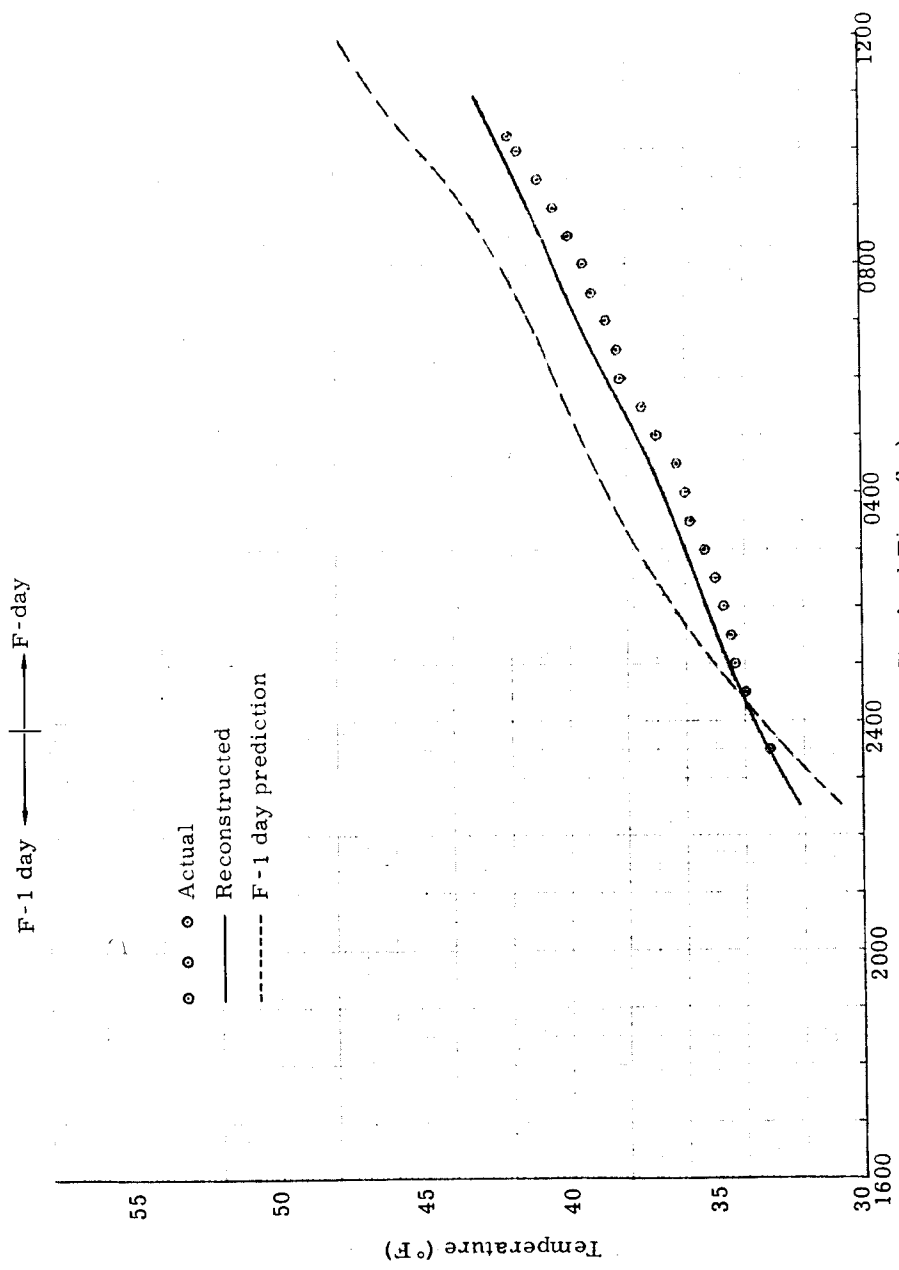

Fig. III-14. Stage I Oxidizer Tank Bottom Probe Temperature (Meas 4128)

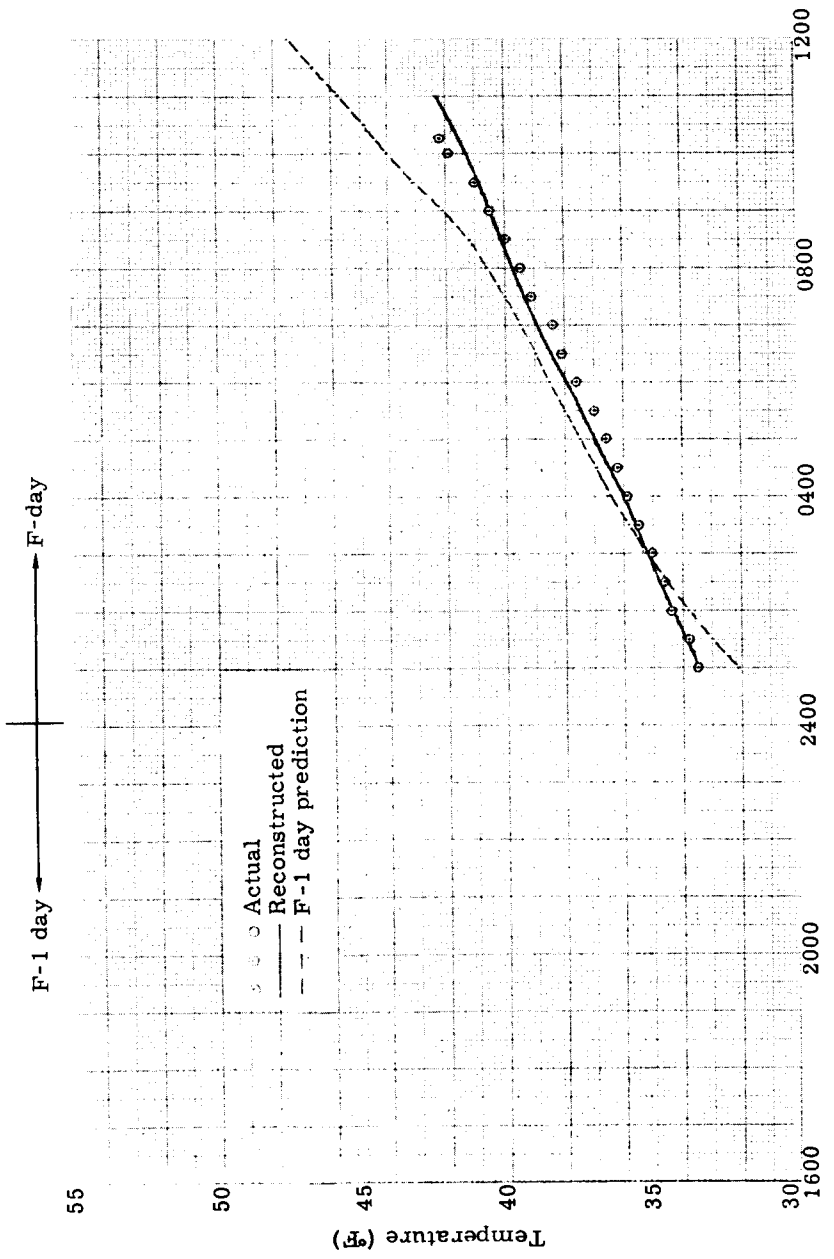

Fig. III-15. Stage I Fuel Tank Bottom Probe Temperature (Meas 4124)

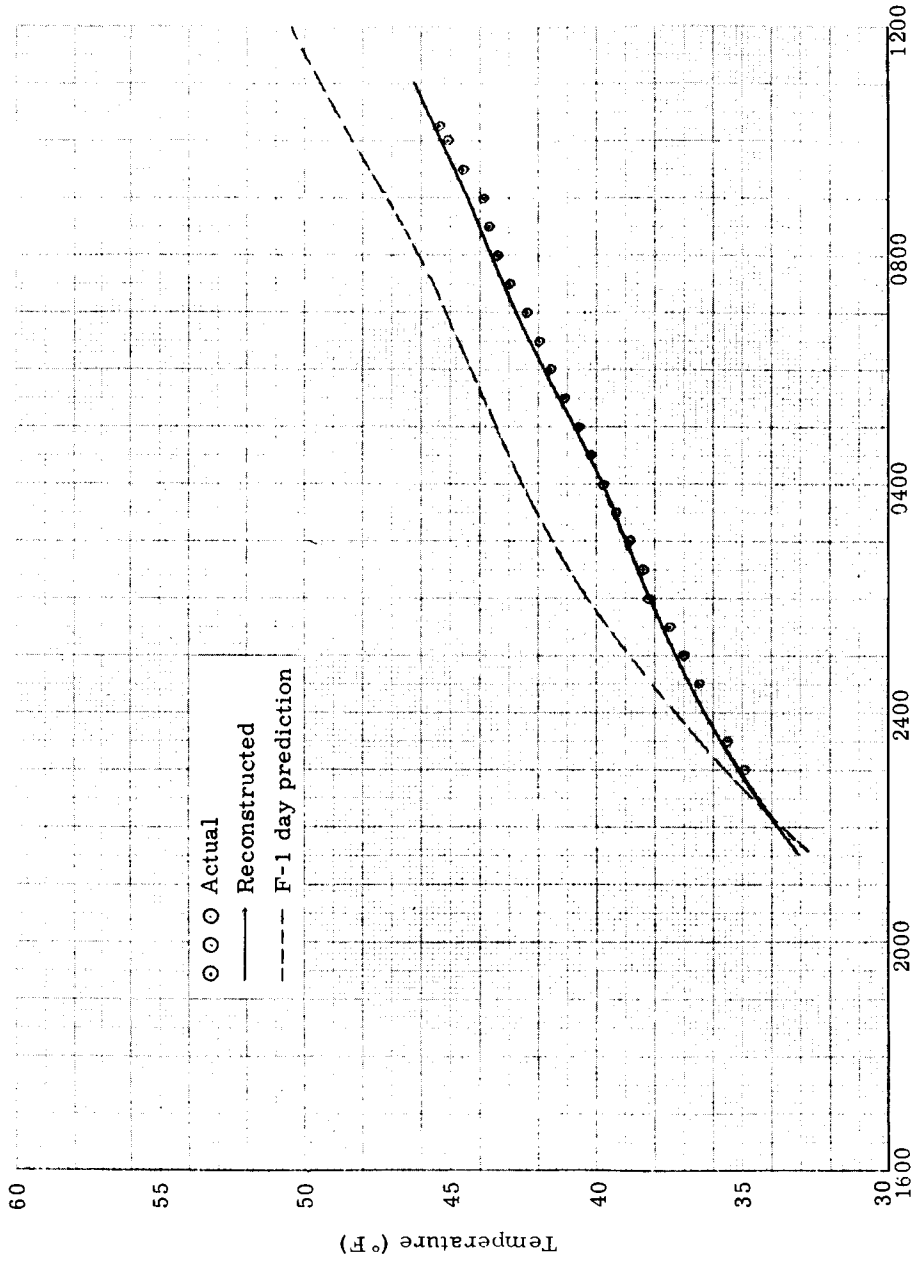

Fig. III-16. Stage II Oxidizer Tank Bottom Probe Temperature (Meas 4604)

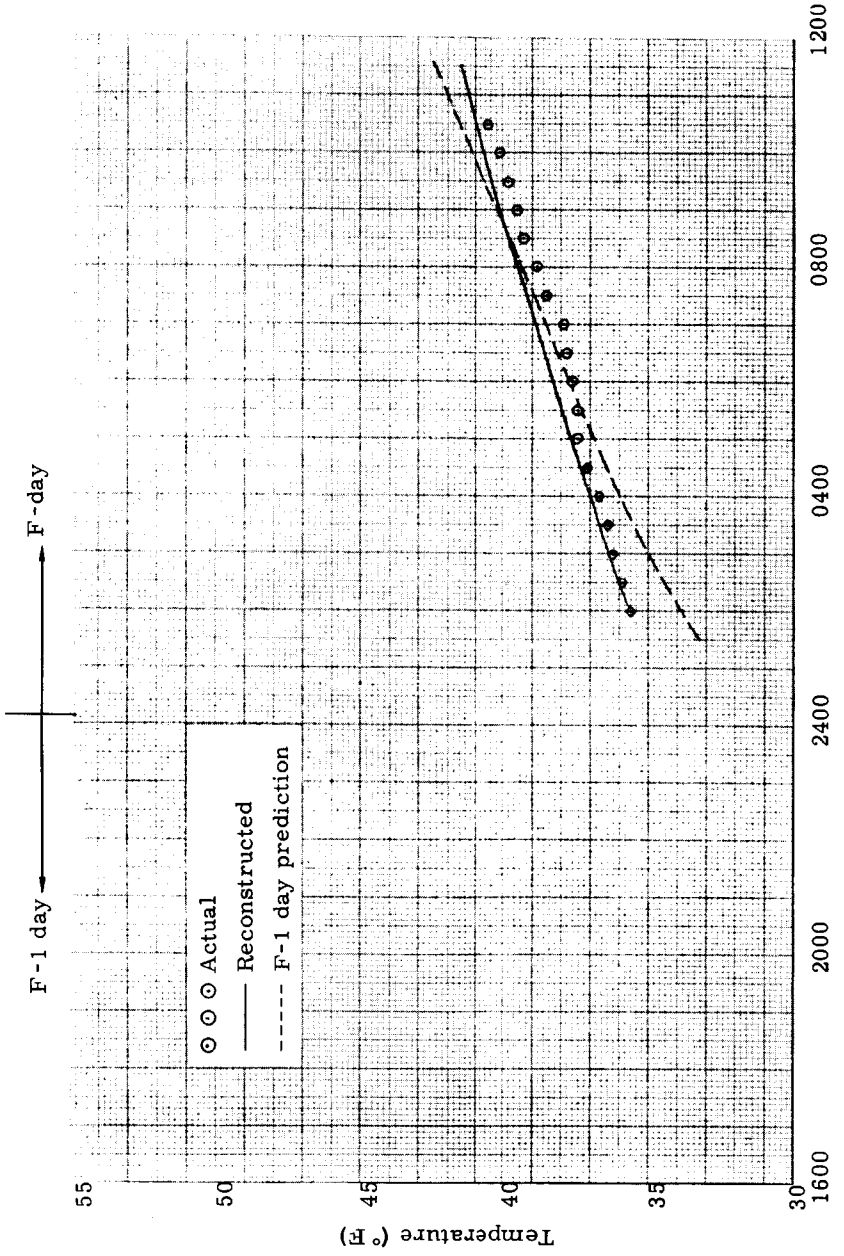

Fig. III-17. Stage II Fuel Tank Bottom Probe Temperature (Meas 4601)

f. Suction temperatures

Inflight pump inlet temperatures were generally in good agreement with the predicted temperature profiles. These data are shown in Figs. III-18, III-19, III-20 and III-21. The discrepancy in Stage II oxidizer temperature results from less stratification of the propellant than predicted. Since this has occurred on previous Gemini launches, the profile of the suction temperatures will be modified for future flights beginning with GT-5.

With the exception of Stage II oxidizer, the shape of temperature versus time curves was in good agreement with predicted shape, although uniformly low. This was a result of the difference between predicted and actual weather conditions.

A comparison has been made between the suction and tank bottom temperature probe readings at various times after FS_1. In this manner, each probe tends to measure the same element of fluid and a realistic comparison results. It may be seen that Meas 0024 is more representative of the actual temperature than is Meas 0023.

The tank bottom probe and the pump inlet temperatures recorded at various times after FS_1 are shown in Table III-24.

TABLE III-24

Comparison of Tank Bottom Probe and Pump Inlet Temperatures

System	Time (sec)	Suction Probe Temperature (°F)	Tank Bottom Probe Temperature (°F)	ΔTemperature (°F)
Stage I fuel	$FS_1 + 5$	42.8	42.2	0.6
Stage II fuel	$FS_1 + 25$	41.1	41.4	-0.3
Stage I oxidizer	$FS_1 + 6$	41.4	42.0	-0.6
Stage II oxidizer	$FS_1 + 22$	44.7	45.4	-0.7

3. Propellant Feed System

a. Feedline transients

The maximum transient pressures recorded at the pump inlet instrumentation transducers are presented in Table III-25.

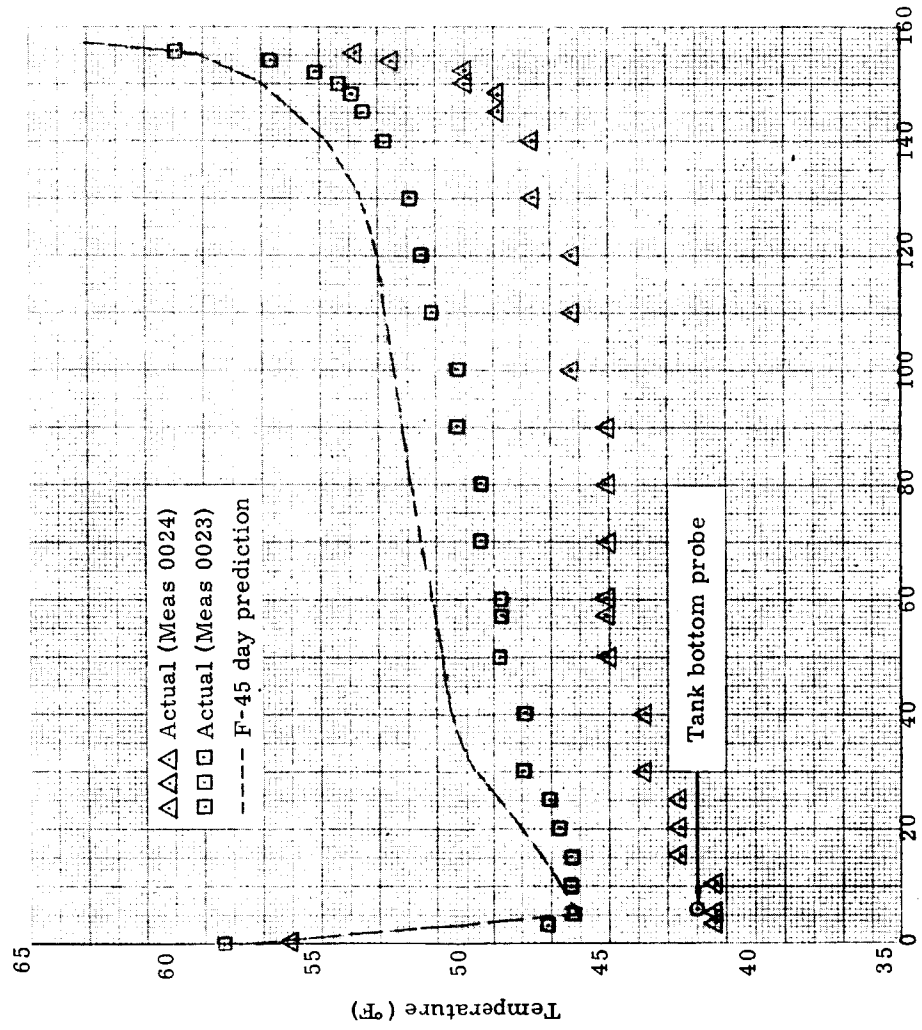

Fig. III-18. Stage I Oxidizer Pump Inlet Temperature (Meas 0023 and 0024)

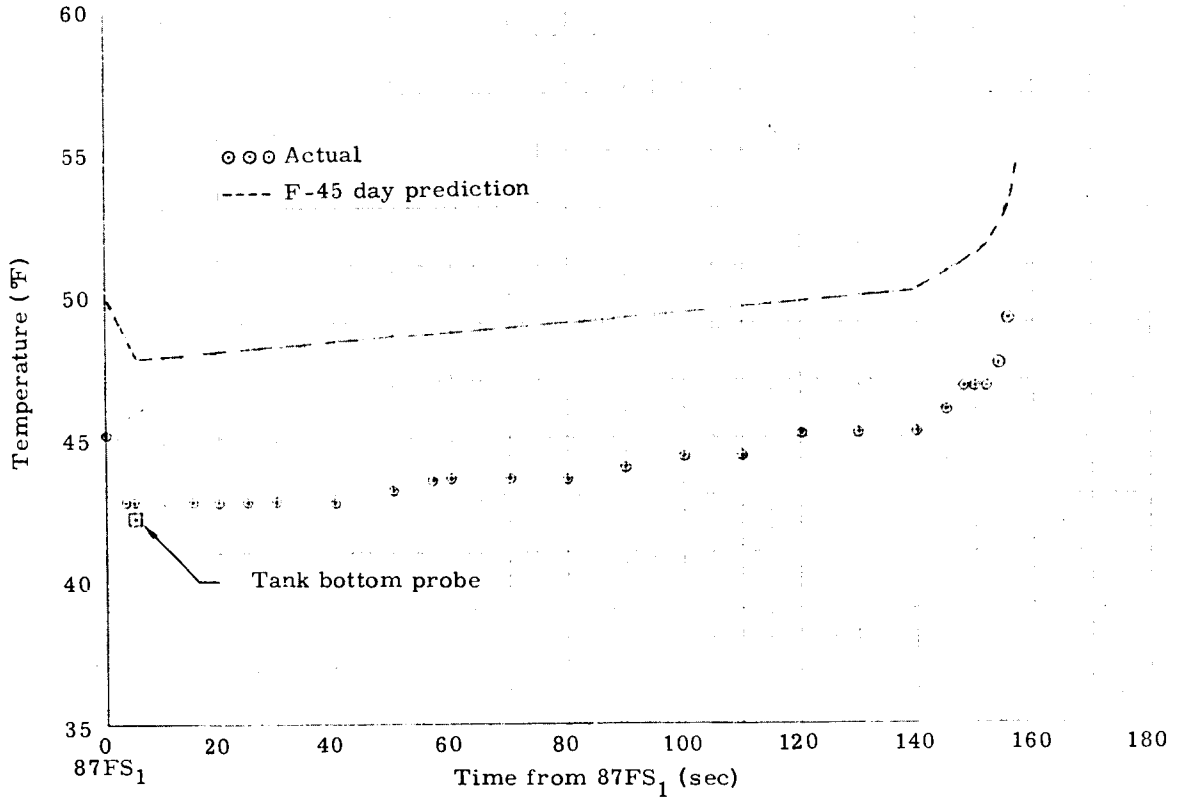

Fig. III-19. Stage I Fuel Pump Inlet Temperature (Meas 0013)

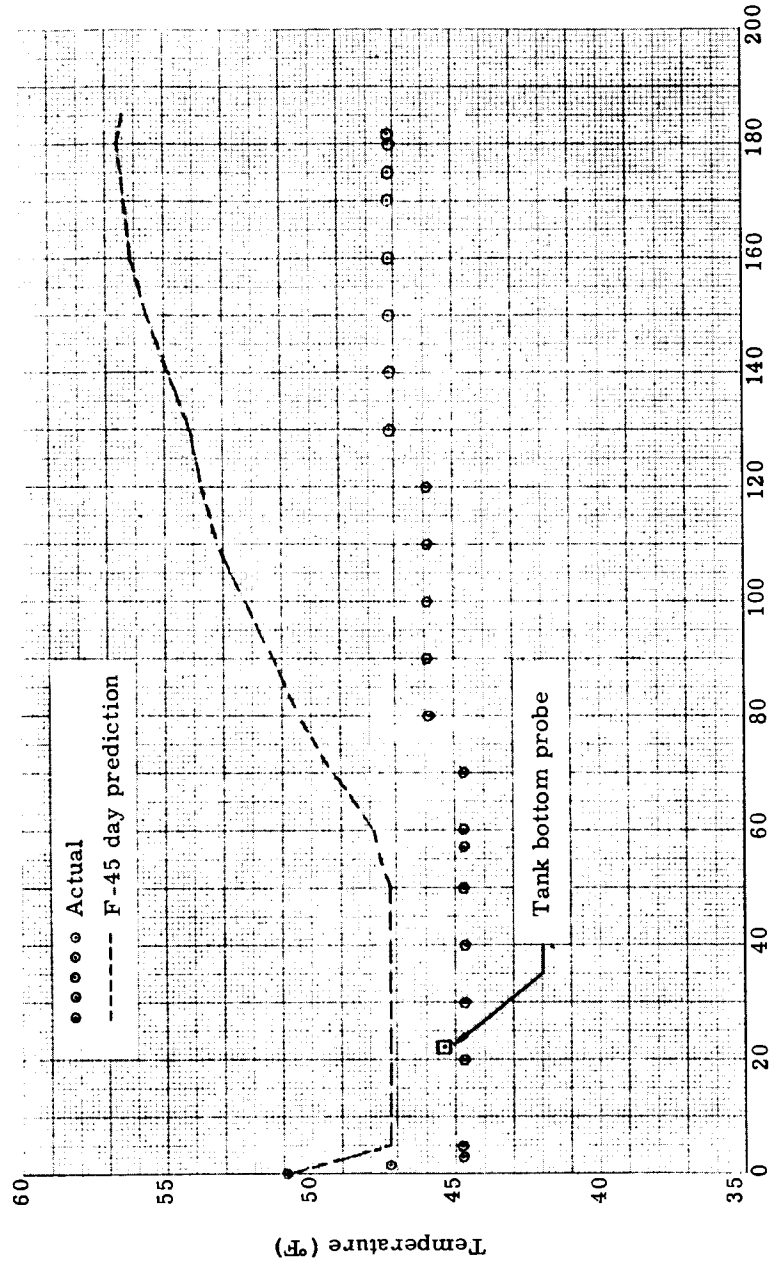

Fig. III-20. Stage II Oxidizer Pump Inlet Temperature (Meas 0514)

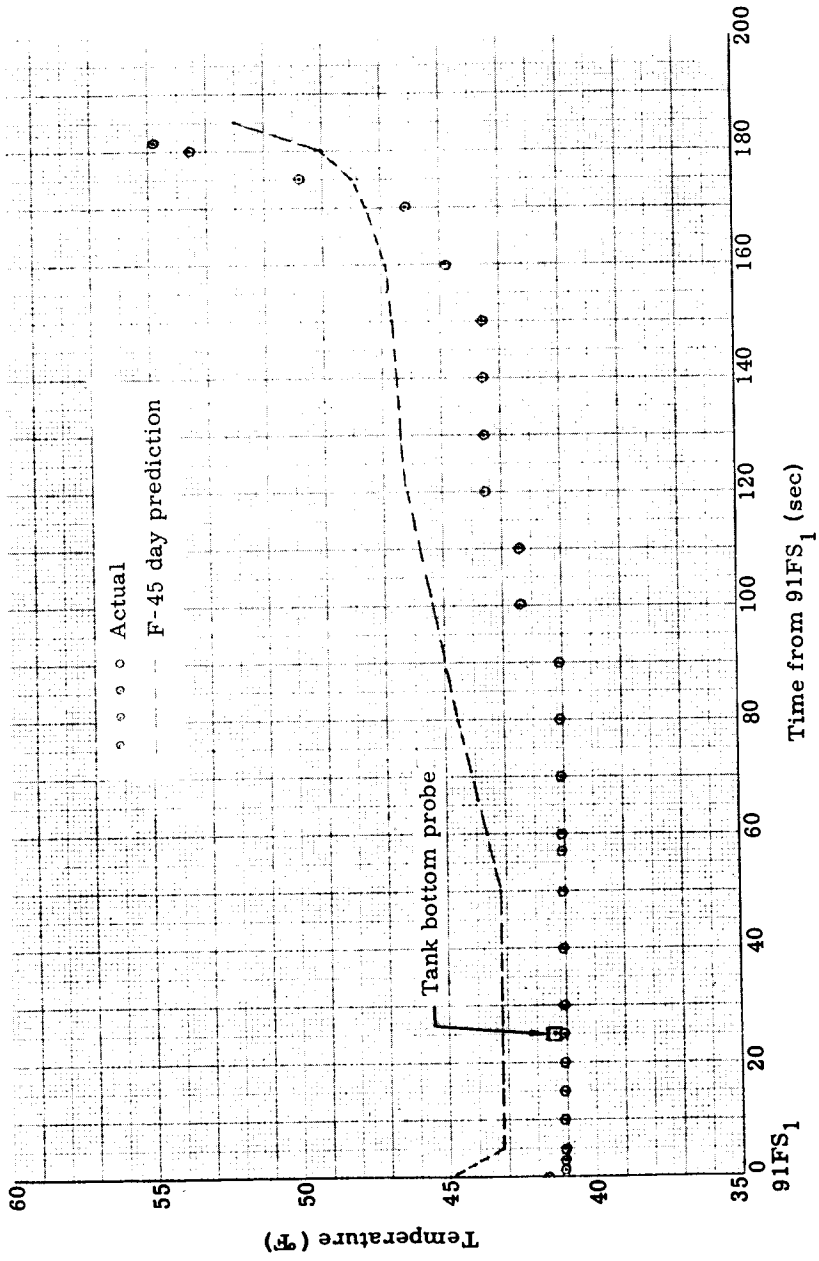

Fig. III-21. Stage II Fuel Pump Inlet Temperature (Meas 0508)

TABLE III-25

Maximum Transient Pressures

System	Meas	ΔP at Prevalve Opening (psi)	ΔP at Initial Pressure Wave (psi)	ΔP at Ignition (psi)	ΔP at TCV Closing (psi)	Design Operating Pressure (psia)
Stage I oxidizer	0017	No data	Negligible?	136	Negligible	215
Stage I fuel	0014	46.0	Negligible?	39	Negligible	55
Stage II oxidizer	0510	74.0	71	*	67	260
Stage II fuel	0507	Negligible	Negligible	*	Negligible	80

*Not available due to telemetry blackout at staging.

Pressure data at the opening of the Stage I oxidizer prevalves were unavailable because these valves were opened prior to the start of telemetry recording. Ignition transient pressures were similar to those on GT-2 and GT-3. Telemetry blackout at staging, during Stage II ignition, eliminates data on the sustainer engine ignition transients.

b. Pump suction pressures

Stages I and II static suction pressures at the suction line measurement locations are shown in Figs. III-22 through III-25. These graphs show the preflight predicted, postflight reconstructed, and best estimate of actual flight pressures.

The postflight reconstructed curves have been based on flight measured values of ullage gas pressure, axial load factors, propellant temperatures and propellant loadings.

The Stage I oxidizer best-estimate curve of the static suction pressures at the measurement transducer (Meas 0017) represents an average of the measured pressure and the two oxidizer standpipe pressures (Meas 0033 and 0034), adjusted to the Meas 0017 transducer location. The Stage I fuel suction pressure best estimate at the Meas 0014 transducer location is an average of the measured pressure and the two fuel accumulator pressures (Meas 0037 and 0038), adjusted to the Meas 0014 location. The Stage II oxidizer and fuel best-estimate suction pressures were obtained directly from Meas 0510 and 0507, respectively.

The difference between reconstructed and measured pressures at the Stages I and II fuel measurement locations (Meas 0014 and 0507)

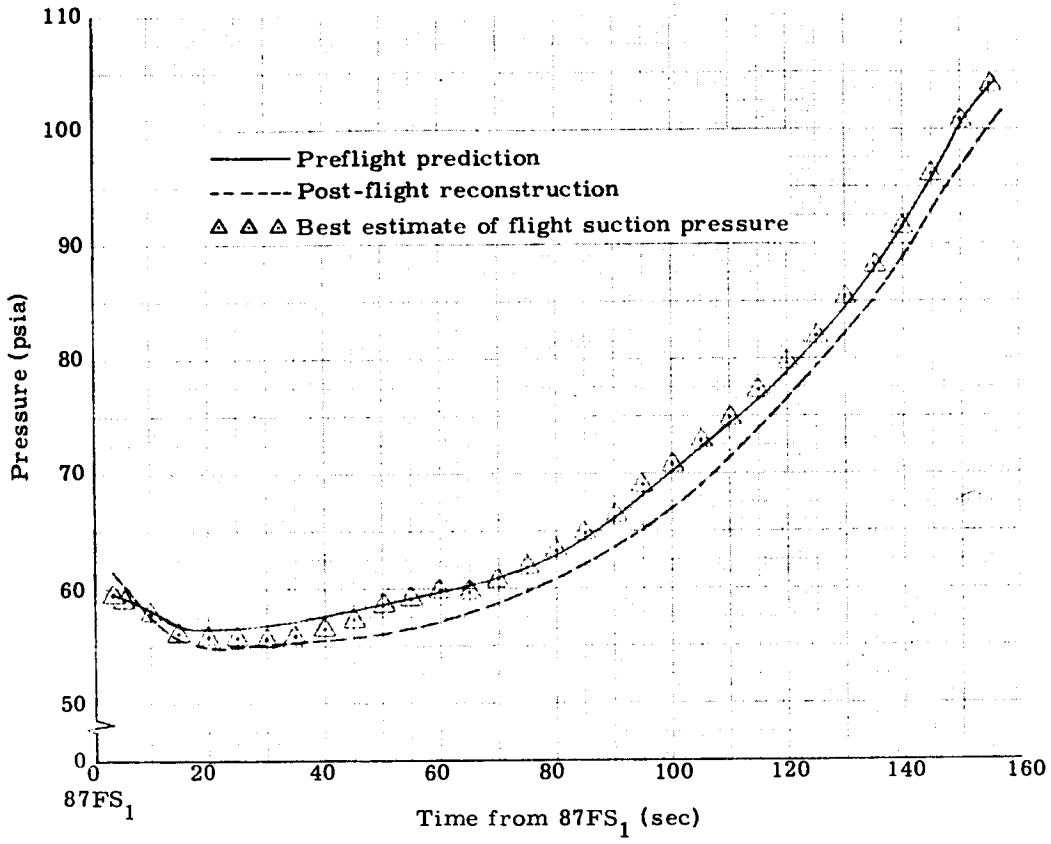

Fig. III-22. Stage I Oxidizer Suction Pressure (Meas 0017)

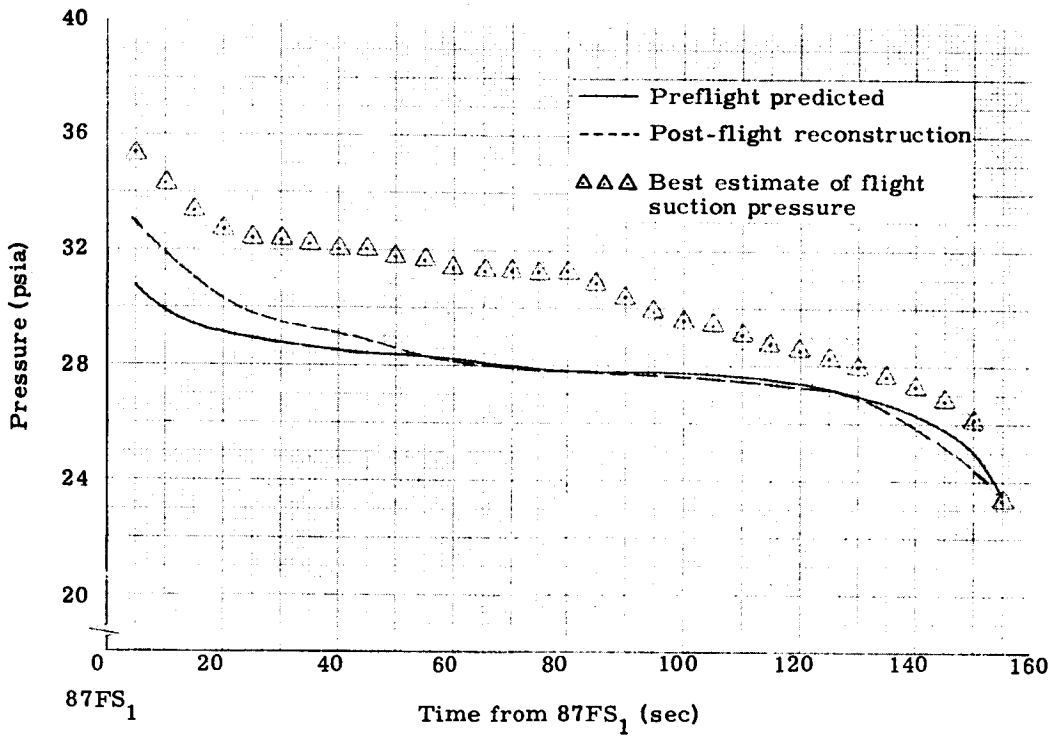

Fig. III-23. Stage I Fuel Suction Pressure (Meas 0014)

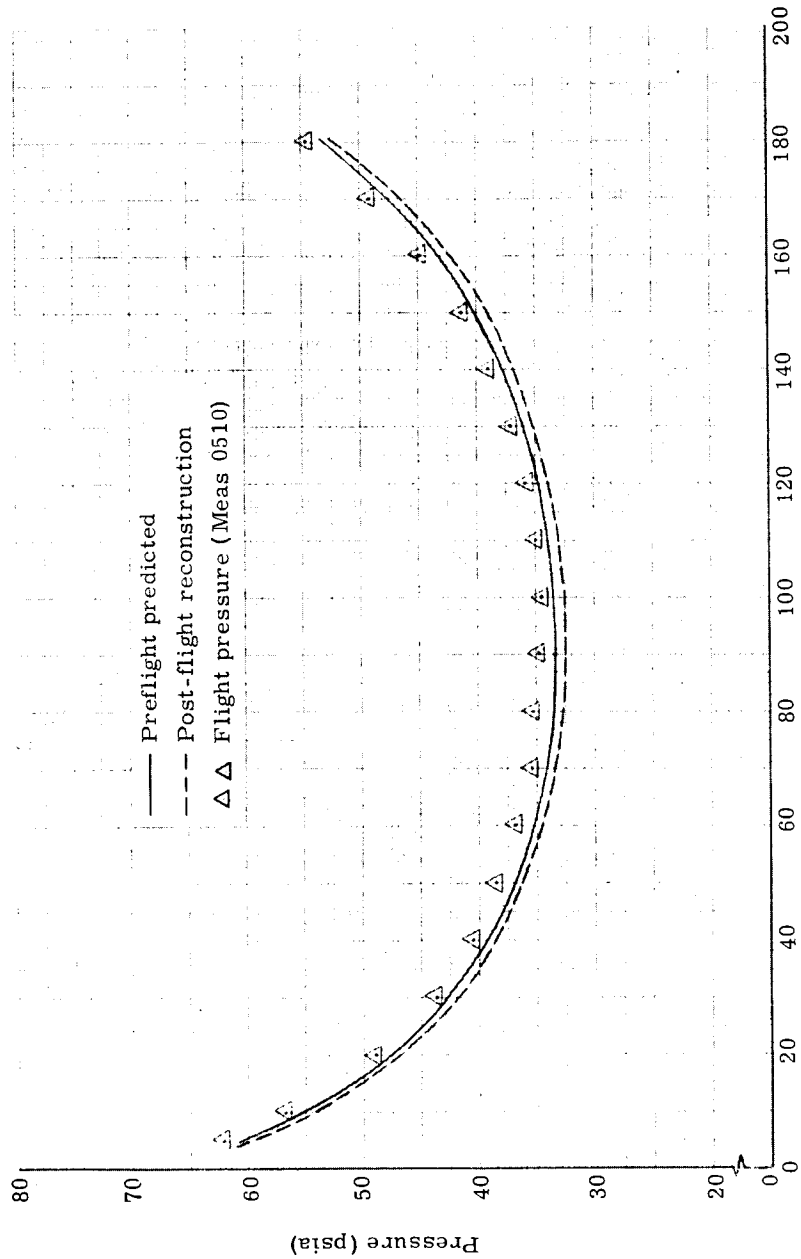

Fig. III-24. Stage II Oxidizer Suction Pressure (Meas 0510)

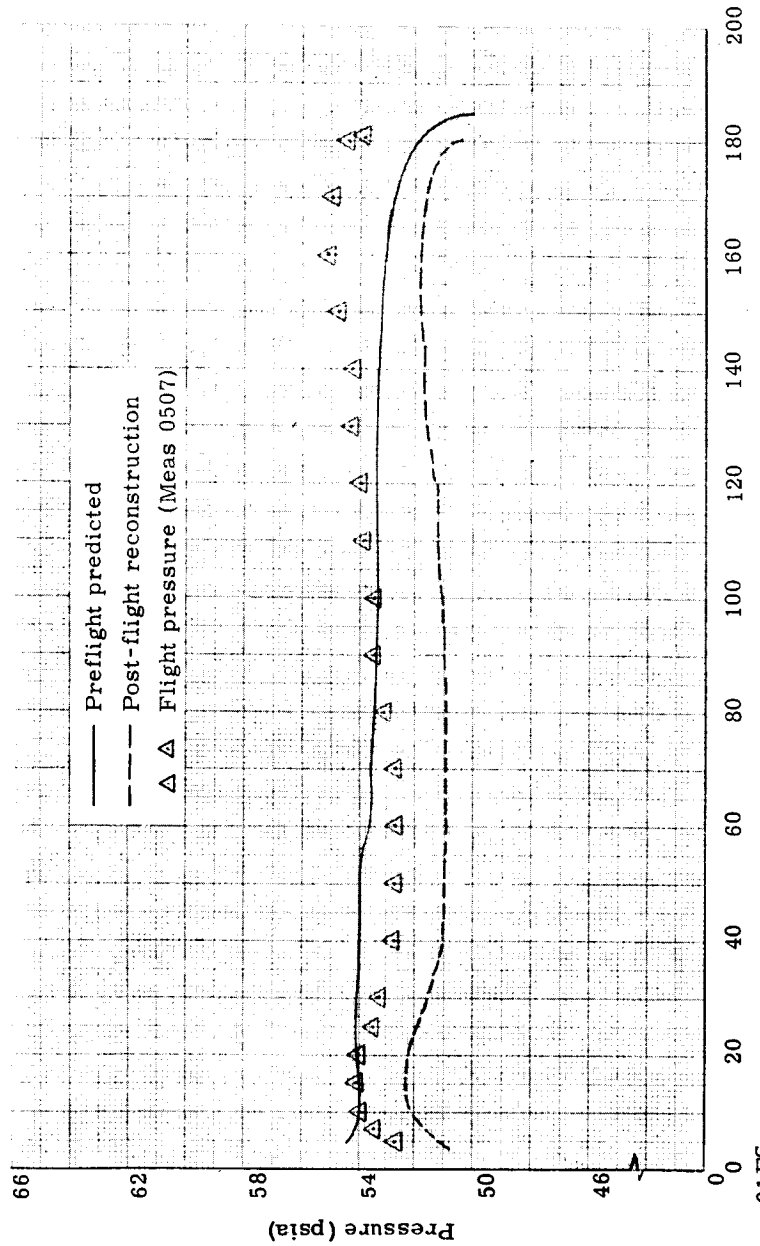

Fig. III-25. Stage II Fuel Suction Pressure (Meas 0507)

exceeds the 2% instrumentation tolerance. An investigation is under way to determine the cause of these discrepancies.

c. NPSH supplied

The NPSH supplied at the engine turbopump inlets during the start phase and steady-state operation is shown in Table III-26.

4. Propellant Utilization

a. Level sensor operation

Figures III-26 and III-27 show the predicted, actual and reconstructed level sensor uncover times for Stages I and II. Measured level sensor uncover times are also tabulated in Table III-27. The relationship of the predicted to the actual times of sensor uncover reflects the higher-than-predicted flow rates observed on Stages I and II.

Slosh (indicated by on and off signals near the uncovering of both Stage II oxidizer, one Stage II fuel, and one Stage I fuel high level sensors) was less than that noted on GT-1, GT-2 or GT-3, and on many Titan II flights. The longest duration of slosh was 0.7 second for the Stage II oxidizer high level sensor. The recover on the Stage II fuel high level sensor (Meas 0540) occurred sufficiently after the uncover signal and thus did not affect interpretation of the data.

b. Best estimate of level sensor uncover times

Table III-28 contains the best estimate of average level sensor uncover times for the GT-4 flight. The measured average uncover times shown in Table III-27 are decreased by 0.06 second to allow for the built-in level sensor delay of 0.033 second and the telemetry sampling time interval of 0.05 second.

The decrease in the Stage II fuel high level sensor uncover times incorporated in previous GLV postflight reconstructions was not used for GLV-4. The following factors were considered in arriving at this decision:

(1) The analytical procedures used to determine the propellant consumption between ignition and high level sensor uncover times have been improved.

(2) The propellant tank stretch was re-evaluated, resulting in a reduction of approximately one cubic foot in the volume below the high level sensor.

TABLE III-26

Minimum NPSH Supplied

System	Minimum NPSH Supplied During Start Transient (psia)	Starting ① NPSH Required (psia)	Limited ② Operation NPSH Required (sec)	Minimum Steady-State NPSH Supplied (psia)	Unlimited ① Operation NPSH Required (psia)
Stage I oxidizer	29.0	38.4	28.2 psia for 135	56	46.1
Stage I fuel	30.0	17.1	17.1 psia for 120	23	23.1
Stage II oxidizer	③	38.4	19.2 psia for 120	29	22.4
Stage II fuel	③	39.8	39.8 psia for 120	51	43.4

① Oxidizer values represent NPSH required at FS_1; fuel values at engine start.

② Time represents maximum cumulative operating time from engine acceptance at the given NPSH levels.

③ Not available due to telemetry blackout.

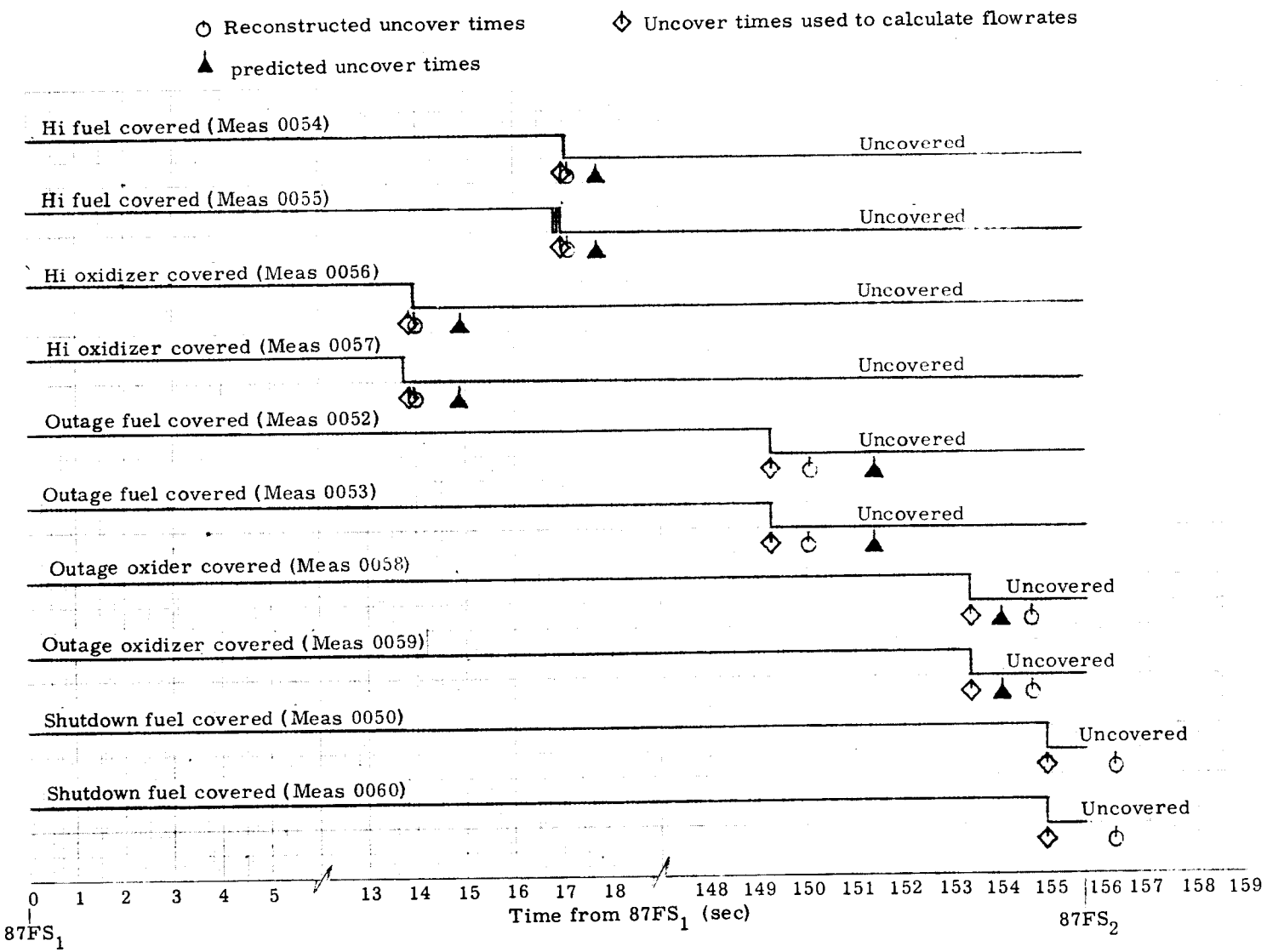

Fig. III-26. Stage I Level Sensor Operation

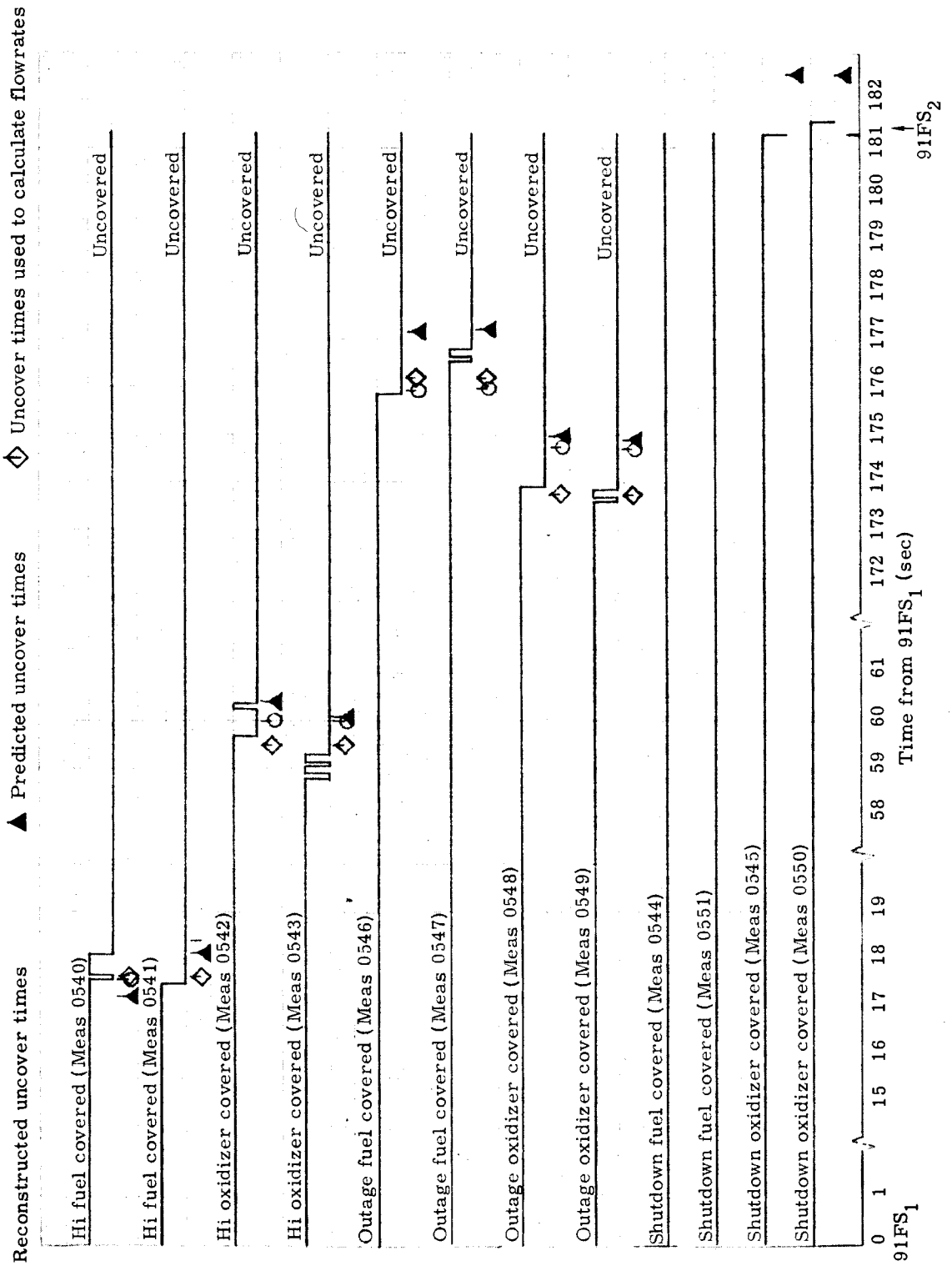

Fig. III-27. Stage II Level Sensor Operation

TABLE III-27

Measured Level Sensor Uncover Times

Meas	Sensor Description	Uncover Time (hr GMT)	Average Uncover Time (hr GMT)	Remarks
0056	Stage I oxidizer high	1516:10.296	1516:10.196	Clean
0057	Stage I oxidizer high	1516:10.096		Clean
0058	Stage I oxidizer outage	1518:29.710	1518:29.710	Clean
0059	Stage I oxidizer outage	1518:29.710		Clean
0054	Stage I fuel high	1516:13.396	1516:13.321	Clean
0055	Stage I fuel high	1516:13.246		Single-slosh cycle, 0.1 sec
0052	Stage I fuel outage	1518:25.599	1518:25.604	Clean
0053	Stage I fuel outage	1518:25.609		Clean
0050	Stage I fuel shutdown	1518:31.250	1518:31.255	Clean
0060	Stage I fuel shutdown	1518:31.260		Clean
0542	Stage II oxidizer high	1519:32.026	1519:31.526	Single-slosh cycle, 0.7 sec
0543	Stage II oxidizer high	1519:31.026		Two slosh cycles, 0.50 sec
0548	Stage II oxidizer outage	1521:25.899	1521:25.812	Clean
0549	Stage II oxidizer outage	1521:25.724		Single-slosh cycle, 0.25 sec
0540	Stage II fuel high	1518:49.897	1518:49.685	Single-slosh cycle, 0.65 sec, recover after 140 sec
0541	Stage II fuel high	1518:49.472		Clean
0546	Stage II fuel outage	1521:27.839	1521:28.252	Clean
0547	Stage II fuel outage	1521:28.664		Single-slosh cycle, 0.25 sec
0545	Stage II oxidizer shutdown	1521:33.290	1521:33.420	
0550	Stage II oxidizer shutdown	1521:33.550		Clean
0544	Stage II fuel shutdown	--	--	Did not uncover
0551	Stage II fuel shutdown	--	--	Did not uncover

TABLE III-28

Best Estimate of Average Level Sensor Uncover Time

Quadrant	Meas	Sensor Description	Best Estimate of Uncover Time (GMT)	Δt (sec)
I III	0056 0057	Stage I oxidizer high level Stage I oxidizer high level	1516:10.138	139.514
I/IV II/III	0058 0059	Stage I oxidizer outage Stage I oxidizer outage	1518:29.652	
I III	0054 0055	Stage I fuel high level Stage I fuel high level	1516:13.652	132.283
III II	0052 0053	Stage I fuel outage Stage I fuel outage	1518:25.546	
-- I III	-- 0050 0060	Stage I oxidizer shutdown Stage I fuel shutdown Stage I fuel shutdown	-- 1518:31.197	--
IV II	0542 0543	Stage II oxidizer high level Stage II oxidizer high level	1519:31.468	114.286
I/IV II/III	0548 0549	Stage II oxidizer outage Stage II oxidizer outage	1521:25.754	
I III	0540 0541	Stage II fuel high level Stage II fuel high level	1518:49.627	158.567
I III	0546 0547	Stage II fuel outage Stage II fuel outage	1521:28.194	
II IV	0545 0550	Stage II oxidizer shutdown Stage II oxidizer shutdown	1521:33.362	--
II IV	0544 0551	Stage II fuel shutdown Stage II fuel shutdown	--	

Tank	Average Temperatures Between Uncoverings (° F)	Corresponding Density (lb/ft^3)
Stage I oxidizer	45.8	91.935
Stage I fuel	44.1	57.155
Stage II oxidizer	46.4	91.888
Stage II fuel	42.8	57.197

Table III-28 also shows the integrated average temperatures between level sensor uncoverings and the corresponding propellant densities.

Table III-29 contains the level sensor volumes and the delta volumes used in the level sensor flow rate analysis. The Stage II oxidizer level sensor volumes were reconstructed to reflect the volume below the high level sensor which had been calibrated at Cape Kennedy, using the propellant transfer and pressurization system (PTPS).

TABLE III-29

Averaged Tank Volumes at Level Sensor Locations

Tank	Sensor	Averaged Volumes (stretch included) (cu ft)	ΔVolumes (cu ft)
Stage I oxidizer	High-level	1714.38	1674.67
	Outage	39.71	
Stage I fuel	High-level	1405.62	1337.76
	Outage	67.86	
Stage II oxidizer	High-level	285.61	262.40
	Outage	23.21	
Stage II fuel	High-level	351.69	333.55
	Outage	18.14	

c. Flow rates

Table III-30 presents the predicted and the actual volumetric flow rates between level sensors.

TABLE III-30

Propellant Volumetric Flow Rates

Tank	Predicted (ft^3/sec)	Actual (ft^3/sec)
Stage I oxidizer	12.039	12.004
Stage I fuel	10.006	10.113
Stage II oxidizer	2.286	2.296
Stage II fuel	2.086	2.104

This tabulation also reflects the higher-than-predicted flow rates for Stages I and II engines. The resistances in the engine analytical model were adjusted to reflect the actual flow rates in the reconstruction of the engine performance.

d. Mixture ratio

Table III-31 shows the comparison of Stages I and II predicted and actual engine mixture ratios between level sensors for GT-4. Also shown are the mixture ratios (MR) predicted on launch day as a result of the propellant temperature monitoring procedures.

TABLE III-31

Engine Mixture Ratio

System	Predicted Mixture Ratio*	Actual Mixture Ratio	Predicted Mixture Ratio (F-0 day)
Stage I	1.9305	1.9093	1.9350
Stage II	1.7522	1.7536	1.7637

*Ref. 19.

By applying pressure and temperature corrections to the predicted (F-45 day) mixture ratios, the run-to-run variation has been calculated. The mixture ratio deviation along with the allowable run-to-run dispersions are presented in Table III-32.

TABLE III-32

Mixture Ratio Deviation

System	Predicted Mixture Ratio (corrected for pressure and temperature variations)	Actual Mixture Ratio	Deviation (%)	Run-to-Run Dispersion (%)
Stage I	1.9360	1.9093	-1.38	±1.38
Stage II	1.7657	1.7536	-0.68	±2.28

The mixture ratio shift on GT-4 was more than that experienced on GT-1, GT-2 and GT-3, but was within the expected tolerance band for run-to-run repeatability.

e. Outage and trapped propellants

The statistical mean and maximum (99%) outages predicted for GT-4 in both the F-45 day preflight report (Ref. 19) and during the F-0 day propellant temperature monitoring exercise appear in Table III-33. The actual outages are also shown, as calculated using the information contained in the reconstructed propellant inventories (Tables III-16 and III-17).

TABLE III-33

Outage Prediction

	Predicted (F-45 day)		Predicted (F-0 day)		
	Mean	Max (99%)	Mean	Max (99%)	Actual
Stage I Total steady-state propellant (%)	0.220	0.645	0.258	0.674	0.239 (oxidizer)
Weight (lb)	567	1659	664	1734	614
Stage II Total steady-state propellant (%)	0.344	1.026	0.421	1.105	0.264 (fuel)
Weight (lb)	207	617	253	664	160

Outages are presented in percent of total steady-state propellants and in pounds weight. The value used for total steady-state propellants for Stage I was 257, 240 pounds, and the value for Stage II was 60, 102 pounds.

The predicted and actual trapped propellant weights for Stages I and II are shown in Table III-34.

TABLE III-34

Trapped Propellants

System	Oxidizer (lb)		Fuel (lb)	
	Predicted	Actual	Predicted	Actual
Stage I				
Above interface	0	0	20	95
Below interface	235	235	309	309
Stage II				
Above interface	0	0	0	0
Below interface	20	20	14	14

f. Start and holddown propellant consumptions

The predicted and actual propellant consumptions during the Stage I ignition and holddown periods are presented in Table III-35.

TABLE III-35

Stage I Ignition and Holddown Propellant Consumption

Interval	Oxidizer (lb)		Fuel (lb)	
	Predicted	Actual	Predicted	Actual
Start consumption ($87FS_1$ to TCPS)	204	204	40	40
Holddown (TCPS to liftoff)	2159	2210	1138	1201

Predicted values were derived from data in Ref. 21, and actual values were calculated from the Martin PRESTO engine performance program.

The Stage II predicted and actual propellant consumptions during the time from $91FS_1$ to $91FS_2$ + 1.2 seconds are listed in Table III-36.

TABLE III-36

Stage II Start Propellant Consumption

Interval	Oxidizer (lb)		Fuel (lb)	
	Predicted	Actual	Predicted	Actual
Start consumption ($91FS_1$ to $91FS_1$ + 1.2 sec)	131	131	51	51

The predicted and actual values were derived using data from Ref. 21.

g. Vapor retained

Predicted and actual values of vapor retained in the tanks, as a result of pressurization gases and liquid vaporization during flight, are shown in Table III-37.

TABLE III-37

Pressurization Gas Inventory

	Oxidizer (lb)		Fuel (lb)	
	Predicted	Actual	Predicted	Actual
Stage I				
Vapor retained				
Oxidizer tank	324	324	93	97
Fuel tank	8	7	93	97
Vaporized	8	8	0	0
Stage II				
Pressurization				
Fuel tank	4	4	51	49
Vaporization				
Oxidizer tank	21	21	-	-

The actual values were taken from the reconstructed flight pressure profile of the pressurization computer program runs.

h. Shutdown

Stage I shutdown was due to fuel exhaustion. The predicted and actual values for the propellants consumed during shutdown are listed in Table III-38. The actual values were obtained by integrating a curve (derived from PRESTO) of flight flow rate versus time after $87FS_2$.

Stage II shutdown was initiated by a guidance command; hence, the propellants were not exhausted as in Stage I. The predicted and actual values for the propellants consumed during shutdown are shown in Table III-38. The actual values were computed from the altitude shutdown impulse.

TABLE III-38

Shutdown Propellant Consumption

System	Oxidizer (lb)		Fuel (lb)	
	Predicted	Actual	Predicted	Actual
Stage I	446	361	27	60
Stage II	86	79	69	63

5. POGO Performance

The Stage I longitudinal oscillation levels for this flight were slightly higher than those of previous Gemini flights. Nevertheless, propulsion data, other than standpipe pressures, did not exhibit significant structural frequency responses. All propulsion measurements were smooth and normal at the time of maximum POGO oscillation (LO + 121 seconds). A presentation of selected filtered measurement data is presented in Chapter XII of this report.

Table III-39 presents unfiltered pressure amplitudes at various Stage I flight times. The amplitudes were of the same general magnitude as those observed on the GT-2 and GT-3 flights.

TABLE III-39

Propulsion POGO Parameters

Time from $87FS_1$ (sec)	Oxidizer Standpipe Max Pressure Amplitude, Zero-to-Peak (psi)*		Fuel Accumulator Max Pressure Amplitude, Zero-to-Peak (psi)	
	Meas 0033, S/A 1	Meas 0034, S/A 2	Meas 0037, S/A 1	Meas 0038, S/A 2
45	2	2	8	8
100	4	4	8	4
123**	5	4	9	4
135	3	4	8	6
145	8	10	6	4
155	12	10	5	4

*Unfiltered PCM data.
**Max longitudinal oscillation.

Fuel and oxidizer cavitation indices are given in Fig. III-28. These parameters have partial correlation with POGO levels and have been included for reference only. The results are similar to these of previous Gemini flights.

6. Components

a. Prevalves

During the launch countdown, all prevalve functions were performed without incident. On replacement of the "dummy" prevalves with flight units in preparation for the launch, the installed Stage II oxidizer prevalve was found to leak across the butterfly seal. The unit was replaced. Prevalves installed for the flight are identified in Chapter XVII.

b. Level sensors

GLV-4 incorporated 22 Bendix optical type propellant level sensors (Table III-40). All units performed satisfactorily during propellant loading and in flight.

Measurement 0540, a Stage II high level fuel sensor, gave an erroneous cover signal approximately 140 seconds after a normal uncover. The 12 fuel sensors flown were of the shielded prism configurations.

c. Ball valves

Performance of the AGE ball valves was completely satisfactory during the launch effort on GT-4.

d. Oxidizer standpipes

The GLV-4 oxidizer standpipe assemblies were modified to accommodate a remote charge system (RCS). The airborne portion of this change replaced the manually operated valves with remotely operated valves and also replaced the charging line end caps with pull-away disconnects. The AGE portion included a small oxidizer tank with level sensors and vent system servicing each separate airborne standpipe; a common nitrogen gas pressurization system (hand loader and regulator), and appropriate valves, blockhouse monitor and control devices; and the plumbing necessary to charge and bleed nitrogen gas and liquid oxidizer (N_2O_4) from each standpipe.

The RCS regulator and hand loader were adjusted at T-24 hours at a charge pressure of 62 psig. A final check at T-246 minutes gave a reading of 63 psig, indicating proper regulator performance.

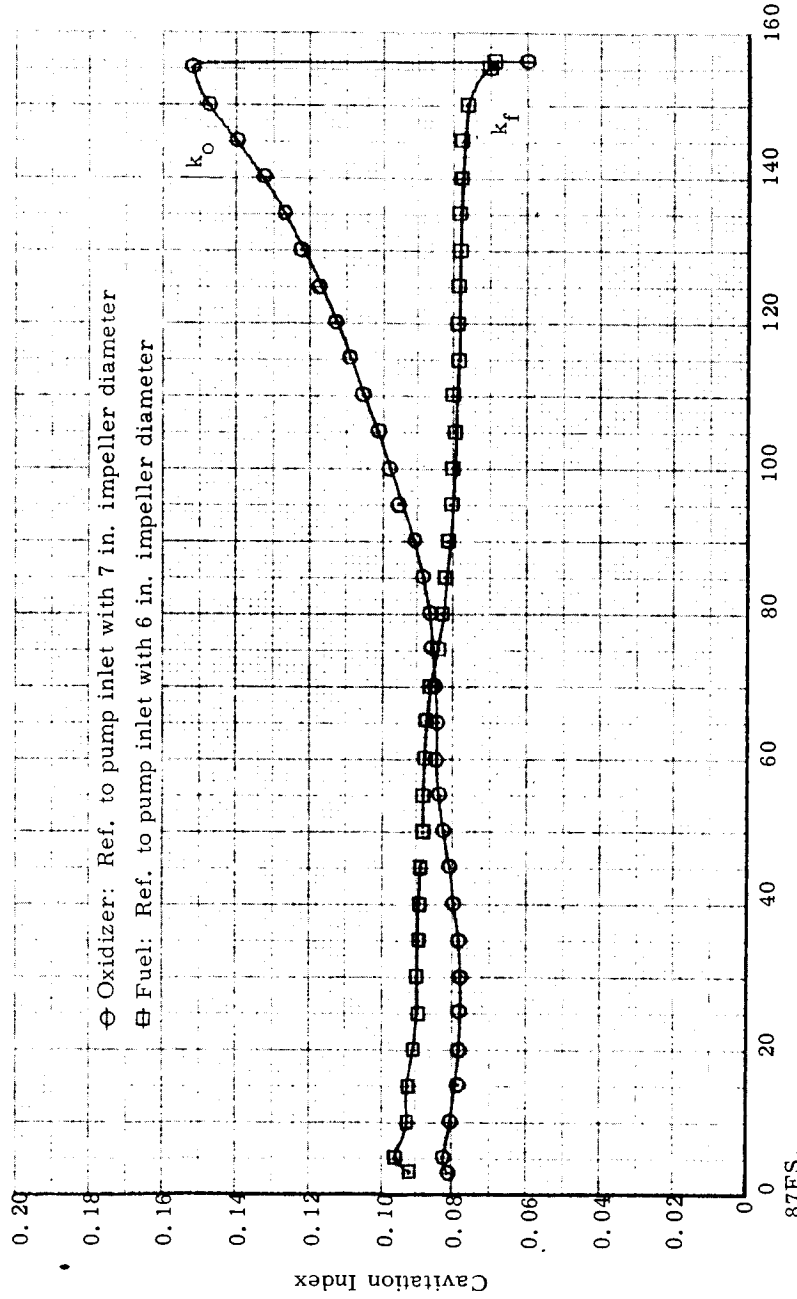

Fig. III-28. GT-3 Cavitation Indices (quasi-steady state)

TABLE III-40

Propellant Level Sensor Serial Numbers and Locations in GLV-4

Function	Stage I					Stage II				
	Meas	Location (quadrant)	Volume (ft^3)*	Serial No.	Dash No.	Meas	Location (quadrant)	Volume (ft^3)*	Serial No.	Dash No.
Oxidizer Tank										
High level	0057	III	1714.47	000422	-009	0543	II		000246	-039
High level	0056	I	1714.28	000062	-009	0542	IV		000345	-039
Outage	0059	II/III	39.54	000392	-009	0549	II/III		000169	-009
Outage	0058	I/IV	39.87	000409	-009	0548	I/IV		000266	-009
Shutdown	None	--				0545	II		000358	-009
Shutdown	None	--				0550	IV		000256	-009
Fuel Tank										
High level	0054	I	1405.56	000327	-059	0541	III	350.74	000199	-049
High level	0055	III	1405.67	000251	-059	0540	I	352.50	000167	-049
Outage	0052	III	68.10	000312	-049	0547	III	18.18	000190	-049
Outage	0053	I	67.62	000192	-049	0546	I	18.09	000222	-049
Shutdown	0060	III	8.31	000295	-049	0544	II	2.24	000218	-049
Shutdown	0050	I	8.31	000244	-049	0551	IV	2.20	000350	-059

*Volume to interface including tank stretch at uncover time.

The RCS was actuated at T-231 minutes, and each standpipe was charged properly at this time.

Monitoring of the blockhouse control/display panel (CP 2807) indicated that level sensor actuation time was the same for each subassembly (approximately 69.4 seconds). This fact verifies the desired similarity in hydraulic characteristics between each half of the remote charge system. RCS development tests at Martin-Baltimore had established that the average time from initiate charge to level sensor cover was about 66.8 seconds, with a mean vent system pressure of 2 psig. Vent system pressure for GT-4 was about 5 psig, or 3 psi more than that of the development test, hence the slightly longer time for charging.

All flight data indicated that the standpipes were satisfactorily charged. Standpipe pressure Meas 0033 and 0034 appeared normal. A comparison of S/A 1 and S/A 2 standpipe pressures is shown in Fig. III-29.

e. Fuel accumulators

The fuel accumulators used on GLV-4 incorporated one modification from the GLV-3 configuration. Blue teflon replaced white teflon at both the piston bearing and shaft bearing locations.

Response of the piston displacement Meas 0035 and 0036 was satisfactory throughout the flight. Figure III-30 shows a history of indicated accumulator piston displacement. The response was similar to that on GT-3. The amplitude of S/A 1 was generally greater than that of S/A 2, particularly in the first 50 seconds of flight. The high speed playback of the flight data shown in Fig. III-30 indicates, as on GT-3, that the large overall S/A 1 amplitudes were the result of a 5- to 6-cps motion superimposed on the predominant 22-cps motion.

Dynamic friction levels for dry accumulators were measured prior to installation of the accumulator assemblies and again prior to flight. A summary of these friction measurements is presented in Table III-41 as peak-to-peak values (twice the equivalent friction force in one direction).

TABLE III-41

Accumulator Friction

S/A	Serial No.	Peak-to-Peak Friction (psi)*	
		Bench Test	Preflight Check
1	B015	1.3	1.0
2	B016	0.8	0.9

*Max acceptable value = 2.0 psi.

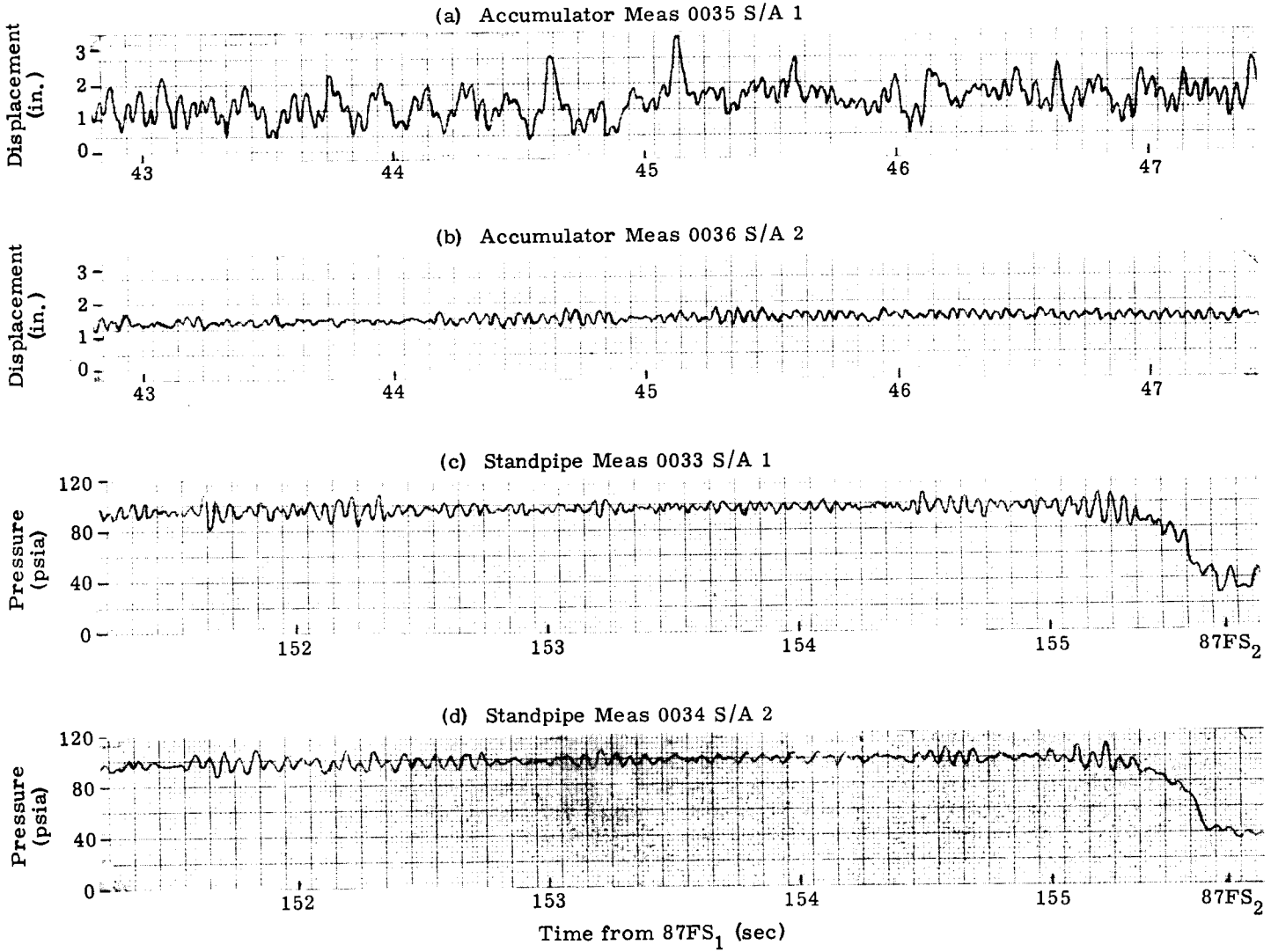

Fig. III-29. Fuel Accumulator and Oxidizer Standpipe Measurements

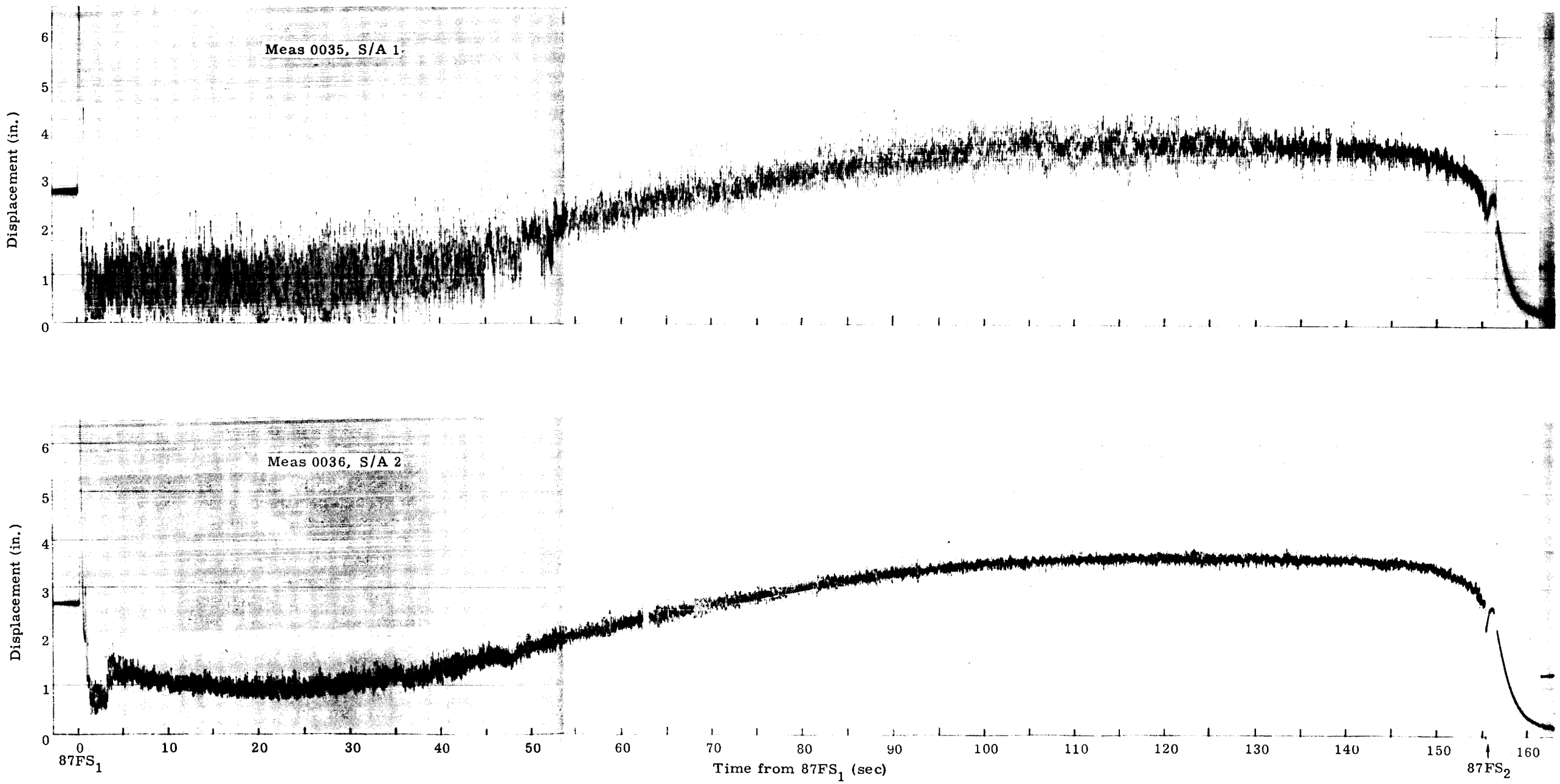

Fig. III-30. GT-4 Fuel Accumulator Piston Travel

C. PRESSURIZATION SUBSYSTEM

1. Prelaunch Pressurization

At approximately T-195 minutes, all propellant tanks were pressurized, through the AGE, from blanket pressure level to flight pressure levels. The resultant time-pressure profiles (Fig. III-31) indicate that the process was normal. The tank ullage lockup pressures obtained from landline measurements made at T-0 and the related normal operating pressure ranges are presented in Table III-42.

TABLE III-42

Tank Ullage Lockup Pressures

Meas	Parameter	Normal Range (psia)	Measured (psia)
4125	Stage I fuel tank pressure	27.5 to 31.5	28.8
4129	Stage I oxidizer tank pressure	30.5 to 34.5	33.0
4602	Stage II fuel tank pressure	49.5 to 54.5	52.0
4605	Stage II oxidizer tank pressure	53.5 to 57.5	54.5

Data from the GT-3 flight countdown indicated that the Stage I fuel tank ullage gas pressure dropped approximately 0.8 psi when the prevalves were opened, and would have resulted in activation of the pressure switch low launch circuit light if the switch pressure tolerance had been on the high side. To prevent this from occurring on GT-4, the lockup pressure of the tank was increased by 1.0 psi. This was an interim measure, and further studies are being made to determine corrective action for GT-5 and up.

2. Flight Pressurization

Stages I and II ullage gas pressure time histories are shown in Figs. III-32 through III-35. These graphs show flight-measured, preflight-predicted, and postflight-reconstructed pressure histories. The flight-measured pressures were obtained by averaging the telemetered output from each pair of pressure transducers in the individual tanks. The preflight-predicted curves were taken from Ref. 19. The postflight reconstruction was based on measured values of engine performance, propellant temperatures and propellant loadings. A comparison of significant pressurization system parameters taken at FS + 100 seconds is given in Table III-43.

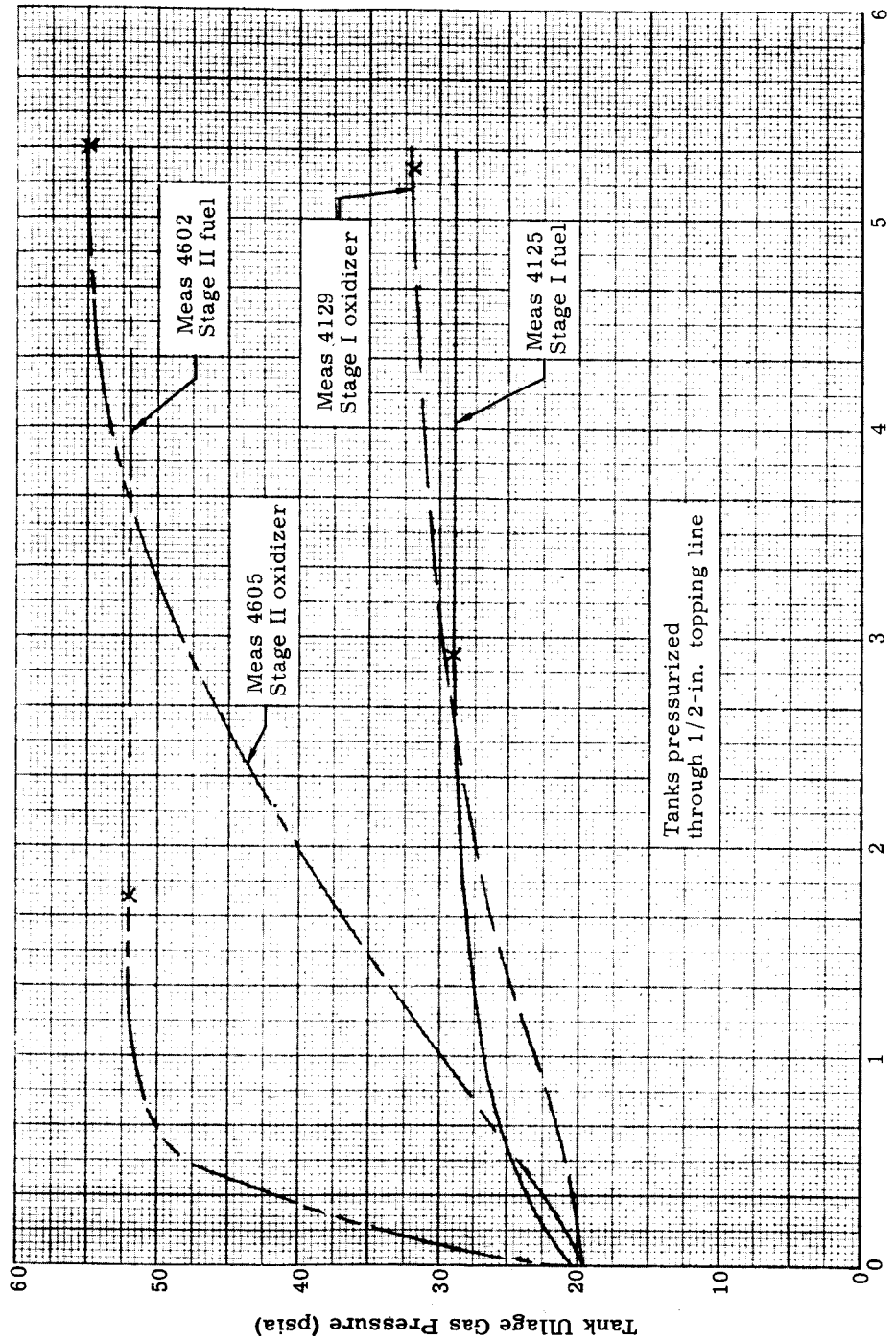

Fig. III-31. Tank Pressurization Cycle (blanket to flight pressure)

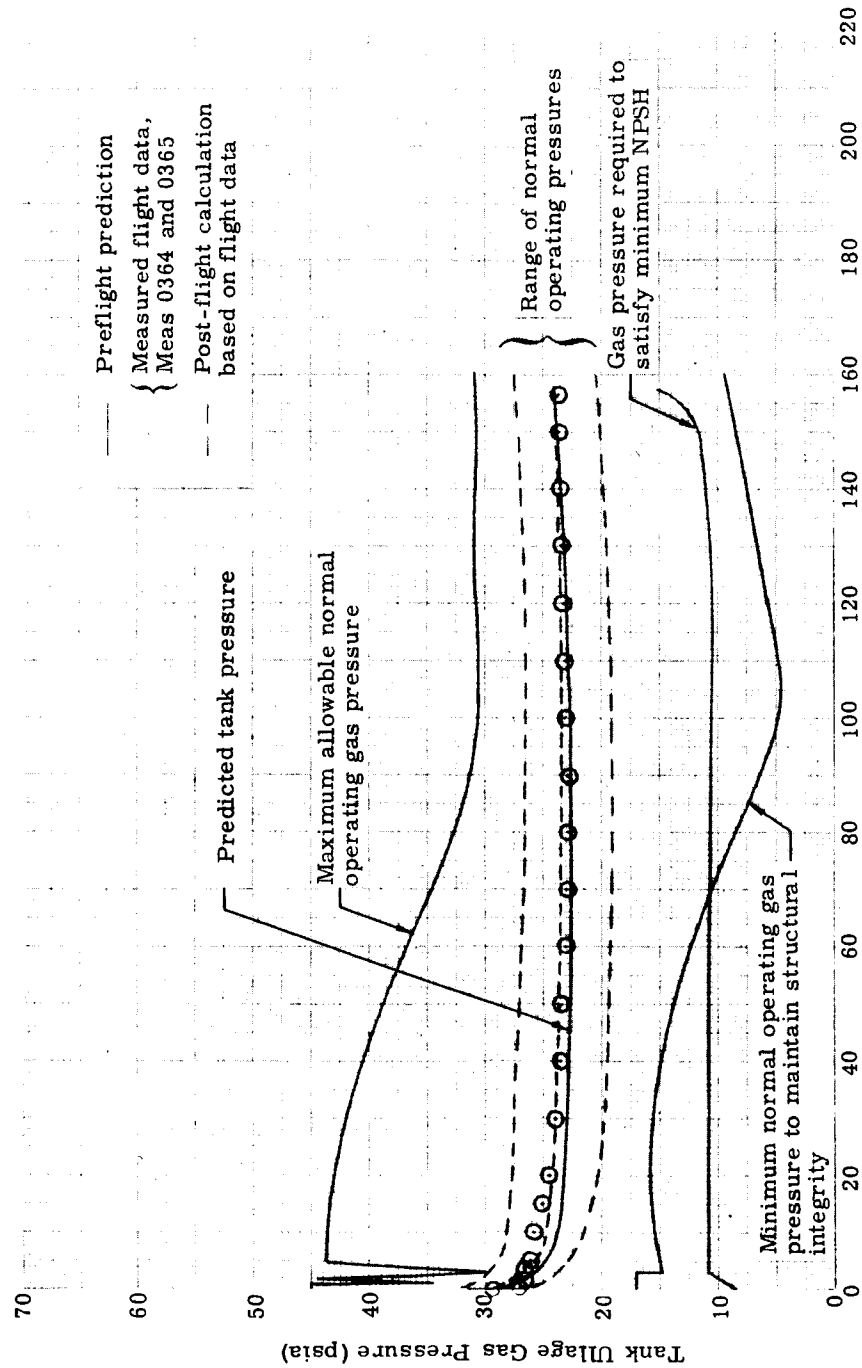

Fig. III-32 Stage I Fuel Tank Ullage Pressure History

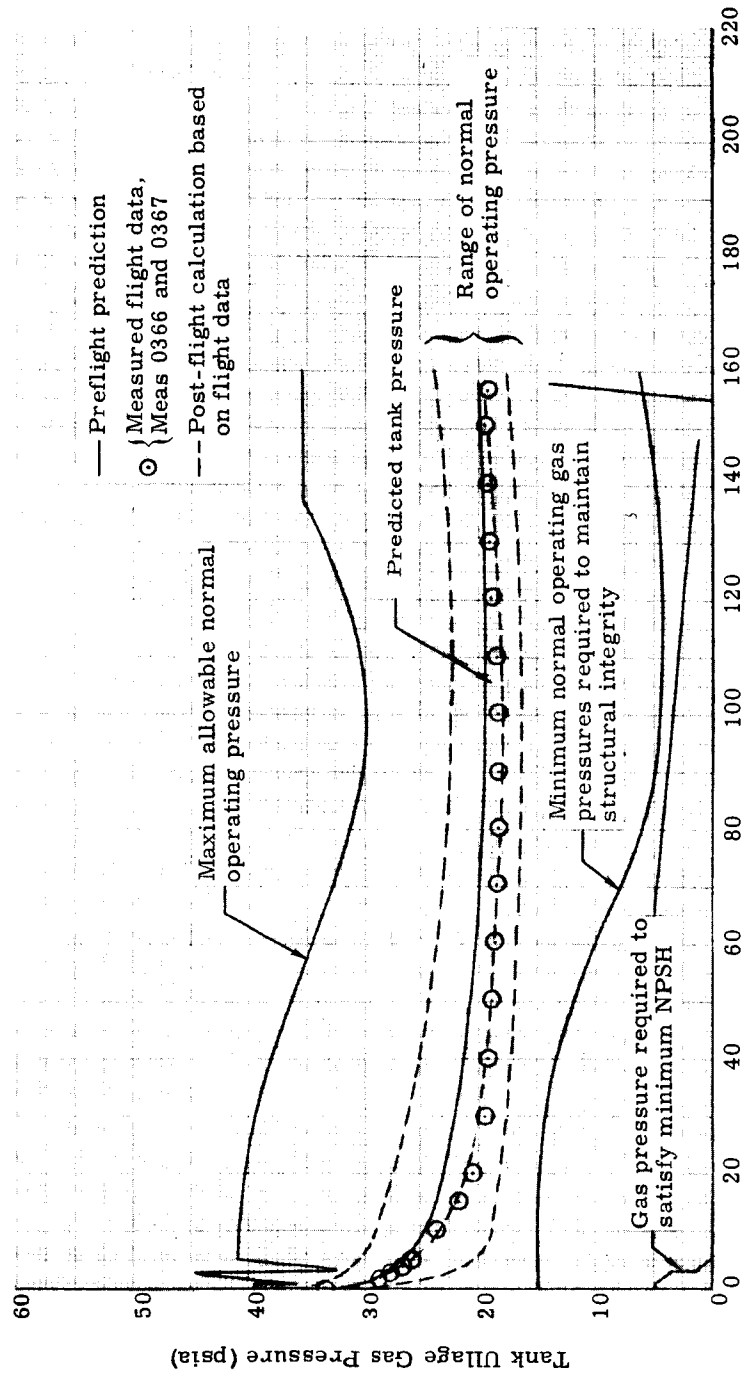

Fig. III-33. Stage I Oxidizer Tank Ullage Pressure History

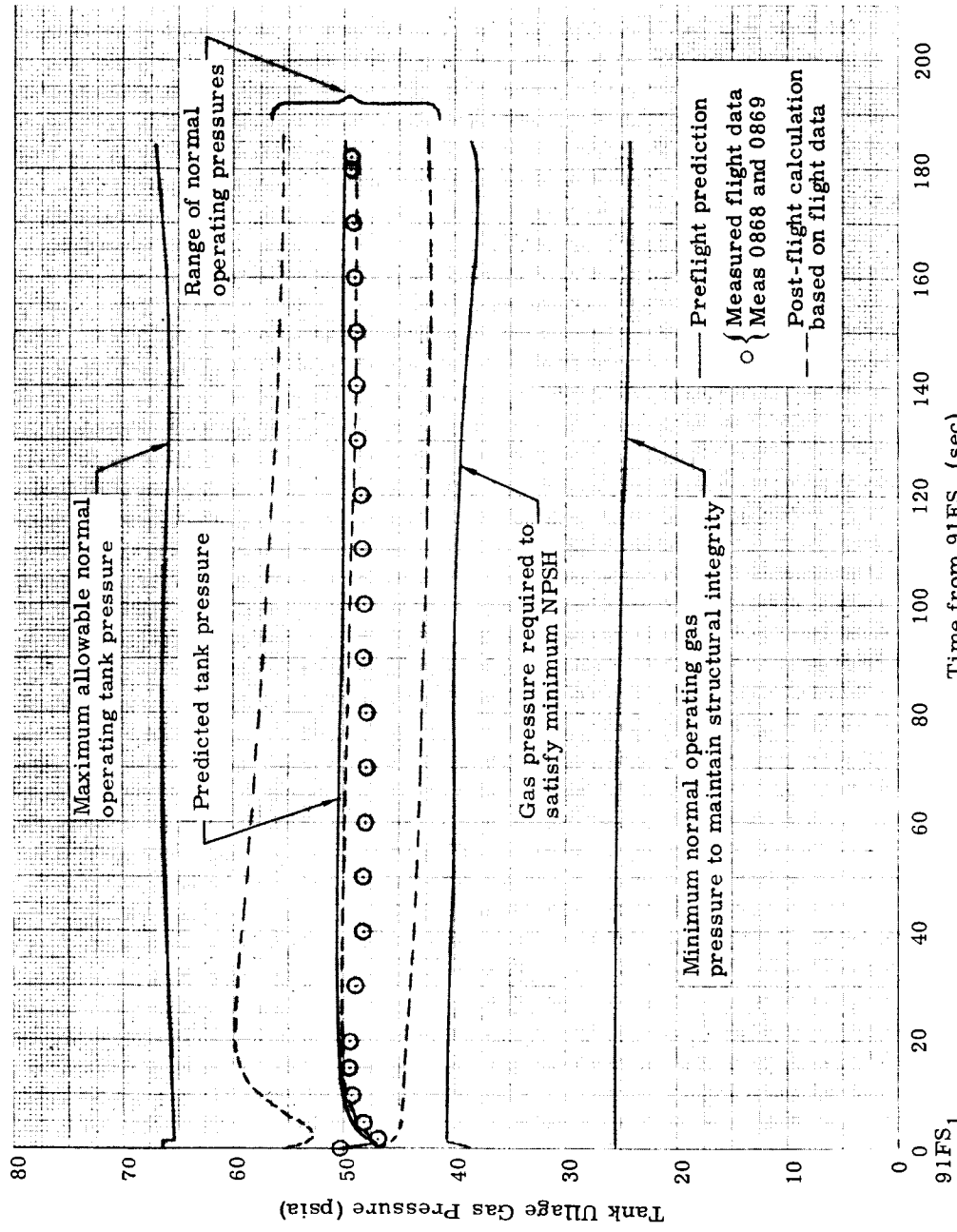

Fig. III-34. Stage II Fuel Tank Ullage Pressure History

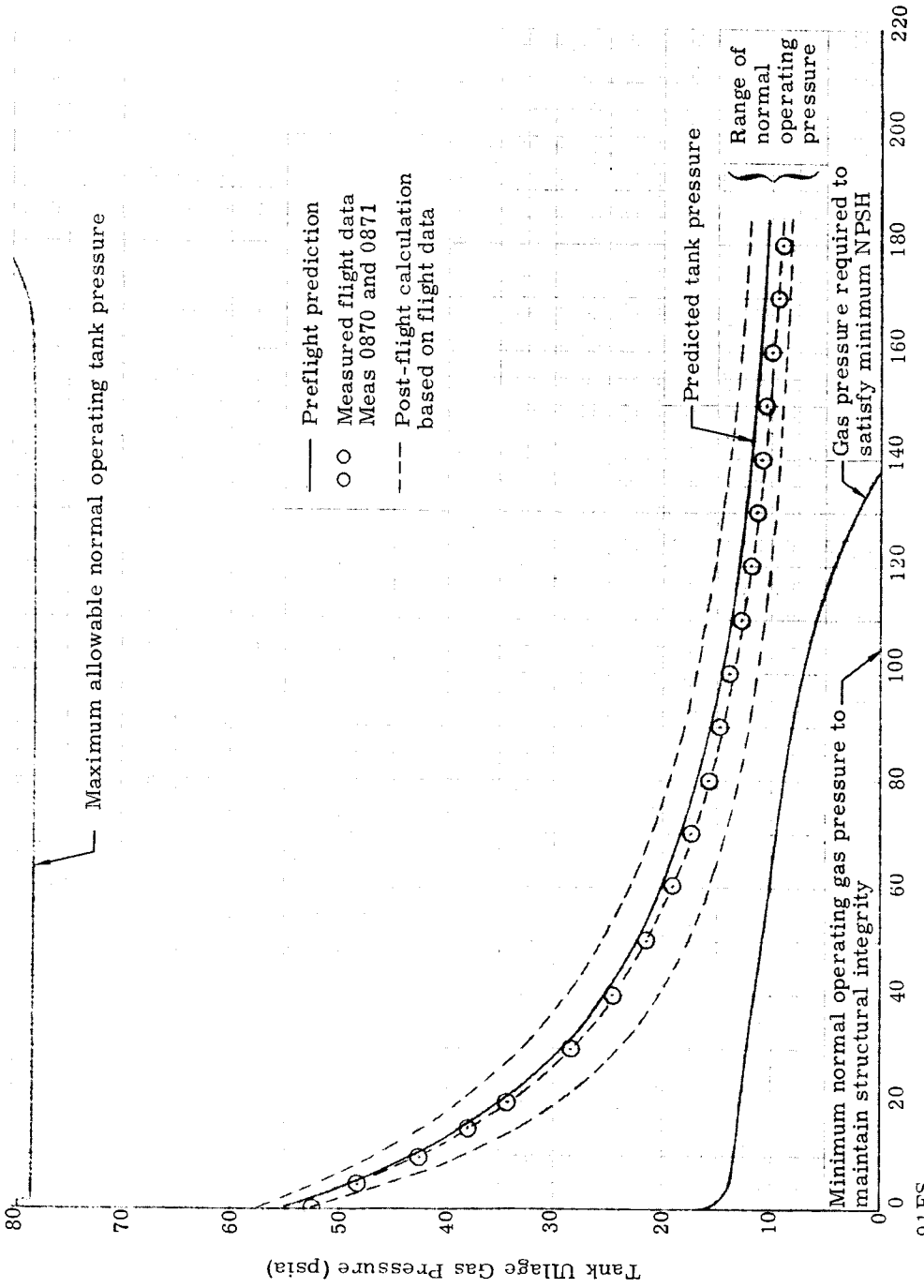

Fig. III-35. Stage II Oxidizer Tank Ullage Pressure History

TABLE III-43

Stages I and II Pressurization System
Parameters at FS_1 + 100 Seconds

Parameter	Preflight Predicted	Flight	Postflight Reconstructed
Stage I fuel tank			
Tank pressure, P_{FT} (psia)	22.82	23.01	23.30
Nozzle inlet pressure, P_{FPOI} (psia)*	254.	262.	262.
Nozzle inlet temperature, T_{FPOI} (° F)	242.	231.	231.
Flow ratio, W_{FP}/Q_{FS} (lb/cu ft)	0.0655	0.0656	0.0656
Stage I oxidizer tank**			
Tank pressure, P_{OT} (psia)	19.52	18.40	18.07
Orifice inlet pressure, P_{OPOI} (psia)	503.	482.	482.
Orifice inlet specific enthalpy, H_{OPOI} (Btu/lb)	362.	344.	344.
Flow ratio, W_{OP}/Q_{OS} (lb/cu ft)	0.1727	0.1729	0.1729
Stage II fuel tank			
Tank pressure, P_{FT} (psia)	50.15	48.13	49.50
Nozzle inlet pressure, P_{FPOI} (psia)***	407.	405.	405.
Nozzle inlet temperature, T_{FPOI} (° F)	229.	263.	263.
Flow ratio, W_{FP}/Q_{FS} (lb/cu ft)	0.1446	0.1377	0.1377
Stage II oxidizer tank			
Tank pressure, P_{OT} (psia)	14.65	13.74	13.34
Propellant flow rate, Q_{OS} (cu ft/sec)	2.275	2.292	2.292

*Nozzle diameter, Stage I fuel = 0.48 in.
**Flow control Venturi coefficient = 0.0510
***Nozzle diameter, Stage II fuel = 0.26 in.

Figures III-36, III-37 and III-38 present the preflight-predicted and the inflight-measured pressurization parameters at the orifice or nozzle inlet. Autogenous gas temperature at the nozzle inlet, T_{FPOI}, in the Stage II fuel autogenous system increased abnormally during flight (Fig. III-38). The temperature appeared normal until $91FS_1$ + 6 seconds, after which it increased to a value of 277° F at $91FS_1$ + 180 seconds. This temperature level was out of the flow box specified in the Martin/Aerojet Interface Document (Ref. 23). Autogenous gas pressure at the nozzle inlet was normal. The probable cause of the abnormal temperature was one of the following:

(1) Reduction in the coolant flow rate of the gas cooler.

(a) Coolant leak overboard upstream of the gas cooler.

(b) Restriction in the coolant flow circuit.

(2) Coolant leak within the gas cooler into the hot gas autogenous flow stream.

A coolant leak or a restriction to the coolant flow rate which would reduce the effective coolant capability by approximately 6% is required to increase the nozzle inlet temperature to the levels noted on this flight.

A coolant leak into the hot gas autogenous flow stream could also increase the nozzle inlet temperature to that noted during flight. The coolant is liquid fuel consisting of a 50% blend of hydrazine and unsymmetrical dimethylhydrazine (UDMH). At approximately 500° F, this blend decomposes into its constituent parts and the hydrazine may undergo a chemical reaction liberating its heat of combustion. This additional energy added to the autogenous pressurizing gas may have caused the nozzle inlet temperature to be higher than expected.

The Stage II fuel tank pressure had an unexplained deviation from the preflight predicted curve, and differs from the postflight-reconstructed pressures (Fig. III-34). The maximum difference between flight-measured pressure and postflight-reconstructed pressure is 2 psi at $91FS_1$ + 60 seconds. A shift in the molecular weight of the autogenous pressurizing gas, initiated by the abnormal gas cooler performance, can account for this pressure deviation.

3. Component Performance

All MDS tank pressure sensors functioned normally. The maximum and mean pressure differences between pairs (A and B sensors) of sensors in each of the individual propellant tanks are shown in Table III-44.

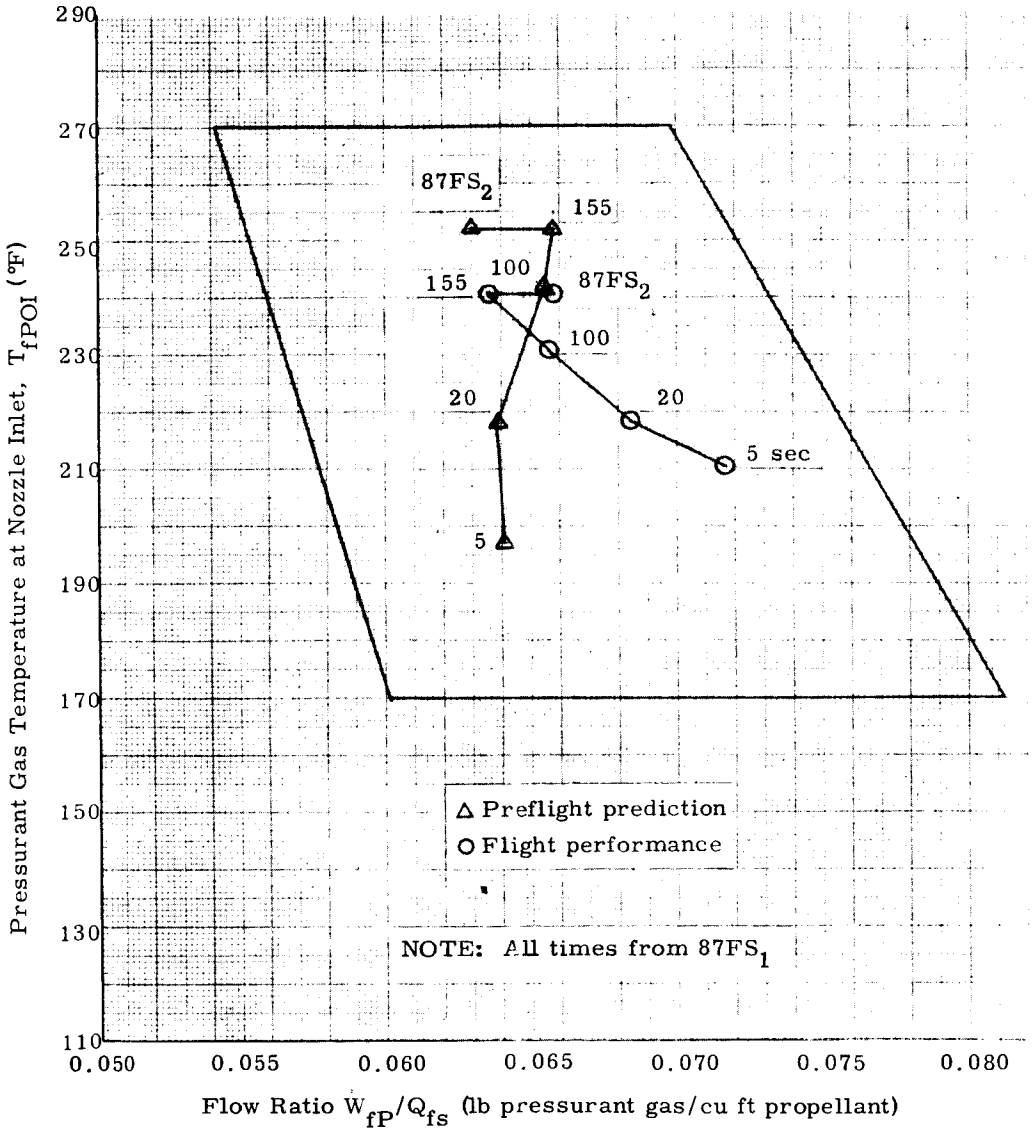

Fig. III-36. Stage I Fuel Tank Pressurant Performance

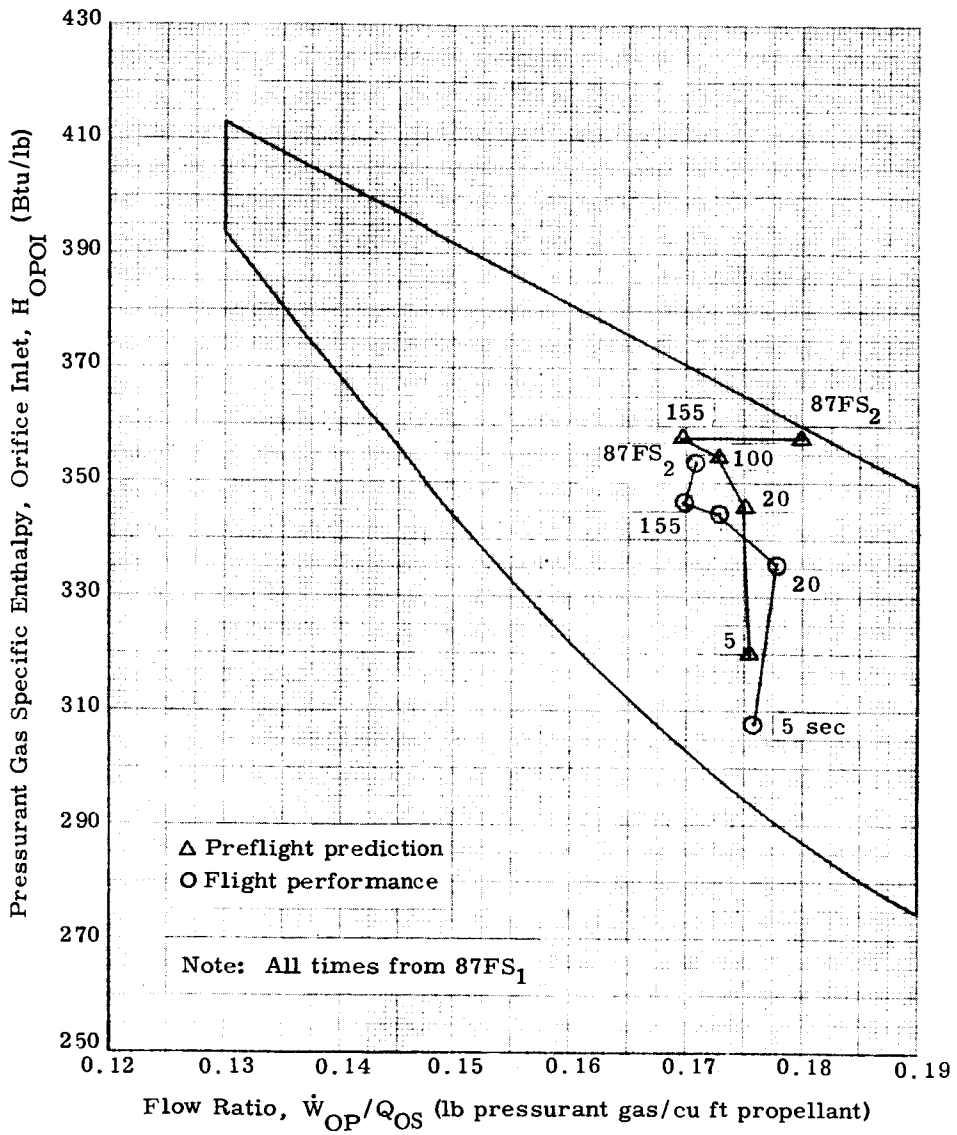

Fig. III-37. Stage I Oxidizer Tank Pressurant Performance

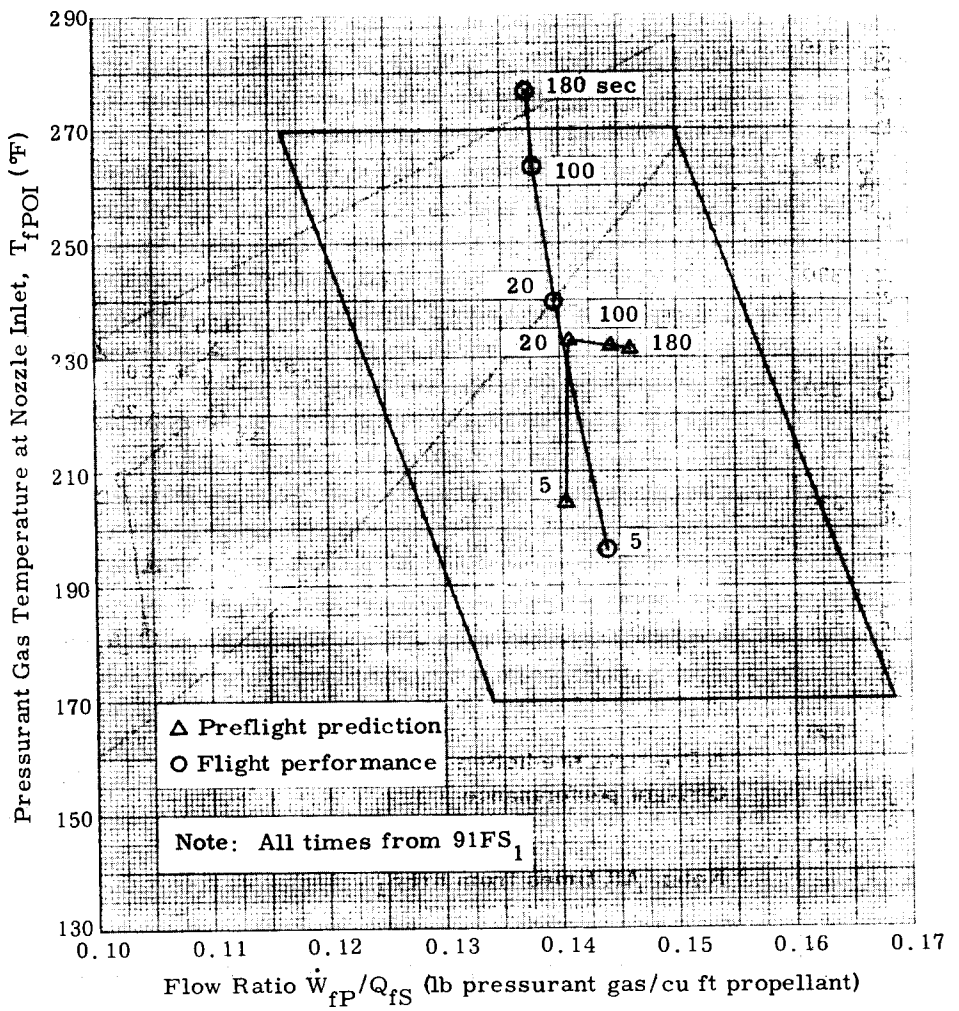

Fig. III-38. Stage II Fuel Tank Pressurant Performance

TABLE III-44

Comparison of Tank Pressure Sensor Pairs

Tank	Maximum Difference (psi)	Mean Difference (psi)	Maximum Allowable Difference (psi)
Stage I oxidizer	0.19	0.06	1.50
Stage I fuel	0.37	0.15	1.50
Stage II oxidizer	0.29	0.12	2.25
Stage II fuel	0.39	0.26	2.25

The Stage I fuel tank pressure and vent topping quick disconnect (2DFVT) did not release by lanyard actuation at 11 inches of rise, as planned, but was separated from the launch vehicle when the disconnect failed as a result of the taut umbilical hose after the vehicle had risen approximately 20 feet. This malfunction is discussed in Chapter XIII of this report.

D. ENVIRONMENTAL

1. Launch Vehicle Air-Conditioning System

The air-conditioning system, which serves launch vehicle Compartment 2 and all engine start cartridges, was operative continuously during the prelaunch activities until vehicle liftoff. The system operated satisfactorily. Table III-45 presents a summary of the system parameters.

2. Stage I Oxidizer Tank Dome Pressure at Staging

Pressure rise on the Stage I oxidizer tank dome during the staging sequence was measured by one high-frequency pressure transducer (Meas No. 1085) located on the tank dome surface at Station 607, WL 58 and BL 27R. This location was identical to that on GLV-2 and GLV-3. Figure III-39 depicts the recorded pressure-time profile and indicates that a maximum peak pressure of 69.5 psia occurred at 0.685 second after $91FS_1$. This measurement will not be included on GLV-5 and subsequent launch vehicles.

TABLE III-45

Air-Conditioning System Performance

Meas	Description	Observed Range	Specified Range	Remarks
4403	Launch vehicle supply air temperature	49° to 53° F	48° to 65° F (Compartment 2) 48° to 58° F (Engine start cartridges)	Temperature of air supplied to launch vehicle Compartment 2 and the engine start cartridges
4405	Compartment 2 supply air mass flow rate	Approximately 90 lb/min	82 lb/min (minimum)	
4418	Compartment 2 exhaust air temperature	56° to 63° F	40° to 75° F	Manual hold parameter
4045	Start cartridge temperature S/A 1	59° F (at liftoff)	42° to 90° F	S/N 0003340 manual hold parameter
4046	Start cartridge temperature S/A 2	61° F (at liftoff)	40° to 88° F	S/N 0002720 manual hold parameter
4612	Start cartridge temperature S/A 3	59° F (at liftoff)	35° to 83° F	S/N 0859279 manual hold parameter

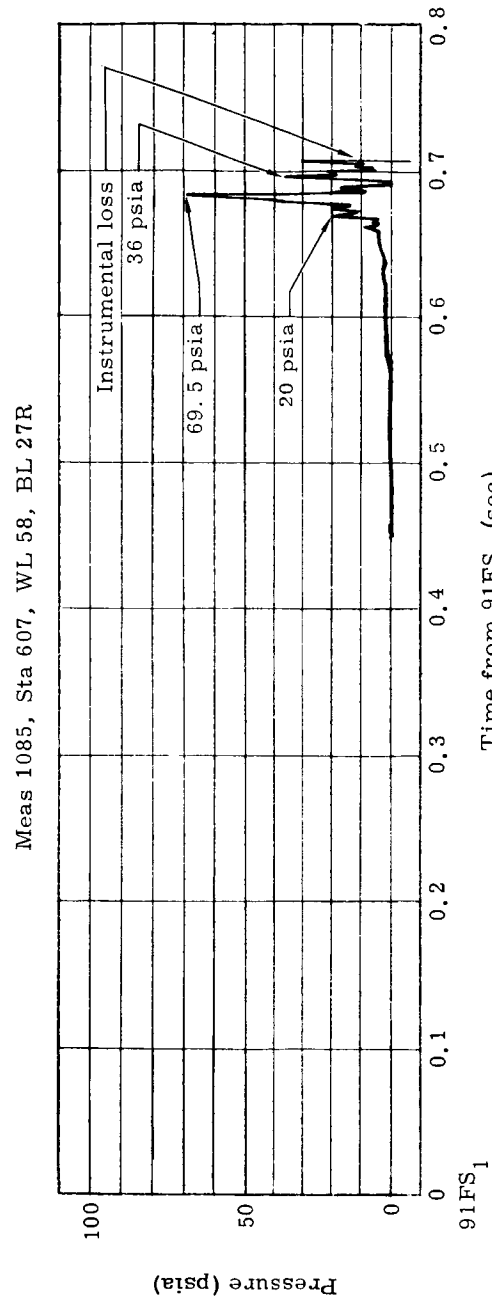

Fig. III-39. Stage I Oxidizer Tank Dome Pressure During Staging

IV. FLIGHT CONTROL SYSTEM

Analysis of the GLV-4 control system performance indicated satisfactory operation during both Stage I and Stage II flight. The primary flight control system (FCS) was in command throughout the flight, and no switchover to the secondary system was required.

A. STAGE I FLIGHT

1. Ignition and Liftoff Transients

Peak actuator travels and rate gyro disturbances recorded during the ignition and holddown period are presented in Table IV-1.

TABLE IV-1

Transients During Stage I Holddown Period

Actuator Designation	Maximum During Ignition		Maximum During Holddown Null Check (in.)	
	Travel (in.)	Time from T-O (sec)		
Pitch, 1_1	-0.142	-2.444	+0.010	
Yaw/roll, 2_1	+0.231	-2.444	-0.020	
Yaw/roll, 3_1	+0.151	-2.444	+0.010	
Pitch, 4_1	-0.040	-2.444	-0.020	
	Maximum Rate Stage I Gyro (deg/sec)		Maximum Rate Stage II Gyro (deg/sec)	
Axis	Primary	Secondary	Primary	Secondary
Pitch	+0.19	-0.28	+0.29	+0.30
Yaw	+0.19	+0.10	-0.29	+0.19
Roll	+0.58	+0.60	--	--

The combination of thrust misalignment and engine misalignment at full thrust initiated a roll transient at liftoff. The response of the FCS to correct the offset kept the roll rate to a maximum of 0.8 deg/sec CW at 0.3 second after liftoff (Fig. IV-1). The rate oscillation had a basic frequency of 4.6 rad/sec, damping out in 1.2 seconds. As shown on the roll error curve in Fig. IV-1, a roll bias of 0.3 degree CW was introduced at liftoff by the equivalent engine misalignment of 0.06 degree.

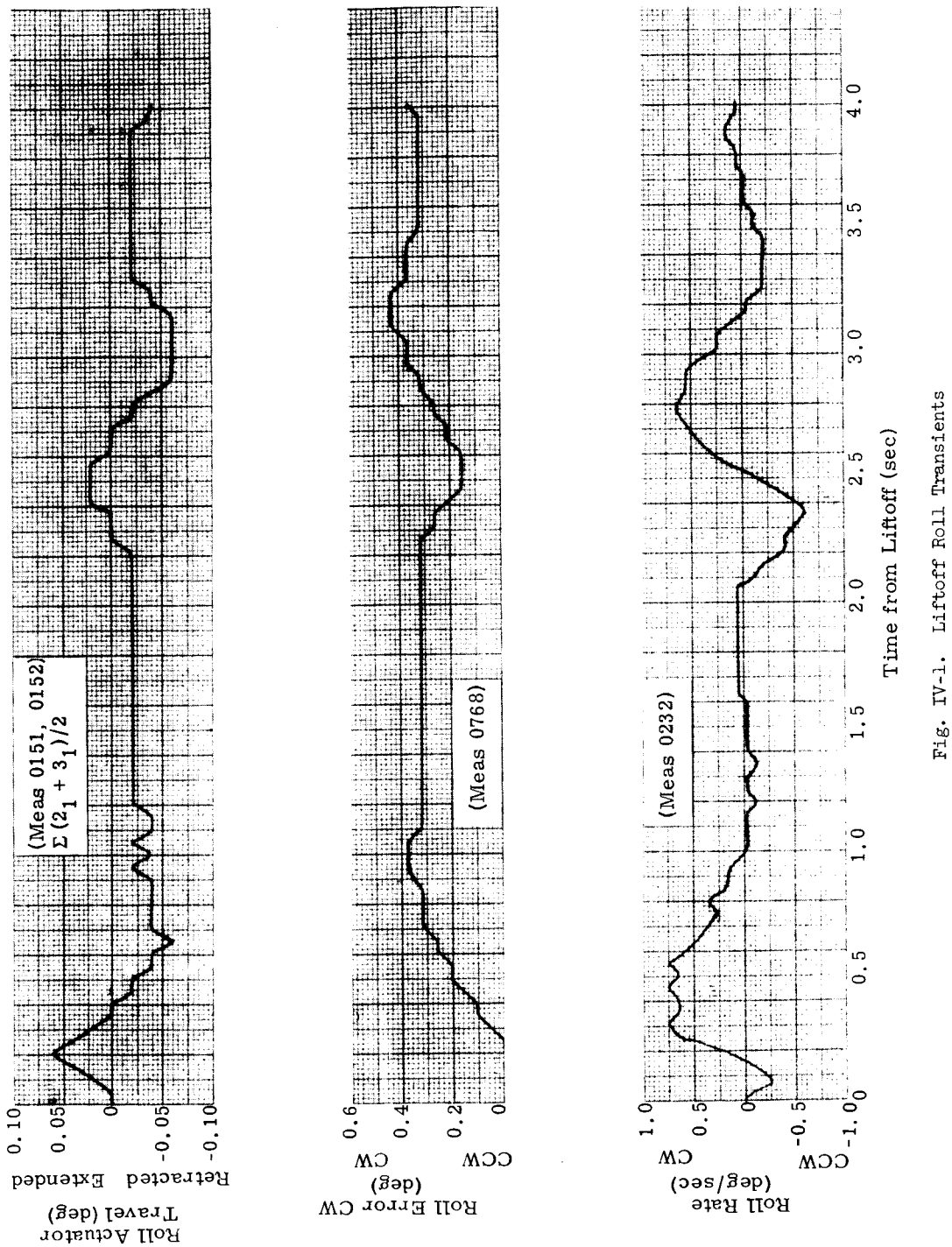

Fig. IV-1. Liftoff Roll Transients

2. Post Liftoff Roll Transient

At LO + 2.1 seconds, a second roll transient occurred. Because the vehicle's acceleration and roll rate (Fig. IV-1) preceded the roll error signal and the actuator motion, it is concluded that the transient was due to an external vehicle disturbance. The roll control system responded to correct for the disturbance. The maximum rates experienced during the disturbance were -0.6 and +0.75 deg/sec. The maximum roll error was 0.4 degree CW. As in the liftoff transient, the rate oscillation contained the basic rigid body frequency of 4.6 rad/sec and was damped out in less than 1.5 seconds.

A six-degree-of-freedom analog simulation has been initiated in an effort to reconstruct the vehicle motions and to ascertain the magnitude and time duration of the external forcing function.

3. Roll and Pitch Programs

Measured flight data reflecting performance of the TARS roll and pitch programs are shown in Table IV-2. Within telemetry accuracy, the rate gyros indicate that proper roll and pitch programs were executed during flight. The maximum roll and pitch rates, which occurred at the start of their respective programs, were 1.6 deg/sec CW for roll and 0.7 deg/sec pitch-down.

TABLE IV-2

TARS Roll and Pitch Programs

Program	Flight Event Time from LO (sec)	Nominal Time (sec)	Flight Data, Stage I Rate Gyro (deg/sec)		Torquer Monitor Rates (deg/sec)	Nominal Rates (deg/sec)
			Primary	Secondary		
Roll						
Start	10.10	10.16	+1.23	+1.14	+1.22	+1.25
Stop	20.40	20.48				
Pitch Step 1						
Start	22.95	23.04	-0.67	-0.66	-0.69	-0.709
Pitch Step 2						
Start	88.21	88.32	-0.47	-0.57	-0.50	-0.516
Pitch Step 3						
Start	118.66	119.04	-0.18	-0.28	-0.25	-0.235
Stop	162.07	162.56				

4. TARS and IGS Comparison (Stage I)

The TARS and IGS attitude signals during Stage I flight for pitch, yaw and roll are presented in Figs. IV-2, IV-3 and IV-4.

The dispersion between the TARS and IGS attitude signals was caused by a combination of TARS and IGS gyro drifts, errors in open-loop guidance programs and reference axis cross-coupling. The dispersions at BECO and the known contributing factors are given in Table IV-3.

TABLE IV-3

TARS and IGS Dispersion at BECO

Axis	Total Dispersions (deg)	Contributing Factors					
		TARS Drift				TARS Guidance Program Errors (deg)	Uncertain Dispersions (deg)
		Anticipated Drift at BECO (deg)	Preflight Drift Rate				
			On Null (deg/hr)	Off Null (deg/hr)	g Sensitive (deg/hr/g)		
Pitch	+1.15	-0.06	-0.59	-1.86	--	+1.23	-0.02
Yaw	-0.63	-0.18	-3.52	-1.74	--	--	-0.45
Roll	-1.5	-0.46	-3.30	-1.44	19.86	-0.25	-0.79

The Stage I pitch dispersion was predominantly caused by a low TARS pitch program, as indicated in Table IV-3. There was no evidence of any appreciable TARS or IGS drift or IGS pitch program errors.

The Stage I yaw dispersion is largely unexplained, as noted in Table IV-3. However, the magnitude was not excessive, and was well within the TARS 3σ drift limits.

A significant contributor to the dispersion in roll is attributed to the axial g sensitive drift term, acting on the TARS roll gyro. The magnitude listed in Table IV-3 (0.46 degree CCW) assigned to TARS roll drift was primarily due to the g sensitive drift. This quantity was derived using the preflight measured drift rate and the g compensation level set into the gyro, and is well within the 3σ limits.

The uncertain dispersions are attributed to cross-coupling effects in IGS, IGS gyro drifts, IGS guidance program errors and additional TARS gyro drifts.

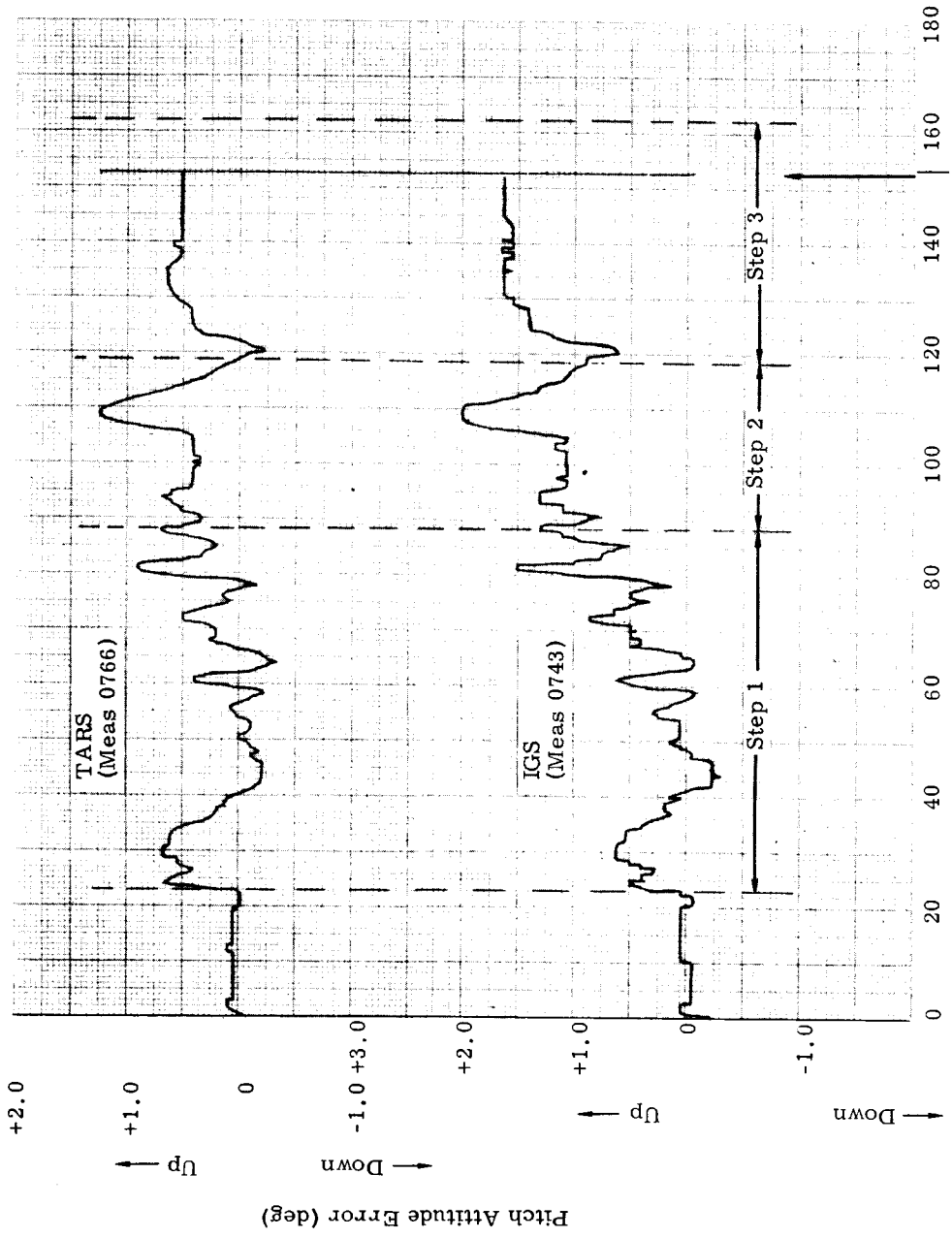

Fig. IV-2. Pitch Attitude Error History During Stage I Flight

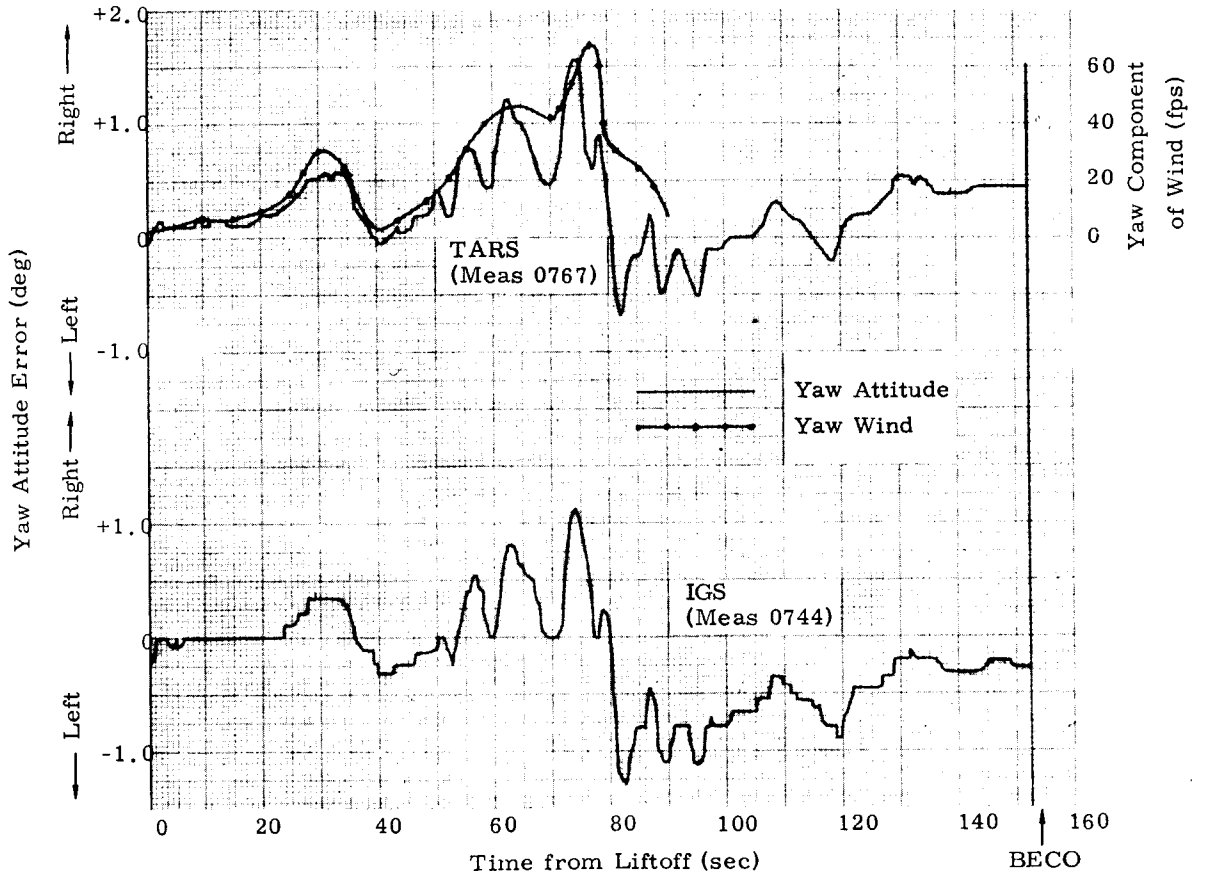

Fig. IV-3. Yaw Attitude Error History During Stage I Flight

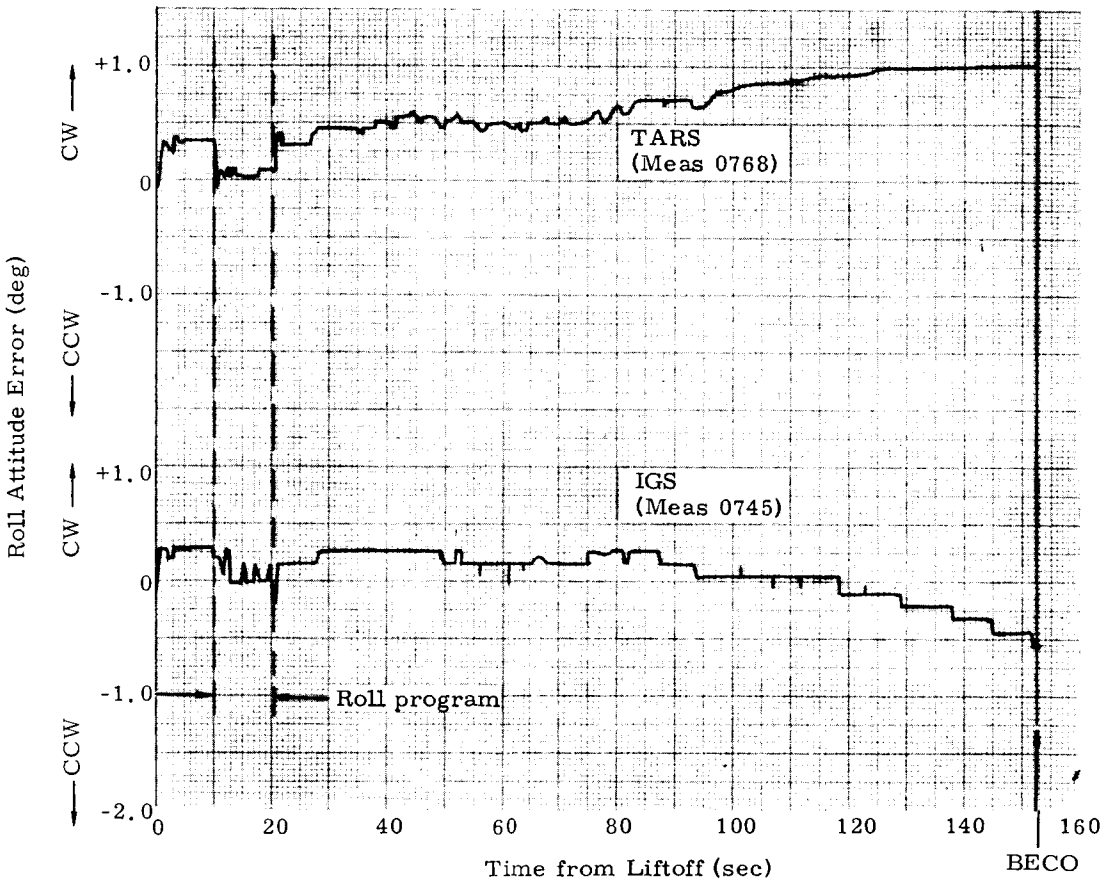

Fig. IV-4. Roll Attitude Error History During Stage I Flight

5. Stage I Flight Disturbances

Analysis of the primary FCS TARS attitude signals (Figs. IV-2, IV-3 and IV-4) show responses to wind disturbances and to the guidance programs.

Vehicle disturbances during flight were caused by the prevailing winds aloft. For example, the comparison of the yaw component of wind velocity with the actual vehicle yaw attitude is shown in Fig. IV-3. The control system response to these disturbances was normal and well controlled. During these wind disturbances, oscillations occurred in pitch and yaw at the predicted GT-4 rigid body oscillatory mode frequencies, varying with flight condition, between 1.0 and 1.6 rad/sec with an average peak-to-peak overshoot amplitude of less than 0.5 degree of attitude error. In roll, the oscillations occurred at the roll rigid body natural frequency of approximately 1 cps with an average peak-to-peak amplitude of 0.1 degree. These oscillations were similar in nature to those experienced on the previous Gemini flights, due to wind disturbances.

At the time of gain change (LO + 104.7 seconds), there was a noticeable (but very highly damped) pitch transient reaching a maximum of 1.2 degrees nose-up. Prior to gain change, the pitch attitude error was 0.37 degree nose-up. The reduction of the attitude and rate gains reduces the amount of engine deflection thus causing the transient to occur. Analyses indicate that the control system reacted properly to the flight conditions which existed before and after gain change.

Toward the end of Stage I flight, the propellant slosh mode was excited in the yaw channel. The limit cycle oscillation exhibited low amplitude rates of less than 0.2 deg/sec with no appreciable changes in attitude.

The maximum rates and attitude errors recorded during Stage I flight are shown in Table IV-4.

TABLE IV-4

Stage I Maximum Rates and Attitude Errors

	Stage I Rates (deg/sec)		Time from Liftoff (sec)	
Axis	Primary	Secondary	Primary	Secondary
Pitch	-1.07 +0.38	-1.15 +0.30	82.614 0.406	82.564 0.306
Yaw	-0.66 +0.56	-0.74 +0.58	80.100 83.114	80.114 82.914
Roll	+1.61 -0.58	+1.61 -0.69	10.8 2.356	10.7 2.356

TABLE IV-4 (continued)

Axis	Attitude Error* (deg)	Time from Liftoff (sec)
Pitch	+ 1.310 - 0.256	108.2 64.0
Yaw	+ 1.623 - 0.617	74.0 82.1
Roll	+ 1.101 0.0	141.0 10.6

*Bias removed.

6. Static Gains

The primary FCS static gains (as determined from telemetry data) were within the instrumentation inaccuracy of preflight evaluations, and indicate that no static gain deterioration was experienced during Stage I boost flight.

B. STAGE II FLIGHT

1. Stage Separation

During the staging event, moderate rates and attitude errors of the sustainer vehicle were observed. The maximum attitude errors recorded were as follows:

Pitch	+ 0.427 deg at BECO + 1.1 sec
Yaw	+ 1.206 deg at BECO + 2.6 sec
Roll	- 1.256 deg at BECO + 1.1 sec

The maximum sustainer vehicle rates recorded during staging were as follows:

Axis	Rate (deg/sec)		Time from BECO (sec)	
	Primary	Secondary	Primary	Secondary
Pitch	- 0.96	- 0.99	1.1	1.1
Yaw	+ 0.78	+ 0.77	1.4	1.4
Roll	- 2.83	- 2.58	0.4	0.4

These were also the maximum recorded rates for the entire Stage II flight, except for a guidance-induced pitching rate of the maximum -2.0 deg/sec about 2.6 seconds after guidance initiation.

In general, all staging-induced sustainer rate transients were completed by BECO + 4 seconds; a 15-second lightly-damped pitching rate oscillation of approximately 0.8 cps was observed with a maximum peak-to-peak rate of about 0.3 deg/sec (Fig. VI-1), and an accompanying peak-to-peak displacement error of less than 0.1 degree. From linear analyses, this frequency is in agreement with that of the Stage II oxidizer slosh mode.

2. Slosh-Induced Oscillations

From LO + 200 to LO + 310 seconds, propellant slosh modes caused vehicle limit cycle oscillations in pitch, varying between 1 and 2 cps. The sloshing perturbations in pitch coupled into roll at the same frequency and exhibited a low amplitude (approximately 0.15 degree peak-to-peak in attitude and a maximum of 0.5 degree peak-to-peak in rate) limit cycle in both pitch and roll. The sloshing oscillation in yaw attitude and rate was less than that observed in pitch. The differences in magnitude between the limit cycle in pitch and yaw are attributed to the combination of FCS static gain and dynamic parameter spread about the nominal design value in the respective channels. For GT-4, the pitch channel static gains and dynamics combine to produce the larger rate limit cycle oscillation. The probable causes for excitation of the sloshing mode were the pitching motions of the vehicle due to guidance commands, as well as by the disturbance caused by the constantly changing center of gravity of the vehicle, and the attitude bias error adjustment which was immediately evident when the separation transient disappeared. In all cases, the FCS operated within its design specification requirements.

3. Pitch and Yaw Attitude Biases

The FCS indicated an attitude bias in both pitch and yaw during Stage II flight which was well within predicted limits. The attitude error signals in pitch and yaw are shown in Figs. IV-5 and IV-6. The attitude biases are caused by engine thrust vector misalignment due to structural deformation at the engine gimbal assembly, center-of-gravity travel off the vehicle longitudinal axis, and the position of the roll thrust vector off the longitudinal axis. The GT-4 yaw bias of + 1.3 degrees compares favorably with the GT-3 bias of 1.4 degrees and is similar to the biases experienced on other Gemini flights. The GT-4 pitch bias of - 0.32 degree is the same order of magnitude as the - 0.6 degree observed on GT-3. The pitch actuator length adjustment incorporated on GT-2 and subsequent vehicles greatly reduced the pitch bias from that experienced on GT-1. The deviation of the pitch and yaw

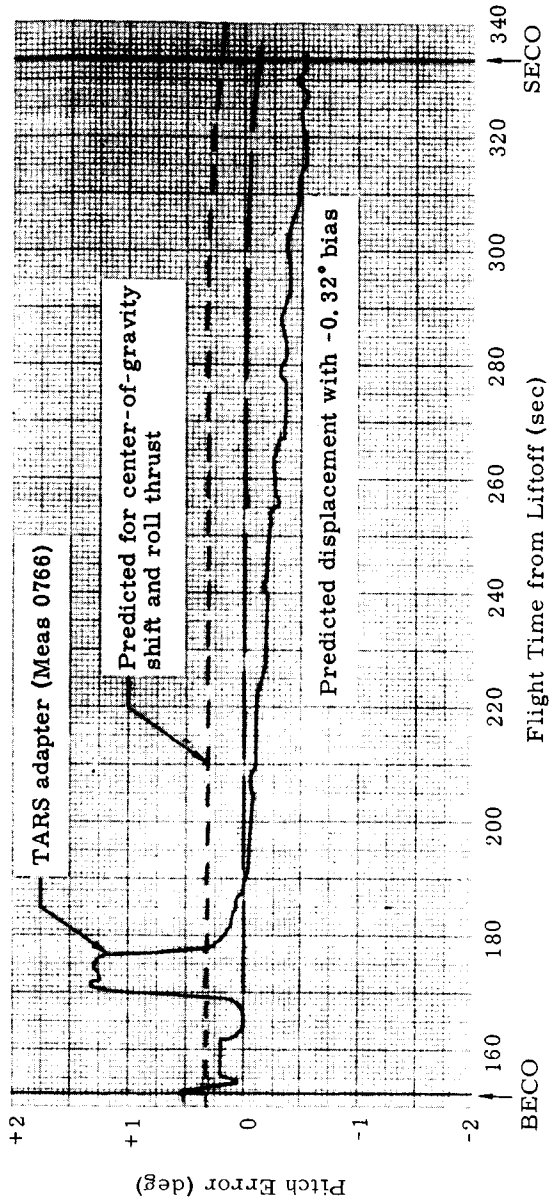

Fig. IV-5. Pitch Axis Displacement Error During Stage II Flight

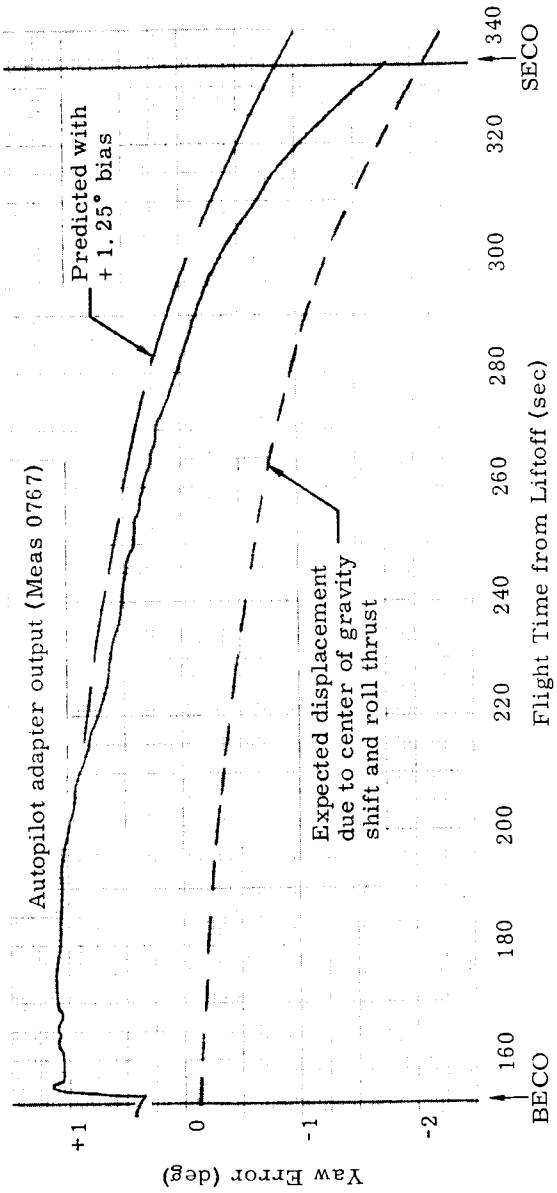

Fig. IV-6. Yaw Axis Displacement Error During Stage II Flight

attitude errors from the predicted values (which assumed fixed bias, center-of-gravity shift and roll thrust bias) toward the end of Stage II flight is similar to that experienced on previous Gemini flights. This is partially attributed to the fact that the vehicle experiences a g loading which is higher than the fixed 2.2 g nominal TARS roll gyro drift compensation at this time. Even though this drift is not reflected in roll attitude error and, consequently, not corrected by the roll FCS, it is sensed as a component in pitch and yaw.

4. Guidance Initiate

The guidance enable command was generated by the TARS timer at LO + 162.033 seconds. The first pitch guidance command was received at LO + 168.68 seconds and consisted of a small command followed by a full 2.0 deg/sec pitch-down command for 6.5 seconds. Low magnitude pitch commands occurred during the remainder of the flight. The first yaw command was received at LO + 169.47 seconds and all commands were of low magnitude, not exceeding 0.05 deg/sec for all of Stage II flight. The rate gyro signals substantiated the correct response to the guidance commands.

5. Static Gains

The primary FCS static gains as determined from telemetry data were within the instrumentation inaccuracy of preflight calculations.

C. POST-SECO FLIGHT

1. Vehicle Motions

Prior to SECO, the pitch actuator was retracted, producing a sustainer engine gimbal deflection of 0.0466 degree to correct for a pitch error of -0.644 degree nose-down. In yaw, the error was -1.785 degrees with an equivalent engine gimbal deflection of 0.257 degree. At SECO, the roll error was 0.117 degree CCW.

Pitch, yaw and roll attitude errors and rates during the period from SECO through spacecraft separation are shown in Fig. IV-7. Aside from the transient disturbances at approximately 3.1 and 10.8 seconds after SECO, the maximum rates measured during the period following SECO appear in Table IV-5.

TABLE IV-5

Vehicle Rates Between SECO and Spacecraft Separation

Pitch Axis	Rate (deg/sec)
Max positive rate at $91FS_2$ + 3.3 sec	+ 1.2
Max negative rate at $91FS_2$ + 18.6 sec	- 0.3
Rate at $91FS_2$ + 20 sec	- 0.3
Rate at spacecraft separation ($91FS_2$ + 31.7 sec)	- 0.1
Yaw Axis	
Max positive rate at $91FS_2$ + 6.8 sec	+ 0.4
Max negative rate at $91FS_2$ + 1.7 sec	- 0.6
Rate at $91FS_2$ + 20 sec	+ 0.2
Rate at spacecraft separation ($91FS_2$ + 31.7 sec)	+ 0.3
Roll Axis	
Max positive rate at $91FS_2$ + 1.6 sec	+ 0.4
Max negative rate at $91FS_2$ + 9.8 sec	- 0.7
Rate at $91FS_2$ + 20 sec	+ 0.2
Rate at spacecraft separation ($91FS_2$ + 31.7 sec)	- 0.3

The Stage II redundant engine shutdown system was used for the second time on GT-4. With this type of shutdown, the roll nozzle thrust decay precedes the sustainer thrust decay. Again, as on GT-3, the initial portion of the sustainer engine and roll nozzle thrust decay was very rapid in comparison to the same GT-1 and GT-2 parameters with the singular thrust chamber valve shutdown. These two factors caused the vehicle's post-SECO rates to be less severe than those experienced on the GT-1 and GT-2 flights, and of the same order of magnitude as those exhibited on GT-3.

Successful spacecraft separation was accomplished at 31.7 seconds after $91FS_2$. However, maximum vehicle rates were only 0.3 deg/sec and the sustainer residual thrust at SECO + 20 seconds was less than the 60 pounds specified for successful spacecraft separation. Consequently, it is concluded that successful spacecraft separation could have been accomplished at that time.

The GT-4 spacecraft lateral damping system was employed approximately 2 seconds before separation. The effect of this can best be seen in the total change in the vehicle's pitch attitude error (Fig. IV-7) and the reduction of the pitch rate to almost zero for a brief period of time. Because at $91FS_2$ + 30 seconds the sustainer thrust was nearly zero, the lateral damping system was effective in rapidly reducing the vehicle pitching rate.

2. Post-SECO Transients

Noticeable vehicle disturbances in certain telemetered parameters occurred at SECO + 3.14 and SECO + 10.85 seconds. The phenomenon and resultant transients were similar to those observed on the GT-1 and GT-2 flights, and on numerous Titan II flights.

The vehicle pitch, yaw and roll rates observed during the two transient periods are shown in Figs. IV-8 and IV-9. The maximum changes in vehicle rates during the two transients are as follows:

Transient	Rate Changes (deg/sec)		
	Pitch	Yaw	Roll
SECO + 3.14 sec	0.69	1.0	0.80
SECO + 10.85 sec	1.0	0.66	0.37

The axial accelerations and the pitch and yaw engine deflections that occurred during the post-SECO transients are shown in Figs. IV-10 and IV-11. During the first transient, the axial acceleration response was 0.21 g peak to peak, as measured by the + 0.5 g accelerometer located in Compartment 1. The same response was 0.07 g peak to peak during the second transient period. The frequencies of the oscillations have been calculated to be 7.8 cps for the first disturbance and 6.3 cps for the second. These have been determined from the actuator motions as well as from the filtered rate and axial acceleration data. There was no change in the chamber pressure level during either of the transients. The two perturbations, which persisted for less than 0.4 second, had no discernible effect on the actual vehicle attitude.

The torque which must have been applied to the Stage II engine nozzle to produce the actuator motions (equivalent yaw engine deflection of 0.32 degree peak to peak and pitch engine deflection of 0.16 degree peak to peak) during the SECO + 3.14 second transient has been calculated to be 4.96×10^4 in.-lb. During the second disturbance at SECO + 10.85 seconds, the torque necessarily applied to produce the yaw and pitch engine deflections of 0.16 and 0.23 degree peak to peak, respectively, has been calculated to be 3.88×10^4 in.-lb.

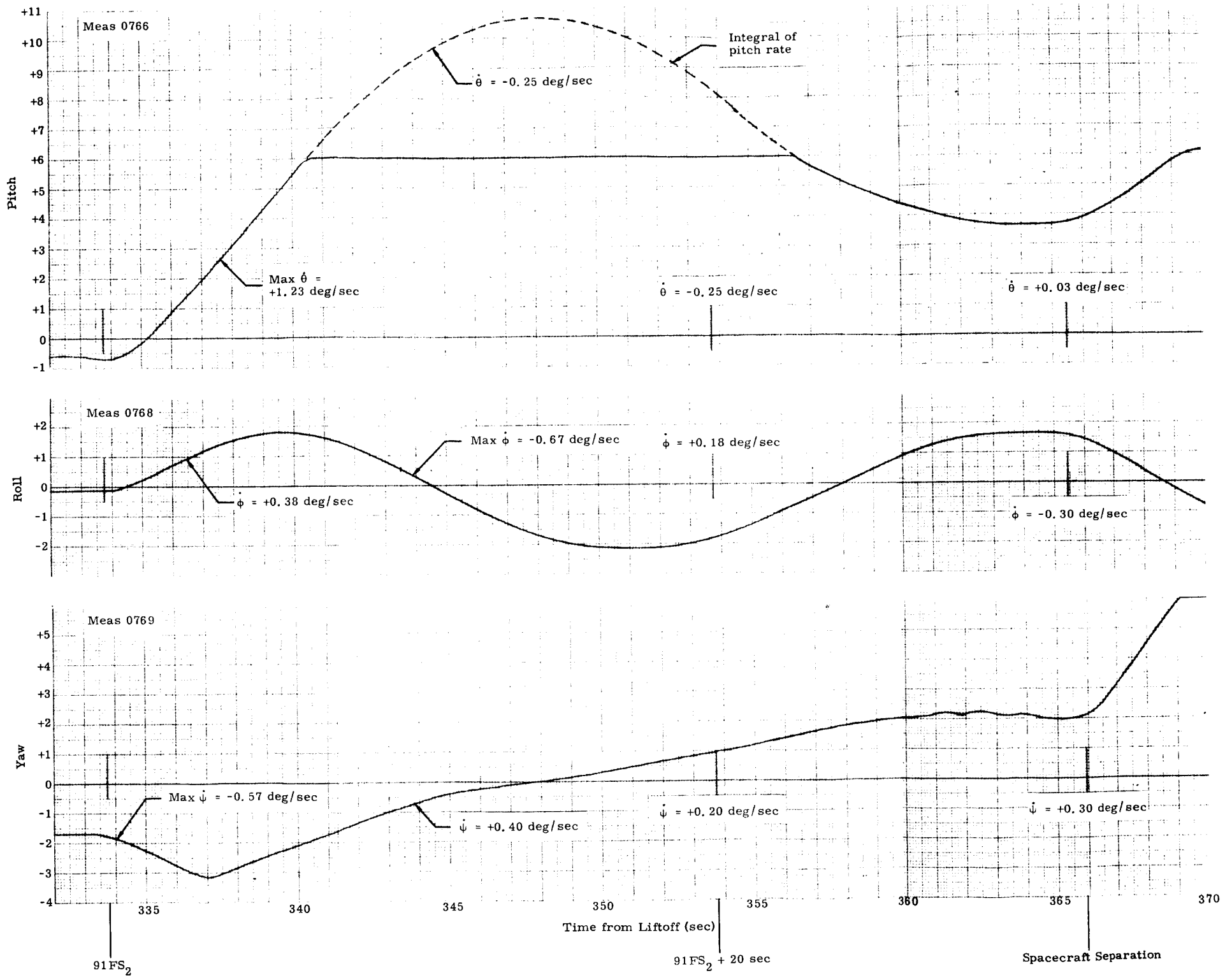

Fig. IV-7. Pitch, Roll and Yaw Attitude Errors During Post-SECO Flight

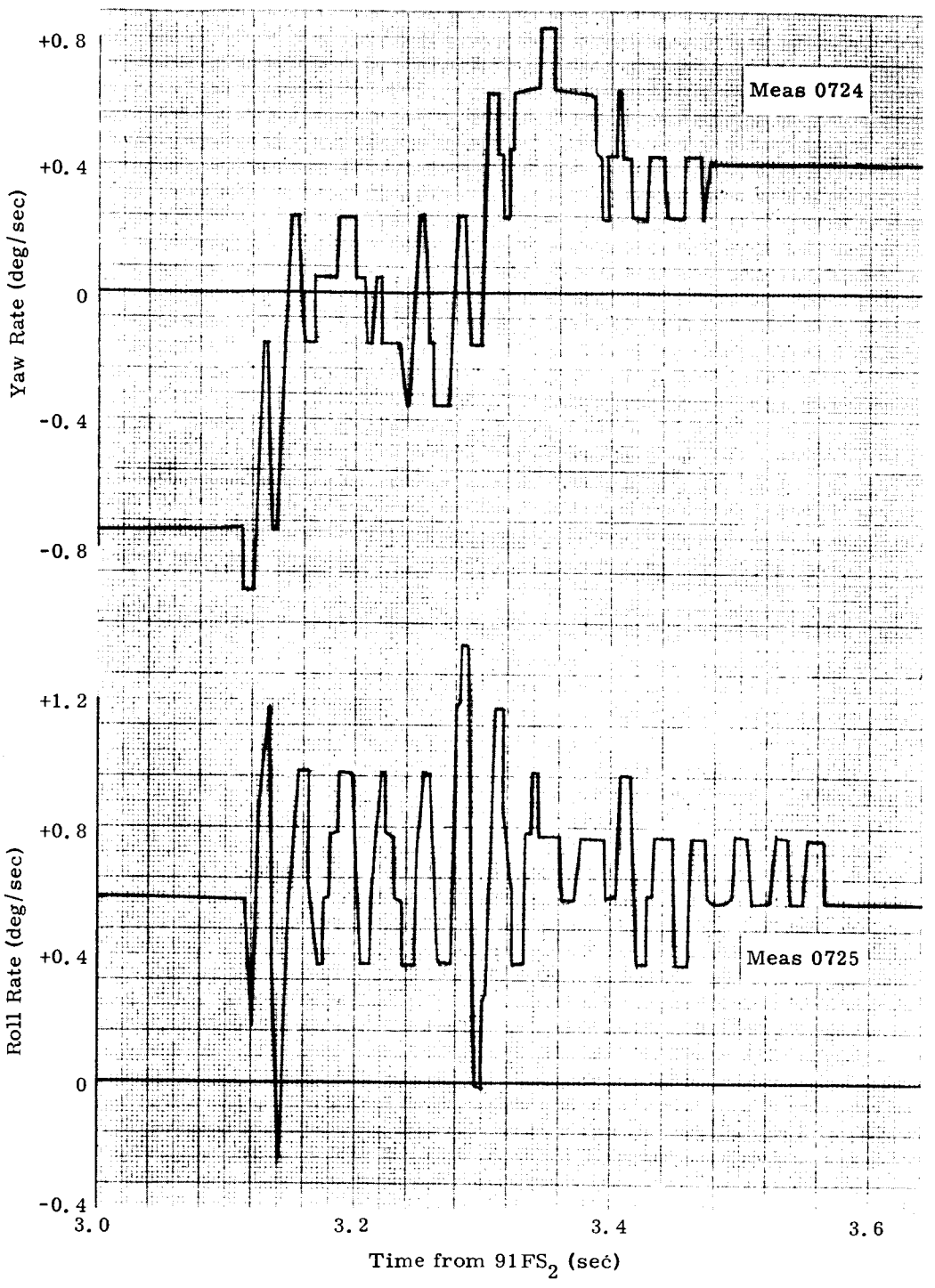

Fig. IV-8. Pitch, Yaw and Roll Rates During First Post-SECO Transient

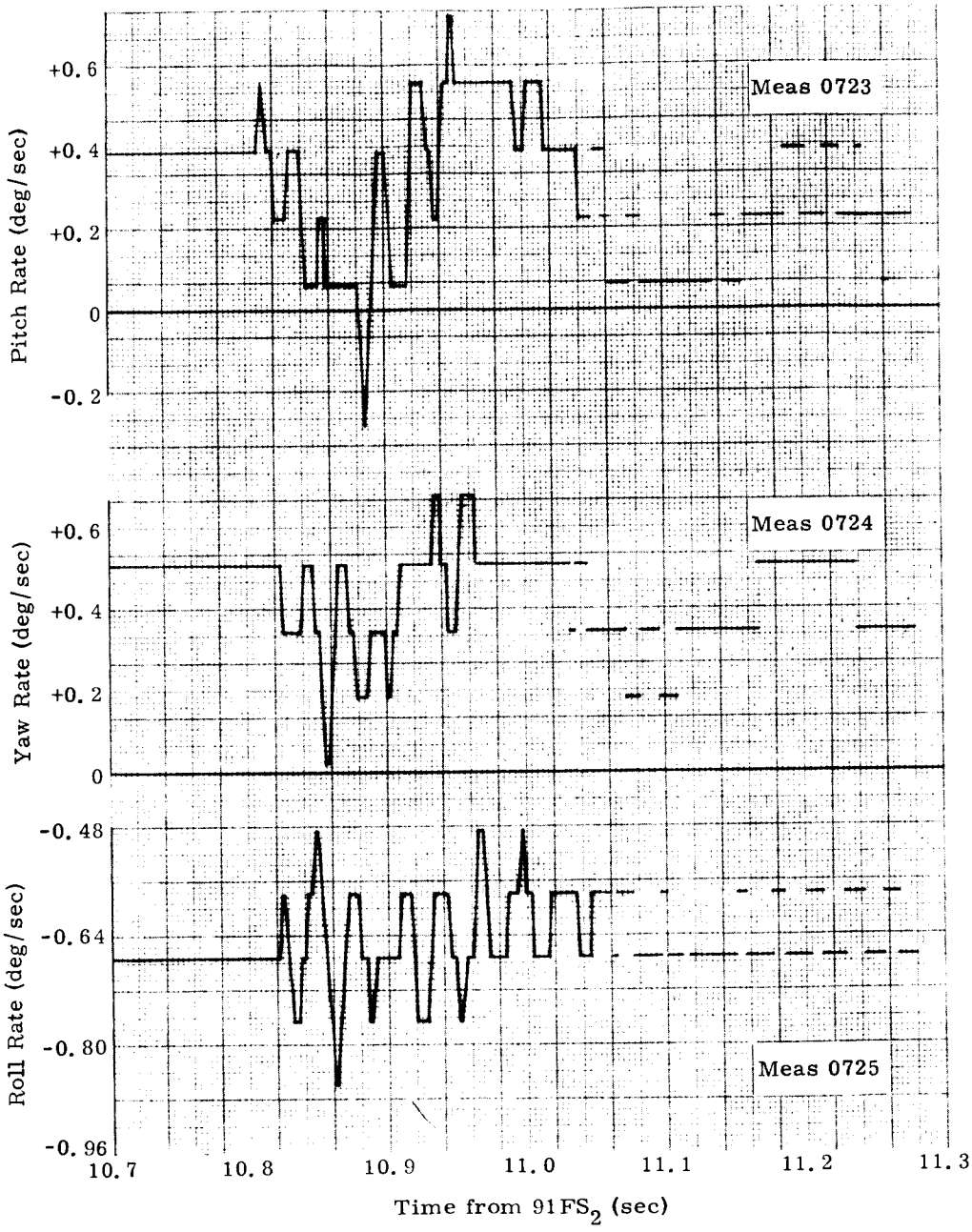

Fig. IV-9. Pitch, Yaw and Roll Rates During Second Post-SECO Transient

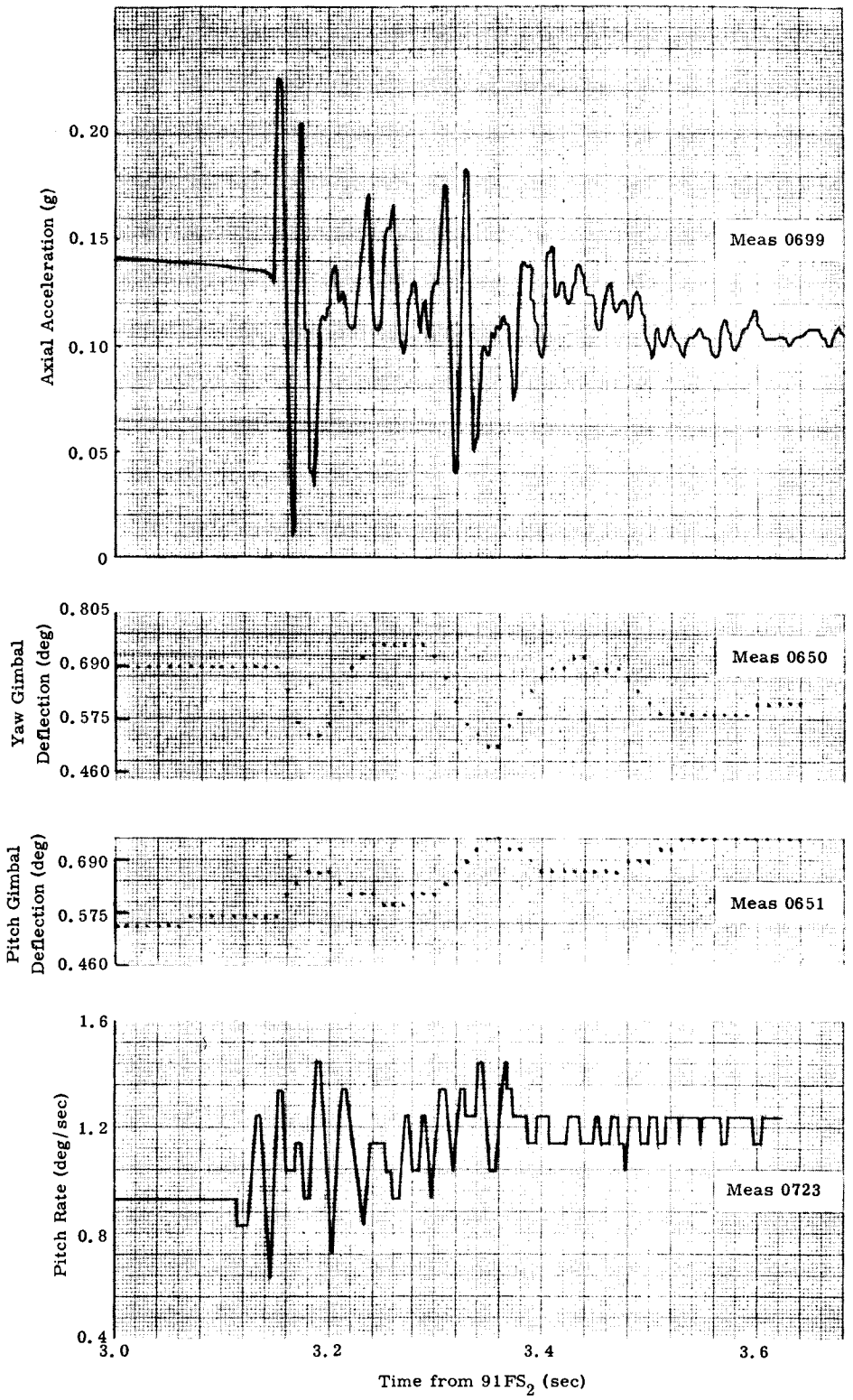

Fig. IV-10. Axial Accelerations and Pitch and Yaw Engine Deflections During First Post-SECO Transient

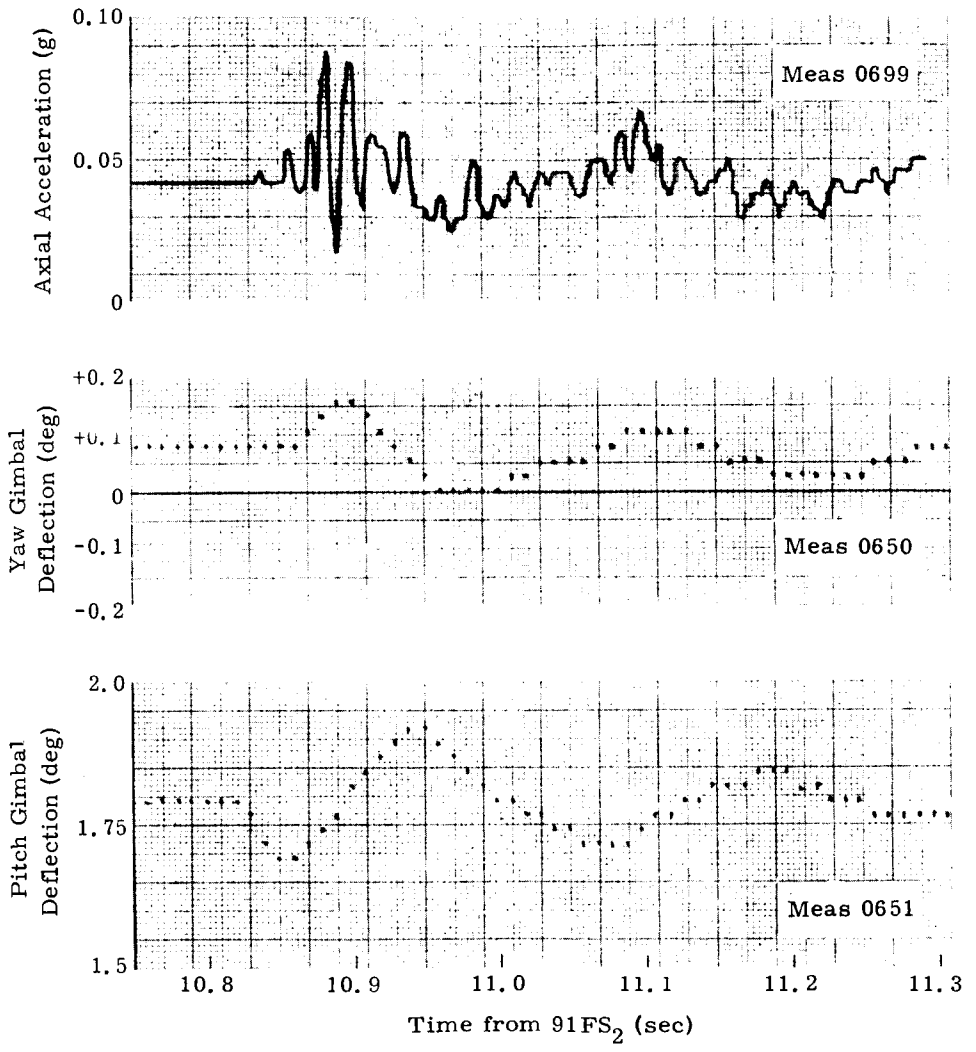

Fig. IV-11. Axial Accelerations and Pitch and Yaw Deflections During Second Post-SECO Transient

From the stability and control aspect, it is significant that all recorded vehicle parameters did not exhibit any level changes due solely to the disturbance. The ensuing history of these functions continued as if the disturbance did not occur. This observation was true also for the GT-1 and the GT-2 flights as well as for all Titan II flights that were examined.

V. HYDRAULIC SYSTEM

The GLV-4 hydraulic systems performed satisfactorily during Stages I and II flights.

Prior to the launch of GT-4 (between WMSL and SFT), the engine-driven hydraulic pumps were replaced with newly cleaned units, thereby minimizing the possibility of contamination during vehicle systems tests requiring hydraulic power. The newly installed pumps were checked with a Gaussmeter to verify free and proper compensator motion. The pump response during engine start was normal (Fig. V-1), and there was no evidence of stiction.

A. STAGE I

1. Primary Subsystem

The output of the Stage I electric motor pump was automatically switched from the secondary to the primary subsystem at T-110 seconds. This event pressurized the primary subsystem and resulted in normal system operation. The indicated accumulator precharge was 1790 psia. Electric motor pump pressure was a normal 3075 psia at T-0. Engine start transients starting at $87FS_1$ + 0.77 second produced flow demands which dropped primary pressure to 2300 psia at $87FS_1$ + 0.90 second. Pressure recovery occurred immediately, indicating proper pump compensator response. The pressure overshoot on recovery peaked at 3345 psia at $87FS_1$ + 1.11 seconds. A steady-state pressure of 2984 psia was reached at $87FS_1$ + 1.67 seconds. There were no significant pressure perturbations at liftoff or during flight. Pressure decayed normally to 2910 psia at staging.

The static reservoir level was 58.4% full prior to T-110 seconds, decreasing to a normal 37.8% full at T-0. The level increased during flight to 51.8% full at staging. This 14% increase is consistent with the observed fluid temperature rise from 93.5° F at T-0 to 177° F at staging.

The steady-state reservoir levels and the level changes during system pressurization were normal.

Primary and secondary system pressures and pressure switch actuation points are shown in Fig. V-1. A comparison of primary system pressure for GT-3 and GT-4 launches during engine start and holddown is presented in Fig. V-2.

The pressure values quoted were obtained from telemetered data. It has been determined that the primary pressure data readings are low by

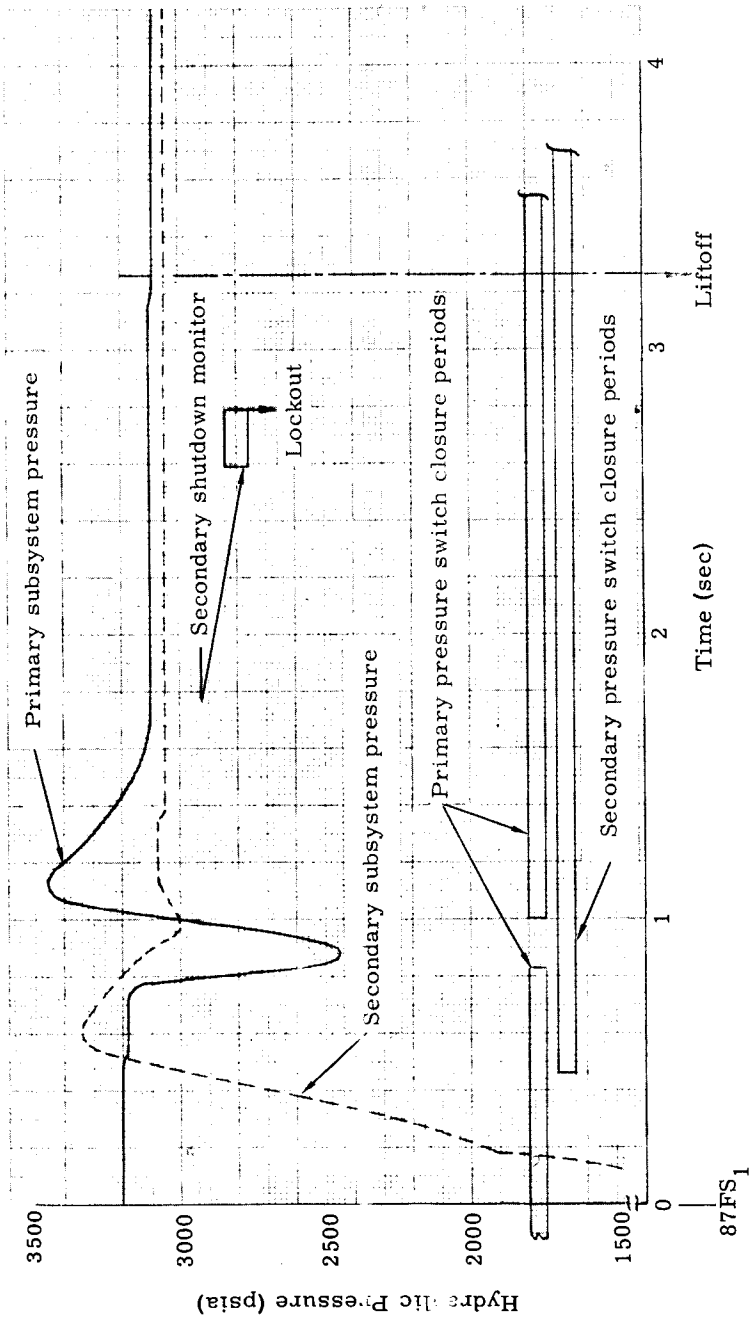

Fig. V-1. Stage I Hydraulic System Pressure Variation During Engine Start and Holddown

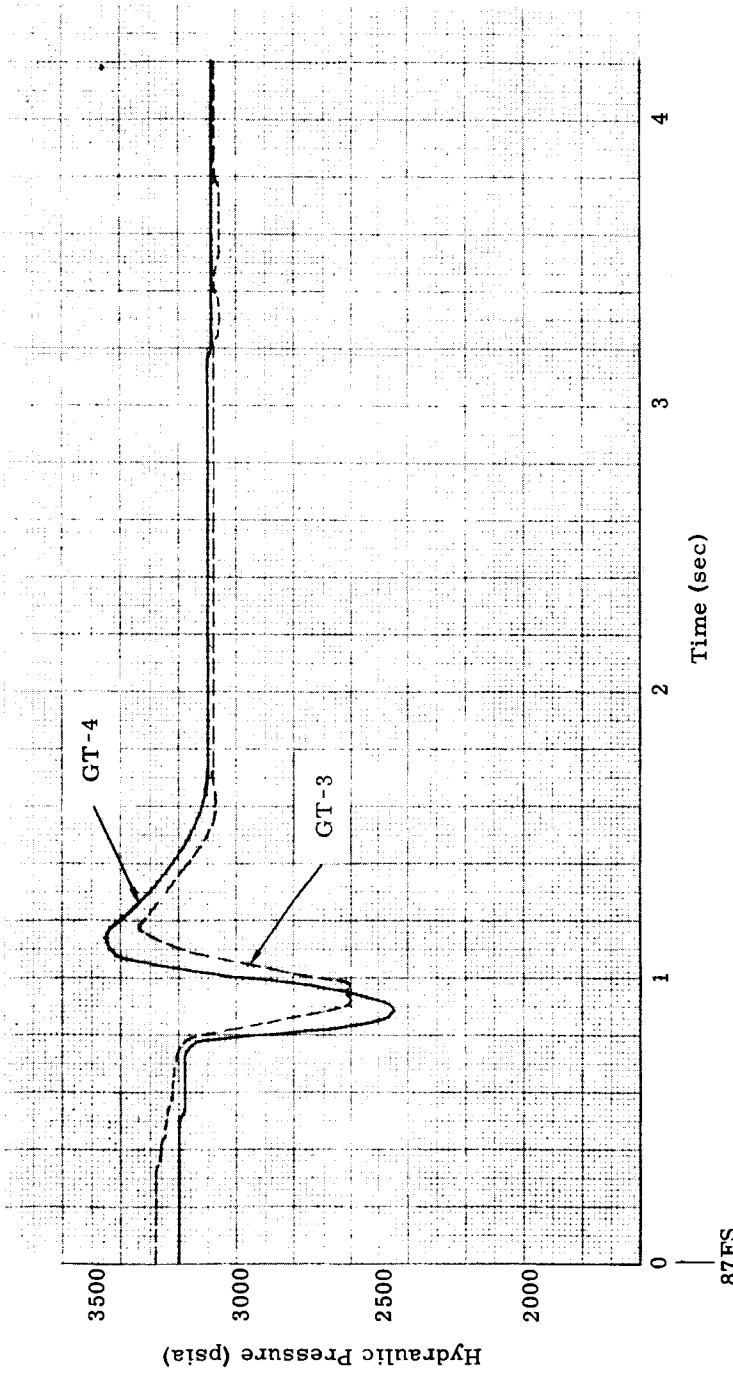

Fig. V-2. Comparison of Primary System Hydraulic System Pressure During Engine Start and Holddown

approximately 123 psi. This bias was due to a change in the transducer output subsequent to calibration by the vendor. Such changes are attributed to transducer aging. The magnitude of the error was determined by comparing vendor acceptance data on the Stage I pumps with the telemetered data. Vendor test showed that the electric motor pump pressure at a flow of 1 gpm was 3215 psia. This agrees very well with the value of 3210 psia read from Sanborn records of secondary subsystem operation prior to engine start. The secondary pressure indication after engine start was 3052 psia which agrees fairly well with the vendor data on the engine pump of 3095 psia at 1 gpm. The primary system pressure indications were 3075 psia from the electric motor pump and 2984 psia from the engine-driven pump. The vendor component acceptance test readings were 3215 psia for the electric motor pump (140 psi higher) and 3090 psia (106 psi higher) for the engine-driven pump.

Therefore, in Fig. V-1, a correction of +123 psi has been applied to the primary pressure curve.

2. Secondary Subsystem

The secondary subsystem was pressurized by the electric motor pump from T-180 to T-110 seconds. The indicated accumulator precharge was 1910 psia. Motor pump pressure was a normal 3210 psia at T-110 seconds.

The static reservoir level was a normal 54.7% full prior to pressurization at T-3 minutes, and had decreased to 30.0% full at T-110 seconds. These levels and the level changes during system pressurization and depressurization were normal.

At T-0, the system was unpressurized or "soft." Pressure began to develop immediately as the start cartridge rotated the engine turbine. Pressure overshoot reached a maximum of 3355 psia, indicating very good pump compensator response. A steady-state pressure of 3065 psia was reached at $87FS_1$ + 1.15 seconds. During the pressure shutdown monitor period from TCPS + 1.6 seconds to shutdown lockout, the pressure remained at a steady 3052 psia.

There were no pressure perturbations during flight as the system remained in a stand-by condition. Pressure decayed normally to 2880 psia at staging.

The reservoir level stabilized at 32.8% full after engine start, increasing during flight to 43.5% full at staging. This 10.7% increase was consistent with the observed fluid temperature rise from 90° F at T+10 seconds to 168° F at staging.

A comparison of secondary system pressures from GT-3 and GT-4 launches during engine start and holddown is presented in Fig. V-3.

B. STAGE II

Prelaunch checkout of Stage II hydraulics was initiated at T-4 minutes, and followed by normal system operation. The indicated accumulator precharge was 1850 psia. Electric motor pump pressure stabilized at a normal 3170 psia. The static reservoir level was 67.2% full, decreasing to 38.8% full after pressure application, and again increasing to 65.6% full upon removal of pressure at T-3 minutes.

During engine startup at staging, the indicated precharge was 1810 psia, and pressure overshoot was to 3680 psia. Steady-state pressure after engine start was 3000 psia, decreasing to 2870 psia at SECO. No significant pressure perturbations occurred during flight. After SECO, the pressure fluctuated with the engine rpm, a normal reaction to the low and variable turbine speeds occurring during this period.

The reservoir level was a normal 66.6% full prior to staging. After staging, the level stabilized at 39.7% full, gradually increasing to 41.8% full at SECO. This level increase of 2.1% is normal and consistent with the fluid temperature rise from 68° F at staging to 116° F at SECO.

The reservoir levels and changes in level during system pressurization and depressurization were normal.

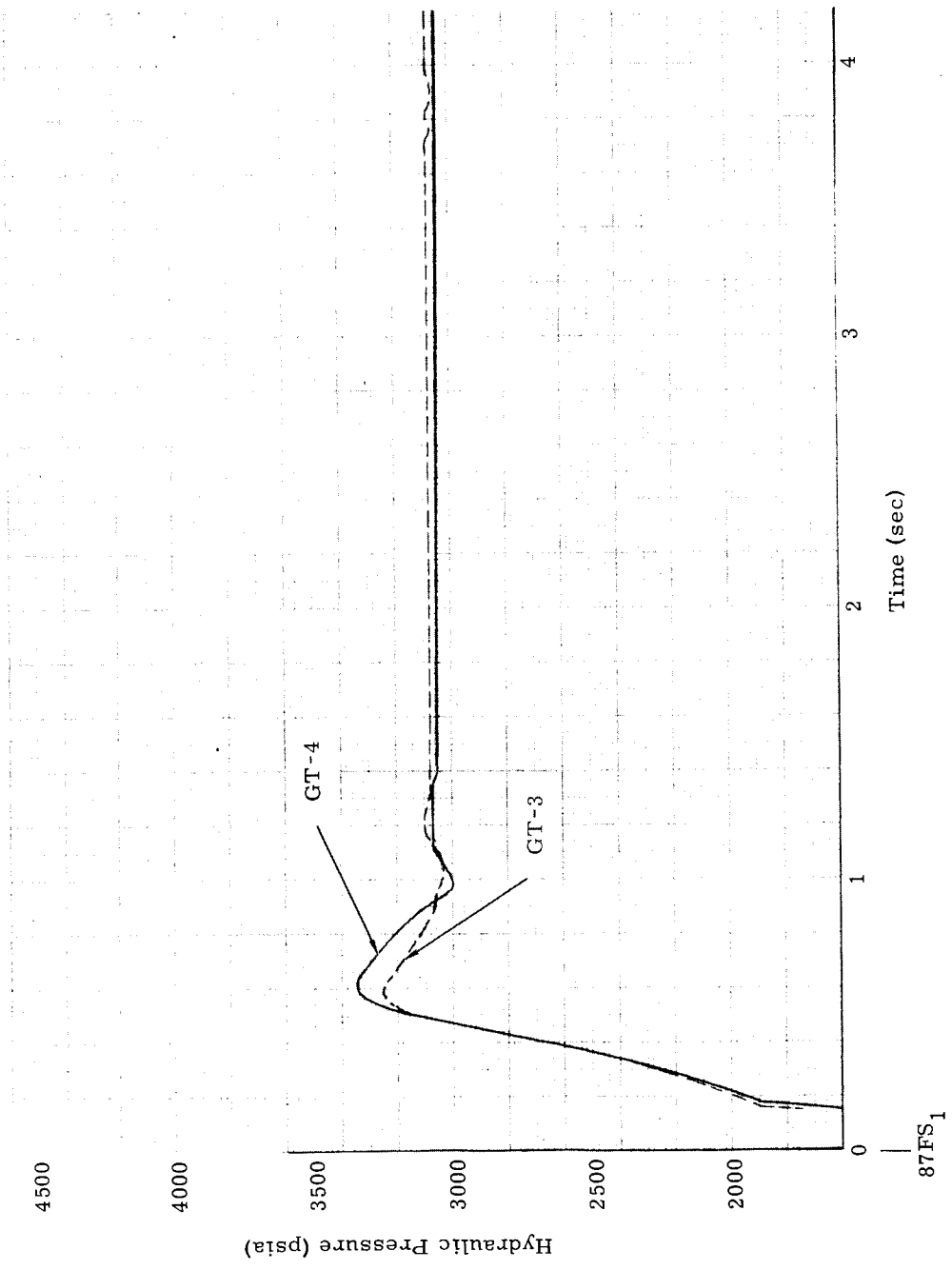

Fig. V-3. Comparison of Secondary System Hydraulic System Pressure During Engine Start and Holddown

VI. GUIDANCE SYSTEMS

A. RADIO GUIDANCE SYSTEM PERFORMANCE

1. Rate Beacon

Rate beacon performance was satisfactory throughout the flight. Good lock was maintained up to engine ignition and from LO + 47 to SECO + 64 seconds. Momentary loss of lock at engine ignition is considered normal. Relock occurs as the primary antenna is brought into favorable ground station view.

Values of the rate beacon telemetered functions during flight are listed in Table VI-1.

2. Pulse Beacon

Pulse beacon performance was also satisfactory throughout the flight. Good lock was maintained through engine ignition and up to SECO + 58.3 seconds.

Normal oscillations during the antenna crossover period were observed in the AGC output from approximately LO + 40 to LO + 73 seconds. During this time, the minimum signal level received by the beacon was -54 dbm.

The normal ground station signal level increase occurred at LO + 83.5 seconds. This increase was approximately 15 db.

Values of the pulse beacon telemetered functions are listed in Table VI-1.

TABLE VI-1

Guidance System Parameters

	Meas	Max Value	Min Value
Rate beacon			
Received signal No. 1	0750	3.95 v	3.85 v
Phase detector	0751	3.05 v	2.56 v
Power out	0752	3.97 v	3.92 v
15-volt power supply	0747	4.30 v	4.30 v

TABLE VI-1 (continued)

	Meas	Max Value	Min Value
Pulse beacon			
Magnetron current	0753	3.30 v	3.20 v
AGC	0754	>-10 dbm	-41.4 dbm*
30-volt power supply	0746	2.88 v	2.88 v
Decoder			
+ 10-volt power supply	0748	4.50 v	4.40 v

*Does not include antenna crossover period.

3. Decoder

Decoder performance was satisfactory. Telemetry data comparisons with the Burroughs computer-generated output indicate that pitch and yaw steering signals, and the SECO discrete commands were properly executed. No noticeable decoder null drift in pitch or yaw was observed.

Values of the decoder telemetered functions are listed in Table VI-1.

4. Guidance Commands

a. Pitch steering

A profile of early closed-loop pitch steering in terms of computer commands, decoder pitch telemetry, TARS gyro torquer monitor, and primary Stage II rate gyro is given in Fig. VI-1.

TARS discrete No. 3 (RGS enable) was issued at approximately LO + 162.0 seconds, thereby energizing the airborne guidance initiate relay. Simultaneously, pitch program No. 3 was terminated. This effect can be observed on the pitch torquer monitor and the rate gyro plots of Fig. VI-1.

An initial pitch-down command of 0.19 deg/sec, which lasted 0.5 second, was issued at LO + 168.5 seconds. Following this, a 2.0 deg/sec pitch-down command was issued for 6.5 seconds.

Throughout the remainder of the flight, except immediately prior to SECO, the pitch commands were small, varying between 0 and 0.1 deg/sec pitch-down. At approximately SECO - 4.0 seconds, there was a slow pitch-down variation that reached a maximum of 0.3 deg/sec. Computer commands were terminated at SECO - 2.3 seconds.

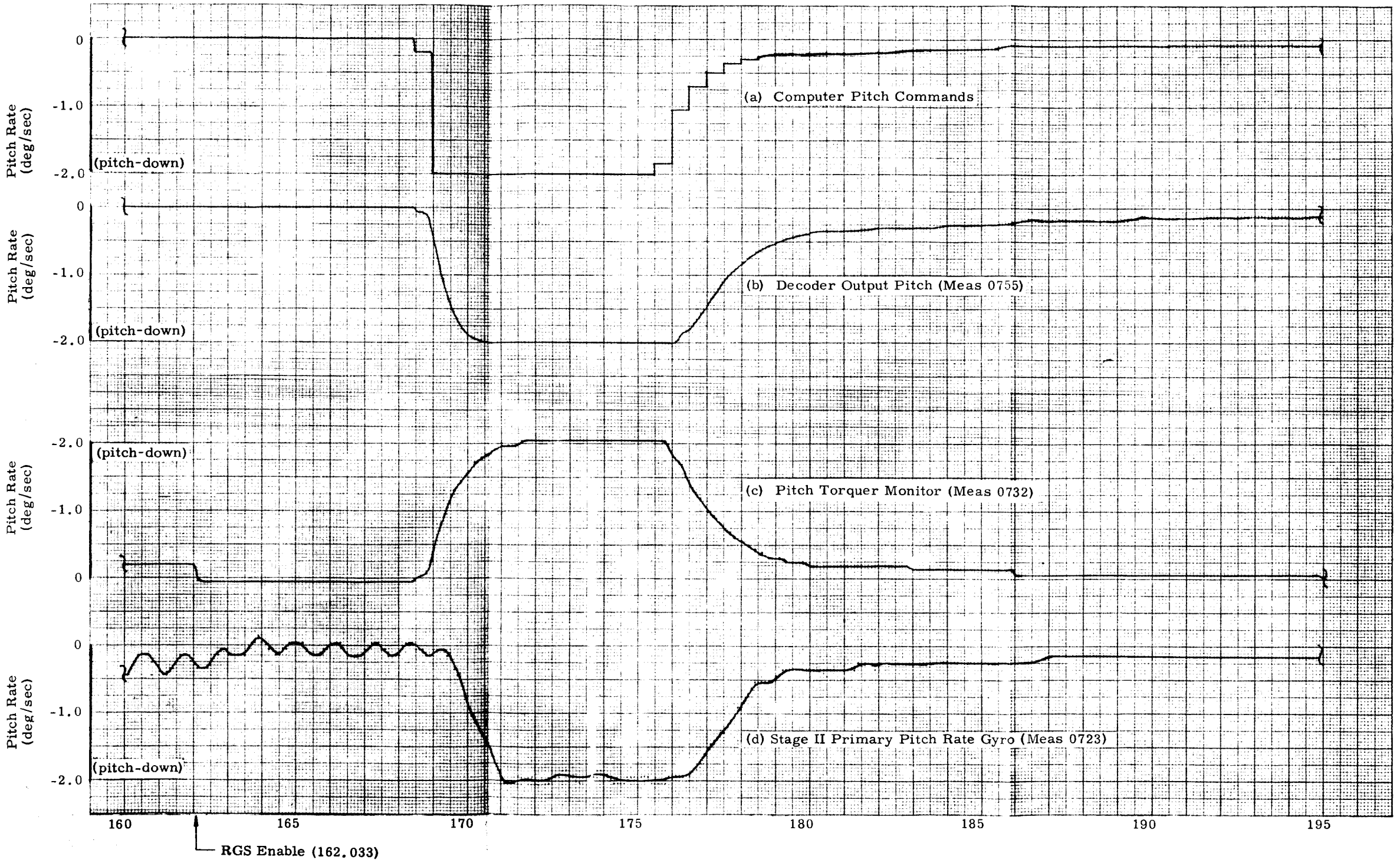

Fig. VI-1. Stage II Pitch Guidance Flight History

The decoder output, torquer monitor and rate gyro reactions were proper for the computer commands as shown in Fig. VI-1.

b. Yaw steering

Computer yaw commands were initiated at LO + 169.4 seconds. Throughout the flight, yaw command magnitudes were small and within telemetry resolution ($\leq$ 0.08 deg/sec, approximately).

c. Discrete commands

The times for the computer-generated SECO/ASCO command and the vehicle hardware reactions are presented in the following tabulation.

Signal	Meas	Time from Liftoff (sec)
Ground station SECO/ASCO	-	333.707 $\pm$ 3 ms
Decoder discrete output	0777	333.744 $\pm$ 5 ms
$91FS_2$	0519	333.754 $\pm$ 5 ms
ASCO	0799	333.837 $\pm$ 25 ms

These data indicate that the SECO time delay from ground station issuance to $91FS_2$ was 47 $\pm$ 8 milliseconds.

5. Vibration Environment

A vibration transducer located in Compartment 2 on the truss adjacent to the pulse beacon was used to measure lateral vibration (Meas 1697). The maximum vibration level observed during the ignition and liftoff period was 1.73 g rms. The maximum level during Stage I flight was 1.60 g rms, which occurred at LO + 57 seconds. This measurement was recorded during Stage I flight only.

B. SPACECRAFT INERTIAL GUIDANCE SYSTEM ASCENT PERFORMANCE

1. Prelaunch Nulls

The prelaunch IGS attitude error null signals were as follows:

Pitch = - 0.230 degree
Yaw = - 0.234 degree
Roll = - 0.120 degree

These null signals were well within the specification values of ± 0.37 degree in pitch and yaw, and ± 0.25 degree in roll.

2. Stage I

IGS performance during Stage I flight correlated well with the primary system (TARS), as shown by the comparison of the IGS and corresponding primary system attitude errors presented in Figs. IV-2 through IV-4. The BECO dispersions between IGS and primary system attitude errors are shown in Table IV-3 and are discussed in Chapter IV.

The IGS Stage I gain change discrete was issued at LO + 104.733 ± 0.025 seconds, which is well within the specification time of LO + 104.96 ± 1% seconds.

3. Stage II

IGS pitch, yaw and roll performance during Stage II flight appeared normal. The attitude error dispersions which had built up between the IGS and the primary system during Stage I flight in pitch, yaw and roll were carried over into the early portion of Stage II flight as shown in Figs. VI-2 and VI-3.

a. Pitch

IGS Stage II pitch attitude error is shown in Fig. VI-2. Primary system pitch attitude error and RGS pitch steering commands are also shown for purposes of comparison.

The ramp buildup of IGS pitch attitude error between approximately LO + 162.5 and LO + 168 seconds is attributed to the fact that the primary system third pitch rate ends at LO + 162.56 seconds, whereas the IGS third pitch rate remains in until the start of closed-loop guidance. This incompatibility will be rectified by an IGS change for GT-5 and up.

IGS closed-loop pitch guidance commenced at LO + 168.122 seconds. IGS pitch attitude error saturated at + 5.93 degrees shortly after guidance initiate, and remained saturated for approximately 7 seconds. Figure VI-2 shows that the TARS pitch attitude error builds up during this same time period to about + 1.3 degrees, due to the RGS - 2.0 deg/sec pitch rate command. The reason for the large difference in IGS and TARS attitude errors during this period is due to the fact that, in the primary system, the steering command is limited to a rate of ± 2.0 deg/sec, while the IGS limits attitude error only to a nominal ± 6 degree value. Therefore, IGS pitch behavior during this period appears normal and compares well with primary system behavior in correcting the vehicle for the slightly high Stage I trajectory.

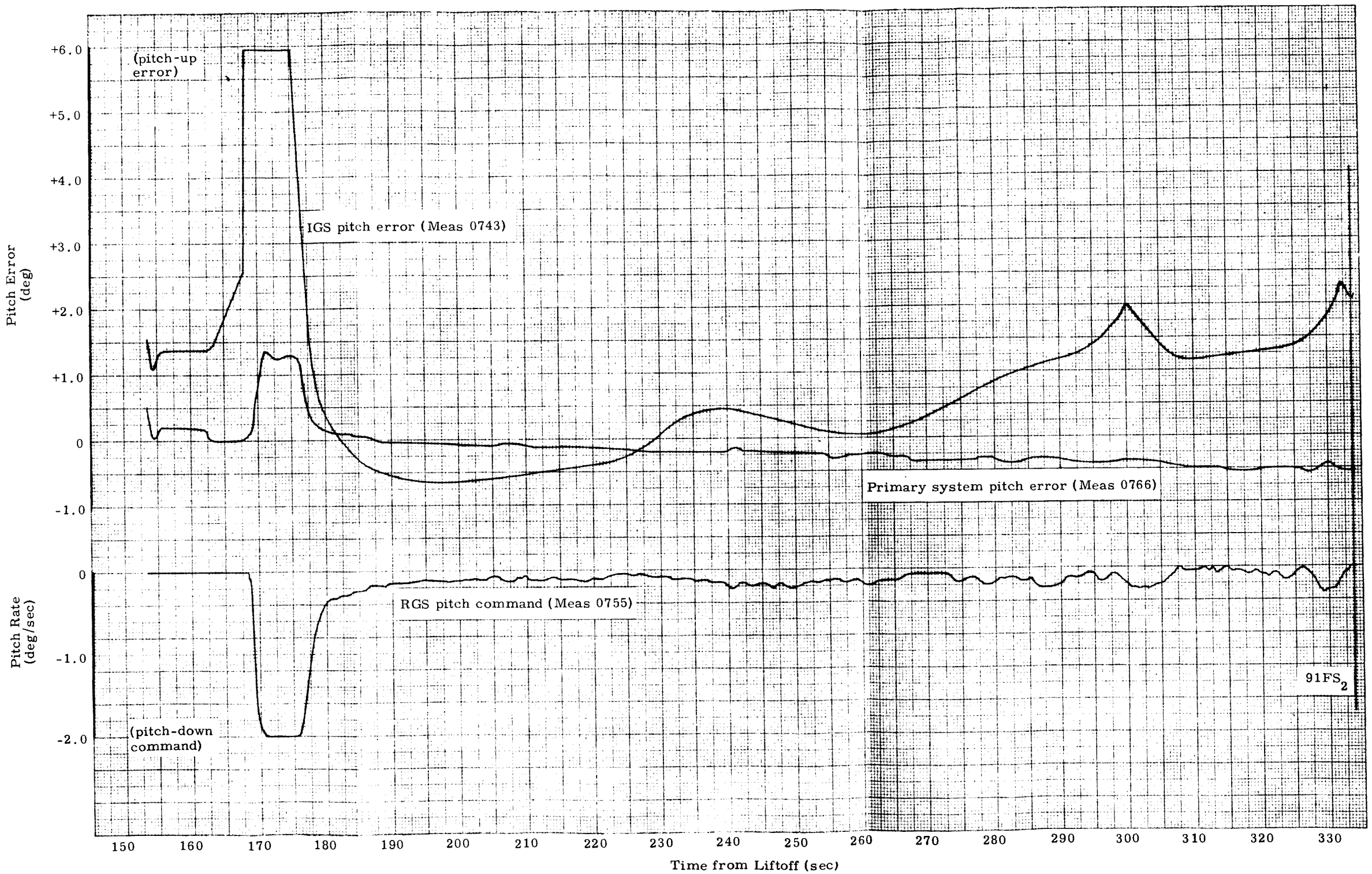

Fig. VI-2. Stage II IGS Pitch Flight History

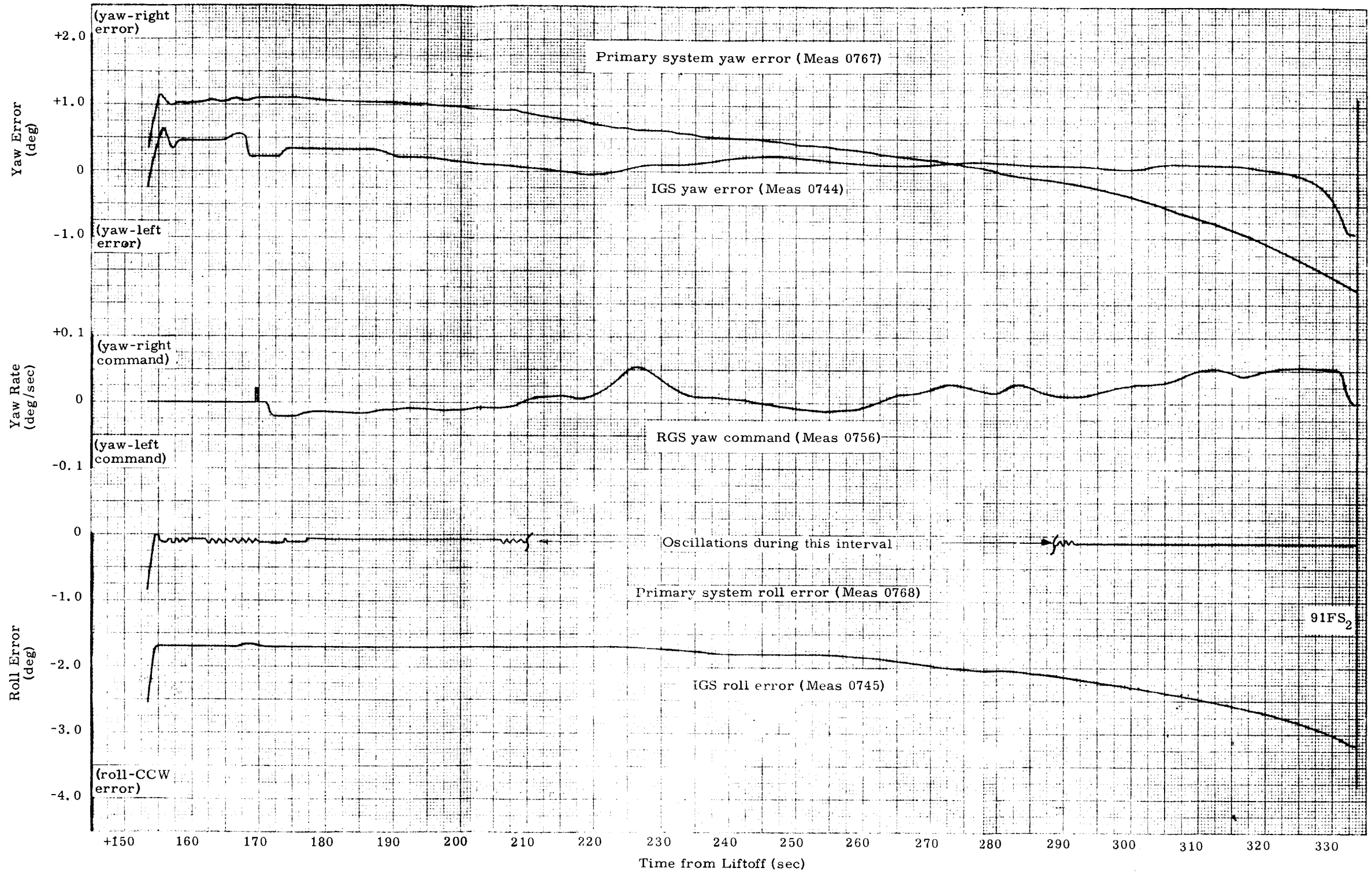

Fig. VI-3. Stage II IGS Yaw/Roll Guidance Flight History

IGS pitch attitude error for the remainder of Stage II flight stayed within acceptable limits. The attitude error peaked at about +2.0 degrees, just slightly after LO + 300 seconds, as shown in Fig. VI-2. This peaking appears to be a characteristic of IGS pitch steering, and coincides with the time at which the IGS starts constant altitude steering. The amplitude of the peak was not excessive.

After LO + 300 seconds, the attitude error decreased to 1.15 degrees, then peaked again to +2.3 degrees at LO + 332 seconds. This was a pitch-down command; Fig. VI-2 shows that the RGS was also commanding pitch-down at this time.

The decrease in IGS pitch error after 332 seconds is attributed to the fact that pitch steering was discontinued, as programmed.

b. Yaw

IGS yaw attitude error during Stage II flight is shown in Fig. VI-3. Primary system yaw attitude error and RGS yaw steering commands are shown for comparison.

IGS yaw performance throughout Stage II flight appeared normal and correlated well with the primary system. Steering commenced at approximately the same time as in pitch. The decrease in IGS yaw attitude error between guidance initiation and LO + 210 seconds is due to the influence of the RGS yaw steering on the vehicle (Fig. VI-3). Thereafter, the IGS yaw attitude error remained within +0.25 degree of null until LO + 325 seconds. At this time, the IGS yaw attitude error began to slope in the negative direction, and by LO + 332 seconds had increased to -0.9 degree, which is a GLV yaw-right command. At this time, steering was terminated, as in pitch. The amplitude of the attitude error was not excessive, and the direction of the attitude error build-up was as expected due to GLV center of gravity drift. A similar effect is apparent on Fig. VI-3 in primary attitude error (in that the error is building up negatively) and in RGS yaw steering (which is commanding the GLV to yaw right).

c. Roll

Relative drift between TARS and IGS roll attitude error was in evidence during Stage II flight (Fig. VI-3) and was in the same direction (CCW, TARS with respect to IGS) as the relative drift observed during Stage I flight. The dispersion which built up during Stage II flight, over and above that which had accumulated during Stage I flight, was -1.45 degrees. Approximately -0.89 degree of this total is due to TARS roll gyro drift. The predominant drift effect is due to the g sensitive drift term. The drift rate is well below the 3σ limit. The unexplained difference of -0.56 degree may be due to a combination of additional TARS drift and IGS drift.

d. IGS SECO

The IGS SECO discrete was issued at LO + 333.704 + 0, -0.10 seconds.* This compares to the RGS SECO time of LO + 333.744 + 0.005 seconds. Thus, if shutdown had occurred by IGS command, the GLV velocity would have been slightly lower at SECO.

4. Conclusions

IGS pitch, yaw and roll performance for the entire GLV flight appeared normal. There was no excessive build-up of IGS attitude error at any point in flight. Dispersions between IGS and primary system attitude errors remained within acceptable limits. There was no discernible evidence of any recurrence of the GT-2 and GT-3 IGS in-flight problems in the pitch axis attitude error.

From the data reviewed, it is concluded that it would have been safe to switch over to the IGS on GT-4 flight.

*IGS SECO time obtained from NASA source.

VII. ELECTRICAL SYSTEM ANALYSIS

A. CONFIGURATION

The launch vehicle airborne electrical system components installed for the GT-4 flight were similar to those used on GT-3. On GLV-4, a flashing beacon light assembly was installed on the second stage.

B. COUNTDOWN AND FLIGHT PERFORMANCE

The airborne electrical system functioned as designed through the entire flight, and all parameters were within specifications. Power transfer to airborne batteries at T-85.6 seconds was comparatively smooth, and liftoff occurred without incident.

During staging, examination of the APS and IPS current traces indicated no ordnance squib shorts to structure. The IPS staging current spike was approximately 2.5 amperes, whereas the APS staging current spike was obscured by the TARS heater cycling.

Currents to the Stage II redundant shutdown squibs at SECO were not detectable on either the APS or IPS traces, although squib operation was confirmed by Meas 0521.

At spacecraft separation, the launch vehicle/spacecraft electrical interface was cut by a guillotine in the adapter. This caused a 31-ampere rise in IPS bus current for approximately 150 milliseconds, indicating a momentary shorting of GLV interface signals to the structure. No similar pulse was indicated on the APS bus. This transient is expected because several active signals are normally maintained across the launch vehicle/spacecraft interface up to separation.

The flashing beacon light assembly began operating after SECO, as planned, at a rate of 68 pulses per minute. Orbital operation was confirmed by astronaut observations.

A summary of electrical system parameters measured at power transfer and during flight is presented in Table VII-1.

TABLE VII-1

GLV-4 Electrical System Parameters

Meas	Description	At Power Transfer			At Liftoff	At $87FS_2/91FS_1$ (Staging)			At Spacecraft Separation		
		Before	During	After		Before	During	After	Before	Peak	After
0800	IPS (volts)	29.4	28.4	29.5	29.3	29.0	28.9	29.0	29.5	28.2	29.3
0804	IPS (amp)	36.6	35.6	36.6	34.8	37.2	39.7	36.6	33.0	64.3	33.0
0801	APS (volts)	29.5	30.5	30.5	29.9	29.8	29.5	29.6	29.8	29.8	29.8
0805	APS (amp)	31.8	32.8	31.8	23.0	23.6	30.8	28.4	21.2	22.4	21.2
0802	400 cps, Phase A (volts)	114.1	114.1	114.1	114.1	114.0	114.0	114.0	114.0	114.0	114.0
0803	400 cps, Phase A (cps)	400.8	400.8	400.8	400.8	400.8	400.8	400.8	400.8	400.8	400.8
0726	25 vdc Power Supply (volts)	25.3	25.3	25.3	25.3	25.3	25.3	25.3	25.3	25.3	25.3

VIII. INSTRUMENTATION SYSTEM

A. AIRBORNE INSTRUMENTATION

1. Prelaunch and Countdown Status

The airborne instrumentation system operated within specified limits during prelaunch testing and countdown. Between WMSL (29 May) and launch, the airborne tape recorder was replaced because of noisy playback of the SFT data.

2. Data Acquisition

The airborne telemetry and instrumentation system, with the exception of Meas 0230, operated satisfactorily during countdown. The measurements program for launch consisted of 172 PCM analog signals, 46 PCM bilevel signals, and 12 FM/FM analog signals. All channels functioned properly throughout flight resulting in 100% data acquisition.

3. Instrumentation System Parameters

Instrumentation system parameters, as measured in-flight, are compared with specified limits in Table VIII-1.

4. Anomalies

The bias voltage level of Meas 0230 (Stage I primary pitch rate gyro output) changed gradually from 2.5 volts to 0.89 volt over a 5.7-minute interval, starting at T-39.8 minutes. At T-1.65 seconds, the bias level returned abruptly to its normal 2.5-volt level. The measurement remained normal and thereafter produced valid data.

This mode of failure was duplicated after the flight by inserting a 10-megohm resistance in series with the output impedance of the signal conditioner module and the input of the PCM encoder. This test narrowed the area of failure to the system circuitry between the output of the phase-sensitive-demodulator emitter follower and the input connection to the encoder. Any failure in the signal-conditioner module forward of the emitter follower would not have provided the 2.5-volt bias necessary to obtain the erroneous 0.89-volt divided signal. There is no known mode of failure for the PCM encoder that could possibly produce the long time constant decay observed.

This is the first indication of this mode of failure and it is not apparent how the high series resistance might have developed or how the condition corrected itself. A detailed study of the countdown

operation was made and there was no time correlation between the failure and CP 2600 console activity or mechanical shock stimulus such as hydraulic pump start or prevalve opening.

5. Telemetry Signal Strength (237.0 and 244.3 mc)

Telemetry signal strength records indicated satisfactory signal levels from the launch vehicle from liftoff to approximately SECO +92 seconds. The anticipated staging blackout lasted approximately 300 milliseconds.

Cape Kennedy's Tel II and Tel III ground stations monitored the entire flight of the launch vehicle. The Grand Bahama Island (GBI) station acquired data from approximately LO+ 47 seconds to the end of flight. The Grand Turk station acquired data during Stage II flight, beginning at approximately LO +190 seconds.

B. LANDLINE INSTRUMENTATION

1. Countdown Status

The entire landline instrumentation system functioned satisfactorily prior to and up to liftoff. All airborne instrumentation hold functions monitored in the blockhouse remained within specification throughout the countdown.

2. Data Acquisition

Data acquisition was 100% on 51 channels programmed as follows:

- 14 propellant temperatures on Bristol multipoint recorder No. 2.
- 3 start cartridge temperatures on Bristol multipoint recorder No. 1.
- 2 air-conditioning system temperatures on Bristol strip chart recorders.
- 1 air-conditioning system pressure measurement on Bristol strip chart recorder.
- 4 launch vehicle tank pressures on Bristol strip chart recorders.
- 8 event signals on a 78-channel Brush events recorder.

- 9 a-c and d-c electric power source measurements on oscillograph recorder.
- 6 BLH base reaction load measurements on Sanborn recorder.
- 1 BLH total vehicle weight measurement on a digital print-out.
- 2 hydraulic pressure switch signals on magnetic tape via voltage-controlled oscillators.
- 1 d-c electric power source measurement on a Sanborn analog recorder.

In addition, data acquisition was 100% on landline instrumentation measurements observed or recorded on the following backup channels:

- 17 voltage-controlled oscillator channels for recording on magnetic tape
- 14 digital voltmeter channels
- 1 vehicle total weight visual digital display

3. Anomalies

Measurement 4601 (bulk Stage II fuel tank temperature) appeared to be reading higher than expected after the propellant loading was complete. Because this was the only bulk temperature probe recorded on magnetic tape, as well as on the Bristol multipoint recorder, the magnetic tape patch cord was removed and the multipoint recorder level dropped 1.1° F. When the magnetic tape recording patch was inserted, the temperature level increased 1.1° F. This indicated that the bridge balance potentiometer was not properly adjusted. This potentiometer was set to its mid-position so that when the magnetic tape patch cord was connected it did not affect the multi-point recording. After the potentiometer adjustment was made, there was no further problem with this measurement.

TABLE VIII-1

Instrumentation System Parameters

Meas	Description	Required PCM Count Required Engineering Units	PCM Count Engineering Units Liftoff	$87FS_2$ $91FS_1$	$91FS_2$	SECO + 20
0810	5-volt power supply	203 ± 1 5.000 v ± 0.035	203/204 5.005/5.026	203/204 5.005/5.026	203 5.005	203 5.005
0811	40-volt power supply	231 ± 3 40.00 v + 0.51 - 0.18	231/232 40.26/40.44	231 40.26	231 40.26	231 40.26
0812	Signal conditioner package temperature	N/A 104° to 126° F	N/A 119.6° F	N/A 116.6° F	N/A 116.6° F	N/A 117.4° F
0813	PCM mercury cell	73 ± 1 1.335 to 1.375 v	73 1.355	73 1.355	73 1.355	73 1.355
0814	PCM mercury cell	73 ± 1 1.335 to 1.375 v	73 1.355	73 1.355	73 1.355	73 1.355
0815	PCM mercury cell	73 ± 1 1.335 to 1.375 v	73 1.355	73 1.355	73 1.355	73 1.355
0816	+30-volt power supply	166 ± 3 29.92 to 30.11 v	167 30.05	167 30.05	167 30.05	167 30.05
0817	-30-volt power supply	198 ± 3 -29.91 - 30.10 v	199 -30.01	199 -30.01	199 -30.01	199 -30.01

IX. RANGE SAFETY AND ORDNANCE

A. COMMAND CONTROL RECEIVERS

1. Countdown

The command receiver ASCO checkout (FIDO from Houston), and the shutdown/destruct checks were made at T-235 minutes. At T-5 minutes, ASCO (FIDO from Cape Kennedy) was checked. All range safety system (RSS) tests were performed satisfactorily. The command receiver telemetry indicated a signal level greater than 125 microvolts from T-5 minutes through liftoff.

2. Flight Results

Command receivers S/N 37 (APS) and S/N 50 (IPS) were flown on GLV-4. The RF carrier remained fairly constant until LO + 66.56 seconds, at which time the Cape switched to the high power FRW-2 and the signal strength was raised to approximately 4000 microvolts. At LO + 115.36 seconds, the RF carrier was transferred from the Cape to Station No. 3 at Grand Bahama Island (GBI), and as the launch vehicle traveled downrange, the RF carrier signal weakened as expected. At approximately LO + 310 seconds, the RF carrier dropped rapidly from 45 microvolts to less than 2 microvolts in 5 seconds. The carrier remained below 2 microvolts for approximately 850 milliseconds, and then returned to 45 microvolts at LO + 320 seconds. The ASCO command was received at LO + 333.837 seconds with the RF carrier signal at 45 microvolts.

One minute after the first incident of the RF carrier dropping to less than 2 microvolts (LO + 375 seconds), the same event was repeated.

A review of the sensitivity test data obtained on the two receivers indicated that if ASCO or shutdown and destruct had been commanded at the time the RF carrier dipped to its lowest level, the receivers probably would have functioned as commanded; if not, the receivers would have functioned within the next 150 milliseconds as the RF carrier level had increased sufficiently in that interval.

The spacecraft digital command system (DCS) utilizes the same RF carrier as the launch vehicle's command receivers. A review of spacecraft telemetry data showed a similar signal drop at LO + 375 seconds but no drop at LO + 315 seconds.

3. Postflight Investigations

Results of the investigations into the cause of the RF carrier signal decreases are as follows:

(1) Between LO + 114.4 seconds and LO + 431 seconds, the RF carrier was being transmitted from GBI.

(2) At LO + 375 seconds, the spacecraft was maneuvering and the OAMS propulsion was in use. At LO + 315 seconds, the spacecraft rockets were not being used.

(3) Only two digital commands were issued to the spacecraft during boost flight--the first at LO + 105 seconds and the second at LO + 145 seconds. When the carrier was not sending commands, it was modulated to send sub-bit 1 to maintain receiver phase lock.

(4) Hatches and covers were removed from the spacecraft at approximately LO + 400 seconds.

(5) GLV antenna pattern null characteristics were not contributory because:

   (a) GT-4 and GT-3 trajectories were similar, and no RF carrier problems were encountered on GT-3 flight.

   (b) The antenna systems at GBI were the same for GT-4 and GT-3 flights.

   (c) Antenna patterns indicate that a null does not exist during boost flight.

   (d) During the first incident (LO + 315 seconds), the launch vehicle did not experience any sudden angular changes.

(6) The FRW-2 system at GBI functioned properly during the flight. The first GBI power monitor tape shows no power output problems. GBI antenna position history and frequency shift data have not been received.

(7) The RGS and MISTRAM RF carrier telemetry data do not show any change at LO + 315 and LO + 375 seconds.

(8) Jamming was considered: however, this would increase RF carrier signal rather than cause a drop.

(9) The flashing light location relative to the command control antennas was reviewed, and is not considered contributory.

(10) Design of the command control antennas and the six-port junction were reviewed and found satisfactory.

(11) Titan II telemetry data were reviewed and no similar incidents were uncovered.

Although the cause of the two RF carrier drops has not been isolated, the investigation is continuing.

B. MISTRAM

1. Countdown

The MISTRAM open-loop checks with the MACK station from T-390 to T-330 minutes and from T-30 to T-10 minutes were performed without incident. A review of MISTRAM telemetry showed that the transponder was locked up to the MACK station signals from T-5 minutes until LO- 0.394 second. The MACK station signal is manually turned off as close to liftoff as possible.

2. Flight Results

a. Airborne transponder

General Electric transponder S/N 97 was installed in GLV-4. Analysis of the MISTRAM telemetry records for Stages I and II boost flight indicates that the overall performance of the airborne MISTRAM system was completely satisfactory. The MISTRAM I station started the sweep of the calibrate channel at LO + 27.258 seconds. The transponder range channel locked on the Valkaria signal at LO + 8.407 seconds and the calibrate channel locked on at LO + 9.707 seconds. Telemetry data show that the transponder did not unlock from first acquisition until SECO (with the possible exception of staging). Since telemetry and ground station data from the transponder are lost because of ionization caused by the Stage II engine plume, it is not possible to verify that the transponder unlocked.

3. Ground Station Operation

a. Valkaria station (MISTRAM I)

Valkaria station started active track at LO + 19.7 seconds and continued through SECO until LO + 393.0 seconds, at which time it was handed over to System II (Eleuthera). The west 100,000-foot leg of the MISTRAM I station lost real-time data during this launch because the central site receiver used for obtaining the west 100,000-foot remote site data was not operating. This problem affected only the real-time data because the received data are stored on magnetic tape for use in reconstructing flight data. Valkaria had reconstructable data from LO + 19.7 seconds until handover. MISTRAM I has four

remote sites (one 100,000-foot and one 10,000-foot west site, and one 100,000-foot and one 10,000-foot south site) permitting the three remaining remote sites to be used as the data source for the range safety impact prediction during 61% of the launch vehicle powered flight.

The source data for the primary and secondary range safety plot boards are included in Table IX-1.

b. Eleuthera station (MISTRAM II)

The Eleuthera station operated in a passive track mode from LO + 128 seconds until LO + 393 seconds, then in active track from LO + 393 seconds until LO + 448 seconds. MISTRAM II was not used as source data for the range safety plot boards.

TABLE IX-1

Range Safety Plot Board Impact Prediction

Primary Plot Board		Secondary Plot Board	
Data Source	Total Time Source Used (sec)	Data Source	Total Time Source Used (sec)
MISTRAM I	259.8	Mod III-G	315.9
GBI (FPS-16)	6.2	GBI	6.7
Merritt Island (TPQ-18)	48.6	Merritt Island	70.3
Patrick AFB (TPQ-18)	83.0	Patrick AFB	2.4
Grand Turk Island (TPQ-18)	122.4	GBI (TPQ-18)	10.6
		Grand Turk Island	114.1
Total	520.0	Total	520.0

C. ORDNANCE SYSTEM

The prevalve, engine start and dropweight ordnance devices operated as required during GLV-4 countdown and launch.

The launch release ordnance operated satisfactorily with all nuts actuating as evidenced by the recovery of all four holddown studs and the four lower launch nuts on Pad 19 after launch. The stage separation system operated as required. The TARS timer arm signals occurred at LO + 144.2 seconds. The 145-second timer signal occurred at LO + 145.3 seconds. Both times were within tolerance.

X. MALFUNCTION DETECTION SYSTEM

A. CONFIGURATION

The malfunction detection system (MDS) and associated hardware performed satisfactorily during the GT-4 countdown and flight. Significant MDS components appear in Table XVII-1.

All MDS components flown on GLV-4 were identical to those which had undergone VTF testing in Baltimore, with the exception of the rate switch package. This package was removed after WMSL for a calibration check, and a new package was installed for the flight.

B. SYSTEM PERFORMANCE

1. Engine Pressure Switches

Operation of the Stage I engine malfunction detection thrust chamber pressure switches (MDTCPS) and the Stage II engine malfunction detection fuel injector pressure switches (MDFJPS) is summarized in Table X-1. These switches are required to "make" in a pressure range of 540 to 600 psia and "break" in a pressure range of 585 to 515 psia. The Stage I engine start transient was of sufficient amplitude and time duration to cause the S/A 1 MDTCPS switches to momentarily respond to the thrust chamber pressure. All MDS engine pressure switches operated properly and within the specification requirements.

TABLE X-1

MDS Engine Pressure Switch Operation

Operation	S/A 1 (Meas 0356)	S/A 2 (Meas 0357)	S/A 3 (Meas 0855)
Make (540-600 psia)	1515:57.174 GMT at 550 psia	1515:57.224 GMT at 580 psia	1518:32.676 GMT*
Break (585-515 psia)	1518:31.961 GMT at 545 psia	1518:31.946 GMT at 530 psia)	1521:33.476 GMT*

* S/A 3 fuel injector pressure was not instrumented on GLV-4; hence, make and break pressures were not available.

2. Switchover

The MDS switchover circuitry responded properly throughout the flight. There were no switchover commands and no switchover was executed, indicating proper performance of the switchover circuitry.

3. Vehicle Rate Detection

The spin motor rotation detectors (SMRDs) contained in the malfunction detection package (MDP) functioned properly. The SMRDs monitor rate switch package (RSP) gyro speed and, thereby, rate sensing capability.

The RSP operated properly throughout the countdown and flight. There were no vehicle overrates detected by the MDS (rate switch operations) and none occurred during flight from liftoff through SECO + 20 seconds. Table X-2 compares the maximum launch vehicle rates (measured during the period from liftoff through SECO) with the RSP switch settings.

TABLE X-2

Maximum Vehicle Rates Versus Rate Switch Settings

		Stage I Flight	Flight Event	Stage II Flight	Flight Event
Rate switch settings (deg/sec)	Pitch	+2.5; -3.0	N/A	±10	N/A
	Yaw	±2.5	N/A	±10	N/A
	Roll	±20.0	N/A	±20	N/A
Maximum vehicle rates (deg/sec)	Pitch	-1.15	Wind shear	-2.08	Staging
	Yaw	-0.74	Wind shear	+0.78	Staging
	Roll	+1.61	Roll program	-2.83	Staging

Following spacecraft separation (SECO + 31.5 seconds), there were four operations of the rate switches. The rate gyro outputs verified that the rate switch performance was in agreement with the RSP calibration data. Table X-3 summarizes the rate switch operation.

XI. CREW SAFETY

A. PRELAUNCH SIMULATIONS

Prelaunch wind measurements from Cape Kennedy were data-card transmitted to Martin-Baltimore and used as input to three computer programs. One digital program evaluated the wind conditions by comparing actual wind measurements against specification wind speeds and wind shears. A second digital program was used to compute the wind-affected trajectory. A third analog program determined the vehicle bending loads and the control system transients for the wind-affected trajectory. Subroutines were then used to establish the first-stage propellant tank underpressure constraints and the slow malfunction action thresholds for flight control system (FCS) switchover. The results were sent periodically by phototelegraphy to Martin-Canaveral and to NASA-MSC prior to the launch.

All portions of the program worked smoothly. Balloon soundings, data-card transmissions, IBM-1620 wind computations, IBM-7094 trajectory computations, analog flight load simulations, communications network (newly extended to MCC-Houston), phototelegraphy of documents to Cape Kennedy and Houston, and delivery of these documents to Complex 19 and the Mission Control Centers at Cape Kennedy and Houston were accomplished on schedule. A brief summary of all computer runs is presented in Table XI-1.

1. Trajectory Simulation

Of the seven wind profiles obtained (Figs. XI-1, XI-2 and XI-3), the soundings released by the Air Force at T-12, T-5 and T-1 hours (Fig. XI-2 and XI-3) were programmed into the IBM-7094 Gemini Trajectory Program. The T-3 hour sounding data release was not programmed because it had not changed from the T-5 hour wind. Results of the T-12 and T-5 trajectory simulations were delivered to both MCCs in time for use in plotboard revisions of the nominal trajectory as affected by winds.

The T-5 hour trajectory simulation indicated that a peak lateral velocity of + 60.26 fps would occur at LO + 84 seconds, and a peak γ of + 27.58 degrees at LO + 75 seconds. The wind effect was to depress the nominal trajectory.

2. Loads Simulation

The winds-aloft launch recommendations for the GT-4 flight were based upon the results obtained from analog computer load simulation runs performed at Martin-Baltimore. Four simulations were run using winds data released at T-12, T-5, T-3 and T-1 hours. These loads,

TABLE XI-1

Summary of Prelaunch Simulations

Run No.	Time of Data Release to Martin-Baltimore	Operation
1	F-2 day 1100 EST 6-1-65	Wind evaluation. Sent to MCC-Cape Kennedy and MCC-Houston.
2	F-1 day 1100 EST 6-2-65	Wind evaluation. Sent to MCC-Cape Kennedy and MCC-Houston. F-2 day data retransmitted to MCC-Houston to provide more legible copies.
3	T-12 hr 2100 EST 6-2-65	Computation of wind evaluation, loads, analog and trajectory simulations and constraints. Data sent to MCC-Cape Kennedy and MCC-Houston. Winds were "go."
4	T-5 hr 0400 EST 6-3-65	Computation of wind evaluation, loads, analog and trajectory simulations and constraints. Data sent to MCC-Houston and MCC-Cape Kennedy. Winds were "go."
5	T-3 hr 0600 EST 6-3-65	Computation of wind evaluation, loads, and analog simulations. Trajectory simulation and constraint computations were canceled because of unchanged winds. Only wind evaluation sent to MCC-Houston and MCC-Cape Kennedy. Unchanged data verified by telephone. Winds were "go."
6	T-1 0800 EST 6-3-65	Computation of wind evaluation, loads, analog and trajectory simulations. All but trajectory sent to MCC-Houston and MCC-Cape Kennedy. Winds were "go."
7	T-1/4* 1000 EST 6-3-65	Computation of wind evaluation. No data sent to MCC-Houston or MCC-Cape Kennedy.

* Launch delay occurred at T-1/2 hr.

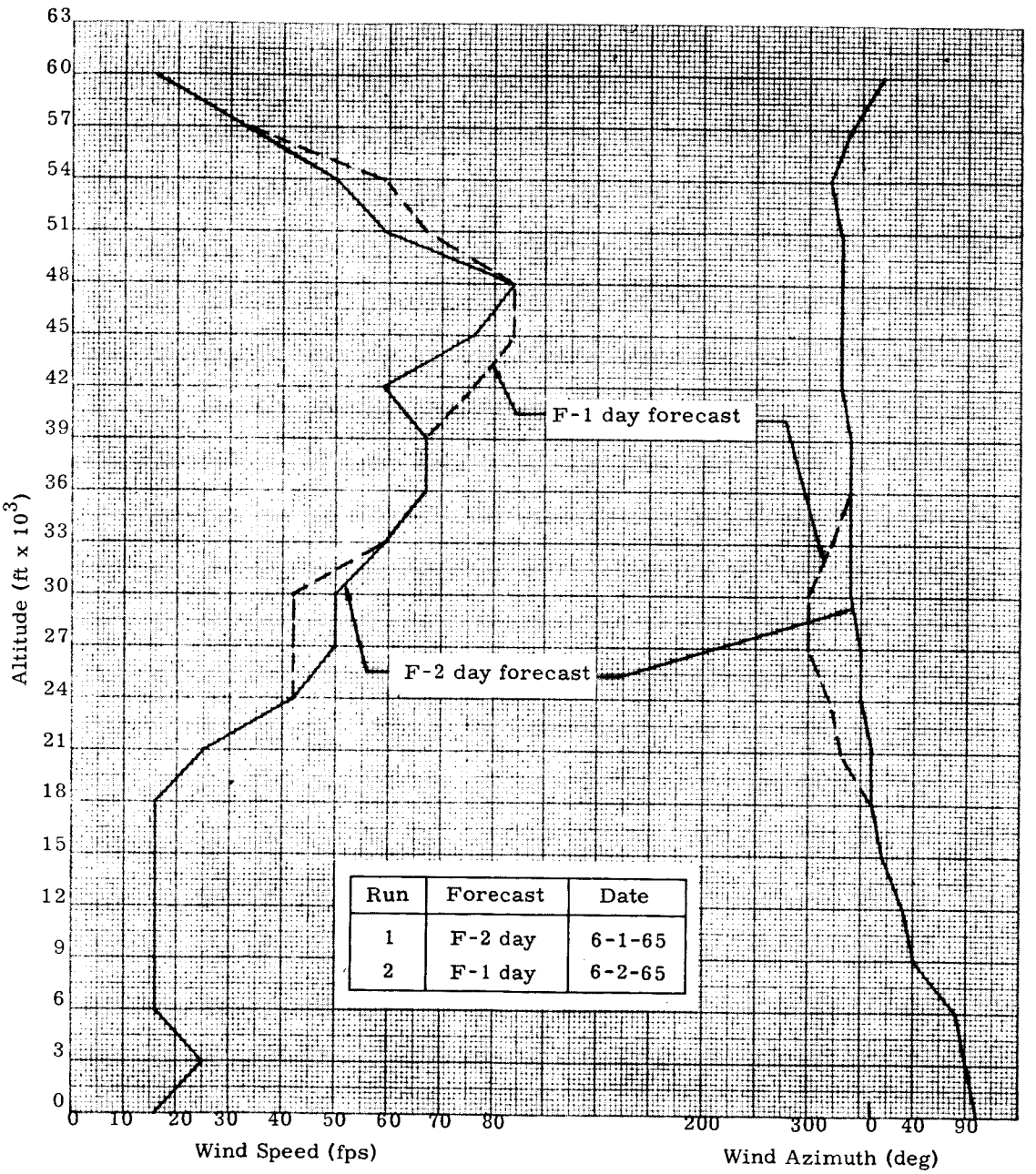

Fig. XI-1. Launch Winds Forecast for T + 0

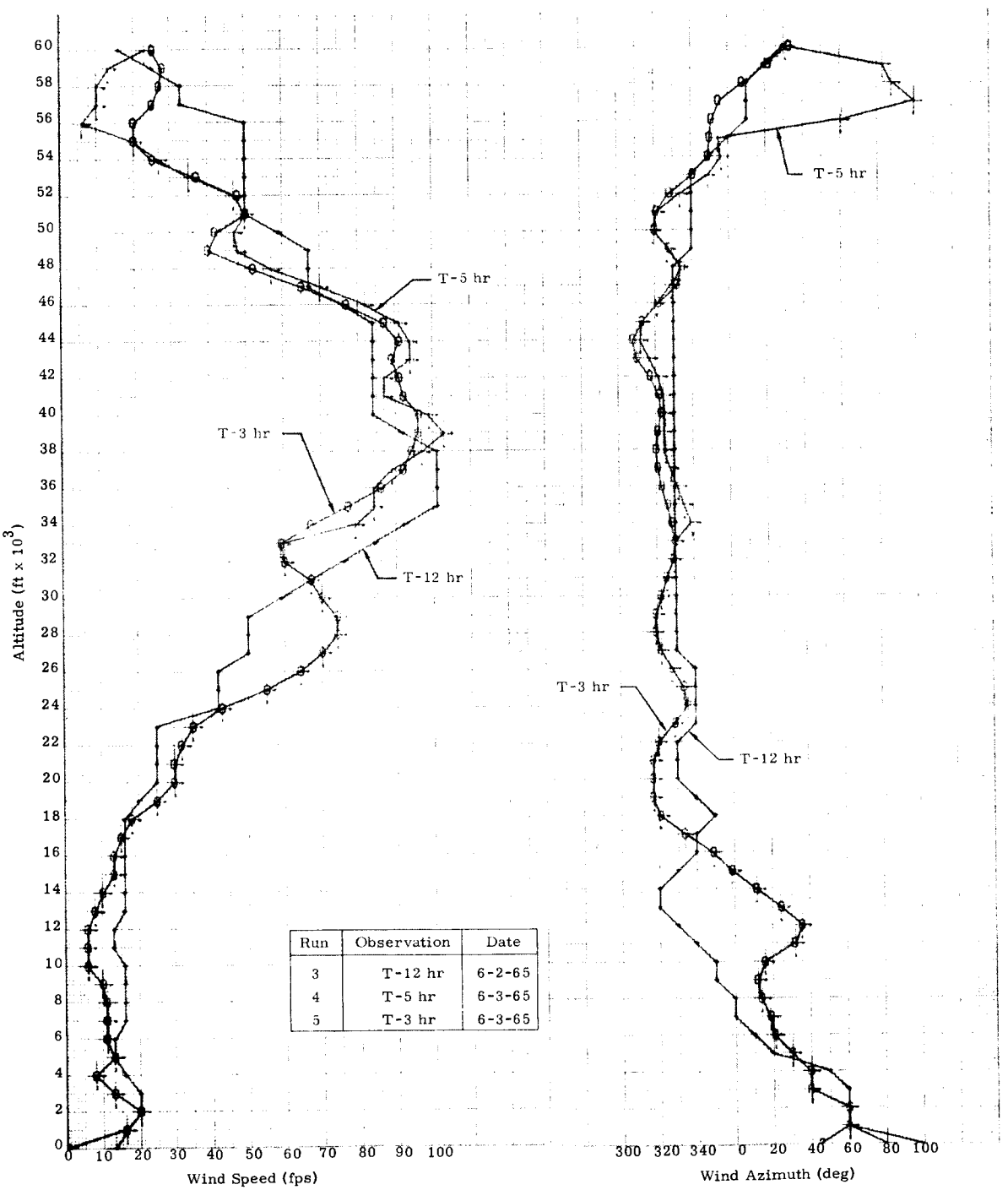

Fig. XI-2. Winds-Aloft Forecast and Observations

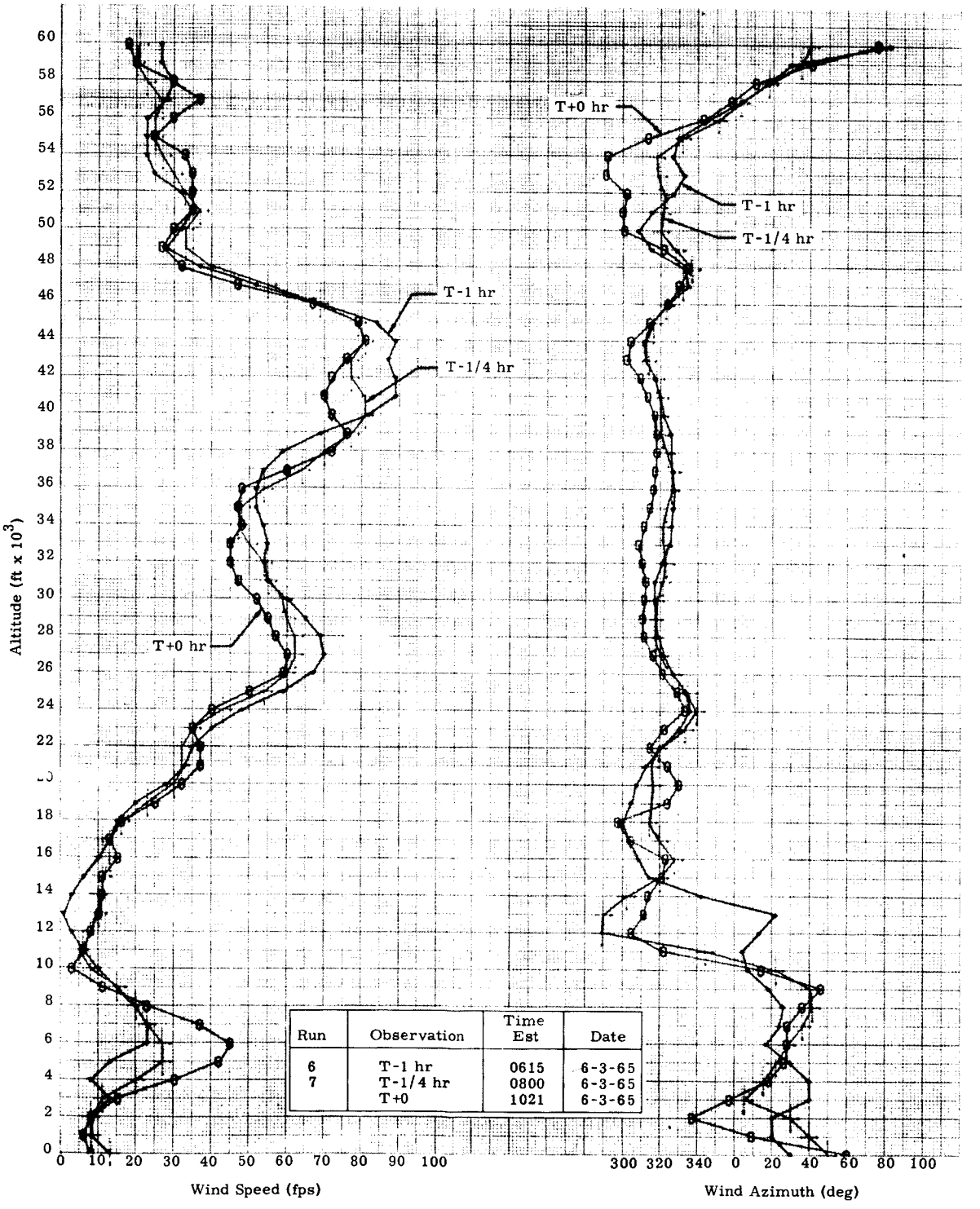

Fig. XI-3. Winds-Aloft Observations

although later shown to be 10% conservative because of a sign error in the computer, were below limit strength--thus, all recommendations were "go." The simulations indicated that peak loads would occur at 65 and 75 seconds after liftoff because of a double-spiked wind profile.

3. Analog Transient Simulations

The engine gimbal angles, attitude errors, and the pitch and yaw angles of attack obtained from the wind load analog simulations were sent to the Monitors in both MCCs and to the flight crew for use as a preview of vehicle and control system responses to the winds aloft.

4. First-Stage Propellant Tank Underpressure Constraints

The Stage I tank underpressure constraints for GT-4 were selected to maintain structural integrity for the simulated loads. The constraints used were lower than the constraints required to withstand design winds which are more severe than those measured during the GT-4 prelaunch operations. The selected constraints were transmitted in timely fashion to both MCCs.

5. Slow Malfunction Switchover Action Threshold

The slow malfunction switchover action threshold was sent to both MCCs in the form of inertial velocity (EUVTIL) and inertial flight path angle (GPTIL). The V-γ threshold was computed from an original set of six functions using average wind velocity increase with altitude and average wind direction, and interpolating to produce the operational threshold. This threshold (in the trajectory pitch plane) was transmitted to the Guidance Monitors in both MCCs.

6. Wind Comparison

Data from seven prelaunch winds-aloft observations are shown graphically in Figs. XI-1, XI-2 and XI-3. Special plots were transmitted to Cape Kennedy for use as a gage of existing wind conditions and as an indicator of the wind trend. These plots included the specification winds and a list of wind shears relative to specification shears. The winds-aloft forecasts for launch, made on F-2 and F-1 days, are shown in Fig. XI-1. A peak speed of 84 fps (57 mph) at a 45,000-foot altitude from an azimuth of 330 degrees (78 degrees left of tail) was forecast.

The launch day winds-aloft observations are shown in Figs. XI-2 and XI-3. These graphs show the wind profile varying from the forecast to a double-spike profile with a maximum speed of 81 fps at a 44,000-foot altitude from an azimuth of 304 degrees at launch.

Table XI-2 shows that the GT-4 wind speed was the lowest experienced of the four missions flown but its direction shows more cross-wind component. The GT-4 winds were half the intensity of those on the GT-2 and GT-3 flights and were essentially of the magnitude of the GT-1 mission. Seasonal wind conditions account for these differences.

TABLE XI-2

Comparison of Mission Simulations

Item	GT-1	GT-2	GT-3	GT-4
Sounding Data	T-2 hr	T-1 hr	T-1 hr	T-1 hr
Launch azimuth (deg)	72	105	72	72
Date of launch	4-8-64	1-19-65	3-23-65	6-3-65
Peak wind speed (fps)	107	195	185	89
Altitude of peak speed (ft)	44,000	69,000	43,000	41,000
Wind azimuth of peak speed (deg)	310	243	289	320
Wind off tail (deg)	58 L	42 R	37 L	68 L
Structural load Limit strength (%)	74	83	82	76

Table XI-3 lists definitive parameters of the GT-4 simulations and of the measured winds-aloft. The T-3 and T-1 hour updating information sent to the guidance Monitors was comparable to the T-12 and T-5 hour simulations that had been used to modify the plotboards in the MCCs. The launch wind (balloon released at liftoff) parameters listed in Table XI-3 also compare well with the prelaunch soundings. This agreement indicates that the prelaunch winds were representative of the actual conditions which existed in flight.

TABLE XI-3

Summary of GT-4 Simulation Data

Item	T-12 hr	T-5 hr		T-3 hr		T-1 hr		T-1/4 hr		T-0 Liftoff Balloon	
Time of wind sounding (EST)	-	-		-		-		0800 (6-3-65)		1021 (6-3-65)	
Time of data release (EST)	2100 (6-2-65)	0400 (6-3-65)		0600 (6-3-65)		0800 (6-3-65)		1000 (6-3-65)			
Altitude of peak (ft)*	35,000	28,000	39,000	28,000	39,000	27,000	41,000	27,000	40,000	27,000	44,000
Peak wind speed (fps)	101	74	103	74	96	70	89	62	81	60	81
Wind speed/spec wind (%)	60	47	56	47	51	48	49	41	44	38	42
Wind azimuth at peak (deg)	330	319	324	319	321	322	320	320	320	316	304
Wind degrees off tail	78 L	67 L	72 L	67 L	69 L	70 L	68 L	68 L	68 L	64 L	52 L
Structural load limit strength (%)	80	77	75	77	77	76	76	No simulations		No simulations	
Wind shear downward, 3000 ft from peak (sec^{-1})	0.0084	0.0083	0.0075	0.0083	0.0035	0.0087	0.0104	0.0084	0.0063	0.0083	0.0052
Wind shear spec (%)	26	33	22	33	10	37	28	36	18	35	14
Launch recommendation	Go	Go		Go		Go		No simulations		No simulations	
Max GPTIL (nominal 28.03 deg)	27.55	27.58		Canceled		27.53		No simulations		28.15 (flight value)	
Max VYTIL (nominal zero) (fps)	63.01	60.25		Canceled		52.23		No simulations		40 (flight value)	

*Double spike occurred after T-12 hr.

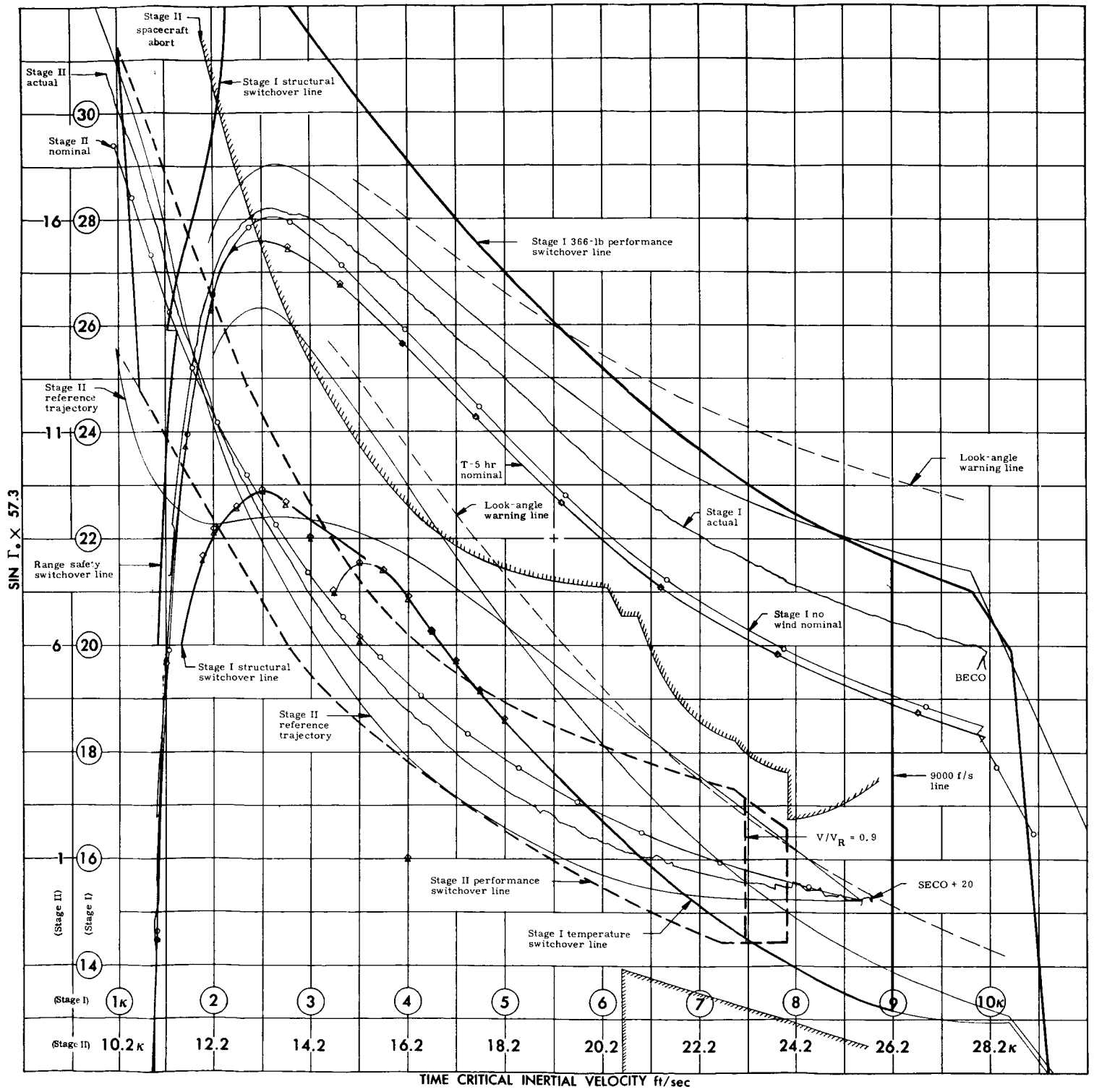

Fig. XI-4. Houston-MCC Plotboard VA, Pitch Plane

B. SLOW MALFUNCTION MONITORING

The prime slow malfunction monitoring facility for GT-4 was the Mission Control Center (MCC) at MSC-Houston, with the MCC at Cape Kennedy utilized in a back up mode for the boost phase. Hand-over procedures were effected to transfer control to MCC-Cape Kennedy, if required. However, MCC-Houston remained prime throughout the GT-4 mission.

1. Countdown

The Baltimore prelaunch wind simulations and performance predictions were received on schedule. The T-5 hour simulation was utilized to develop the $V_I - \tilde{\gamma}_p$ (Plotboard VA, Figs. XI-4 and XI-5) and the $V_y - T_E$ (Plotboard IIIA, Figs. XI-6 and XI-7) displays. The performance switchcover constraint was developed to incorporate a -67 pound payload pad at the 0900 liftoff. The hold for the erector lowering problem did not affect performance significantly as the payload pad was -62 pounds at actual liftoff. The accepted ground rule for revising performance a· ·on lines requires a change of 50 pounds or more; therefore, the 5-pound increment was not utilized.

There were no anomalies or discrepancies requiring Monitor action through the countdown and both guidance facilities were "go" prior to T-0.

2. Stage I Flight

a. Pitch

The lofted trajectory was apparent on Plotboard VA. $\tilde{\gamma}_p$ was 1.54 degrees high at BECO (Plotboard VA), and $\bar{h}$ was approximately 1 naut mi high at BECO ($\bar{h}$ information from Burroughs). The low pitch program was confirmed by the nose-down command from the IGS attitude error display on SCR No. 1 (Figs. XI-8 and XI-9). Thrust appeared normal on the velocity versus elapsed time display on Plotboard IIIA (Fig. XI-7) at MCC-Cape Kennedy; however, the same display on Plotboard IIIA (Fig. XI-6) at MCC-Houston indicated an apparent low thrust. Postflight investigation of the thrust difference between MCC-Cape Kennedy and MCC-Houston showed an erroneous operation of the ordinate axis (elapsed time) drive on the Houston $V_I - T_E$ display. Cognizant NASA personnel are investigating this problem for resolution prior to GT-5 operations.

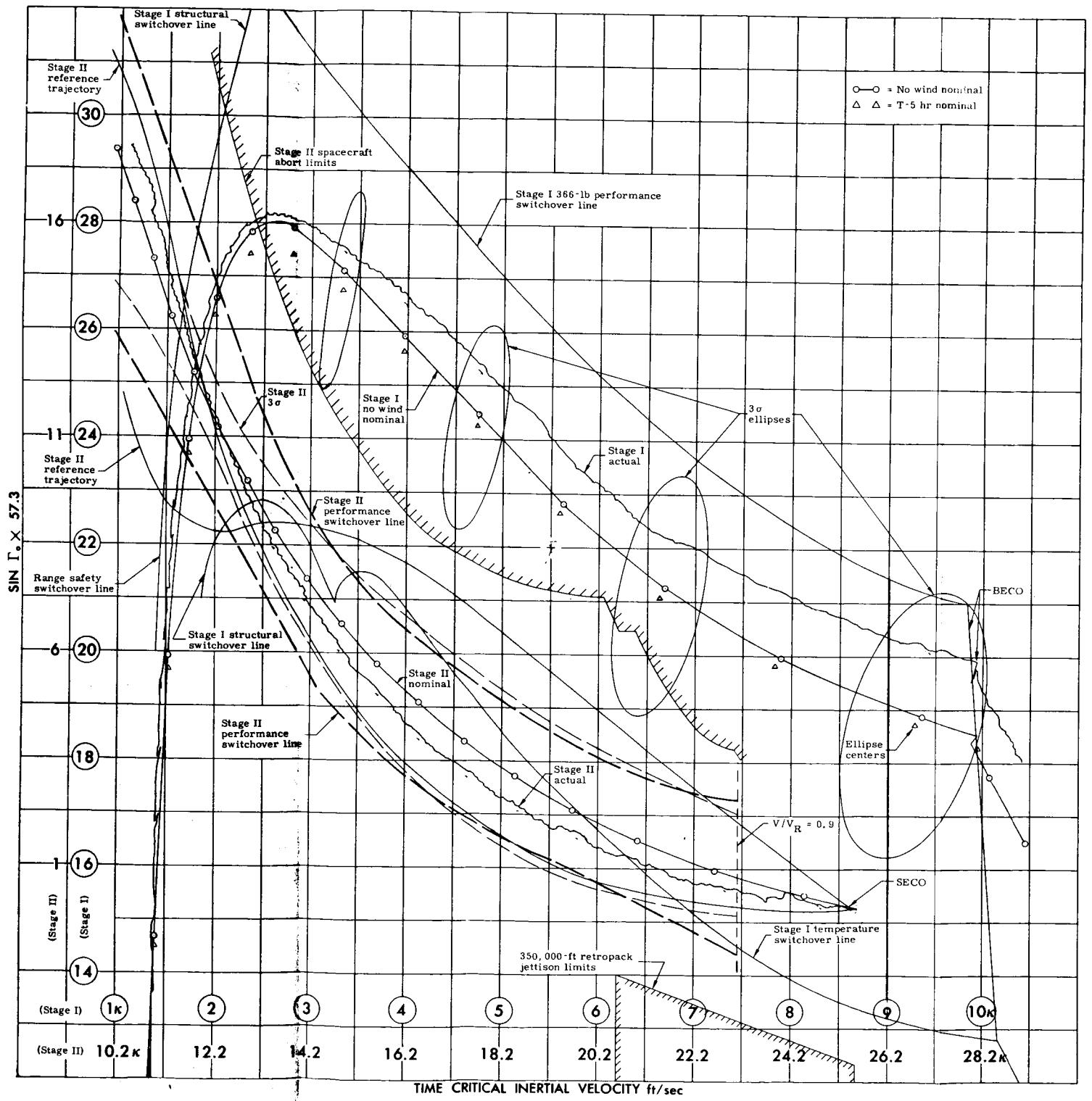

Fig. XI-5. GT-4 ETR Plotboard VA, Pitch Plane

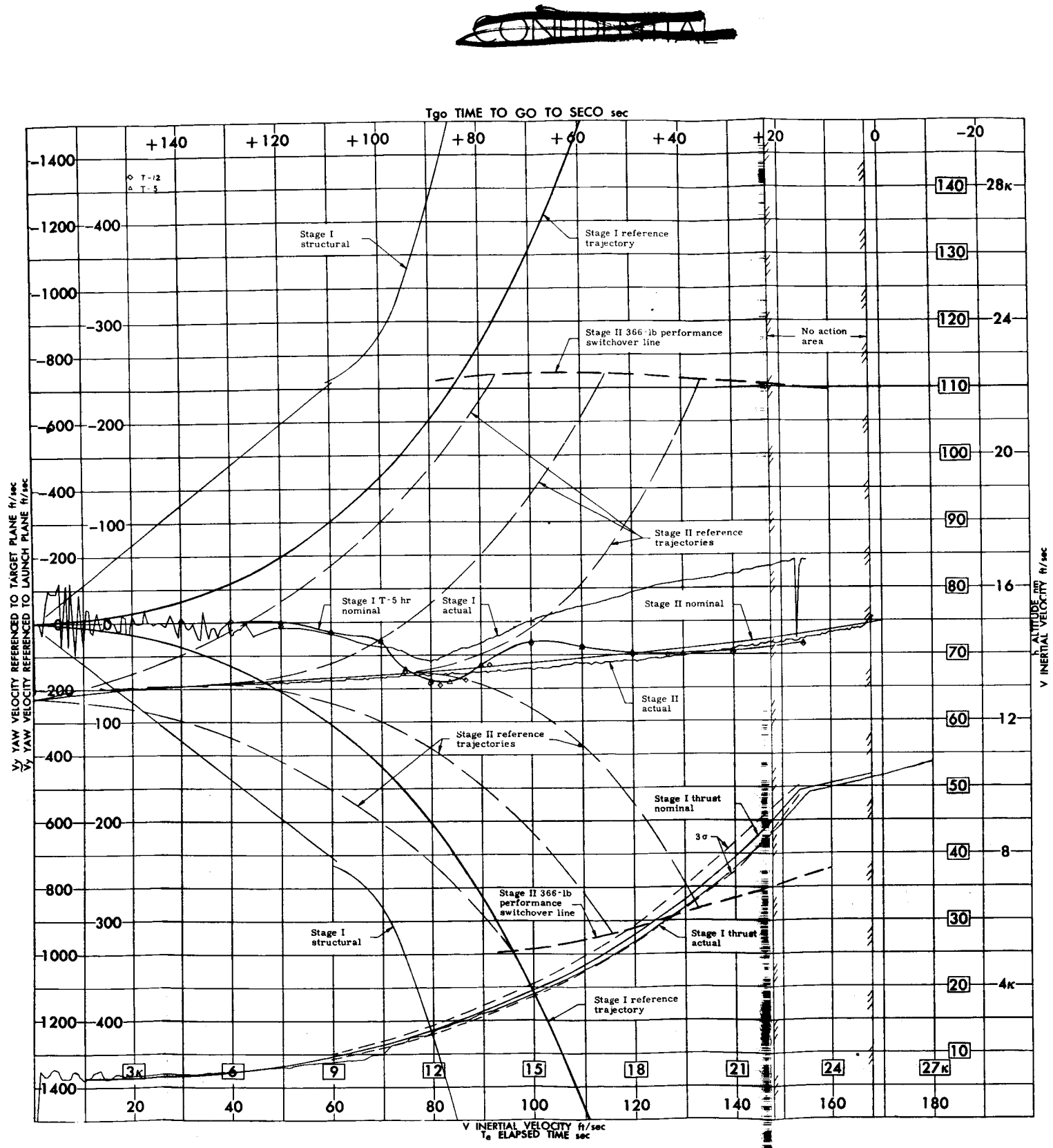

Fig. XI-6. Houston-MCC Plotboard IIIA, Lateral Velocity

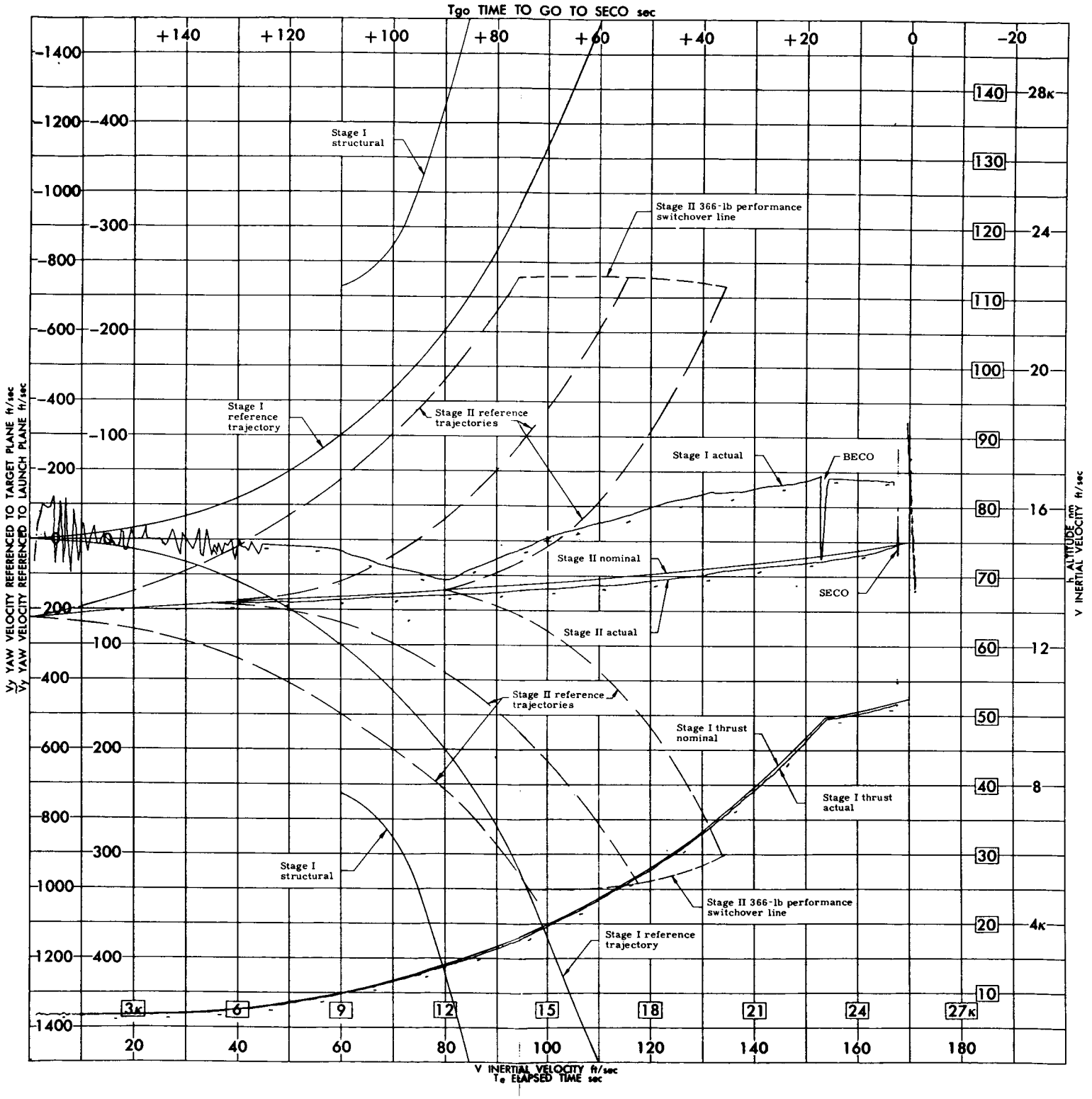

CONFIDENTIAL

ER 13227-4

Fig. XI-7. GT-4 ETR Plotboard IIIA, Lateral Velocity

Stage II	Stage I	
1-Sec Marks from Liftoff		1
$\theta_{e_s} \pm 6°$	$\theta_{e_s} \pm 6°$	1
SWO		2
$\theta_{e_p} \pm 7°$	$\theta_{e_p} \pm 7°$	2
GCP		3
$\delta\beta_p \pm 5°$	$\dot{\theta}_c$	3
GCS		4
$\omega_{pN} \pm 2°/sec$	$\delta\theta_1 \pm 5°$	4
TARS Guid Init		5
$\dot{\theta}_g \pm 2°/sec$	$AP\theta_1 \pm 5°$	5
$\delta_6 = 1$ A-1 Computer Guid Start		6
$\omega_{pS} \pm 0.25°/sec$	$\delta\theta_2 \pm 5°$	6
$\delta_7 = 1$ A-1 Computer SECO		7
$\delta\theta \pm 3°$	$AP\theta_2 \pm 5°$	7
SSCO		8
N/A	$\dot{\phi}_c$	8
1-Sec Marks from Liftoff		9

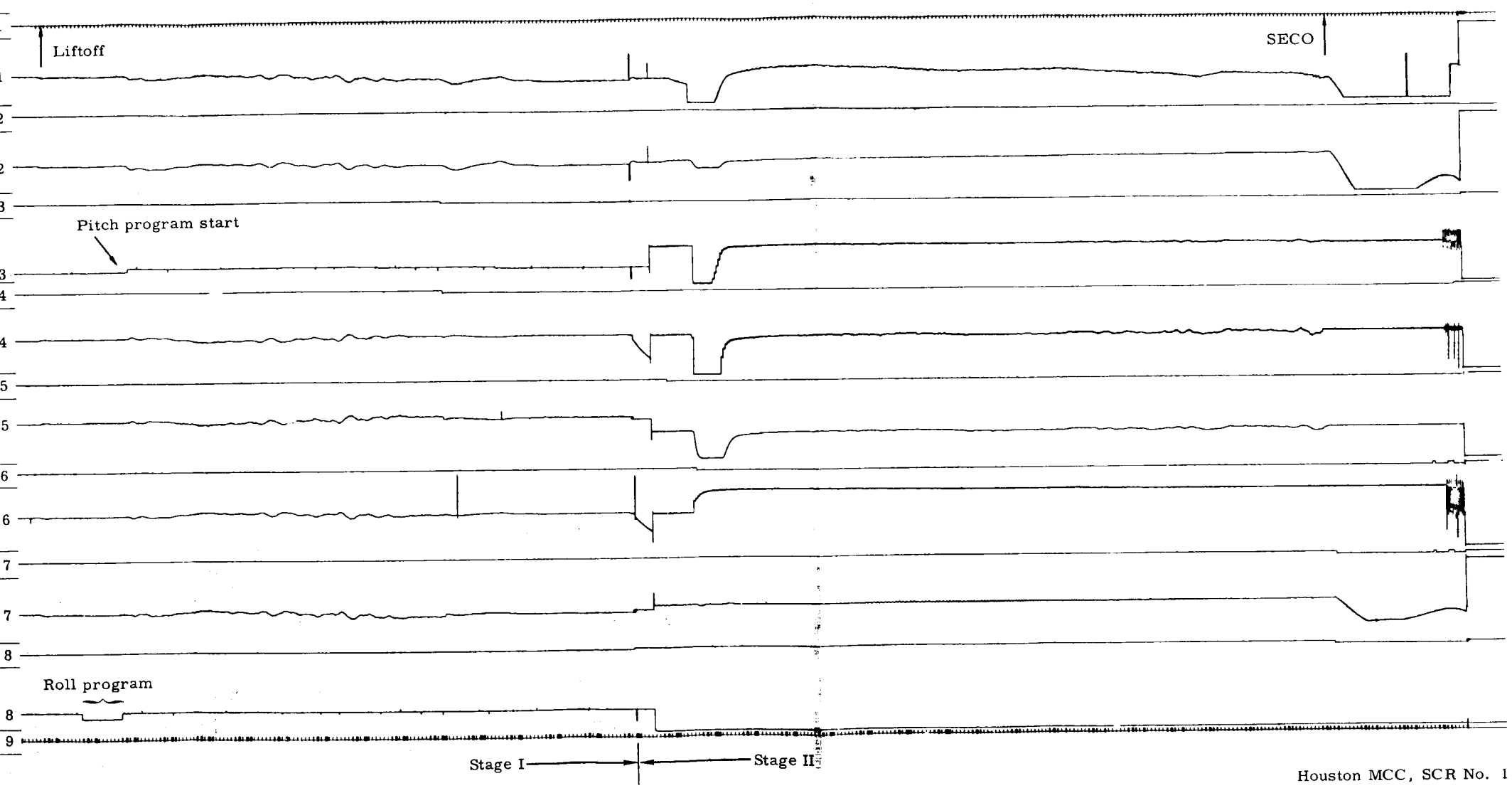

Houston MCC, SCR No. 1

Fig. XI-8. Telemetry III Pitch Axis Recording (Houston MCC)

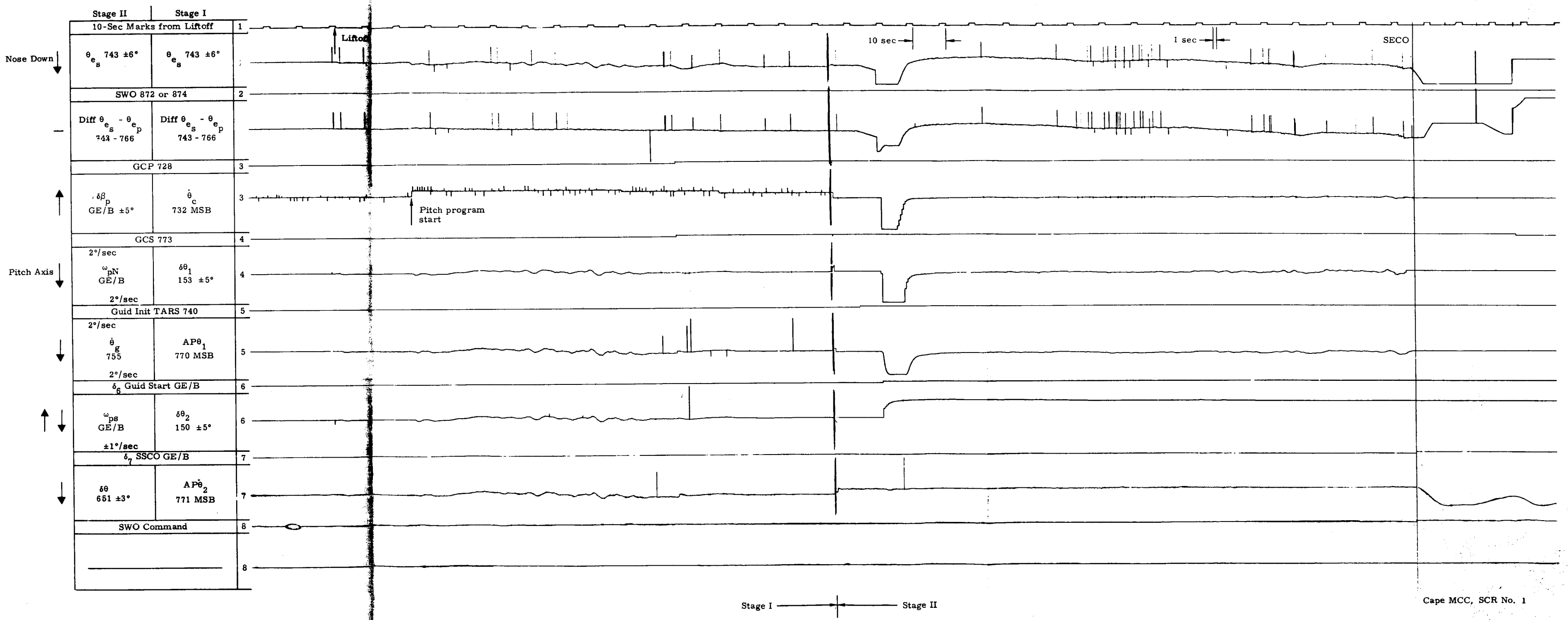

Fig. XI-9. Telemetry III Pitch Axis Recording (Cape MCC)

b. Yaw

The yaw-left velocity (Plotboard IIIA, Figs. XI-6 and XI-7) at BECO (-60 fps) was the result of a cross-coupling effect created by roll-axis error and the thrust differential between the two subassemblies. The yaw-left error was confirmed by the demand nose-right command from the IGS attitude error display on SCR No. 2 (Figs. XI-10 and XI-11).

c. Roll

The TARS roll drift was approximately 23 deg/hr CCW as confirmed by the roll clockwise command from the IGS attitude error display on SCR No. 2 (Figs. XI-10 and XI-11). The TARS roll gyro drift apparently resulted from the "g" sensitivity of the roll axis. MCC-Houston encountered an intermittent dropping of a significant bit in Meas 0768 (Fig. XI-10) (primary roll adapter output) starting approximately 12 seconds prior to BECO. The bit dropout did not impair the monitoring effort and NASA is investigating the cause of this anomaly.

3. Stage II Flight

a. Pitch

RGS steering responded properly to the high dispersed conditions at BECO. The A-1 computer quantity, ω_p N, was saturated nose-down at 2 deg/sec for approximately 6 seconds from LO + 163 to LO + 174 seconds. IGS appeared nominal throughout the guided portion of the flight. Cape Kennedy Plotboard VA (Fig. XI-5) stops plotting at δ_7 (SECO) and Houston Plotboard VA (Fig. XI-4) continues to plot data until SECO + 20 seconds. The slight pitch engine oscillation (1 cps and 0.12 degree peak-to-peak) was the result of cross-coupling from the roll-nozzle oscillation, and was present from $97FS_1$ until LO + 320 seconds. The oscillation presented no problem and required no Monitor action.

b. Yaw/Roll

Both RGS and IGS were nominal throughout the guided portion of the flight. The yaw decoder output Meas 0756 at MCC-Houston experienced dropouts similar to Meas 0768 in Stage I (SCR No. 2, Fig. XI-10). The problem is under investigation by NASA. The roll nozzle displayed an oscillation of 1 cps and 2.3 degrees peak-to-peak that was present from $97FS_1$ until LO + 320 seconds. The oscillation presented no problem and no Monitor action was required.

Stage II	Stage I	
1-Sec Marks from Liftoff		1
$\phi_{e_s} \pm 6°$	$\phi_{e_s} \pm 6°$	1
SWO		2
$\phi_{e_p} \pm 7°$	$\phi_{e_p} \pm 7°$	2
GCP		3
$\psi_{e_s} \pm 6°$	$\psi_{e_s} \pm 6°$	3
GCS		4
$\psi_{e_p} \pm 7°$	$\psi_{e_p} \pm 7°$	4
TARS Guid Init		5
$\omega_{yN} \pm 2°/sec$	$\delta\psi_1 \pm 5°$	5
$\delta_6 = 1$ A-1 Computer Guid Start		6
$\dot{\psi}_g \pm 2°/sec$	$AP\psi_1 \pm 5°$	6
$\delta_7 = 1$ A-1 Computer SECO		7
$\delta\psi \pm 3°$	$\delta\psi_2 \pm 5°$	7
SSCO		8
$\delta\phi \pm 33°$	$AP\psi_2 \pm 5°$	8
1-Sec Marks from Liftoff		9

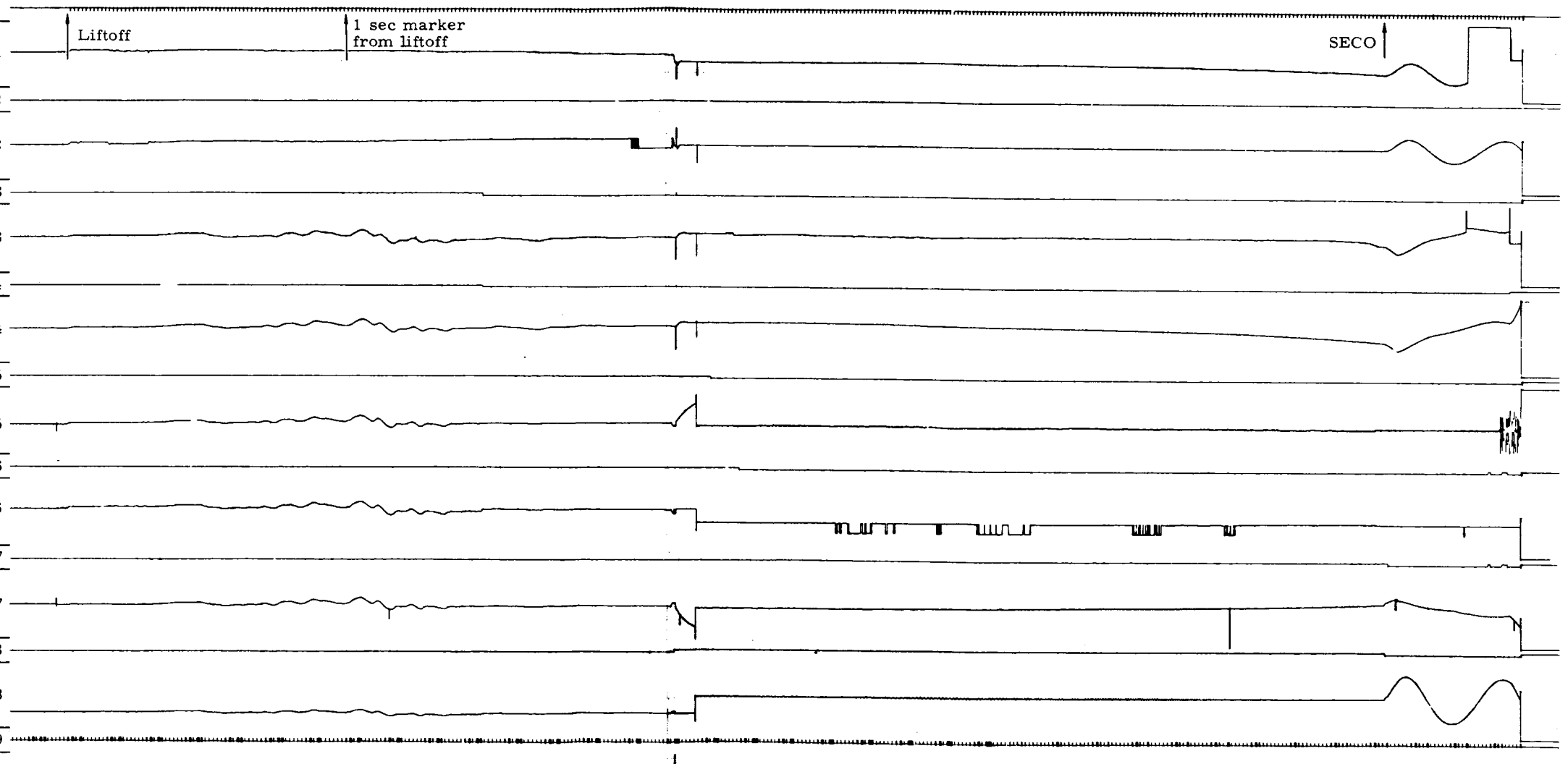

Fig. XI-10. Telemetry III Yaw-Roll Axis Recording (Houston MCC)

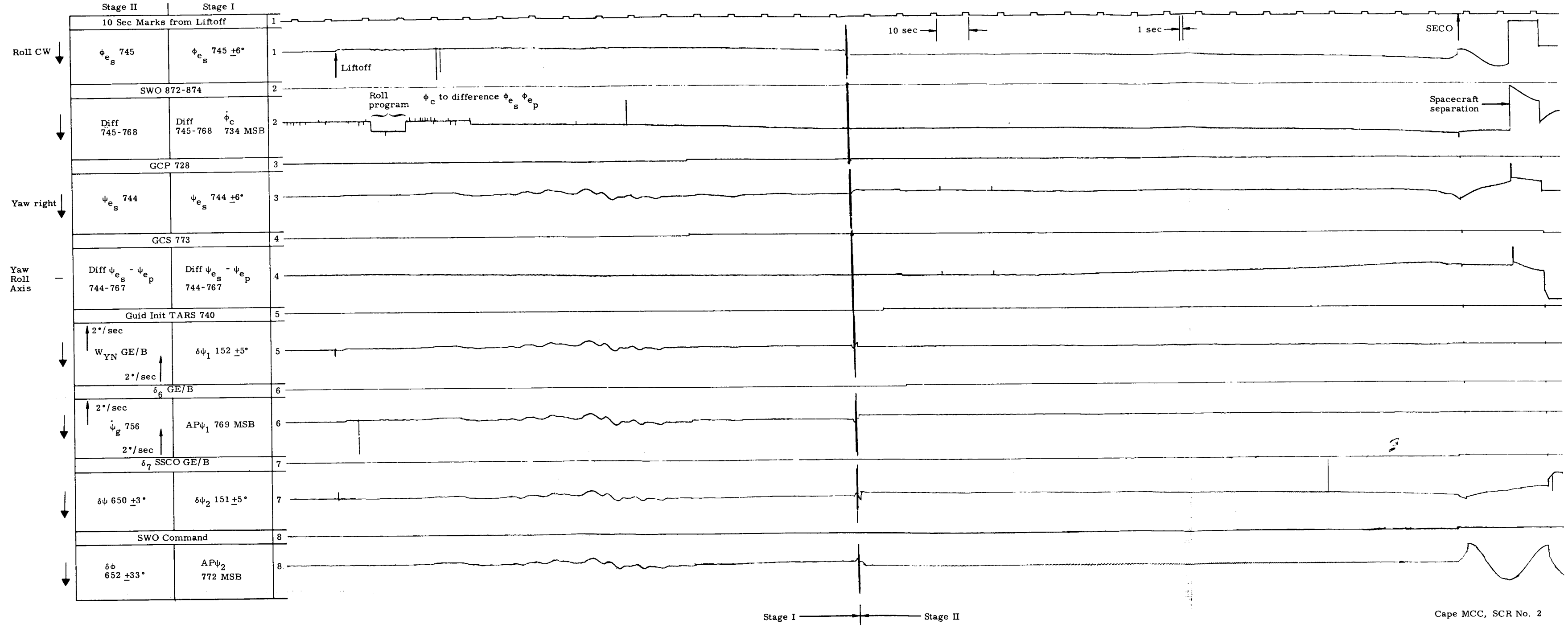

Fig. XI-11. Telemetry III Yaw-Roll Axis Recording (Cape MCC)

c. Discretes

All real time monitored discretes occurred within their specified tolerances.

4. Problem Areas

Data/TV display formats No. 0200 and No. 0201 at MCC-Houston experienced a 30 to 40 second data loss, apparently caused by computer buffer overflow. The aforementioned formats were not prime for the GT-4 mission; however, the problem is under investigation by NASA.

5. Recommendations

A request has been made to SSD/Aerospace to change the scaling on the ω_{pS} display from ± 0.25 deg/sec to ± 0.50 deg/sec to facilitate the diagnosis of dispersed trajectory guidance recovery maneuvers. The ω_{pS} change has been requested for GT-5.

C. ACTUATOR IMPULSE LOADS

The GT-4 Stage I actuator deflections at engine start were of the same general magnitude and characteristic shape as those observed on previous Gemini and Titan II flights. The engine start transient applied tension impulse loading to the yaw/roll actuators and compression impulse loading to the pitch actuators.

The measured GT-4 actuator travel responses to the impulse loads and the actuator load parameters derived from measured responses are presented in Table XI-4. The table also lists the same parameters for GT-2, GT-3 and includes the failure levels of the ground tested speciment (Ref. 22).

A review of Table XI-4 shows that the peak actuator loads for GT-4 were within the range defined by the maximum and minimum loads recorded for GT-2 and GT-3. The review also indicates that the peak GT-4 loads were well within the capability of the present actuator design. The margin of safety for the maximum GT-4 actuator load (27,900 pounds, Actuator 3_1) was 29%, based on a limit load of 36,000 pounds.

TABLE XI-4

Stage I Actuator Response to Engine Ignition Loads

Measured and Calculated Actuator Parameters	GLV Modified Actuator Impulse Test Failure Point	GT-2				GT-3				GT-4			
		1_1	2_1	3_1	4_1	1_1	2_1	3_1	4_1	1_1	2_1	3_1	4_1
Max deflection (in.)	0.328	0.094	0.24	0.202	0.122	0.148	0.264	0.096	0.048	0.184	0.272	0.260	0.068
Max deflection rate (in./sec)	19.8	6.6	12.5	8.7	7.15	8.7	10.4	6.85	3.28	7.2	12.0	12.16	4.8
Max load (lb)	47,000 ** 36,000 ***	20,900 *	28,200 *	23,500 *	21,500 *	23,500*	25,200 *	21,400 *	15,050 *	21,700 *	27,600 *	27,900 *	18,400 *
Impulse Energy (in.-lb)	24,630 ** 13,420 ***	3300 *	8170*	4850 *	3700 *	4850 *	6280 *	3580 *	1315 *	3760 *	7850 *	7960 *	2130 *
Max cylinder pressure (psi)	9625 ** 7500 ***	4600*	6000 *	5000 *	4600 *	5000 *	5400 *	4580 *	3140 *	4650 *	5900 *	5920 *	4000 *

* Loads parameters derived from maximum deflection rates and loads model of Ref. 22.

** Inherent mechanical limit; failure not correctable by switchover.

*** Internal hydraulic failure results in a null shift in the primary system; failure correctable by manual switchover (see Figs. X-19, X-24 and X-31 and Appendix D of Ref. 22).

XII. AIRFRAME SYSTEM

A. STRUCTURAL LOADS

GT-4 flight data analysis indicates that the structural loads imposed on the vehicle were within design limits. The most critical loading condition occurred at BECO where the load aft of Station 320 reached 101% of its design limit; however, this was only 75% of the tested strength of the vehicle at that station. A discussion of loads associated with specific flight periods follows.

1. Preignition

The static axial load consists of the 1 g deadweight distribution only (Fig. XII-1). There were no axial or lateral loads of significance which occurred prior to ignition. The maximum response to ground winds occurred at T-100 seconds, and caused only a 60,000-in.-lb bending moment at the BLH station. The winds were approximately 5 mph from a direction 40° east of north. There were no measurable wind-induced oscillations at the time of ignition.

2. Launch Prerelease

Prerelease lateral dynamic responses (from the BLH) occurred in the second and third structural modes, and in what appears to be the Stage I engine mode. The resulting loads are presented in Fig. XII-2.

The influence of wind-induced oscillation was negligibly small on engine deflection at ignition; however, a yaw side load of approximately 2350 pounds existed, indicating a net equivalent engine misalignment angle of 0.314 degree.

The prerelease axial dynamic loads resulting from the engine start transient were of smaller magnitude than those experienced on any previous Gemini flight. This can be attributed to a much smoother ignition of the hypergolic propellants, as recorded by the BLH measurement system (e.g., the Stage I fuel tank dome load factor was only 61% of the corresponding value recorded on GT-3). The resulting envelope of static plus dynamic axial loads is shown in Fig. XII-3. Propellant tank dome load factors associated with GT-4 thrust buildup in the Stage I engines are shown in Table XII-1.

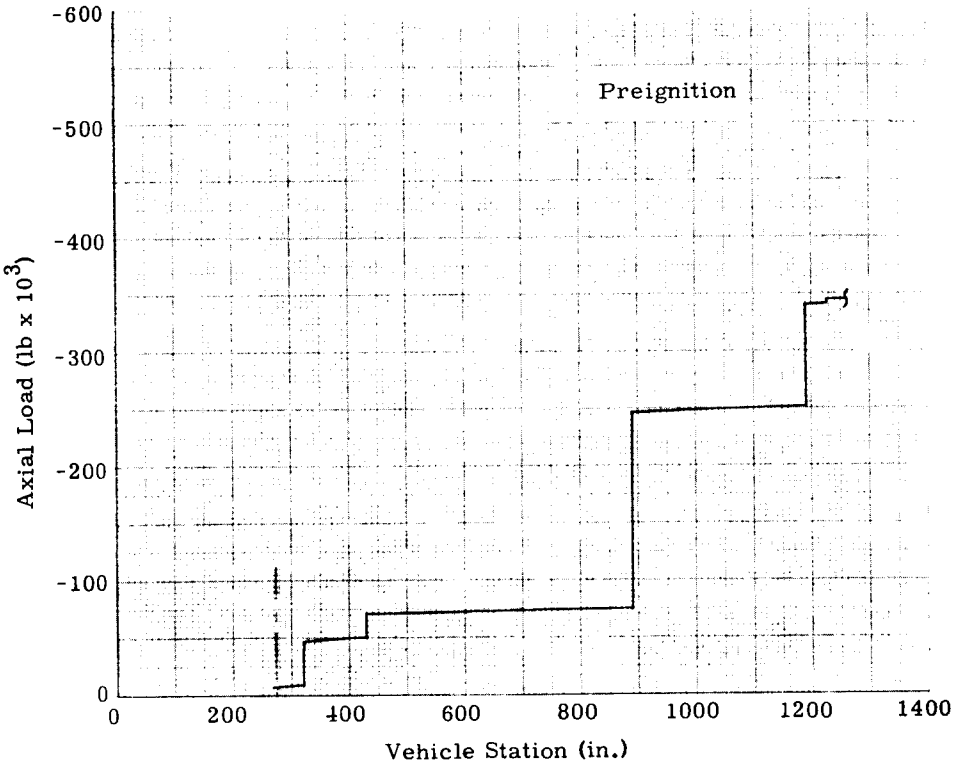

Fig. XII-1. Steady 1 g Axial Load

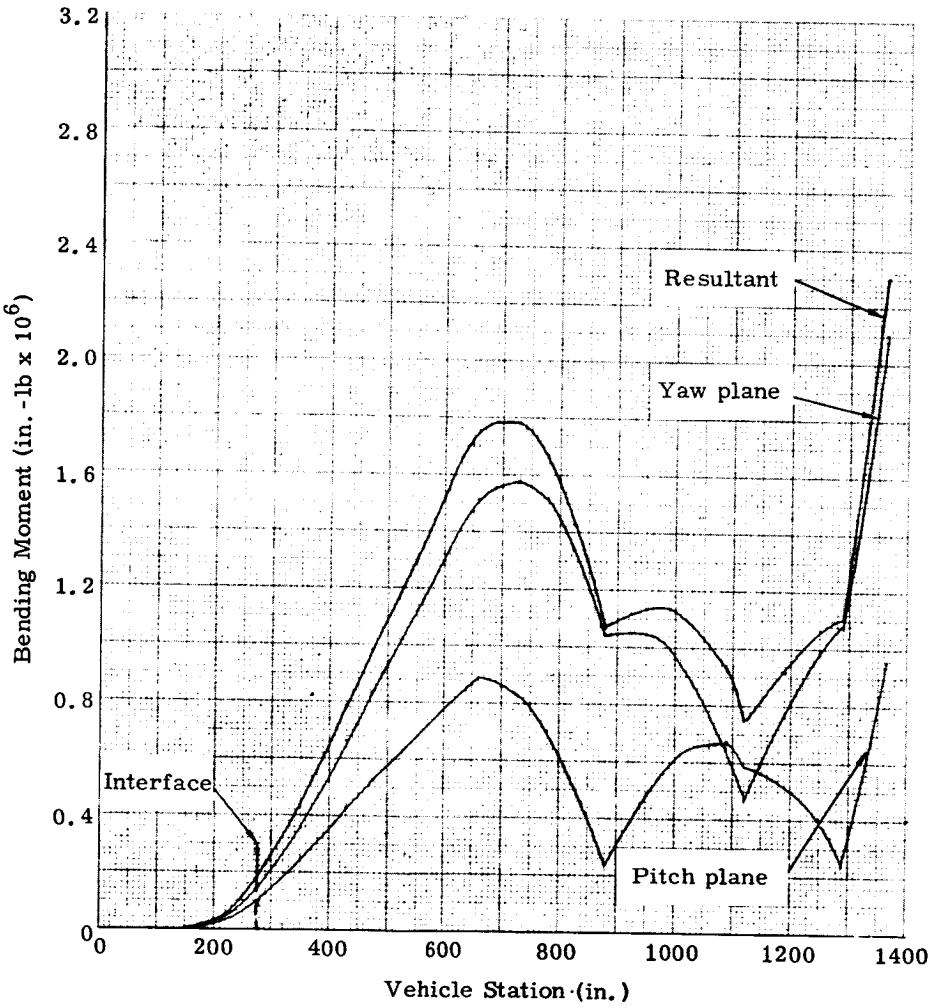

Fig. XII-2. Lateral Dynamic Bending Moment Envelope: Prerelease

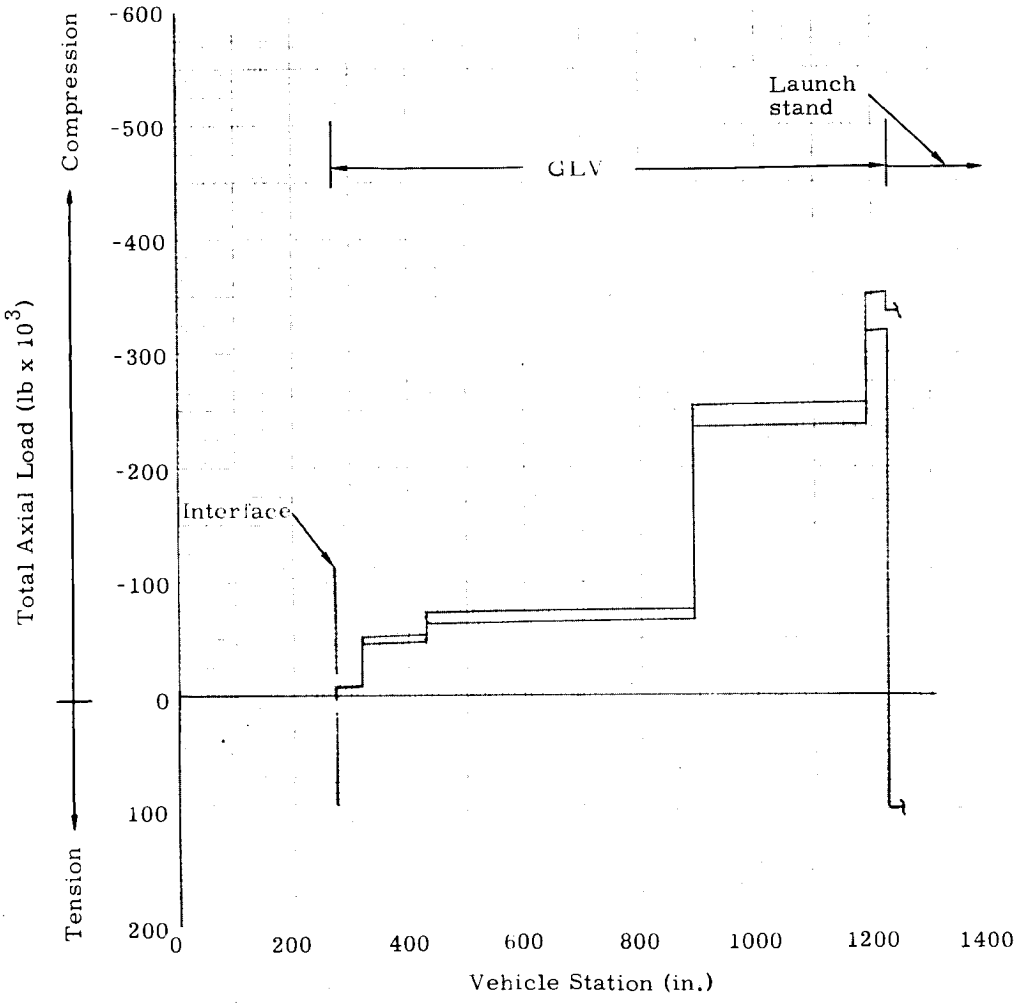

Fig. XII-3. Total Axial Load Envelope: Prelaunch

TABLE XII-1

Maximum Axial Loads in Propellant Tank Domes

Configuration	Prerelease		Launch Design Load Factor (g)
	Load (lb)	Load Factor* (g)	
Stage II oxidizer dome	47,765	1.238	2.76
Stage II fuel dome	27,959	1.264	3.54
Stage I oxidizer dome	182,668	1.062	1.91
Stage I fuel dome	114,663	1.277	2.85

*Based on actual loaded propellant weight.

3. Launch Postrelease

The liftoff axial load factor for GT-4 was 1.27, typical of all Gemini flights to date. Launch transients--a result of the sudden release of the vehicle from its cantilevered position on the launch stand to a free-free flight condition--were quite similar to those experienced on GT-3. The primary lateral bending modes of response were the first structural and Stage I oxidizer slosh modes; peak amplitudes were less than 0.1 g. Of the probable axial modes, only the first axial mode (8 cps) was in evidence at release.

Lateral loads resulting from postrelease transients are shown in Fig. XII-4.

4. Stage I Flight

The most significant periods of flight for vehicle loading occurred at Mach 1 (LO + 60 seconds) and at Max q α C_{N_α} (LO + 76 seconds). The greatest loads were due to the quasi-steady conditions (both thrust and winds aloft). The lateral dynamic loadings for these periods of flight (in addition to measured/calculated vibration frequency correlation) are shown in Figs. XII-5 through XII-10. The total combined loadings in terms of equivalent axial load (P_{eq}) are shown in Figs. XII-9 and XII-10.

Assuming that the Compartment 1 pressure differential was approximately 2 psi (as it was on GT-1 and GT-2), the resulting total interface loadings were therefore well within the vehicle's structural capability for this flight period.

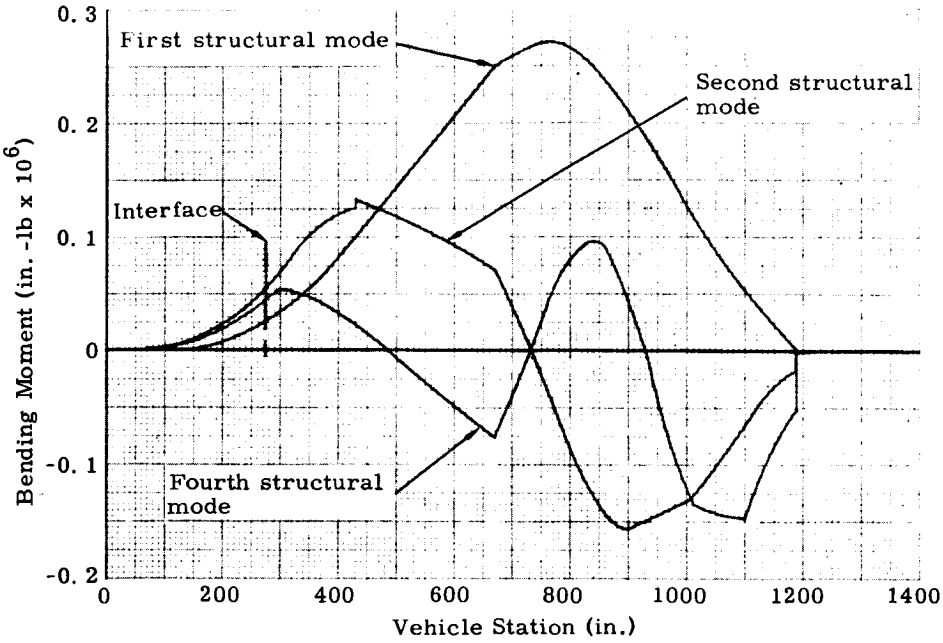

a. Modal Moment Distributions

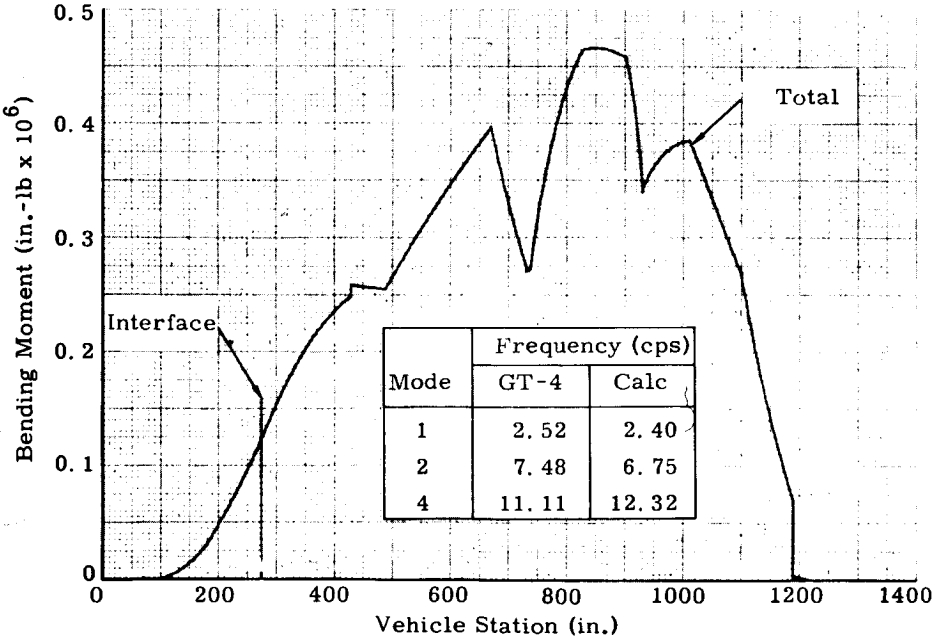

Mode	Frequency (cps)	
	GT-4	Calc
1	2.52	2.40
2	7.48	6.75
4	11.11	12.32

NOTE: Data based upon rate gyro response.

b. Summation of Modal Moments

Fig. XII-4. Total Lateral Load Envelope--Post-release

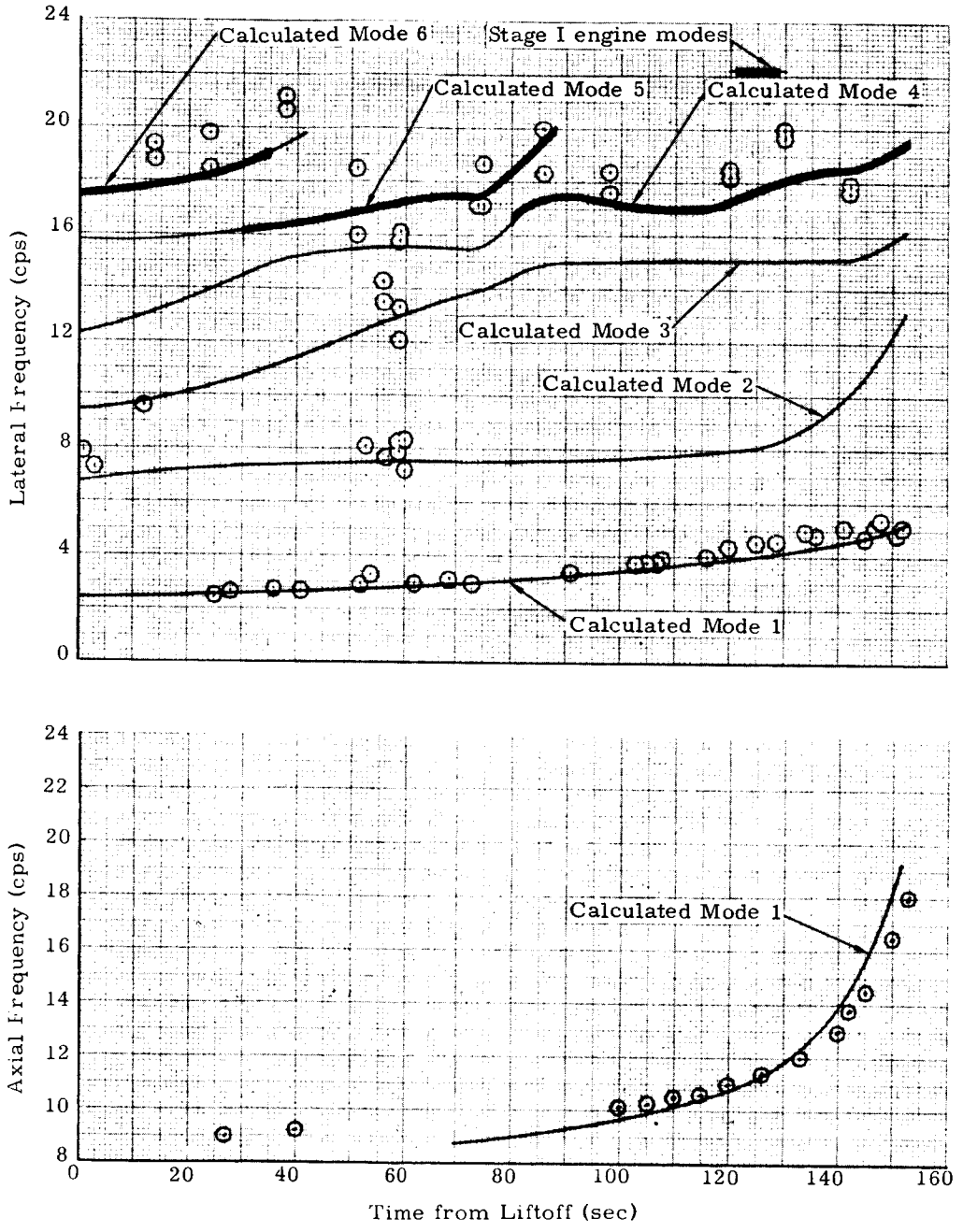

Fig. XII-5. Stage I Flight Vibration Frequency Correlation

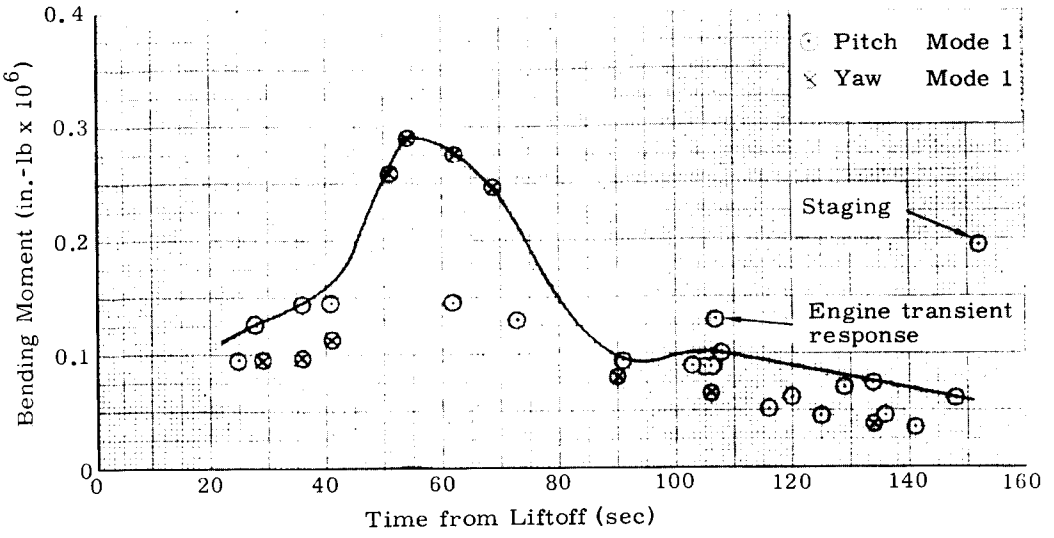

Fig. XII-6. Peak Modal Bending Moment as Determined by Compartment 1 Accelerometers

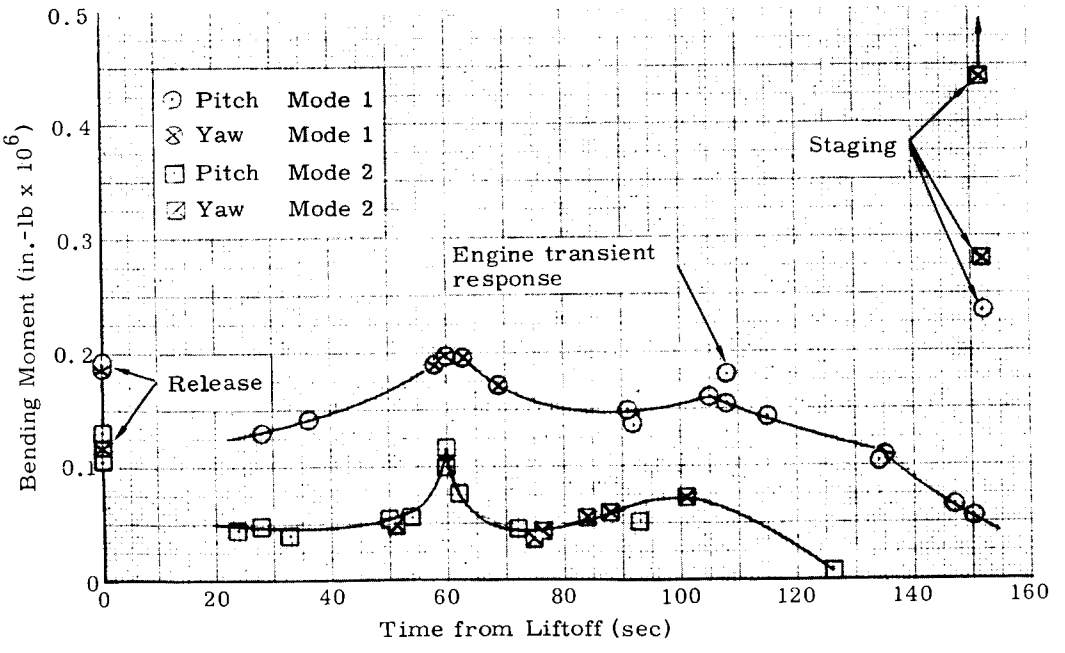

Fig. XII-7. Peak Modal Bending Moment as Determined by Stage II Rate Gyros

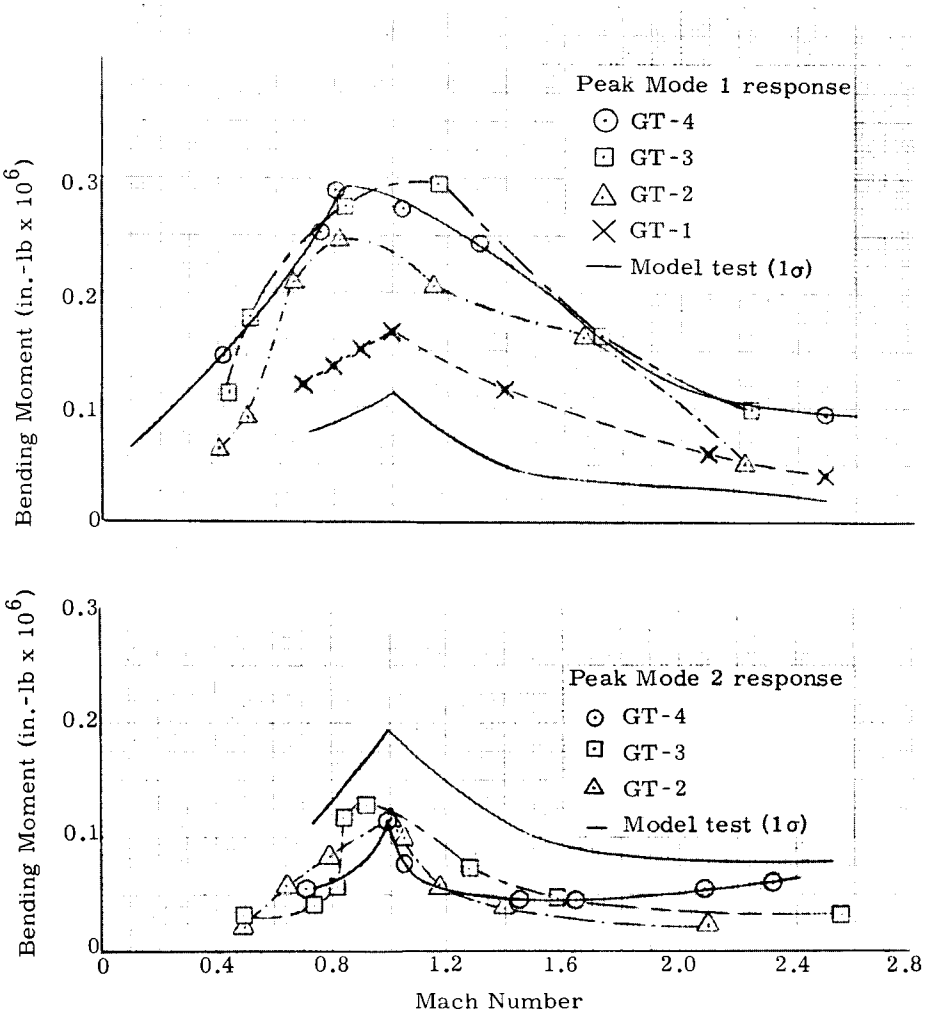

Fig. XII-8. Peak Modal Bending Moment Response to Transonic Buffet: Lateral

Mode	Frequency (cps)	
	GT-4	Calc
1	2.99	2.93
2	7.85	7.55
4	15.8	15.59
I engine	16.7	17.47

NOTE:
Data based upon rate gyro response.

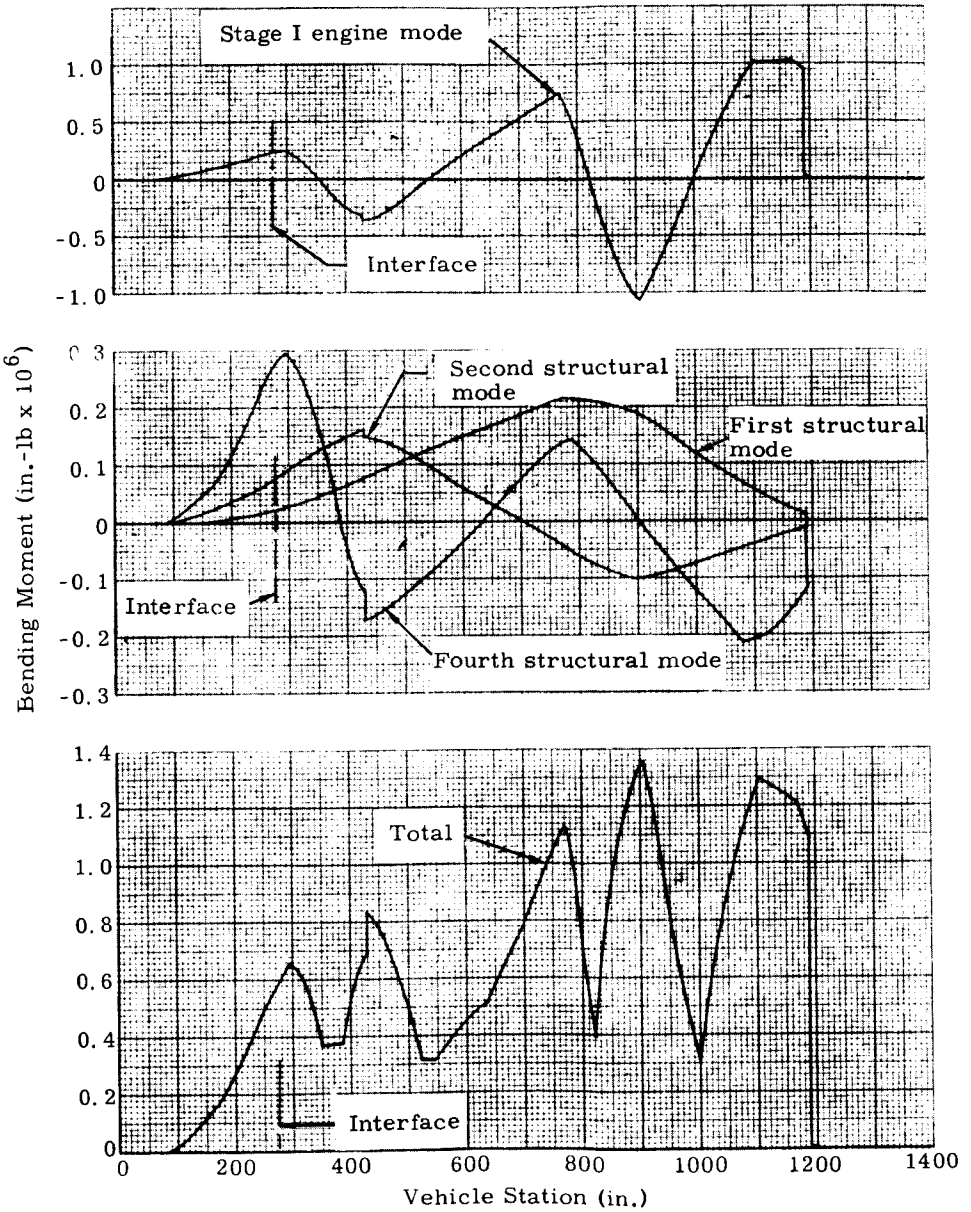

Fig. XII-9. Total Lateral Load Envelope--Transonic Buffet

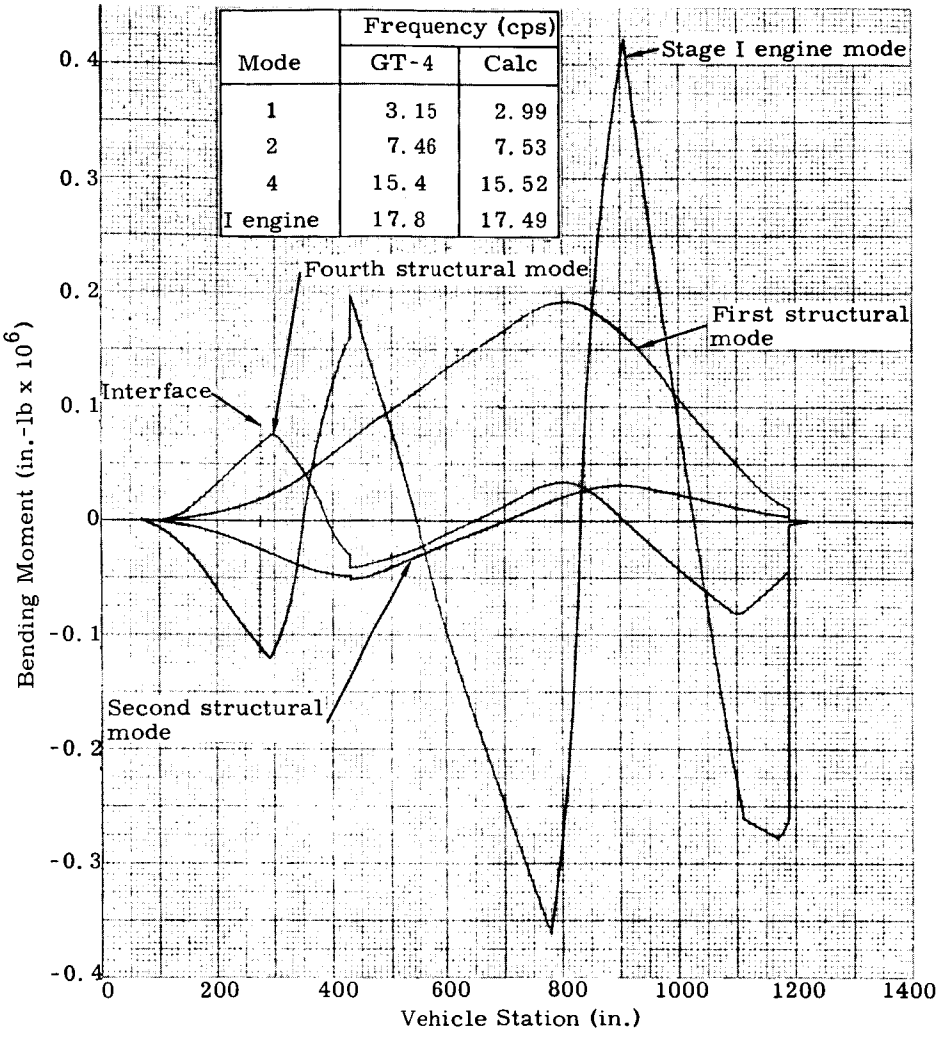

NOTE:

Data based upon rate gyro response.

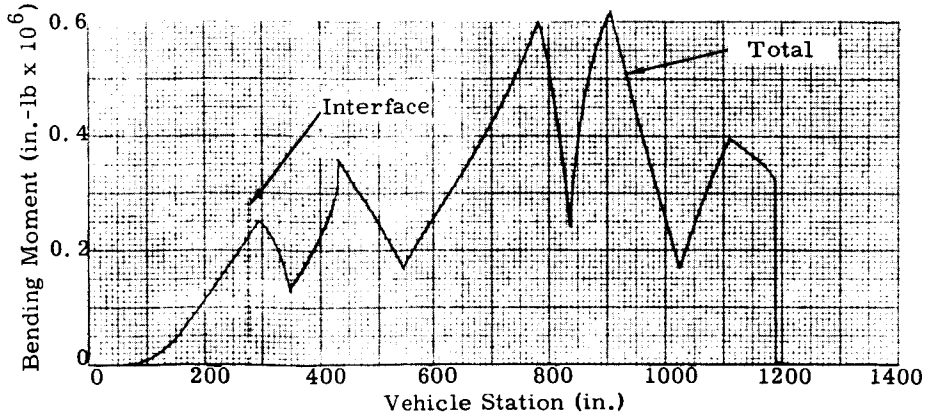

Fig. XII-10. Total Lateral Load Envelope--Max $q\alpha$ C_{N_α}

A notable increase in the second structural bending mode response occurred in the transonic region on the GT-4 flight--over that which occurred on previous flights (Fig. XII-8). It is also significant that peak bending loads associated with the Stage I engine mode were as large as those recorded on GT-1. The engine mode frequency was not as well defined on GT-2 and GT-3; hence, loads for those flights are presented as considerably lower than for GT-1 or GT-4.

5. Pre-BECO

Typical occurrence of lateral and axial dynamic responses were noted from rate gyro and accelerometer responses at the pre-BECO period of flight. However, the greatest component of structural loading resulted from the quasi-steady axial acceleration of 5.63 g. The pre-BECO lateral load envelope is presented in Fig. XII-11.

6. Stage II Flight

The quasi-steady axial acceleration reached a maximum value of 7.42 g at the end of Stage II flight. The dynamic responses which occurred during this portion of flight were of low magnitude ($\pm$ 0.07 g).

Continuous low frequency (1 to 2 cps) oscillations occurred during Stage II flight from LO + 270 to LO + 310 seconds; the resultant amplitude at the crew station was less than $\pm$ 0.25 inch. This response was approximately double the magnitude experienced on previous flights; however, the corresponding equivalent axial load was estimated to be only 400 pounds at Station 276, and is not considered critical.

Two low amplitude post-SECO pulses (0.09 g at SECO + 3.14 seconds and 0.05 g at SECO + 10.83 seconds) were observed. These were similar to those recorded on GT-1 and GT-2 (none occurred on GT-3). These transients were of no consequence to the structural loading of the vehicle.

7. Total Airframe Loads

A summary of the total airframe loads (quasi-steady plus dynamic; axial plus equivalent axial from lateral bending moments) for the significant structural loading conditions is presented in Table XII-2. Individual loading conditions are presented in detail in Figs. XII-12 through XII-18.

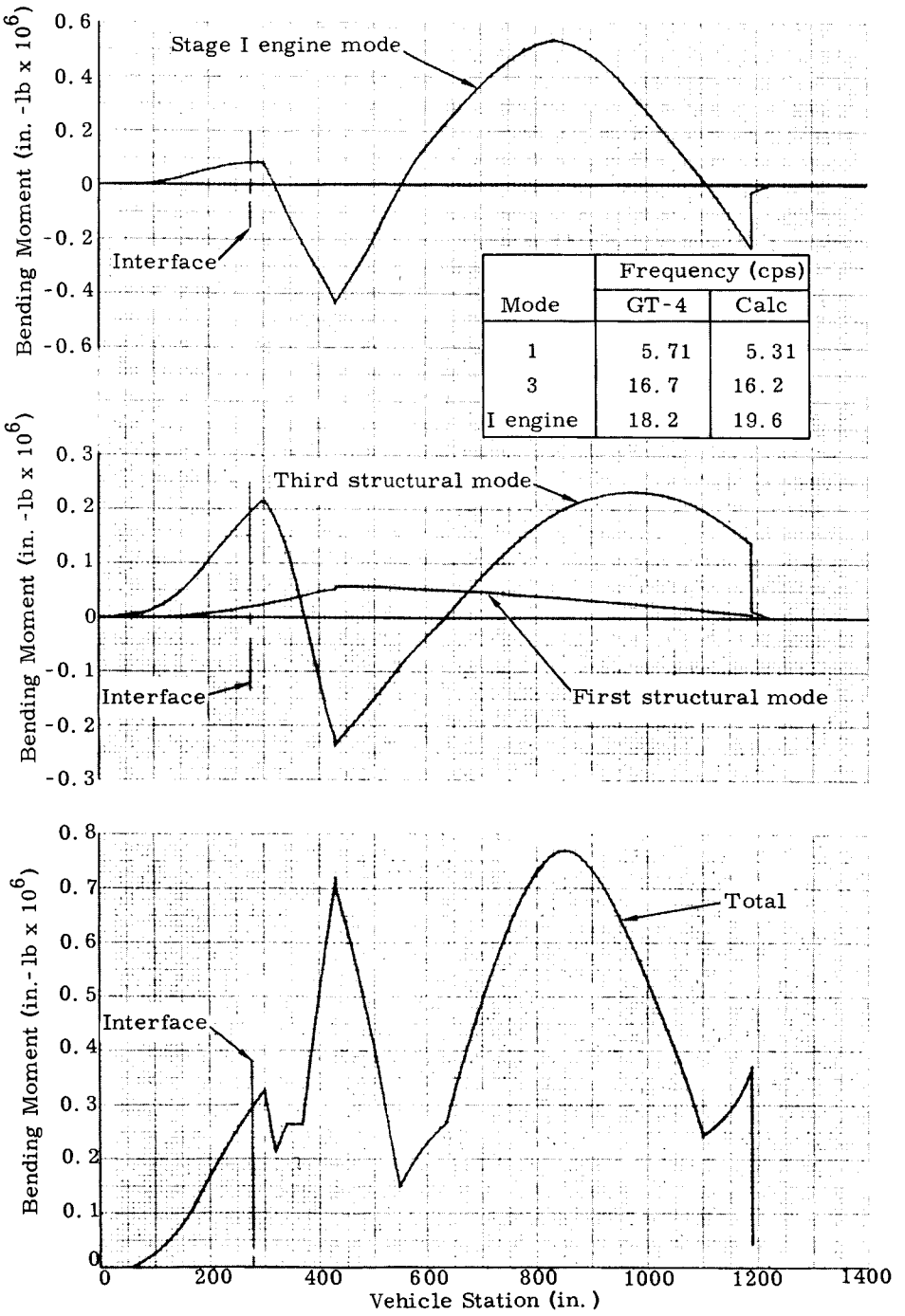

Fig. XII-11. Total Lateral Load Envelope: Pre-BECO

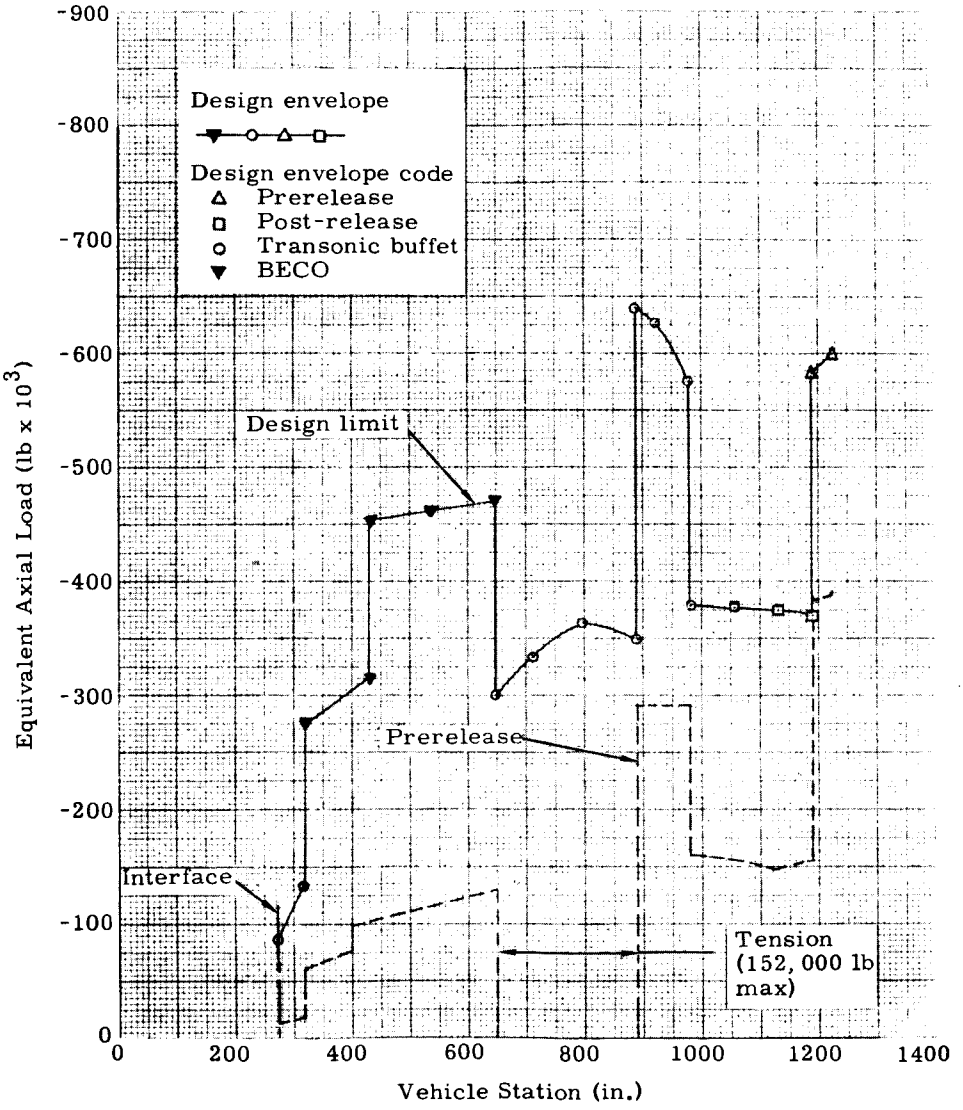

Fig. XII-12. Equivalent Axial Load: Prerelease

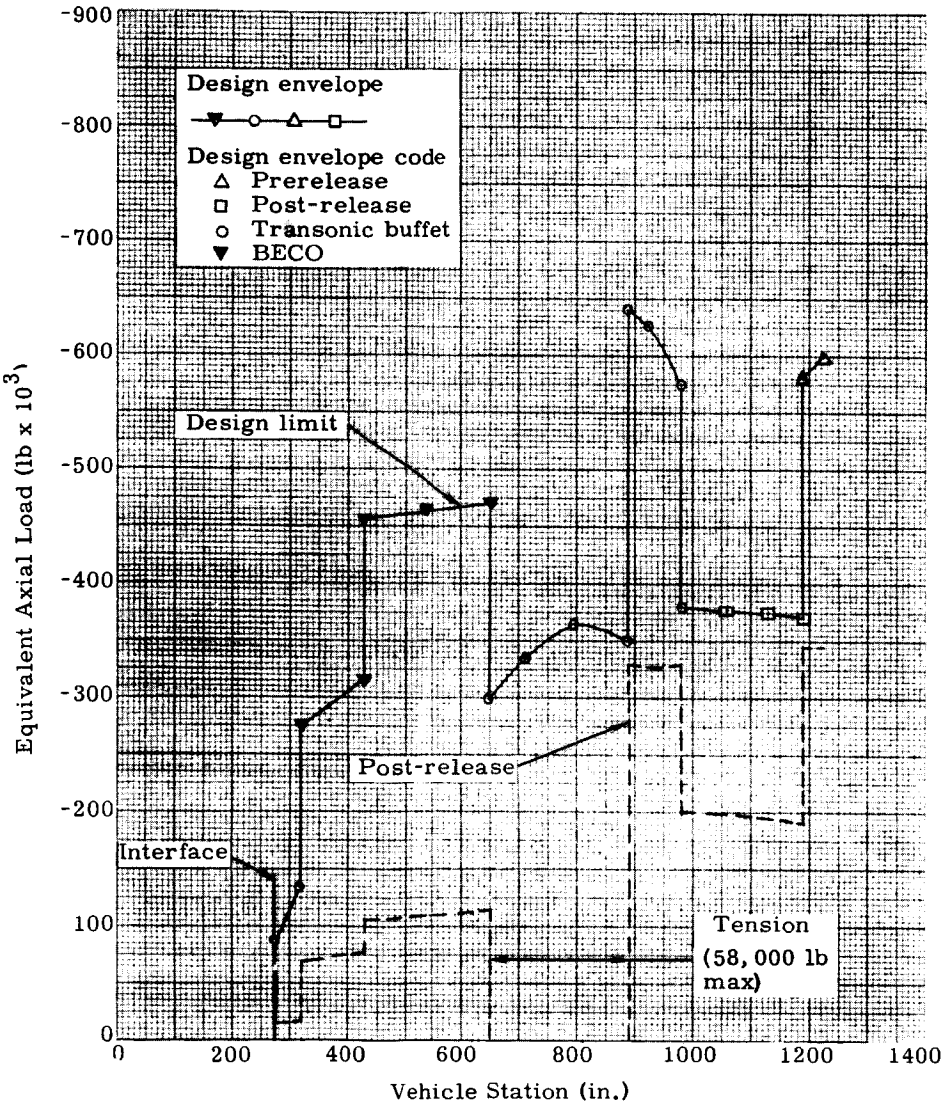

Fig. XII-13. Equivalent Axial Load: Post-release

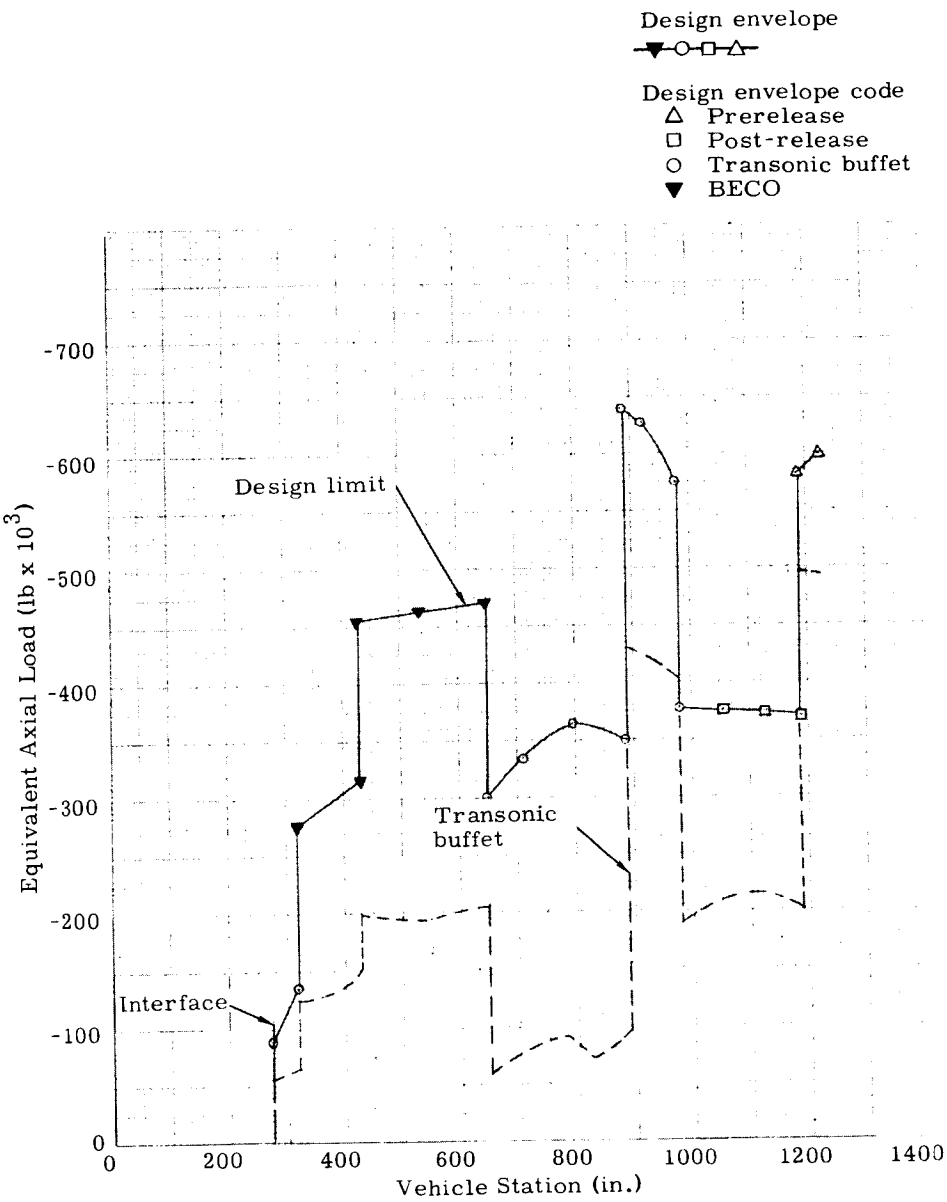

Fig. XII-14. Equivalent Axial Loads: Transonic Buffet

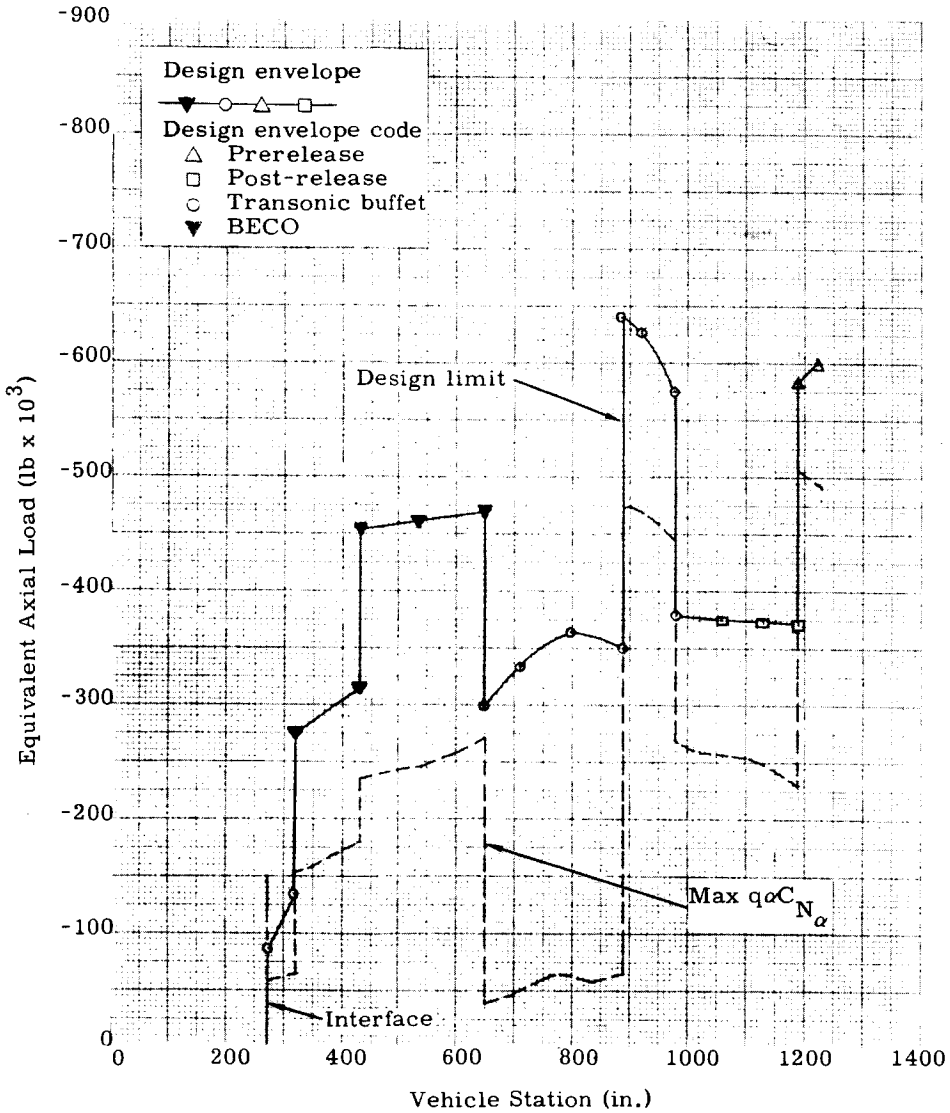

Fig. XII-15. Equivalent Axial Load--Maximum $q\alpha\ C_{N_\alpha}$

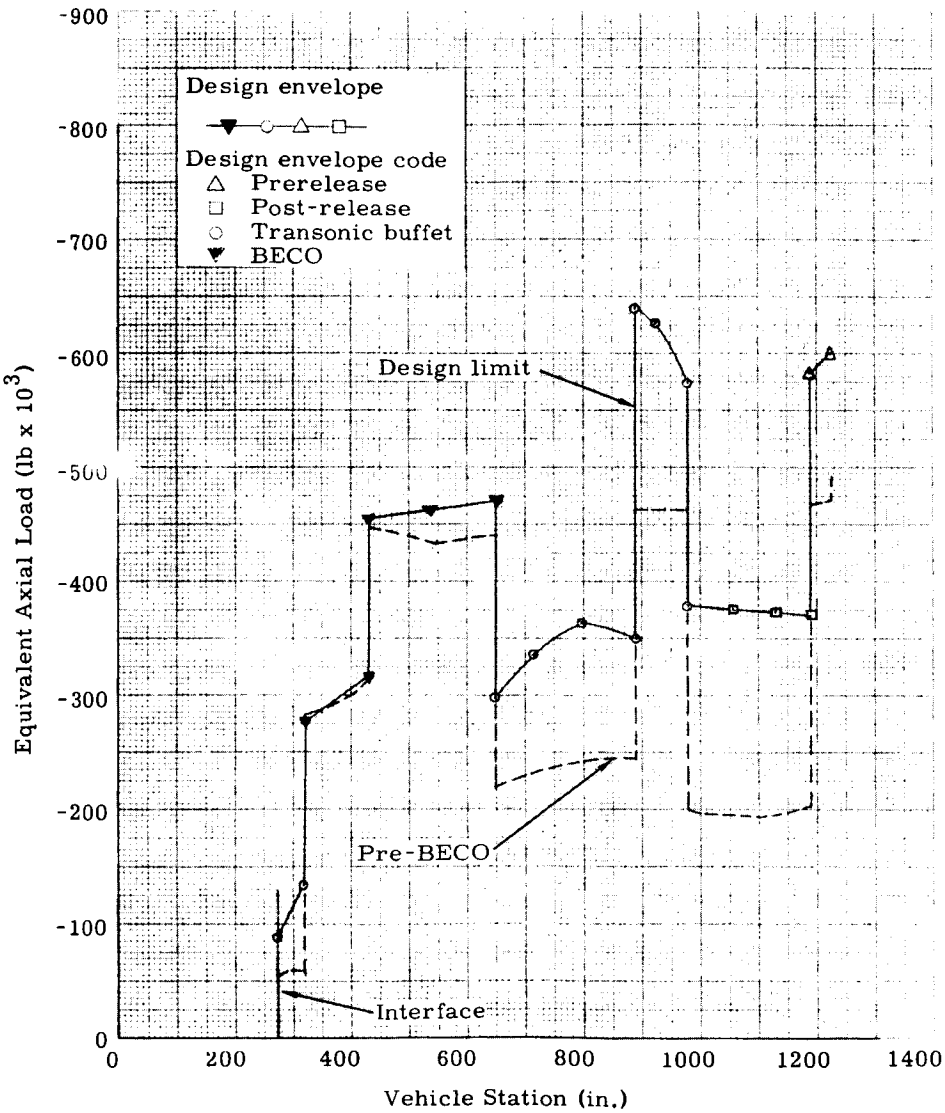

Fig. XII-16. Equivalent Axial Load: Pre-BECO

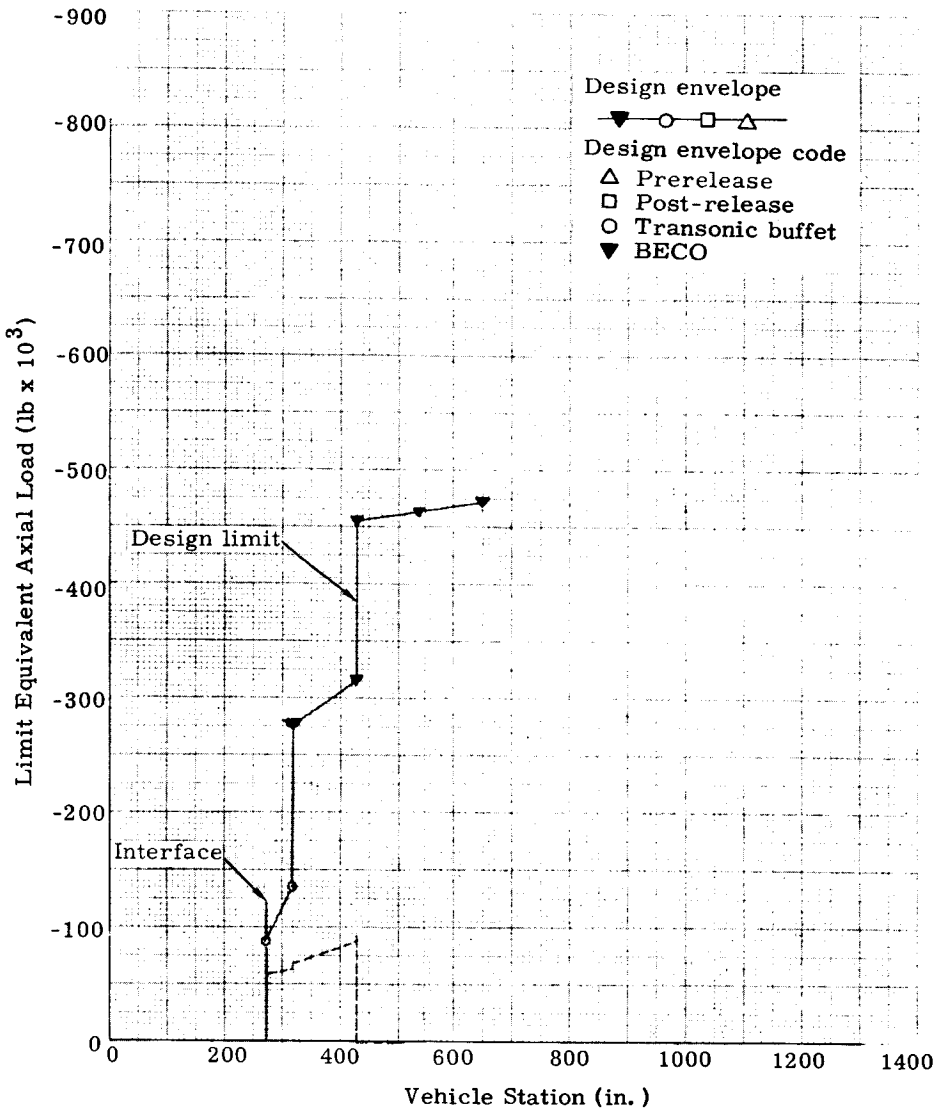

Fig. XII-17. Equivalent Axial Load: SECO

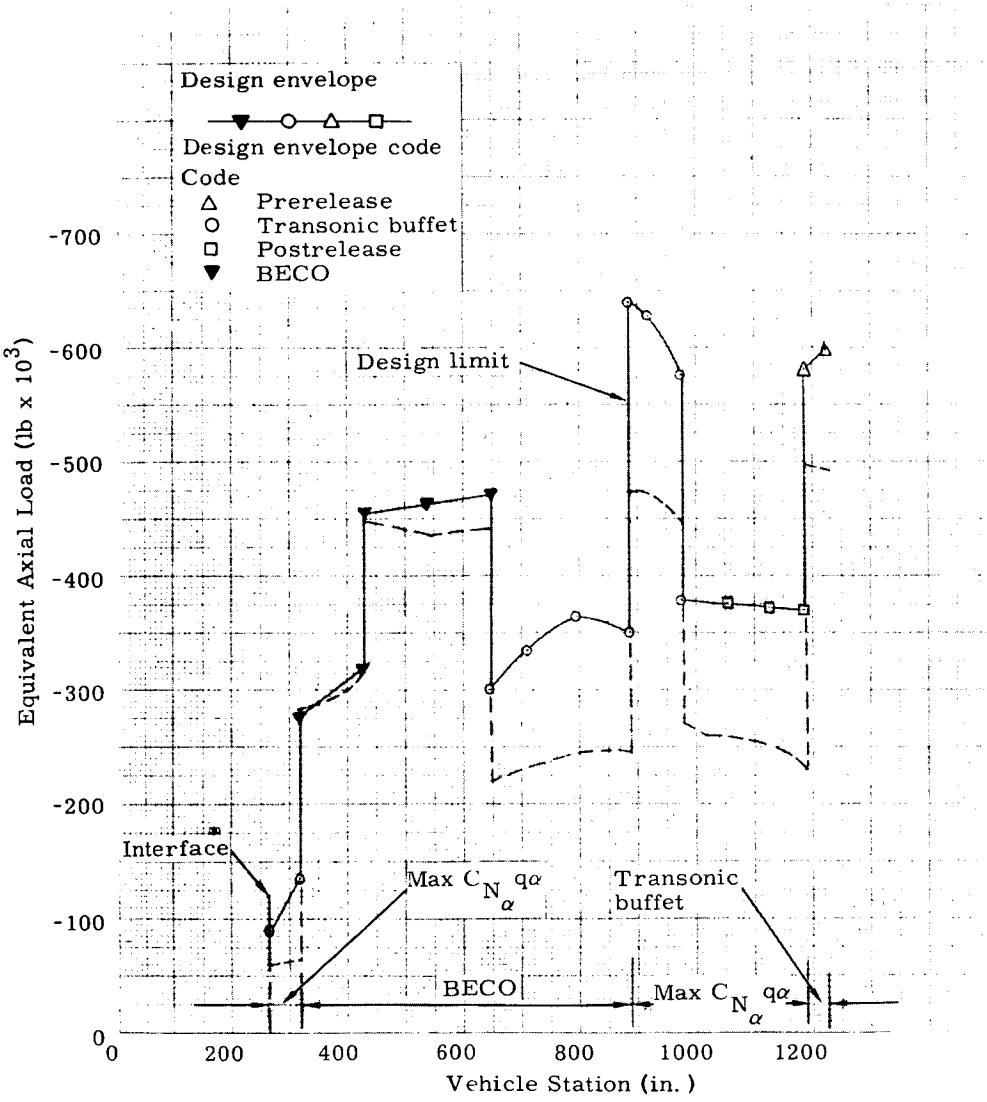

Fig. XII-18. Maximum Structural Load Envelope

TABLE XII-2

Summary of Total Airframe Loads

Structural Loading Condition (nominal)	Calculated Load in Percent of Design Limit Load at Critical Station	Critical Station
Prerelease (LO-0)	65	1188**
Postrelease (LO+0)	58	1188**
Transonic (LO+60)	84	1188**
Max q α C_{N_α} (LO+76)	85	1188**
Pre-BECO (LO+150)	101*	320**
Pre-SECO (LO+330)	66	277

*While this load is in excess of design limit, it is only 75% of tested strength of the vehicle.

**Indicates just aft of that station.

B. ENVIRONMENT

1. Vibration

Only one high frequency vibration measurement (Meas 1697) was made on GT-4, the results of which were very similar to those obtained on previous flights. Maximum response (1.73 g rms) occurred at liftoff and was well below the 14.3 g rms specification level. A g rms time history is presented in Fig. XII-19. The telemetry system limits Meas 1697 to 660 cps; therefore, the actual overall intensity was probably somewhat greater than that shown. Data were obtained up to LO + 140 seconds. Similarity exists between the vibration and sound pressure level (SPL) data of Fig. XII-19.

2. Acoustic

Two external sound pressure level measurements were made on GT-4; the results are presented in the following tabulation.

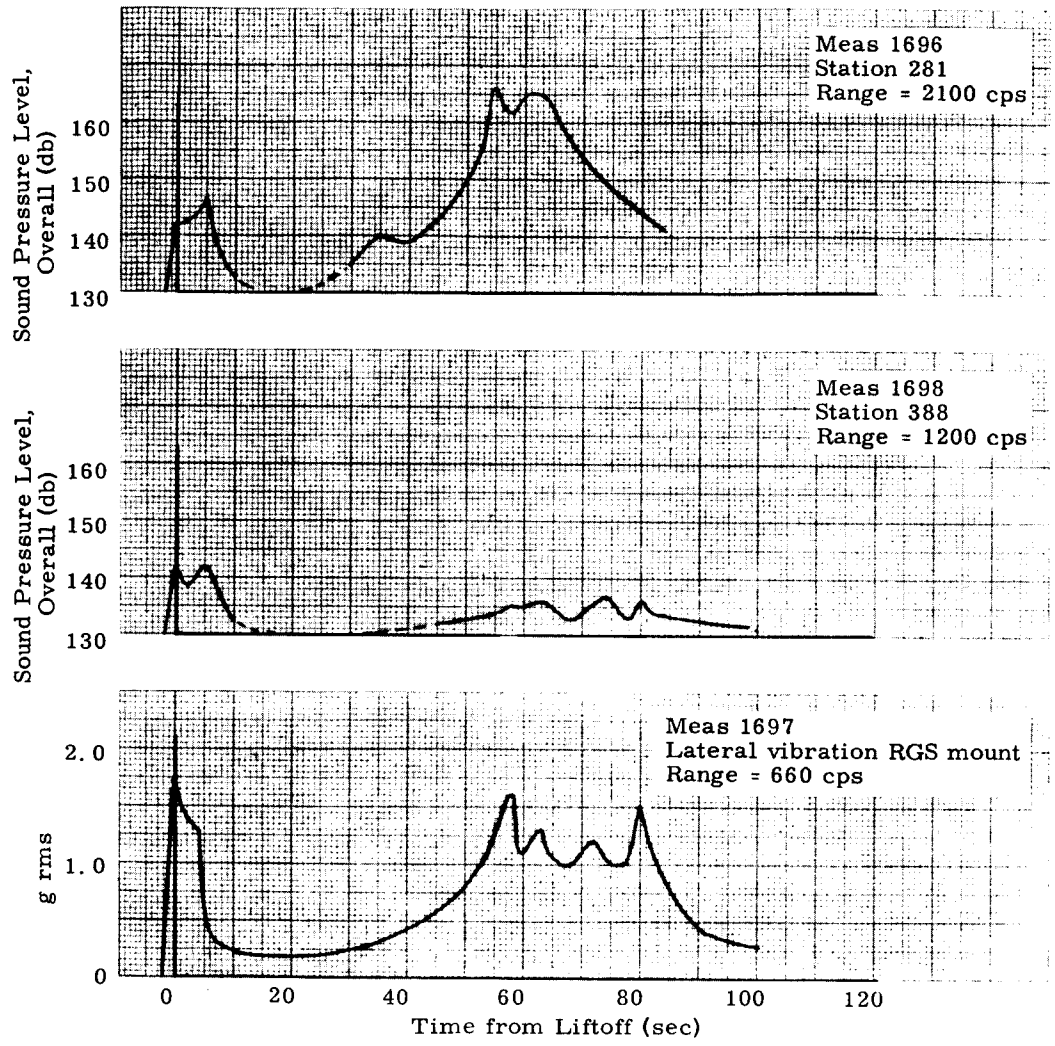

Fig. XII-19. History of Environment Intensities

Meas	Location	Response
1695	Compartment 2, Station 388	130 to 165 db (1200 cps cutoff)
1696	Compartment 1, Station 281	130 to 165 db (2100 cps cutoff)

Correlation of the measured SPL with that predicted for the launch period is shown in Fig. XII-20. Two distinct levels existed during this period, one at liftoff (after the engines had reached full thrust) and one at LO + 5 seconds (when the vehicle was approximately 200 feet off the pad). The measured SPLs at Compartments 1 and 2 locations were equal at liftoff, but at LO + 5 seconds, the Compartment 1 level was significantly greater than the Compartment 2 level. Although no explanation is offered for this trend, the possibility exists for peculiar sound reflection characteristics associated with the launch complex when the vehicle is above the deck. The transducers were located in Quadrant IV which was the side protected from the deflected exhaust blast. Figure XII-21 shows the sound pressure frequency spectrum, based on a 1/3 octave band analysis, for the launch period.

The sound pressure data in flight are presented in Figs. XII-22 through XII-24. The highest intensity (166.5 db) occurred at the Compartment 1 measurement (Meas 1696) at LO + 55.5 seconds (Mach 0.85). In this time period, Meas 1696 was somewhat clipped, since the transducer capability was exceeded from LO + 54 to LO + 66 seconds. This occurred during the transonic region of flight with attendant shock wave disturbances. The time history of the overall decibel level of acoustic environment during flight is presented in Figs. XII-22 and XII-23. Good agreement in the trend of the measured data exists with the predicted data. The maximum GT-4 measured SPL (Compartment 1, clipped) was 12.5 db higher than the qualification level of 154 db for that compartment. Based upon Titan II flight data, a 10-db attenuation can be expected across the vehicle structure from externally mounted acoustic instrumentation to internally mounted equipment.

The results of 1/3 octave band analyses, for flight conditions, are presented in Fig. XII-24. This figure shows that high SPL intensities exist over the entire frequency range considered, and that good trend correlation exists.

In summary, the GT-4 correlation with buffet model data indicates that dynamically scaled model pressure fluctuations can be used adequately for data trends but that the overall sound pressure levels so obtained are unconservative.

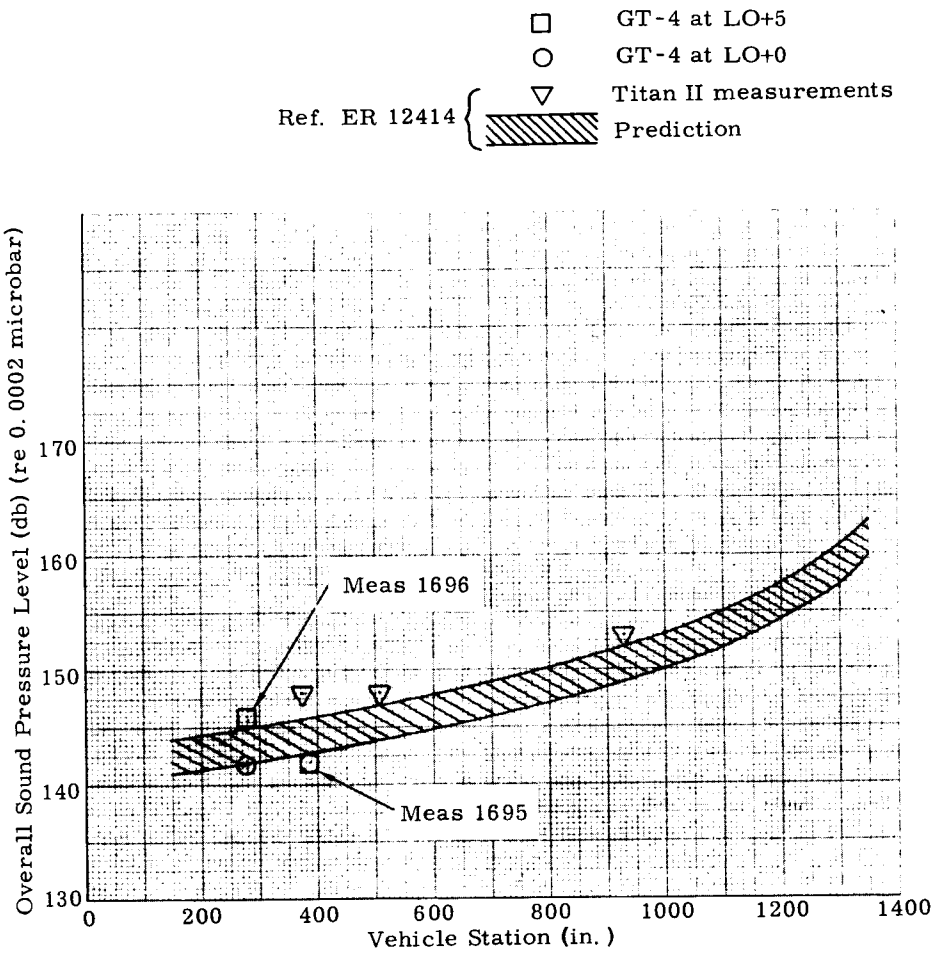

Fig. XII-20. GT-4 Acoustic Environment Variation of Intensity with Vehicle Station During Launch

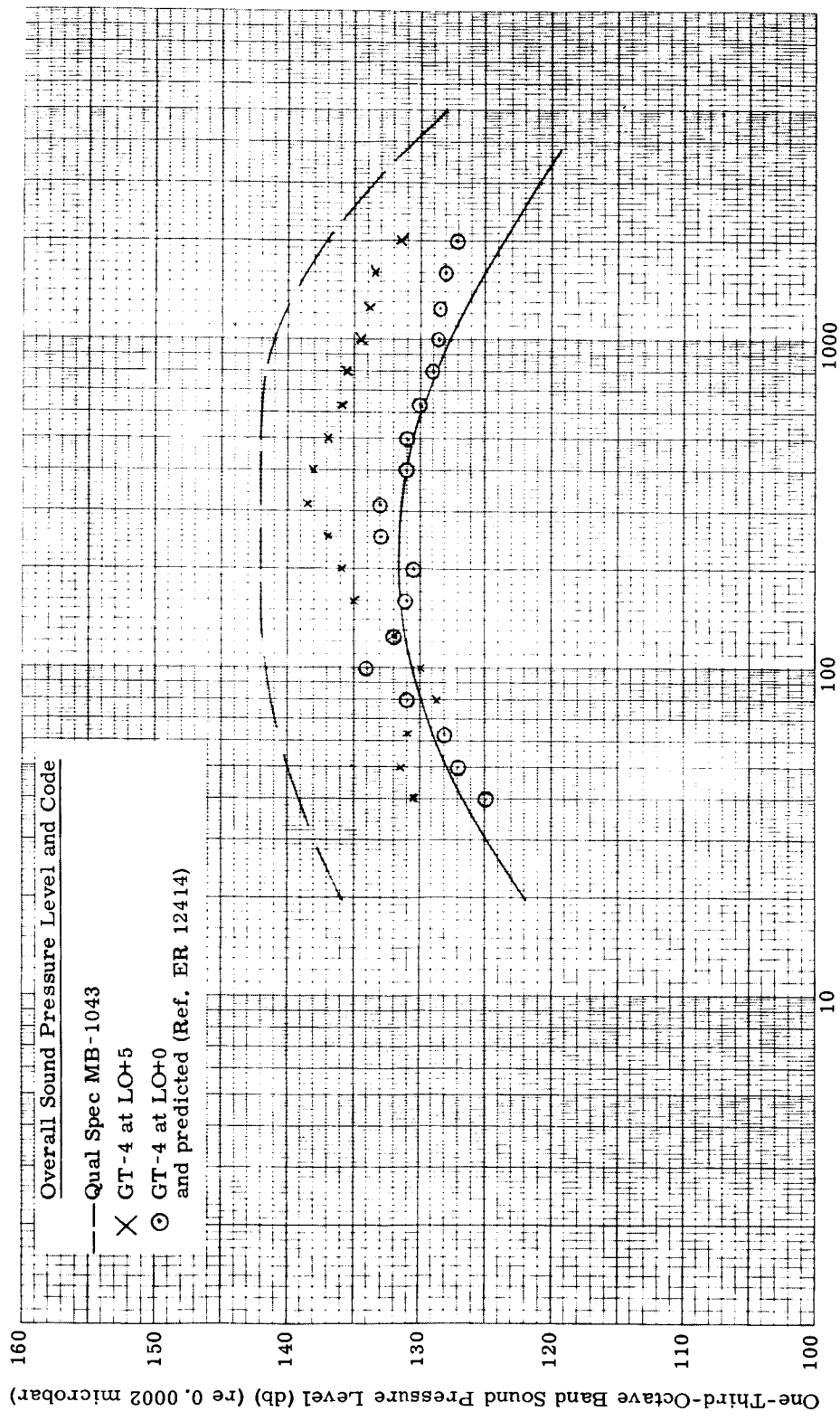

Fig. XII-21. Acoustic Environment in Compartment 1 During Launch

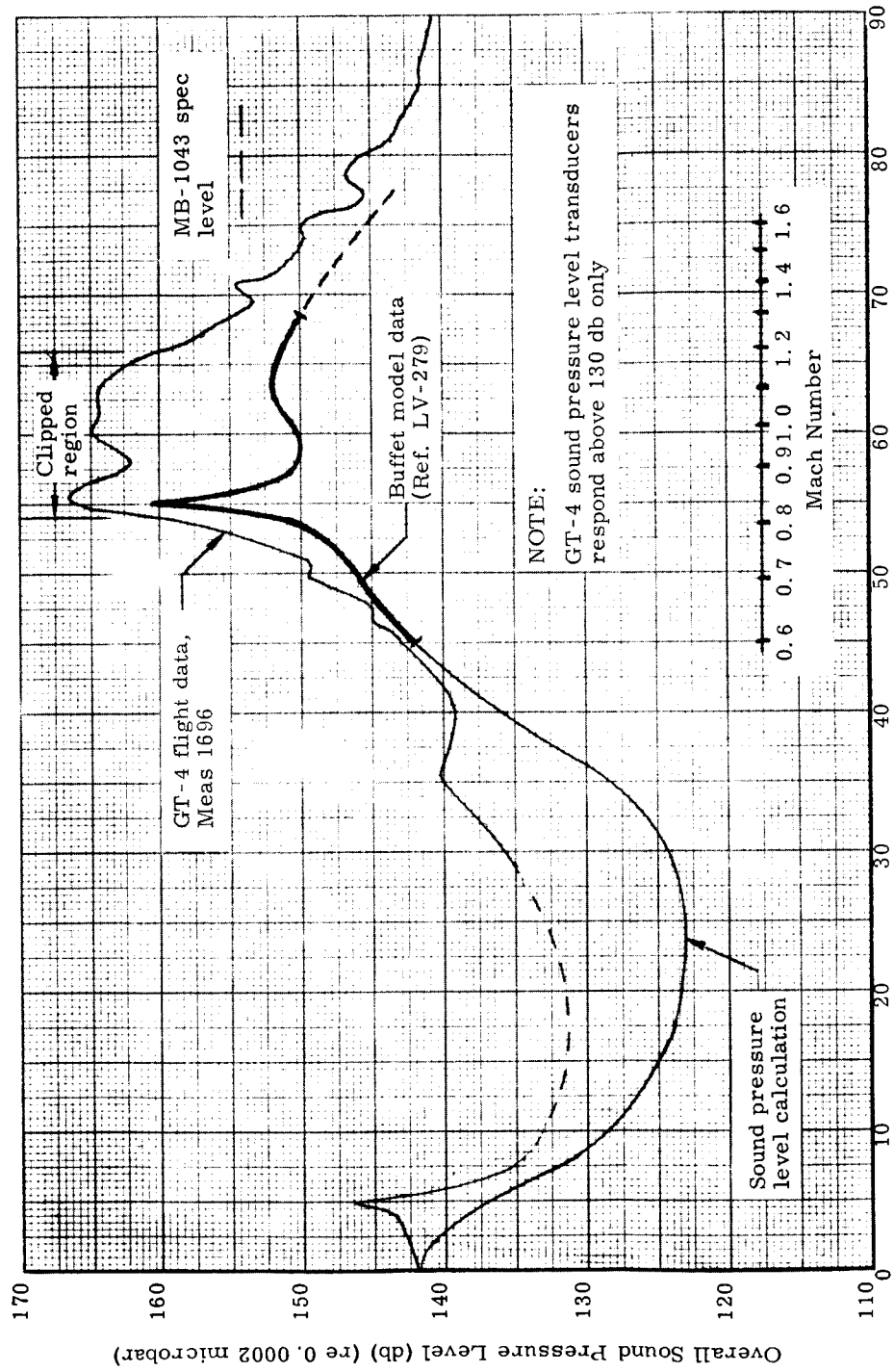

Fig. XII-22. Acoustic Environment Correlation with Buffet Model Data in Compartment 1

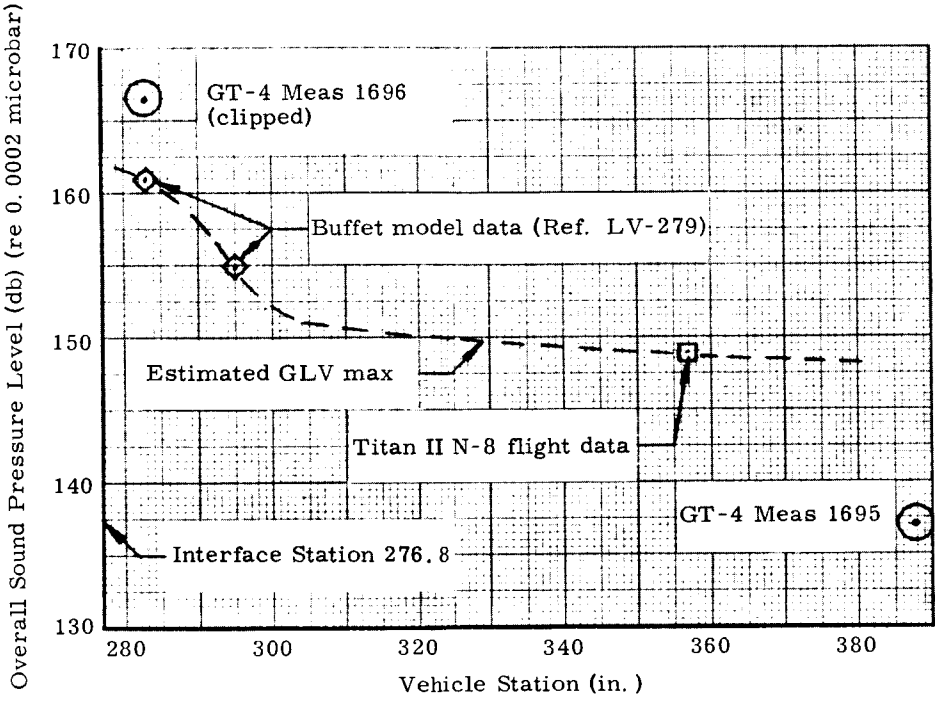

Fig. XII-23. Acoustic Environment Variation of Intensity with Vehicle Station During Flight

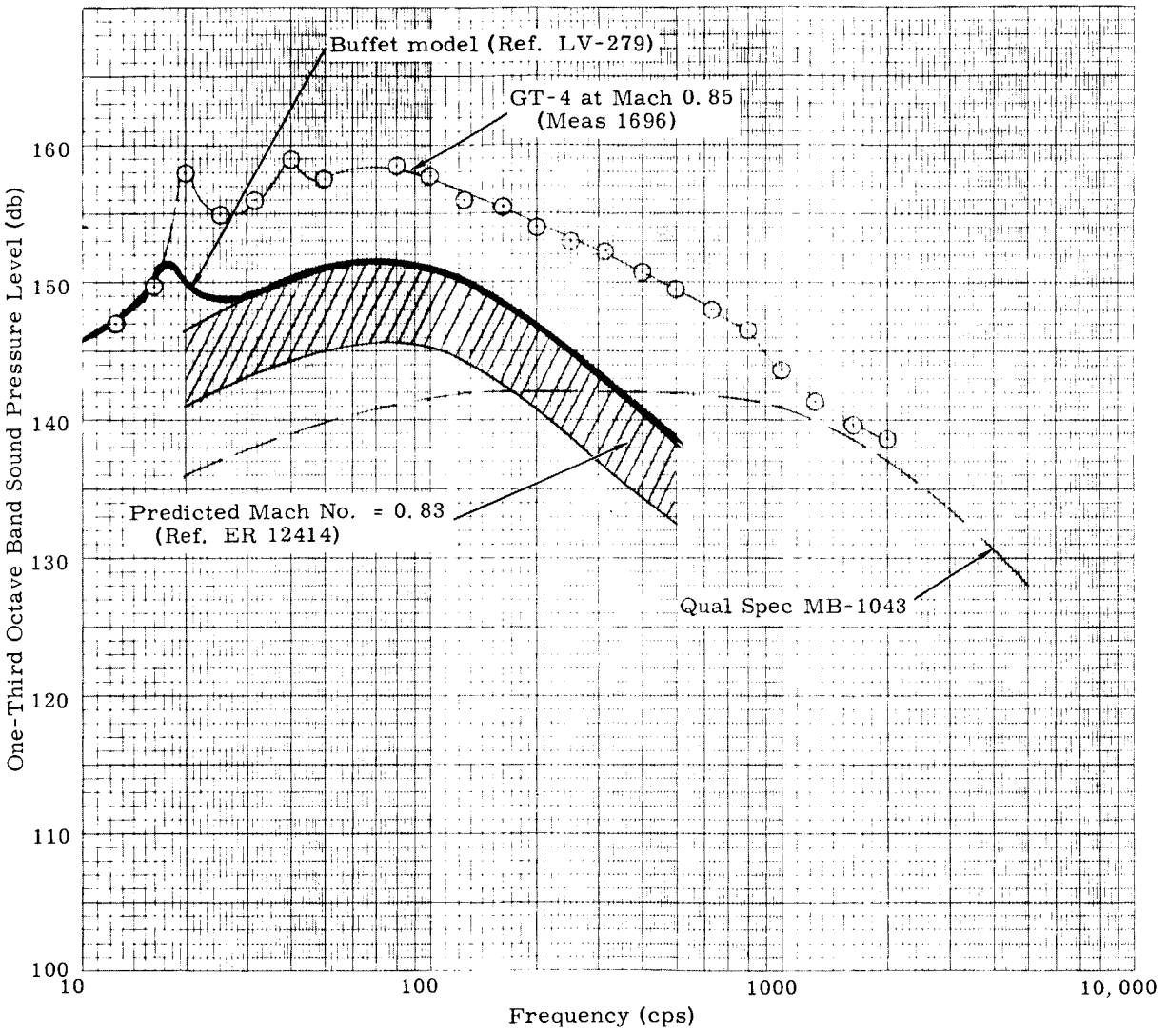

Fig. XII-24. Acoustic Environment in Compartment 1 During Flight

C. LONGITUDINAL OSCILLATION (POGO)

The GT-4 flight data indicate that the prescribed criterion of 0.25 g (zero-to-peak) at Station 280 was not exceeded. The suppression system operated satisfactorily and successfully attenuated the POGO instability. The signals from the launch vehicle axial accelerometers (located at Station 280 on the Compartment 1 skirt near the spacecraft interface and at Station 1209 on the aft fuel tank longeron of Compartment 5) were analyzed by narrow band analog filtering to determine the magnitude and frequency of the primary oscillation. The results of this analysis show that at Station 280 a maximum response of 0.22 g (zero-to-peak) at a frequency of 11.0 cps occurred at LO + 122 seconds (Fig. XII-25). An additional peak response of 0.20 g (zero-to-peak) at a frequency of 13.8 cps occurred at LO + 143 seconds. The correlation of calculated with measured axial mode frequencies was good (Fig. XII-5).

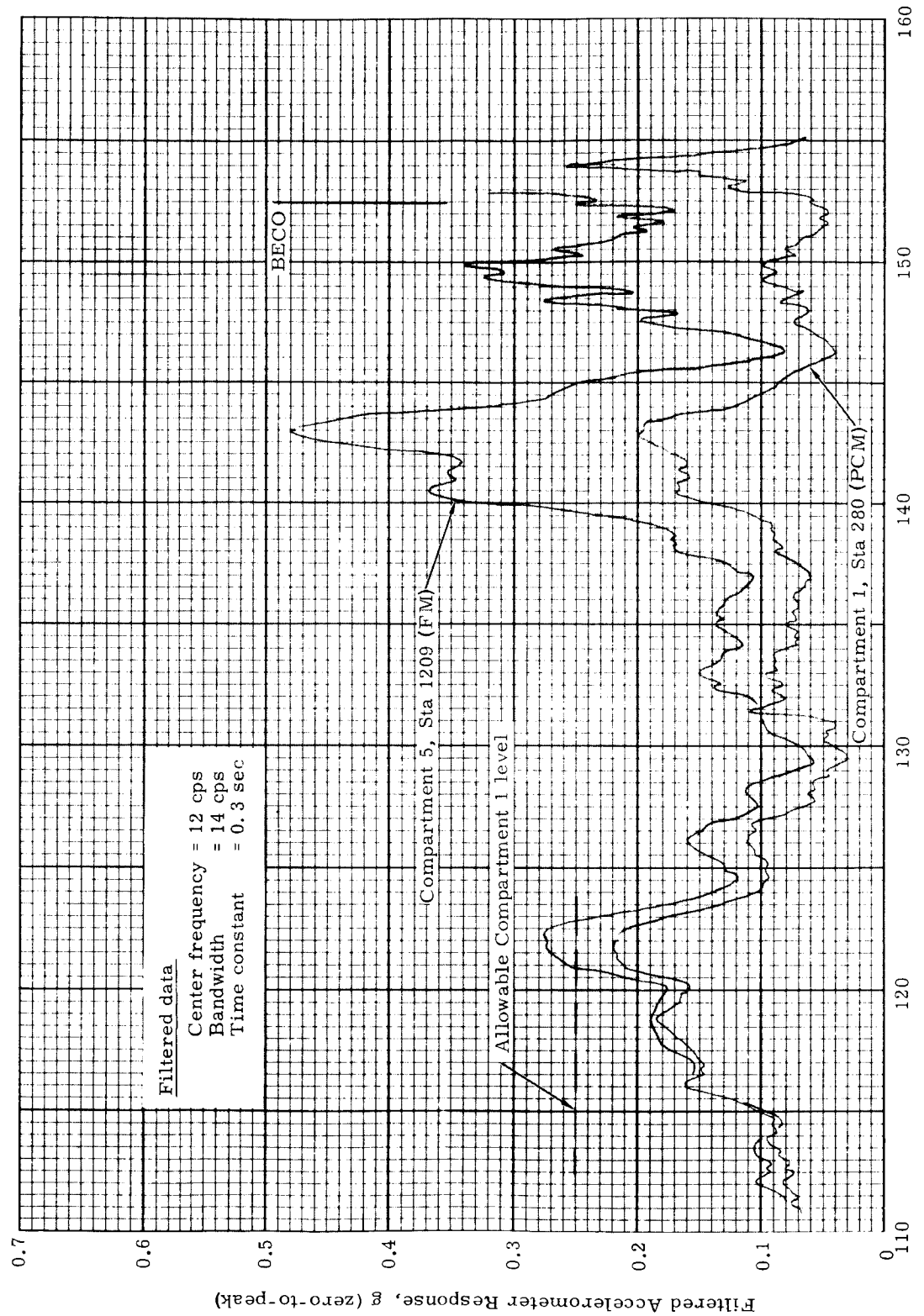

Fig. XII-25. GT-2 Longitudinal Oscillations

XIII. AGE AND FACILITIES

A. MECHANICAL AGE

1. Precount Operations

The mechanical AGE equipment utilized during precount operations is primarily employed during transport and erection of Stages I and II. Both stages of GLV-4 were again airlifted successfully to Cape Kennedy by the B-377PG aircraft. All equipment functioned as designed.

2. Countdown

All mechanical AGE used during the countdown functioned normally.

3. Launch

The spacecraft umbilical dropweight system was released at launch nut fire signal, and successfully disconnected and retracted the three spacecraft umbilicals.

Analysis of magnetic tape recordings of functions carried through the umbilicals and inspection of films confirm that the launch vehicle electrical umbilicals disconnected in the planned sequence as indicated (Table XIII-1).

TABLE XIII-1

Electrical Umbilical Disconnect Sequence

Umbilical Designation	Time of Disconnect (GMT)	Δ Time (sec)
3D1M/3D2M	1515:59.55	0
3D1E	1515:59.820	0.270
3D2E	1515:59.958	0.408
3B1E	1516:00.172	0.622
2B1E	1516:00.322	0.772
2B2E	1516:00.335	0.785

Analysis of motion pictures of the launch revealed that a malfunction occurred in the separation of the Stage I fuel vent topping umbilical disconnect (2DFVT). The disconnect did not release by lanyard actuation at 11 inches of vehicle rise, as planned, but separated after approximately 20 feet of vehicle rise (1516:01.92 GMT) when the flexible hose

umbilical became taut. At this point, the ground portion of the disconnect broke apart from the airborne half. Failure analysis has not been completed, and neither the cause of the malfunction nor the mode of final separation has been determined. Film coverage indicates that the launch vehicle was not damaged by the hang-up. The investigation is continuing.

The two oxidizer standpipe remote charging system disconnects, planned to be separated by lanyard actuation at liftoff, were manually disconnected at approximately T-140 minutes because of some concern that the disconnect might strike the engine bell if actuated by lanyard. ECP GLV-MM-521 has been submitted to revise the lanyard installation for this system to preclude any possibility of the disconnect penetrating the engine/nozzle launch envelope.

The design revision to the thrust mount flame shield, as defined in ECP 492, functioned satisfactorily. No flames shields were buckled.

There was considerably less blast damage to mechanical AGE than after GT-3 launch. However, the 1/2-inch diameter rods (tack-welded to the stiffening bars on the blast covers of Booms 3, 4 and 4-1/2) have been consistently blown off with no discomfort to the blast covers themselves. A design revision is being prepared to remove these rods, and thereby reduce the number of "projectiles" that could cause more extensive damage. This will further relieve the cost of refurbishment.

B. ELECTRICAL AGE

1. Configuration

The AGE launch and checkout equipment was modified for GLV-4 to incorporate the oxidizer standpipe remote charger system into the propulsion control set. The system was used to charge the oxidizer standpipes and the sequence was initiated at T-165 minutes. The hold-fire check (H/F D1) at T-3:30 to T-3:28 minutes was "go."

2. Power Distribution Control Set (PDCS)

The PDCS Equipment functioned properly throughout prelaunch and launch operations. The APS, IPS, 25 vdc and inverter monitors did not indicate a hold or shutdown condition, thereby verifying satisfactory operation of the transformer/rectifiers and associated equipment before, during and after power transfer.

3. Propellant Loading

All electrical counters on the propellant loading system operated properly, and no discrepancies occurred.

4. Launch Damage to Cables

There was slight damage to electrical umbilical 3D1E. The engaging ring and thrust washer were replaced. All other umbilicals were undamaged.

C. MASTER OPERATIONS CONTROL SET (MOCS)

Analysis of the MOCS automatic sequence records shows that all functions were performed properly. At T-34:59 minutes, a hold was called due to inability to lower the erector. After a hold of one hour and sixteen minutes, the automatic sequence was picked up at T-34:59 minutes and proceeded to a successful liftoff. MOCS T-0 occurred at 1515:56.2 GMT followed by TCPS at T + 1.05 seconds. The following MOCS generated time functions occurred as specified:

TCPS + 1.6 seconds

TCPS + 1.8 seconds

TCPS + 2.0 seconds (fire launch nuts)--1515:59.25 GMT

The launch operation was completed in 3.05 seconds.

The recorders were switched to high speed at T-2 minutes. During the remainder of the count, the operation of the sequencer was compared to the real-time trace. All traces were checked for time of occurrence, proper sequence and coincidence of occurrence, and found to be correct and consistent with the planned operation of the sequencer.

D. FACILITIES

All facility items functioned properly throughout the launch countdown with the exception of the erector which failed to respond to the lowering signal at T-48 minutes. A 76-minute hold ensued before the trouble was corrected.

1. Erector Malfunction

Initiation of the erector lowering signal was made from the blockhouse at T-48 minutes, but the erector failed to move. Before the lowering can be started, the erector leg locks must be unlocked. The "legs unlocked" indicator lamp in the blockhouse was illuminated, indicating that the locks were in the correct state for lowering. Figure XIII-1 presents a schematic of the erector control circuit.

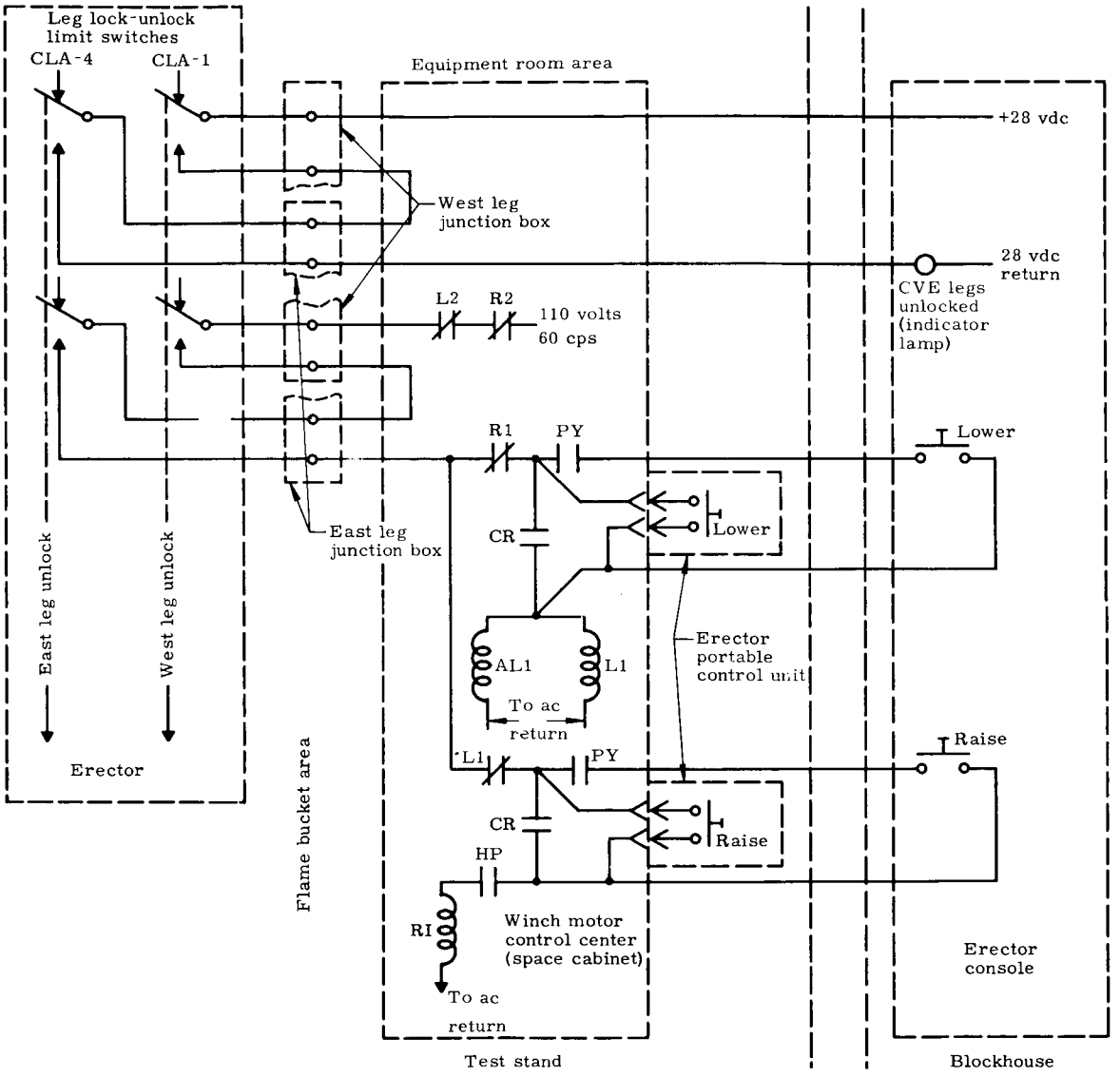

Fig. XIII-1. Erector Control Circuit

An attempt to lower the erector was then made by using the erector portable control unit, but again the erector failed to move. Trouble-shooting revealed that lower relay L1 (which, when energized, starts the lowering sequence) was not engaged when the lowering button was pushed.

The decision was made to manually engage relay L1. When this was accomplished, lowering began, but several seconds later the erector stopped automatically by going into emergency stop. Slack in the motor-erector cable was noted and the erector was raised to remove the slack. It was then found that raise relay R1 (which, when energized, starts the raise sequence) had to be operated manually (the same manner as L1) in order to raise the erector.

Two more unsuccessful attempts were made to lower the erector by the procedure previously described. The emergency stop and cable slack were then determined to be a result of erector overspeed.

Between the second and third attempts, adjustments were made to the cable tension switches, but the erector still would not lower.

The erector was finally lowered by manually engaging both relay L1 and auxiliary lower relay AL1. Relay AL1, when energized, closed a set of contacts which provide dynamic braking current to the erector motor, thus restraining the erector from falling or reaching an overspeed condition by going into an emergency stop condition.

2. Postlaunch Evaluation

Troubleshooting after launch revealed that the CLA-4 leg lock-unlock limit switch control circuit (which should be closed with the legs unlocked) was open with the legs unlocked. This condition prevented relays L1 and AL1 from energizing upon engaging the lower switch and prevented relay R1 from energizing upon engaging the raise switch (Fig. XIII-1). All other contacts of relays in the remainder of the series string had evidently been in the proper configuration for erector lowering and raising.

Further investigation disclosed that wiring to the CLA-4 switch was terminated incorrectly at the junction box in the flame bucket area. The wires in the junction box had been lifted for continuity checks during troubleshooting of the legs-unlocked indicator circuit after the GLV-4 WMSL exercise and were reterminated incorrectly. Wire CV32 was erroneously connected to wire 2 instead of wire 3 of the limit switch.

After GT-4 launch, the junction box terminations were corrected and the circuit retested satisfactorily.

E. PAD DAMAGE

Damage to AGE and facility items caused by engine blast and heat was minor. The damage was less than that which occurred on previous launches. All damaged items will be refurbished to their original configuration. The most significant damaged items were as follows:

(1) Complete vehicle erector (CVE):

(a) Nitrogen system. The gage glass on the southeast side of the CVE (5 feet above deck level) was broken.

(b) Corrugated aluminum siding--east side of CVE. The panels from the deck to the 26 foot 7 inch level were loosened and two large pieces were blown off.

(c) Launch vehicle personnel elevator--west side. The elevator gate from Level No. 1 of the CVE was slightly damaged, and the brace strap at the bottom of the cable trough was broken.

(d) Spacecraft elevator. The arm was bent on the door closer, the guide rail was bent out of line, and the clamp on the lockpin hydraulic line was broken 10 feet above the deck.

(e) Ground strap at the west pivot point was torn out.

(f) Weather curtains. Damage was approximately the same as for GT-1, -2 and -3 (south and west sides to 35 foot 4 inch level).

(g) Electrical items. The waveguide at the west pivot point was damaged, and the outer light fixture glass globe under the 9 foot 8 inch level of CVE was cracked (southwest corner). The cable running up the southeast column to approximately 80-foot elevation pulled loose from the clamps.

(2) Complete vehicle umbilical tower (CVUT)

(a) Desk level. The gage glass on the oxidizer standpipe remote charger was cracked, and the nitrogen line for the prevalve accumulator was bent at approximately the 15-foot level.

(b) Level No. 2. The elevator cable guard screen was broken loose, the light fixture was broken loose from its mounting, and the small umbilical on boom No. 1-1/2 was crimped at the end of the boom.

(c) Level No. 3. The elevator cable guard screen was damaged.

(d) Level No. 4. The door of the nitrogen pressure reducing station was blown open and the lock appeared to be damaged.

(e) Level No. 5. The Stage I topping line quick-disconnect was broken, and the stiffener rod was missing from the inboard cover of boom No. 3.

(f) Level No. 6. The stiffener rods were missing from the covers of boom No. 4, and the "Unistrut" clamps on the cables under boom No. 4 were pulled loose.

(g) Level No. 7. The folding access step (CVUT to CVE) was damaged, and the outer light globe was broken on the east face over boom No. 4-1/2.

(h) White Room air-conditioning duct. The insulation and banding were damaged at the joint near level No. 4.

(3) Second-stage umbilical tower (SSUT)

(a) Conduit and light fixtures were broken loose from mountings at the top level.

(b) Cable cover was broken on the level No. 2.

(c) Bracket support for MITOC station No. 133 was broken loose from the top level.

(4) Complete vehicle erector--thrust mount area

(a) Single-point ground cable was torn loose from the clamps on Quadrant I.

(b) Cabling to the launch nuts was damaged on all four quadrants.

(c) Cabling to the liftoff switches was damaged on all four quadrants.

(d) Hardware was missing on the junction box covers on the thrust mount.

(e) Camera cables and purge lines on the thrust ring were damaged.

(f) Valve handles were missing from the start cartridge air-conditioning ducts.

(g) Several cable clamps for miscellaneous cabling around the thrust mount were missing.

(h) Conduit nipple (1/2 inch) between the "Condulet" and the solenoid for the engine deluge water valve was broken.

(i) Flame shield on the southeast "A" frame (top) was damaged.

(j) Flame shield on the southwest "A" frame leg (bottom) was damaged.

(5) Launch deck area

(a) Structural. The blast cover for the Aerojet engine unit on the north side of the CVE thrust ring was damaged. The south end of the spacecraft elevator ramp was torn loose from the deck.

(b) Mechanical. The water line (1-1/2 inch) to the thrust chamber spray was bent at the north side of thrust ring. The west leg lock hydraulic line was leaking at the connection to the cylinder.

XIV. RELIABILITY

A. ENVIRONMENTAL CRITERIA

GT-4 flight data, relative to launch vehicle environmental criteria, have been reviewed and found to be lower than the qualification test levels in all areas except one. One acoustic noise measurement appeared to be approximately 1-1/2% higher than the qualification test level. A comparison of the flight data with qualification test limits; analytical data; GT-1, GT-2 and GT-3 flight data; and Titan II R&D flight data appears in Table XIV-1.

1. Compartment Temperatures

Compartment 2 and engine start cartridge air-conditioning system exhaust temperatures were recorded prior to liftoff. These temperatures ranged from 56° to 63° F and were within the specified limits of 40° to 75° F. No in-flight compartment temperature measurements were made on GT-4.

2. Skin Temperatures

Launch vehicle skin temperatures on the first three Gemini flights were well within the design limits; consequently, GLV-4 was not instrumented for skin temperature measurements.

3. Random Vibration

Only one high frequency vibration measurement was made on GT-4. It was obtained on the Compartment 2 truss next to the RGS. The maximum lateral (yaw axis) vibration (1.73 grms) of the truss occurred at liftoff; it was well below the 14.3 grms qualification level.

4. Steady-State Accelerations

Longitudinal accelerations on the GT-4 flight were comparable to those obtained on the three previous Gemini flights and, as expected, were well below the qualification test levels. The maximum Stage I measured steady-state acceleration was 5.63 g just prior to BECO.

The Stage II measured steady-state acceleration reached a peak of 7.42 g at the end of Stage II flight.

5. Shock

No separate shock measurements were made on this flight; however, the vibration data include transient responses of the structure during release, staging and the spacecraft separation.

TABLE XIV-1

Environmental Criteria Summary

Parameter	Source	Compartment					
		1	2	3A	3B	4	5
Compartment exhaust air temperature (° F)	Qualification test ①	120	90	100	100	110	160
	Analysis ②	100	75	80	80	100	100
	Flight data, GLV-1	N/A	60 (at T-0)	N/A	N/A	N/A	N/A
	Flight data, GLV-2	N/A	58 (at T-0)	N/A	N/A	N/A	N/A
	Flight data, GLV-3	N/A	61 (at T-0)	N/A	88 (at T-150)	N/A	N/A
	Flight data, GLV-4	N/A	63 (at T-0)	N/A	N/A	N/A	N/A
Maximum skin temperature (° F)	Qualification test	-	-	-	-	-	-
	Analysis ③	372	485	470	305	310	297
	Flight data, GLV-1	153	N/A	N/A	N/A	N/A	N/A
	Flight data, GLV-2	150	236	N/A	152	168	N/A
	Flight data, GLV-3	N/A	258	N/A	177	198	N/A
	Flight data, GLV-4	N/A	N/A	N/A	N/A	N/A	N/A
Random vibration (max g rms)	Qualification test ④	41	65 (truss 14.3)	97	29	44	92.5
	PMT level ④	20.5	32.5 (truss 9)	48.5	14.5	22	46.3
	Flight data, Titan II ④	10	15 (truss 6)	22	21	33	37
	Flight data, GLV-1	2.0 lateral	truss 0.95 axial	N/A	N/A	N/A	12 axial
	Flight data, GLV-2	N/A	truss 1.96 lateral	N/A	N/A	N/A	8.5 axial
	Flight data, GLV-3	N/A	truss 1.45 lateral truss 3.30 vertical	N/A	N/A	N/A	7.0 vertical
	Flight data, GLV-4	N/A	truss 1.73 lateral	N/A	N/A	N/A	N/A
Steady-state acceleration (max g)	Qualification test ⑤	12	12	12	8	8	8
	Flight data, GLV-1	7.35	N/A	N/A	N/A	N/A	5.61
	Flight data, GLV-2	7.70	N/A	N/A	N/A	N/A	5.69
	Flight data, GLV-3	7.50	N/A	N/A	N/A	N/A	5.63
	Flight data, GLV-4	7.42	N/A	N/A	N/A	N/A	5.63
Maximum shock (g)	Qualification test ⑤	None	None	100	None	None	100
	Flight data, GLV-1, -2, -3 and -4 ⑤	N/A	N/A	N/A	N/A	N/A	N/A
Acoustics (db)	Qualification test ⑤	154	151	159	151	154	159
Average inside compartment noise level	Analysis	154	151	159	151	154	159
	Flight data, Titan II	154	151	159	-	154	159
	Flight data, GLV-1, -2 and -3	N/A	N/A	N/A	N/A	N/A	N/A
Outside compartment noise level	Flight data, GLV-4	166.5	137	N/A	N/A	N/A	N/A

① Ref. 16, page 49

② Ref. 17, page 3

③ Ref. 18

④ Ref. 15, Figs. 14, 15 and 16

⑤ Ref. 16, Table 3

N/A = not available

No detrimental effects were experienced or expected from these transients.

6. Acoustic Noise

External sound pressure level measurements were obtained on GT-4 at Stations 281 and 388. The maximum measurement of 166.5 db (clipped) was 12.5 db higher than the 154-db Compartment 1 (inside) qualification level. Based on Titan II acoustic measurements, a 10-db attenuation can be expected from external to internal.

B. PROBABILITY ANALYSIS

1. Countdown

Based on GLV countdown experience (through GT-3), the average number of holds per countdown ($\bar{h}$) was calculated to be 0.25, i.e., one hold per four countdowns. $\bar{h}$ is based on the countdown period from T-420 minutes to T-0. Spacecraft holds and the SCF test were not counted. The countdown experience prior to GT-4 included:

(1)	GLV-1	One countdown including engine ignition
(2)	GLV-2 (attempt)	One countdown completed; tandem actuator failed, engine shutdown on pad
(3)	GLV-2	One countdown including engine ignition
(4)	GLV-3	One countdown, with one hold, including engine ignition

From Ref. 14, the probability of GLV-4 completing the countdown without a hold was predicted to be:

$$P_{c/d}\ (\bar{h} = 0.25) = 0.75$$

Including the GLV-4 countdown (with its one hold), the average number of holds per countdown ($\bar{h}$) is calculated to be 0.4, i.e., two holds per five countdowns. The probability of GLV-5 completing countdown without a hold is predicted to be:

$$P_{c/d}\ (\bar{h} = 0.4) = 0.67.$$

2. Flight

No malfunctions or significant anomalies were experienced in any GLV system during the GT-4 flight. Therefore, the only reliability conclusion is a slight overall increase in the estimate, arising from the increased hours accumulated.

The method of obtaining reliability assessments of engines and RGS units has been reviewed with SSD/Aerospace. Current values of reliability for these systems were included in the evaluation of reliability for the GT-4 flight. The IGS unit is presently under review status; therefore, no new values for this system were included (Ref. 20).

XV. RANGE DATA

A. DATA DISTRIBUTION

1. Quick-Look Range Data

All available quick-look data were supplied by ETR to Martin-Baltimore as shown in Table XV-1.

The PCM serial tape was of good quality and exhibited few drop-outs. The formatted magnetic tape also was of excellent quality and contained no redundancies. Except for approximately 300 milliseconds of transmission blackout during booster staging, the Tel II formatted tape showed that there were no bad data words from LO − 10 to LO + 420 seconds.

TABLE XV-1

Range Supplied Quick-Look Data

Description	Time Requested	Time Received (ETR)	Time Received (Baltimore)
Telemetry magnetic tapes:			
Tel II, Postdetection PCM/FM (1 roll)	T + 1 hr	T + 1 hr	T + 10 hr
Tel II, FM/FM (2 rolls)	T + 1 hr	T + 1 hr	T + 10 hr
Station 1 formatted (2 rolls)	T + 4 hr	T + 3.5 hr	T + 10 hr

2. Martin Data

Test data and records acquired and generated by Martin at Cape Kennedy were received in Baltimore within two days after launch. These data consisted of the following items:

(1) One set of quick-look records from RCA Tape

(2) High speed records of engine parameters

(3) Landline records (events, Bristol, Multipoint and Sanborn) with associated calibrations

(4) BLH tabulation

(5) CP 2600 records (2650, 2660 and events)

(6) Sequencer records with code sheets

(7) Summary of flight events

(8) Dub of Complex 19 landline magnetic tape

(9) Fuel and oxidizer loading records

3. Range Data

All data supplied by the ETR are summarized in Table XV-2. The time requested for delivery to Martin-Canaveral (Ref. 6555th ATW Form 1-116, dated 24 May 1965) and the time received at Baltimore are shown in this table.

TABLE XV-2

Range-Supplied Data

OD Item No.	Description	Time Requested (Canaveral)	Time Received (Baltimore)
1	Position, velocity and acceleration, theodolite	3 CD	7 CD
3	Position, velocity and acceleration, camera	3 CD	7 CD
6	Position, velocity and acceleration, radar	3 CD	7 CD
10	Position, velocity, and acceleration, MISTRAM I	5 CD	11 CD
10	Position, velocity and acceleration, MISTRAM I and MISTRAM II	10 CD	22 WD
5	Attitude, camera	3 CD	7 CD
8	Special parameters, radar	10 WD	9 WD
12	Special parameters, MISTRAM	11 WD	13 WD
4.9/29.9	MISTRAM function recordings	3 WD	13 WD
18	Best estimate of trajectory	14 WD	22 WD
1.5-2	Serial PCM, postdetection magnetic tape	1 hr	6 hr

TABLE XV-2 (continued)

OD Item No.	Description	Time Requested (Canaveral)	Time Received (Baltimore)
1.5-1	FM/FM, postdetection magnetic tape	1 hr	6 hr
1.5-3	PCM formatted, postdetection magnetic tape	4 hr	6 hr
3.5-2	Serial PCM, postdetection magnetic tape	3 CD	6 CD
3.5-1	FM/FM, postdetection magnetic tape	3 CD	6 CD
1.5-6	Signal strength (center frequency) recordings	1 hr	6 CD
1.5-7	Signal strength (center frequency) recordings	3 hr	6 CD
3.5-5	Signal strength (center frequency) recordings	3 CD	13 CD
3.5-6	Signal strength (center frequency) recordings	3 CD	19 CD
7.5-3	Signal strength (center frequency) recordings	3 CD	21 WD
36	Tracking system comparisons, Mod III-G/MISTRAM I	6 CD	13 CD
38	Comparisons involving adjusted trajectory	22 CD	*
1.5-11	Oscillograph records, near real time	1 WD	1 WD
4.8.4.2	Instrumentation data logs	3 CD	*
1.18	Range safety plot charts	1 hr	1 CD
4.7.3.1	Real time computer facility metric data	1 hr	*
1.11-1	Command control function records	3 WD	13 WD
1.11-4	Command control function records	3 WD	*
1.11-5	Command control function records	3 WD	21 WD
1.11-6	Command control function records	3 WD	21 WD
3.11-1	Command control function records	5 WD	21 WD
3.11-2	Command control function records	5 WD	4 WD
3.11-3	Command control function records	5 WD	21 WD
7.11-1	Command control function records	5 WD	*

*Data not received by 7 July 1965.

TABLE XV-2 (continued)

OD Item No.	Description	Time Requested (Canaveral)	Time Received (Baltimore)
7.11-2	Command control function records	5 WD	*
7.11-3	Command control function records	5 WD	*
1	Preliminary test report	2 hr	1 WD
5.4.1	Propellant analysis report	2 WD	*
27	Weather surface observations	1 WD	1 WD
	Weather upper theodolite	1 WD	1 WD
	Weather upper Rawinsonde	1 WD	1 WD
	Weather tower 700/702	1 WD	1 WD
9.2.1.3-8	Special launch parameters, radar 0.18	**	9 WD

*Data not received by 7 July 1965
**Item not requested on Form 1-116, dated 24 May 1965

CD = Calendar days
WD = Working days

4. Agency/Contractor Supplied Data

Table XV-3 presents data received from associated contractors and NASA-MSC.

TABLE XV-3

Agency/Contractor Supplied Data

Description	Supplier	Received (Baltimore)
Mod III-G, AMRO guided missile control facility	GE, ETR	1 CD
Mod III-G, radio guidance system	GE, Syracuse	6 CD
IGS ascent parameters	McDonnell	4 CD
Preliminary vibration and acoustic graphs	NASA	18 CD
Spacecraft measurements	NASA	18 CD

B. FILM COVERAGE

Photographic conditions at Cape Kennedy preceding and during the GT-4 launch were excellent, and motion picture coverage was very good. Table XV-4 contains a listing of the films obtained from the fixed cameras and the tracking cameras. The reduction of film processing requirements resulted in 57% less footage being supplied for GT-4 than on GT-3.

The 70-mm tracking films (Items 1.2-38 and 1.2-40) and the 35-mm tracking film (Item 1.2-39) were reviewed for information pertaining to the booster staging event. Inspection of these films shows that the normal breakup of the first-stage transportation section occurred after Stage II had separated cleanly from Stage I.

TABLE XV-4

Film Coverage and Disposition

OD Item No.	Description	Footage (ft)	Time Received (Baltimore)
1.2-10 16 mm fixed	Missile centered, movement at launch	417	7 WD
1.2-12 16 mm fixed	Spacecraft centered, evaluate at launch	115	8 WD
1.2-14 16 mm fixed	Explosive bolts and first motion	218	4 WD
1.2-16 16 mm fixed	East launch ring, engine	155	5 WD
1.2-17 16 mm fixed	West launch ring, engine	221	5 WD
1.2-18 16 mm fixed	North launch ring, engine	224	5 WD
1.2-19 16 mm fixed	South launch ring, engine	224	4 WD
1.2-20 16 mm fixed	3D1E and 3D2E umbilical plugs	216	9 WD
1.2-21 16 mm fixed	2DFVT umbilical plug	Not Available	
1.2-22 16 mm fixed	1DOVT umbilical plug	223	8 WD
1.2-23 16 mm fixed	3B1E and associated umbilical plugs	222	4 WD
1.2-24 16 mm fixed	2B1E and associated umbilical plugs	224	8 WD
1.2-25 16 mm fixed	Cable cutters	223	4 WD
1.2-26 16 mm fixed	Umbilical Boom 3, "J" bars and lanyards	Not available	
1.2-27 16 mm fixed	Spacecraft upper umbilical plug	223	8 WD
1.2-28 16 mm fixed	Spacecraft upper umbilical plug	226	8 WD
1.2-31 16 mm tracking	LO to LOV pad emergency, spacecraft centered	416	8 WD
1.2-33 16 mm tracking	LO to LOV, missile centered	308	8 WD

TABLE XV-4 (continued)

OD Item No.	Description	Footage (ft)	Time Received (Baltimore)
1.2-35 16 mm tracking	First acquisition to LOV, missile centered	329	8 WD
1.2-38 16 mm tracking	First acquisition to LOV, missile centered and staging	65	9 WD
1.2-39 16 mm tracking	First acquisition to LOV, missile centered and staging	119	9 WD
1.2-40 16 mm tracking	First acquisition to LOV, missile centered and staging	70	8 WD
1.2-42 16 mm tracking	Umbilicals 3D1OC and 3D2OC		17 WD
1.2-39 35 mm tracking	First acquisition to LOV, missile centered and staging	320	8 WD
1.2-38 70 mm tracking	First acquisition to LOV, missile centered and staging	65	13 CD
1.2-40 70 mm tracking	First acquisition to LOV, missile centered and staging	581	12 CD

WD = Working days
CD = Calendar days

XVI. PRELAUNCH AND COUNTDOWN OPERATIONS

A. PRELAUNCH SUMMARY

1. Final Systems Test

The GT-4 simulated flight test (SFT) was performed successfully on 29 May 1965. The test was conducted in accordance with Martin test procedure (Ref. 5). The flight crew was in the spacecraft during the primary run, and the backup crew was in the spacecraft during the secondary run for spacecraft monitoring and training.

The countdown for the secondary run was started at T-45 minutes (1025 EST) and was completed at T+6 minutes (1116 EST). The primary run was started at T-6 minutes (1233 EST) and completed at T+ 6 minutes (1254 EST).

2. Precountdown Preparations

Precountdown preparations were started immediately after the completion of the SFT data review on 29 May. All systems progressed normally; however, the following components were replaced and retested by applicable Martin test procedures:

(1) The airborne tape recorder was replaced because of excessive noise noted during the SFT data review.

(2) The Stage II oxidizer prevalve was replaced because it failed to meet the pressure leak requirement.

(3) Two relays located in the power distribution control chassis (CP 2811) were replaced: K1 relay (malfunction shutdown) and K43 relay (lockout PCS shutdown). These relays were replaced after an investigation showed that excessive current flow due to a pressure sequencing solenoid valve (previously found shorted in S/A 1 of the Stage I engine) may have damaged the relay contacts.

(4) The pressure sequencing valve (PSV) on S/A 2 of the Stage I engine was replaced after the Failure Analysis Laboratory found contamination of alcohol and water in the S/A 1 pressure sequencing solenoid valve which had been replaced.

(5) The 25-volt airborne power supply was replaced after a similar unit at Martin-Baltimore was found to be defective. The unit was replaced with one which had been checked out using the updated manufacturing acceptance process.

(6) The Stages I and II oxidizer flowmeters were replaced because of a discrepancy between the two flowmeter readings during a special tanking exercise performed on the Stage II oxidizer tank on 26 May 1965.

3. Precountdown Activities

Precountdown checks were started at 1400 EST on 2 June 1965, and power was applied to the launch vehicle at 1246 EST. Oxidizer loading was started on 2 June at 2059 EST and completed at 2241 EST. Fuel loading began at 2333 EST and was completed at 0108 EST on 3 June. The precountdown activities were completed by 0500 EST on 3 June.

B. COUNTDOWN SUMMARY

The launch countdown was picked up on schedule at 0500 EST on 3 June. The 240-minute countdown was performed in accordance with Martin test procedure (Ref. 6). The countdown progressed smoothly to T-34:59 minutes, at which time a manual hold was initiated by the Martin Test Conductor because of a malfunction in the launch vehicle erector lowering circuitry. A hold of 76 minutes ensued while the erector malfunction was investigated and the erector subsequently lowered. At 0941 EST, the countdown was resumed at T-35 minutes and continued without incident through liftoff.

The countdown schedule is shown in Fig. XVI-1.

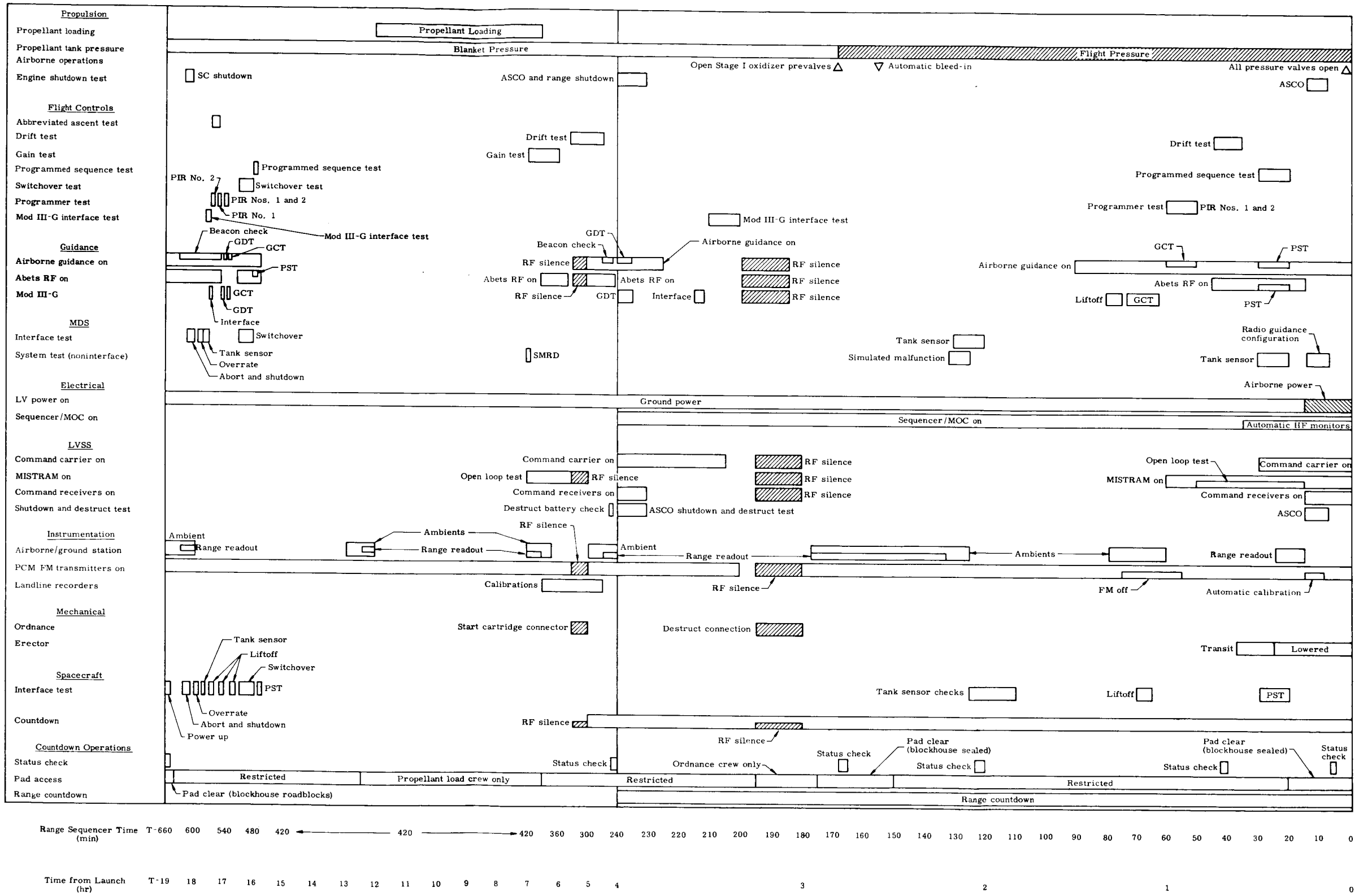

Fig. XVI-1. Precount and Countdown

XVII. CONFIGURATION SUMMARY

A. LAUNCH VEHICLE SYSTEMS DESCRIPTION

The Gemini Launch Vehicle (GLV) is a modified two-stage Titan II intercontinental ballistics missile (ICBM) which has been "man rated" for Gemini usage. The propulsion system in each stage uses hypergolic (self-igniting upon mixture) propellants. Modifications to the basic Titan II vehicle to achieve the "man rated" GLV follow:

(1) Addition of a completely redundant malfunction detection system (MDS).

(2) Replacement of the Titan II inertial guidance system (IGS) with the Mod III G radio guidance system (RGS).

(3) Addition of a three-axis reference system (TARS) to provide attitude reference and open-loop programming to the autopilot.

(4) Addition of a secondary flight control system (FCS).

(5) Addition of a secondary Stage I hydraulic system.

(6) Addition of the capability of switchover to the secondary guidance, flight control, and hydraulic systems.

(7) Provision of redundancy in electrical sequencing by APS and IPS power.

(8) Provision of an engine shutdown capability from the spacecraft.

(9) Provision of a 120-inch diameter cylindrical skirt forward of the Stage II oxidizer tank for mating the spacecraft to the launch vehicle.

(10) Removal of the retrorockets, vernier rockets and associated equipment.

(11) Addition of fuel line spring-piston accumulators and oxidizer line tuned standpipes for suppression of POGO vibrations.

(12) Capability for redundant Stage II engine shutdown (GLV-3 and up).

Significant GLV-4 changes from the GLV-3 configuration are listed in Table XVII-1.

TABLE XVII-1

GLV-4 Modifications

System	Significant Configuration Changes from GLV-3
Stage I Structure	1. Stage I oxidizer feedline conduit circumferential welds changed from lap to butt welded. 2. Helium leak tests of tanks changed from low pressure before and after hydro to low pressure before and high pressure after hydro. 3. Provisions added to Stage I fuel tank aft skirt for remote charging of oxidizer standpipe.
Stage II Structure	1. External protuberance heating insulation removed from Stage II oxidizer tank forward skirt. 2. Helium leak test of tanks changed from low pressure before and high pressure after hydro.
Propulsion	1. POGO installation revised as follows: a. Heat shield added to fuel dampener assembly to protect potentiometer and bearing from heat b. Fuel dampener piston shaft bearing material changed from teflon to ceramic-filled teflon c. Capability for remote charging of oxidizer standpipe added 2. Shields added to all fuel tank level sensors to protect the prism from autogenous gas contamination.

TABLE XVII-1 (continued)

System	Significant Configuration Changes from GLV-3
Flight Controls	1. TARS pitch program revised to make it compatible with GT-4 mission requirements.
Radio Guidance	None.
Hydraulics	None.
Electrical	1. Provisions added for remotely controlling charging or bleeding oxidizer standpipe. 2. Flashing beacon light system added to Stage II.
Malfunction Detection	None.
Instrumentation	1. Sixteen structural integrity measurements removed. 2. Two sound pressure measurements (Compartments 1 and 2) added. 3. Measurements provided for monitoring RGS decoder discretes 2, 4 and 8.
Range Safety and Ordnance	None.

1. Structure

The GLV is primarily of semi-monocoque shell construction (Stage II tank barrels are monocoque) with integral fuel and oxidizer tanks.

The basic diameter of the structural vehicle is 10 feet, and the length is 89.27 feet. Stage I, which includes the interstage transportation section, the fuel tank, and the oxidizer tank, is 70.67 feet long. The transportation section is assembled to the tank assembly by a manufacturing splice located at Vehicle Station 621.

Stage II consists of the fuel tank assembly and the oxidizer tank assembly, and is 28.27 feet in length.

The two stages are joined at Vehicle Station 500 by four studs and eight explosive nuts, the latter being used for staging.

On both Stage I and Stage II, external conduits are provided along the fuel and oxidizer tanks to house and support the propulsion and electric lines which lead into the various vehicle compartments.

a. Stage I

The Stage I structure consists of a fuel tank, an oxidizer tank, skirts at each end of the tanks, an interstage structure and external conduits. Channel-shaped, high strength longerons mounted externally on the fuel tank aft skirt provide separate interfaces for engine truss attachment and for launch stand tiedown. The propellant tanks are capable of withstanding ground and prelaunch loads with no internal pressure applied.

The fuel tank is a completely welded aluminum alloy structure. It consists of an ellipsoidal forward dome, a cylindrical barrel section and the aft cone assembly. An internal conduit, welded to the forward and aft domes, provides for passage of a single oxidizer line from the oxidizer tank through the fuel tank to the engine assembly. An outlet provides the channel for the fuel to pass from the tank to the engine.

The oxidizer tank consists of two end domes welded to a cylindrical section. During the staging event, the forward dome and the surrounding skirt structure are protected from the heat and blast of the Stage II engine exhaust by an ablative coating material.

The interstage section consists of the structure between the stage separation plane and the oxidizer tank forward skirt. A minimum of 7100 square inches of blast port area is provided at the aft end of this section for venting of the Stage II exhaust during staging.

b. Stage II

The Stage II structure includes an oxidizer tank, a fuel tank, skirts at the forward and aft ends of each tank, and external conduits. The tanks are capable of withstanding ground and prelaunch loads with no internal pressure applied.

The fuel tank consists of two ellipsoidal domes, each welded to an extruded aluminum alloy ring frame which forms the juncture of the dome, tank wall and skirt. The cap in the forward dome has a hole to accommodate the passage of the oxidizer line through the tank. The aft dome has provisions for a single fuel outlet. The aft skirt extends to the stage separation plane.

The between-tanks compartment consists of the forward section which is welded to the oxidizer tank aft dome ring frame and the aft section which is welded to the fuel tank forward dome ring frame. Aluminum alloy welded trusses are installed within this structure for support of subassembly components.

The oxidizer tank is similar to the fuel tank. It consists of two ellipsoidal domes, each welded to an extruded aluminum alloy ring frame which forms the juncture of the dome, tank wall and skirt. The aft dome contains the outlet for the oxidizer line. The forward skirt forms the interface between the spacecraft and the launch vehicle. Tension bolts are used in 20 external lugs, which are machined as part of the interface frame, to attach the spacecraft to the launch vehicle.

2. Propulsion System

The two-stage propulsion system for the GLV is adapted from the system used on the Titan II ICBM. Minor changes have been made to "man rate" the vehicle and to eliminate those elements of the Titan II system which are not required for the Gemini mission.

a. Stage I

The Stage I engine is comprised of two independently operated subassemblies mounted on a single engine frame. These subassemblies are designed to operate simultaneously. Each contains a thrust chamber, a turbopump and a gas generator.

The thrust chambers are gimbaled to permit vehicle control and stabilization in flight. Gimbal action is provided by tandem hydraulic actuators that operate in response to signals from the FCS.

Propellants are fed to the thrust chamber by turbopumps. Gas generators, used to drive the turbopumps, utilize the same propellants discharged by the pumps; this allows the engine to "bootstrap" during steady-state operation.

Propellants consist of fuel (50% hydrazine combined with 50% unsymmetrical-dimethyl hydrazine) and oxidizer (nitrogen tetroxide). This hypergolic mixture eliminates the need for combustion chamber igniters.

Solid propellant cartridges provide hot gas to start and drive the turbopumps during the engine start period. Shutdown is controlled by the override solenoid valve on the thrust chamber valve.

The thrust chambers are regeneratively cooled by circulating fuel through coolant tubes within the chamber walls. A dry jacket start is employed.

In-flight propellant tank pressurization is provided by an autogenous (self-generating) pressurization system. The fuel tank is pressurized by small portions of the gas generator exhaust gas output. A heat exchanger is provided to cool the gas generator exhaust before supplying it to the fuel tank for pressurization. The oxidizer tank is pressurized by oxidizer which has been heated to a gaseous state. Liquid oxidizer, supplied under pressure from the turbopump, is directed through a superheater where it is vaporized by the heat from the turbine exhaust.

b. Stage II

The Stage II engine is a single-chamber unit similar in operation to the Stage I engine. However, the engine is designed for maximum operating efficiency at high altitude. An ablative skirt is attached to the regeneratively cooled thrust chamber to increase the nozzle expansion ratio for high altitude performance improvement.

Like Stage I, the thrust chamber is gimbaled. Because only pitch and yaw control is provided in this manner, a roll nozzle is incorporated to permit roll control. The roll nozzle directs gas generator exhaust gas overboard, and roll control is obtained through swivel action of the nozzle.

A redundant means of shutdown is provided through a squib-operated valve in the oxidizer bootstrap line.

An autogenous pressurization system is provided for pressurizing the fuel tank in a manner similar to that of Stage I. The oxidizer tank, however, is pressurized before launch, and no additional pressurization is required.

3. Flight Control System

The redundant flight control system (FCS) consists of the (1) primary guidance and control system, (2) secondary guidance and control system and (3) switchover system.

The primary guidance and control system consists of a three-axis reference system (TARS), an adapter package, a Stage I rate gyro package, an autopilot, the primary servovalves in the Stage I tandem actuators, and the Stage II hydraulic actuators. The GE Mod III G radio guidance system (RGS) provides steering commands to the primary guidance and control system during Stage II flight.

The secondary guidance and control system consists of a duplicate Stage I rate gyro package, a duplicate autopilot, the secondary servovalve in the Stage I tandem actuators, and the Stage II hydraulic actuators. The spacecraft inertial guidance system (IGS) provides stabilization and steering commands to the secondary guidance and control system.

The switchover system consists of the redundant power amplifiers located in the malfunction detection package (MDP), the FCS switchover relays located in the adapter package, the Stage I tandem actuator switchover valve, pressure switches, hardover sensors, and the MDS rate switches.

The TARS is used to establish angular reference along the pitch, roll and yaw axes; to provide roll and pitch open-loop guidance programs during Stage I flight; to accept pitch and yaw radio guidance steering signals during Stage II closed-loop guidance operation; and to provide discrete timing functions.

The main function of the adapter package is to condition attitude outputs from the TARS for inputs to the autopilot. The package also houses the FCS switchover relays.

Two sets of rate gyros are utilized for GLV stabilization: the Stage I rate gyro package (one each for the primary and secondary systems) and the Stage II rate gyros located within the redundant autopilot assemblies. During Stage I flight, signals from both the Stage I and the Stage II pitch and yaw rate gyros are summed in a given proportion.

The autopilot contains an 800-cps static inverter, Stage II rate gyros, gain switching module, channel amplifiers and valve drive amplifiers (VDA). The rate and displacement gyro signals are suitably amplified, demodulated, mixed and dynamically compensated, with filtering, in the autopilot to provide vehicle stability. The autopilot output signals are used to drive the servovalves.

Both the primary and secondary FCS operate at all times during flight. During Stage I flight, each servovalve coil in the Stage I tandem actuators receives control signals. At switchover, control of the tandem actuator is switched from the primary to the secondary servovalve.

4. Radio Guidance System

The GE Mod III G RGS is used to guide the GLV Stage II/spacecraft combination in the proper trajectory. The RGS accomplishes this by using steering commands to torque the pitch and yaw attitude gyros in the TARS. The RGS also supplies the Stage II shutdown signal (SECO) in the primary mode.

The RGS airborne components are the pulse beacon unit, rate beacon unit, decoder unit and antenna system.

Vehicle rates are derived by means of the doppler principle, and position tracking radar is utilized to derive the vehicle position as a function of range, elevation and azimuth. The vehicle position and rate information are used by the ground-based guidance computer to generate the steering commands. The messages that contain the steering commands and SECO discrete are monitored by the decoder for validity. If the message is valid, the steering commands are supplied to the control system as pitch and yaw corrections and the SECO command, when present, is supplied to the engine shutdown circuitry.

5. Hydraulic System

The Stage I hydraulic system is redundant. Separate primary and secondary hydraulic circuits power the four tandem actuators for positioning the two thrust chambers in response to signals from the FCS. The system contains two engine-driven pumps; two accumulator-reservoirs; four tandem actuators; one electric motor pump; one test selector valve; one in-line filter; two coaxial disconnects; and instrumentation transducers. Each tandem actuator contains two hydraulically and electrically separated servo loops which can be switched from primary to secondary by external command or due to a pressure loss in the primary system. Each circuit is powered during engine operation by a variable displacement pressure-compensated pump driven through the accessory gearbox of each subassembly. For tests and during launch countdown, an electric motor pump powers the system.

The Stage II hydraulic system contains an engine-driven pump; two engine actuators, a roll nozzle actuator, an accumulator-reservoir, an electric motor pump, an in-line filter; a coaxial disconnect and instrumentation transducers. The system is not redundant and operation is the same as for a single system on Stage I.

6. Electrical System

The GLV electrical system is divided into a power distribution system and a sequencing system. The power distribution system consists of the accessory power supply (APS) and the instrumentation power supply (IPS).

The APS and IPS buses are provided with airborne power from separate 28 vdc silver-zinc rechargeable batteries.

The APS provides power to the static inverter, the malfunction detection system (MDS), the APS command receiver, the APS shutdown and destruct circuitry, the RGS, the FCS, the sequencing system and the Stage II engine start circuitry. Static inverter output is 115/200 volts, 400 cps at 750 va.

The IPS provides power to the MDS, MISTRAM, the IPS command receiver, the IPS shutdown and destruct circuitry, the FCS, the sequencing system, Stage II engine start circuitry and the airborne instrumentation system.

The sequencing system provides the proper sequencing of events from Stage I engine start to Stage II engine shutdown. Major functions are: reset Stage I prevalves switch; actuate APS and IPS staging switches; shut down Stage I engine; fire staging nuts; and start Stage II engine.

Redundancy in the form of dual power supplies, relays, motorized switches, diodes and wiring is used throughout the GLV electrical system. A separate battery is provided in Stage I to supply power to the engine shutdown and destruct system if inadvertent separation occurs.

7. Malfunction Detection System

The MDS is provided to monitor launch vehicle performance and to supply indications of potentially catastrophic malfunctions and certain significant flight events to the spacecraft. An automatic function is provided for switching from the primary Stage I flight control-guidance-hydraulic combination to the secondary system in the event of a failure in the primary system. Switchover can be initiated by pitch, yaw or roll overrate, Stage I engine hardover, loss of primary system hydraulic pressure or by the flight crew. Switchback to the primary system can be initiated by the flight crew during the Stage II flight.

The main components of the MDS are the malfunction detection package (MDP), the rate switch package (RSP), and the various bilevel

and analog sensors located throughout the launch vehicle. All circuits, components and wiring of the MDS are redundant to provide high reliability.

Functions monitored by the MDS include Stage I engine chamber pressure, Stage II fuel injector pressure, propellant tank pressures, excessive angular rates, staging, loss of Stage I primary hydraulic pressure, engine hardover, and switchover.

8. Instrumentation System

The airborne instrumentation system is comprised of various transducers or measuring points, signal conditioners, a PCM multiplexer, a PCM/FM telemetry unit, an FM/FM telemetry unit, a tape recorder-reproducer, and an antenna system.

The PCM telemetry is a time-multiplexed data system with an input capacity of 196 analog and 48 bilevel channels. The output is a serial pulse train. Samples of input data are as follows:

Analog

Number of Channels	Samples per Second
85	20
35	40
36	100
20	200
20	400

Bilevel

Number of Channels	Samples per Second
40	20
8	100

The major components of the FM telemetry are an FM multiplexer subcarrier oscillator assembly, an RF transmitter and a separate power amplifier. The system has a seven-channel data capacity.

Prior to staging, several FM channels are switched to monitor staging functions, and seven signals are transmitted in real time and paralleled on the tape recorder. The recorder is programmed to play back its recording after completion of the staging event.

9. Range Safety System

The GLV range safety system is comprised of the MISTRAM system, command control system and ordnance destruct systems.

The primary tracking and impact prediction system employed in the GLV is the GE MISTRAM system. It consists of an airborne transponder, antennas and ground stations located at Valkaria, Florida and Eleuthera.

In operation, the airborne transponder receives two CW signals from the ground station, and displaces and retransmits them back to the ground station for computation of accurate position, velocity and impact prediction information.

Because line-of-sight transmission between the GLV and Valkaria is impossible, MISTRAM cannot lock in until the GLV attains an altitude of approximately 8000 feet. A beacon system in the spacecraft combined with an AN/FPS-16 radar is used to supply backup tracking information.

The command control system consists of two Advanced Communications, Inc. (ACI) receivers, four flush-mounted antennas, a six-port junction and an interconnecting cable. The redundant receivers each contain a decoder unit capable of receiving a coded FM signal from the ground station and converting this signal (or tones) into commands for (1) engine shutdown and warning to the spacecraft, (2) destruct (command No. 1 must be received 3.5 seconds before command No. 2 can take effect) and (3) ASCO which is a backup to RGS/IGS Stage II engine shutdown. The ASCO command originates at the Burroughs ground guidance computer.

The ordnance destruct system components consist of destruct initiators, primacord, and bidirectional destruct charges. The initiators are basically out-of-line explosive trains which are armed by AGE prior to liftoff. Each of the initiators is connected to two bidirectional destruct charges which are located 180 degrees apart midway between the fuel and oxidizer tanks in each stage. Upon receipt of command No. 2, the IPS and APS electrical signals cause the initiators to ignite the primacord, thus setting off the destruct charges which rupture the tanks.

The Stage I inadvertent separation destruct system is designed to function up to the time of staging enable (approximately LO + 145 seconds). This system consists of a separate destruct battery, lanyard switches between Stages I and II, and the same Stage I initiators, primacord and destruct charges used in the command control ordnance destruct system. Should Stage I inadvertently separate from Stage II

prior to staging enable, the lanyard switches would route the output of the Stage I destruct battery to Stage I engine shutdown and through a 5.5-second delay timer to the initiators, causing the destruct charges to explode.

10. Ordnance Separation System

The launch separation system uses ordnance devices at the four vehicle-to-pad attachment points. Each attachment point has one interconnecting stud with an explosive nut on each end. Each nut assembly contains a gas pressure cartridge with two independent bridgewires mounted internally. The circuits for these bridgewires are activated by a MOCS signal to the launch release control set two seconds after TCPS make.

The airborne separation system uses ordnance devices at the four Stage I and Stage II attachment points located at Vehicle Station 500. Each attachment point has one interconnecting stud with an explosive nut on either end. Each nut assembly is similar to that of the launch separation system. The cartridges are ignited electrically by the staging command (initiated by TCPS).

B. MAJOR COMPONENTS

The major GT-4 components are as follows:

(1) Spacecraft

(a) Manufacturer: McDonnell Aircraft Corporation

(b) Serial Number: Spacecraft Number 4

(2) Gemini Launch Vehicle

(a) Manufacturer: Martin Company

(b) Serial Number: GLV-4

(c) Air Force Serial Number: 62-12559

(3) Gemini Launch Vehicle systems

The GLV systems and major components are listed in Table XVII-2. Figure XVII-1 shows the general arrangement of the GLV.

TABLE XVII-2

GLV Systems and Major Components

System/Component	Part No.	Serial No.	Manufacturer
Powerplant			
Engine, Stage I	YLR87-AJ-7	1005	Aerojet-General Corp.
Engine, Stage II	YLR91-AJ-7	2003	Aerojet-General Corp.
Propellants			
Level sensor, propellant	424-7491004-009	062	Bendix
Level sensor, propellant	424-7491004-009	169	↑
Level sensor, propellant	424-7491004-009	256	↕
Level sensor, propellant	424-7491004-009	266	↕
Level sensor, propellant	424-7491004-009	358	↕
Level sensor, propellant	424-7491004-009	392	↕
Level sensor, propellant	424-7491004-009	409	↕
Level sensor, propellant	424-7491004-009	422	↕
Level sensor, propellant	PS830900012-039	246	↕
Level sensor, propellant	PS830900012-039	345	↕
Level sensor, propellant	PS830900012-049	167	↕
Level sensor, propellant	PS830900012-049	190	↕
Level sensor, propellant	PS830900012-049	192	↕
Level sensor, propellant	PS830900012-049	199	↕
Level sensor, propellant	PS830900012-049	218	↕
Level sensor, propellant	PS830900012-049	222	↕
Level sensor, propellant	PS830900012-049	244	↕
Level sensor, propellant	PS830900012-049	295	↕
Level sensor, propellant	PS830900012-049	312	↕
Level sensor, propellant	PS830900012-059	251	↕
Level sensor, propellant	PS830900012-059	327	↕
Level sensor, propellant	PS830900012-059	350	Bendix
Switch, pressure	PS718000100-011	0013	Hydra Electric
Switch, pressure	PS718000100-013	0012	↕
Switch, pressure	PS718000100-015	0011	↕
Switch, pressure	PS718000100-017	0012	Hydra Electric

TABLE XVII-2 (continued)

System/Component	Part No.	Serial No.	Manufacturer
Propellants (cont)			
Transducer, temperature	PS741000002-005	700	Rosemount Engineering
Transducer, temperature	PS741000002-005	701	↕
Transducer, temperature	PS741000002-005	702	
Transducer, temperature	PS741000002-005	703	Rosemount Engineering
Transducer, tank pressure	PS746000002-023	1077	Servonics
Transducer, tank pressure	PS746000002-023	1079	↕
Transducer, tank pressure	PS746000002-023	1083	
Transducer, tank pressure	PS746000002-023	1084	
Transducer, tank pressure	PS746000002-025	2082	
Transducer, tank pressure	PS746000002-025	2085	
Transducer, tank pressure	PS746000002-025	2086	
Transducer, tank pressure	PS746000002-025	2088	Servonics
Prevalve, 7 inch	PS475100007-159	0700020	Thiokol, RMD
Prevalve, 7 inch	PS475100007-139	0700018	↕
Prevalve, 4 inch	PS475100006-059	0400004	
Prevalve, 6 inch	PS475100005-159	0600043	
Prevalve, 6 inch	PS475100005-169	0600032	
Prevalve, 6 inch	PS475100005-199	0600025	Thiokol, RMD
Burst disc assembly	PS571300000-009	222	Consolidated Controls
Burst disc assembly	PS571300000-009	223	↕
Burst disc assembly	PS571300000-009	224	Consolidated Controls
Hydraulics			
Tandem actuator, Stage I	PS460000008-149	016	Moog Servocontrols, Inc.
Tandem actuator, Stage I	PS460000008-149	025	↕
Tandem actuator, Stage I	PS460000008-159	023	
Tandem actuator, Stage I	PS460000008-159	024	
Actuator, Stage II	PS460000004-019	008	
Actuator, Stage II	PS460000004-019	010	
Actuator, roll nozzle	PS460000005-019	009	Moog Servocontrols, Inc.

TABLE XVII-2 (continued)

System/Component	Part No.	Serial No.	Manufacturer
Hydraulics (cont)			
Filter, hydraulic, Stage I	PS481000001-009	B-003	Aircraft Porous Media
Filter, hydraulic, Stage II	PS481000001-009	B-015	Aircraft Porous Media
Valve, selector	PS470000029-009	016	Sterer Engineering and Manufacturing Company
Accumulator-reservoir, secondary	PS480000013-009	109	Cadillac Gauge
Accumulator-reservoir, primary	PS480000013-009	129	↓
Accumulator-reservoir, Stage II	PS480000013-009	104	Cadillac Gauge
Motor pump, electric, Stage I	PS483100013-019	C53888	Vickers, Inc.
Motor pump, electric, Stage II	PS483100013-009	C57358	Vickers, Inc.
Pump, Stage I engine, primary	PS483100010-019	A0-23	New York Air Brake
Pump, Stage I engine, secondary	PS483100010-019	A0-18	↓
Pump, Stage II engine	PS483100011-009	A1-159	New York Air Brake
Coaxial disconnect, primary	PS485000001-009	1049	Aeroquip
Coaxial disconnect, secondary	PS485000001-009	1040	↓
Coaxial disconnect, Stage II	PS485000001-009	1004	Aeroquip
Flight Controls			
Package, TARS	PS640900235-089	F-16	Honeywell
Package, TARS adapter	424-7562601-079	B-014	Martin-Baltimore
Autopilot, primary	424-7562200-079	D-021	Martin-Denver
Autopilot, secondary	424-7562200-079	D-014	Martin-Denver
Rate gyro, primary	PS962000001-049	2013	Giannini Controls
Rate gyro, secondary	PS962000001-049	2012	Giannini Controls
Guidance			
Beacon, pulse	66D802028G1	G017	General Electric
Beacon, rate	66D802029G1	G022	↓
Decoder	66D802030G3	G022	General Electric

TABLE XVII-2 (continued)

System/Component	Part No.	Serial No.	Manufacturer
Electrical			
Inverter, static	PS946000001-006	R-12	Bendix
Power supply, 25 volt	CCI 9401A11-1	162	United Controls
Relay, time delay	PS722700003-004	4010	Autronics
Relay, time delay	PS722700004-002	424	↕
Relay, time delay	PS722700004-002	313	↕
Relay, time delay	PS722700005-001	218	Autronics
Relay	PS720200002-001	0053	Leach Company
Relay	PS720200002-001	0056	↕
Relay	PS720200002-001	0074	↕
Relay	PS720200002-001	0075	↕
Relay	PS720200002-001	0096	↕
Relay	PS720200002-001	0102	↕
Relay	PS720200002-001	0113	↕
Relay	PS720200002-001	0138	↕
Relay	PS720200002-001	0228	↕
Relay	PS720200002-001	0232	↕
Relay	PS720200002-001	0211	Leach Company
Relay assembly (gain change)	424-7567018-009	B-005	Martin-Baltimore
Relay assembly (RESS)	424-7567050-009	B-011	Martin-Baltimore
Switch, motor-driven	CCI 7241B3-4	0008	Kinetics Corporation
Switch, motor-driven	CCI 7241B3-4	0009	↕
Switch, motor-driven	CCI 7241B2-8	0109	↕
Switch, motor-driven	CCI 7241B2-8	0118	↕
Switch, motor-driven	CCI 7241B2-8	0133	↕
Switch, motor-driven	CCI 7241B2-8	0123	↕
Switch, motor-driven	CCI 7241B2-8	0110	↕
Switch, motor-driven	CCI 7241B2-8	0191	↕
Switch, motor-driven	CCI 7241B2-8	0167	↕
Switch, motor-driven	CCI 7241B2-8	0143	↕
Switch, motor-driven	CCI 7241B2-8	0198	↕
Switch, motor-driven	CCI 7241B2-8	0134	↕
Switch, motor-driven	CCI 7241B2-8	0137	↕
Switch, motor-driven	CCI 7241B2-8	0025	Kinetics Corporation

TABLE XVII-2 (continued)

System/Component	Part No.	Serial No.	Manufacturer
Electrical (cont)			
Switch, motor-driven	CCI 7241B2-8	0158	Kinetics Corporation
Switch, motor-driven	CCI 7241B2-8	0216	
Switch, motor-driven	CCI 7241B2-14	0028	
Switch, motor-driven	CCI 7241B2-14	0021	
Switch, motor-driven	CCI 7241B2-14	0026	
Vibration isolation assembly	CCI 7241B2-21	0034	
Vibration isolation assembly	CCI 7241B2-21	0035	
Vibration isolation assembly	CCI 7241B2-21	0036	
Vibration isolation assembly	CCI 7241B2-21	0037	
Vibration isolation assembly	CCI 7241B2-21	0038	
Vibration isolation assembly	CCI 7241B2-21	0039	
Vibration isolation assembly	CCI 7241B2-21	0040	Kinetics Corporation
Connector, staging	CCI 8124B1-22	0038	Cannon Electric
Connector, staging	CCI 8124B1-23	0007	
Connector, staging	CCI 8124B1-32	0008	
Connector, staging	CCI 8124B1-33	0007	
Connector, staging	CCI 8124B1-34	0006	
Connector, staging	CCI 8124B1-35	0014	
Connector, staging	CCI 8124B1-36	0009	
Connector, staging	CCI 8124B1-37	0014	
Connector, staging	CCI 8124B1-38	0026	
Connector, staging	CCI 8124B1-39	0022	Cannon Electric
Disconnect, separation	CCI 8119A1-6	0032	Cannon Electric
Disconnect, separation	CCI 8119A1-6	0031	Cannon Electric
Switch, lanyard	CCI 7121B4-1	0019	Kinetics Corporation
Switch, lanyard	CCI 7121B4-1	0020	Kinetics Corporation
Capacitor	CCI 90B15-1	0029	Sprague Electric Company
Capacitor	CCI 90B15-1	0030	Sprague Electric Company
Diode, 5-amp	CCI 7920A7-2	N/A	U.S. Semcor

TABLE XVII-2 (continued)

System/Component	Part No.	Serial No.	Manufacturer
Electrical (cont)			
Umbilical, disconnect	PS812400002 039	004	Cannon Electric
Umbilical, disconnect	PS812400002-039	007	↕
Umbilical, disconnect	PS812400002-049	009	↕
Umbilical, disconnect	PS812400002-049	037	↕
Umbilical, disconnect	PS812400002-049	038	Cannon Electric
Diode box assembly	424-7567020-009	B-010	Martin-Baltimore
Diode box assembly	424-7567020-009	B-058	↕
Diode box assembly	424-7567020-019	B-054	↕
Diode box assembly	424-7567020-019	B-066	↕
Diode box assembly	424-7567020-019	B-067	↕
Semiconductor package	424-7567029-009	B-007	↕
Semiconductor package	424-7567029-009	B-018	Martin-Baltimore
Battery, APS/IPS	PS940300011-001	065	Yardney Electric
Battery, APS/IPS	PS940300011-001	066	↕
Battery, destruct	CCI 9401B15-1	019	Yardney Electric
Microfuse	CCI 8609B7-3	N/A	Littlefuse, Inc.
Microfuse post	CCI 8609B7-4	N/A	Littlefuse, Inc.
Range Safety			
Command receiver, APS	R-423A	37	Advanced Communications, Inc.
Command receiver, IPS	R-423A	50	Advanced Communications, Inc.
Transponder, MISTRAM	764145061	97	GFP
Malfunction Detection			
Package, rate switch	PS830600015-027	4013	Giannini Controls
Package, malfunction detection	424-7569205-189	B-009	Martin-Baltimore
Connector, stage separation	CCI 8119A1-5	0103	Cannon Electric
Connector, stage separation	CCI 8119A1-6	0073	Cannon Electric

TABLE XVII-2 (continued)

System/Component	Part No.	Serial No.	Manufacturer
Malfunction Detection (cont)			
MDTCPS, S/A 1 primary	284321	848	Aerojet-General Corp.
MDTCPS, S/A 1 redundant	284321	847	
MDTCPS, S/A 2 primary	284321	850	
MDTCPS, S/A 2 redundant	284321	849	
MDFJPS, S/A 3 primary	711049-1	789	
MDFJPS, S/A 3 redundant	711049-1	935	Aerojet-General Corp.
Instrumentation			
Multiplexer/encoder, PCM	PS640900237-039	009	Epsco, Inc.
Telemetry unit, PCM-FM	424-7565020-039	D-009	Martin-Denver
Signal conditioner	424-7565006-019	B-004	Martin-Baltimore
Ordnance			
Initiator, destruct	PS601100013-015	34	Thiokol Chemical Corp.
Initiator, destruct	PS601100013-015	27	Thiokol Chemical Corp.
Nut, hold-down	PS335200000-001	15085	High-Shear Corp.
Nut, hold-down	PS335200000-001	15086	
Nut, hold-down	PS335200000-001	15089	
Nut, hold-down	PS335200000-001	15091	
Nut, hold-down	PS335200000-001	15092	
Nut, hold-down	PS335200000-001	15095	
Nut, hold-down	PS335200000-001	15098	
Nut, hold-down	PS335200000-001	15099	
Nut, separation	PS335200000-003	14241	
Nut, separation	PS335200000-003	14243	
Nut, separation	PS335200000-003	14244	
Nut, separation	PS335200000-003	14246	
Nut, separation	PS335200000-003	14247	
Nut, separation	PS335200000-003	14248	
Nut, separation	PS335200000-003	14249	
Nut, separation	PS335200000-003	14251	High-Shear Corp.

TABLE XVII-2 (continued)

System/Component	Part No.	Serial No.	Manufacturer
Ordnance (cont)			
Cartridge, gas pressure-prevalve	PS601100010-001	N/A (12 used)	McCormick Selph
Cartridge, gas pressure-dropweight	PS601100010-001	N/A (4 used)	↕
Cartridge, gas pressure-holddown nut	PS601100010-001	N/A (8 used)	↕
Cartridge, gas pressure-separation nut	PS601100010-001	N/A (8 used)	McCormick Selph
Primacord assembly	424-14060001-009	N/A	The Ensign-Bickford Co.
Primacord assembly	424-14060001-039	N/A	↕
Primacord assembly	424-14060001-049	N/A	↕
Primacord assembly	424-14060001-059	N/A	↕
Primacord assembly	424-14060001-079	N/A	↕
Primacord assembly	424-14060001-089	N/A	The Ensign-Bickford Co.
Destruct charge, bidirectional	PS601100009-001	13, 14, 15, 16	Francis Associates

LAUNCH VEHICLE UMBILICAL SYSTEMS INTERFACE

CODE	FUNCTION	SYSTEM	LOCATION
28A	AIR COND	GUIDANCE AIR COND STG II	STA 371.522 QUAD I 82½° OFF BL 0
S28CV	OXID VENT	OXID STG II	STA 371.522 QUAD II 85° OFF BL 0
28ZE	ELECTRICAL	ELECTRICAL STG II	STA 402.472 QUAD II 82½° OFF BL 0
28IE	ELECTRICAL	ELECTRICAL STG II	STA 402.472 QUAD II 65½° OFF BL 0
28FVT	FUEL VENT TOPPING	FUEL STAGE II	STA 406.491 QUAD II 34° 20' OFF BL 0
S28FV	FUEL VENT	FUEL STG II	STA 406.475 QUAD II 37° 20' OFF BL 0
S38H	HYDRAULIC	HYDRAULIC STG II	STA 470.125 QUAD II 15° OFF BL 0
▲ 38A	AIR CONDITIONING	ENGINE AREA STG II	STA 474.875 QUAD II 30° OFF BL 0
S38F	FUEL FILL AND DRAIN	FUEL STG II	STA 492.250 QUAD II 15° OFF BL 0
38FD	FUEL PRESS SEQ VALVE DRAIN	FUEL STG II	STA 492.250 QUAD II 30° 27' BL 0
S38O	OXID FILL AND DRAIN	OXID STG II	STA 492.250 QUAD II 72° OFF BL 0
38IE	ELECTRICAL	ELECTRICAL STG II	STA 492.250 QUAD II 45° OFF BL 0
ICIFD	TURBO PUMP FUEL DRAIN	FUEL STG I	STA 494.750 QUAD I 75° OFF BL 0
ICOD	TURBO PUMP OXID DRAIN	OXID STG I	STA 494.750 QUAD I 15° OFF BL 0
S1DV	OXID VENT	OXID STG I	STA 670.727 QUAD II 4° WL 60.0
S2DFV	FUEL VENT	FUEL STG I	STA 963.326 QUAD II 40° OFF BL 0
3DIM	MALFUNCTION DETECTION SYS.	MALFUNCTION STG I	STA 214.673 QUAD I 34° 34' OFF BL 0
302M	MALFUNCTION DETECTION SYS.	MALFUNCTION STG I	STA 214.673 QUAD III 34° OFF BL 0
30IE	ELECTRICAL	ELECTRICAL STG I	STA 216.691 QUAD II 20° OFF BL 0
S30F	FUEL FILL AND DRAIN	FUEL STG I	STA 243.560 QUAD I
S30FD	FUEL DRAIN PRE-VALVE	FUEL STG I	STA 1244.123 QUAD III
S300D	OXID DRAIN PRE-VALVE	OXID STG I	STA 1250.560 QUAD II
S30IH	HYDRAULIC SUPPLY AND RETURN	HYDRAULIC STG I PRIMARY	STA 1255.835 QUAD I
S30O	OXID FILL AND DRAIN	OXID STG I	STA 1249.560 QUAD IV
2BOVT	OXID VENT TOPPING	OXID STG II	STA 354.802 QUAD II 4° OFF WL 60
1DOVT	OXID VENT TOPPING	OXID STG I	STA 630.727 QUAD II 60° OFF BL 0
2DFVT	FUEL VENT TOPPING	FUEL STAGE I	STA 963.326 QUAD II 50° OFF BL 0
302E	ELECTRICAL	ELECTRICAL STG I	STA 1216.691 QUAD II 10° OFF BL 0
S302H	HYDRAULIC SUPPLY AND RETURN	HYDRAULIC STG I SECONDARY	STA 1255.835 QUAD II
▲ 3D10C	OXID. REMOTE CHARGING SYSTEM	OXID. STG. I	STA. 1224.311 QUAD III 22½° OFF BL 0
▲ 3D20C	OXID. REMOTE CHARGING SYSTEM	OXID. STG. I	STA. 1224.311 QUAD III 17½° OFF BL 0

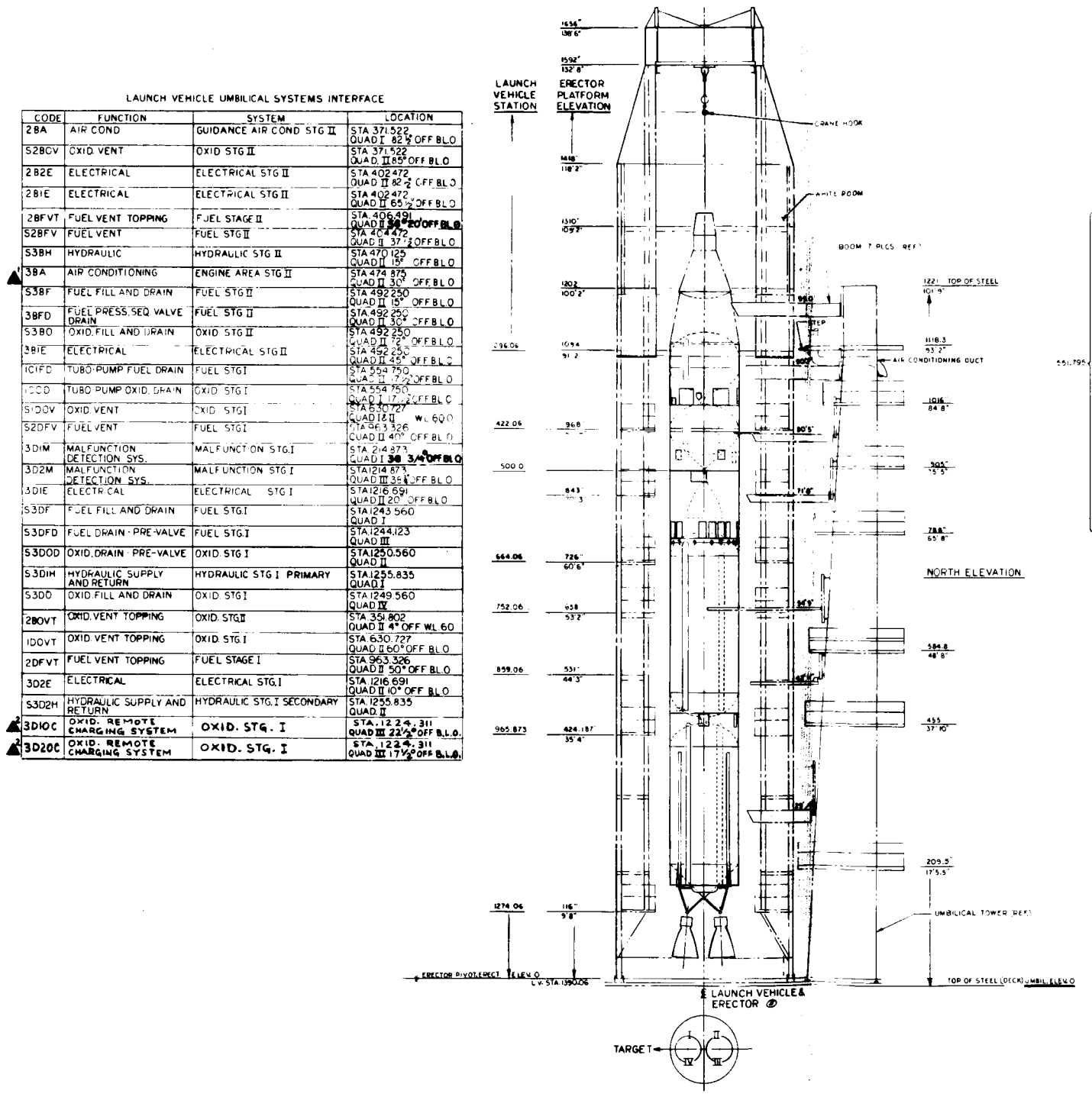

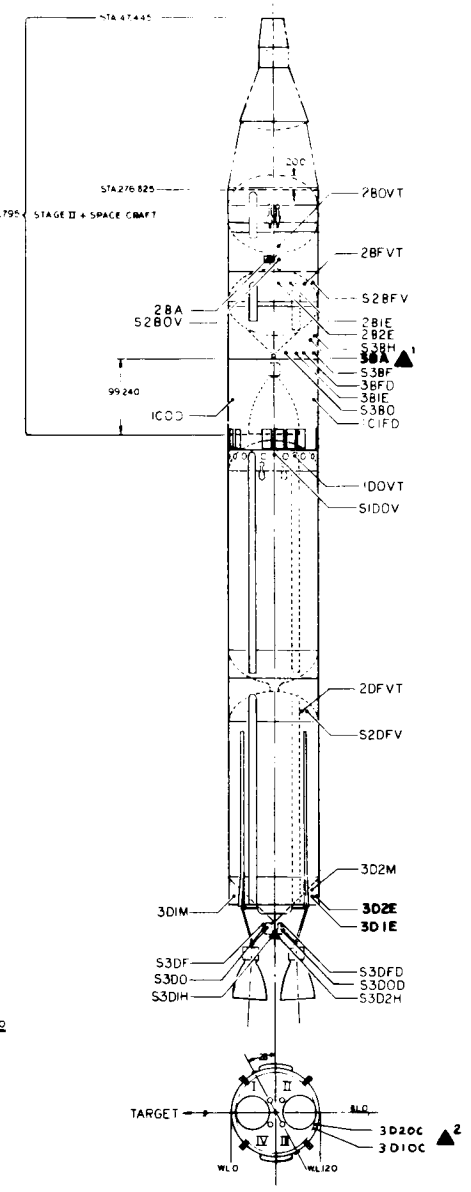

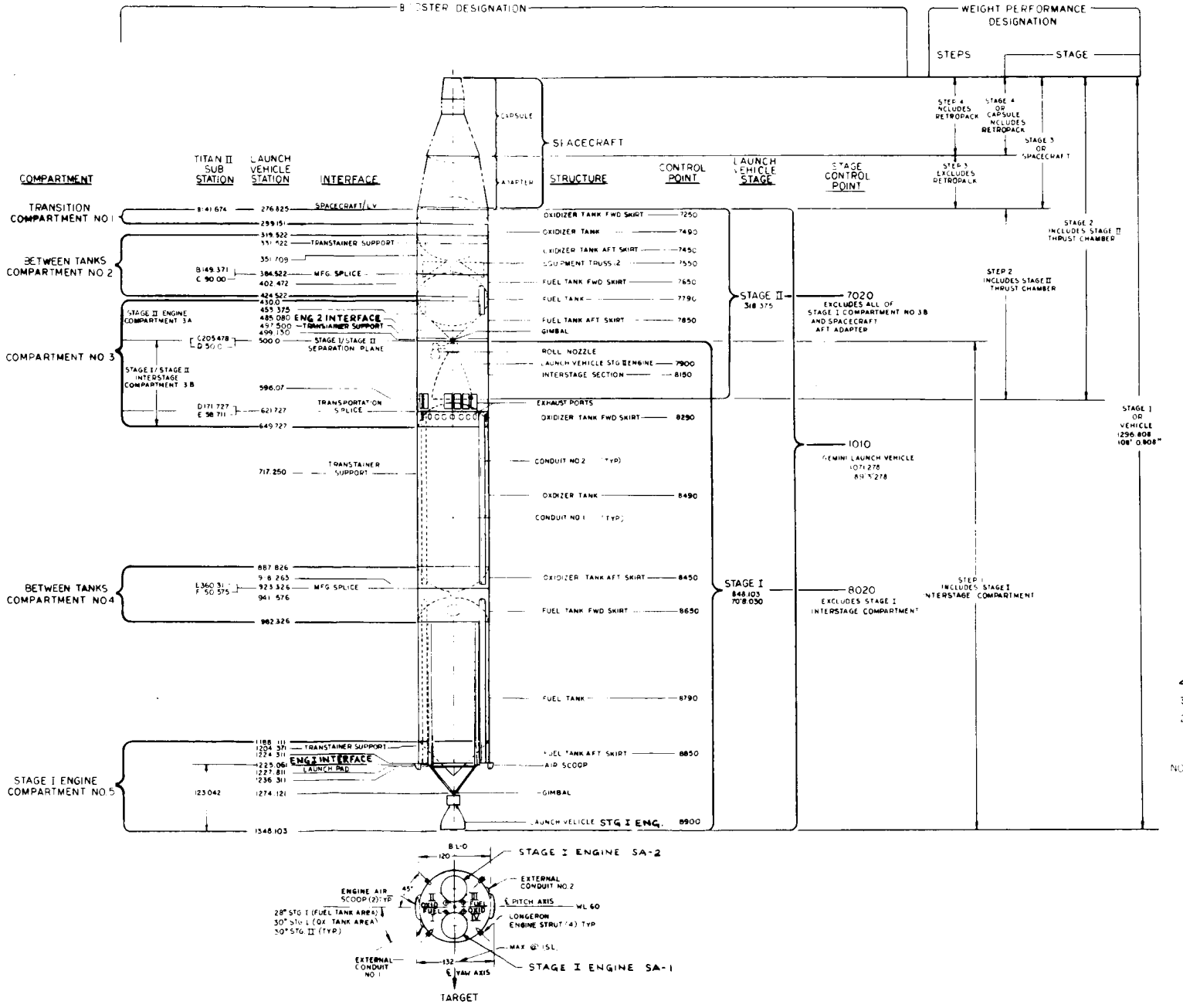

Fig. XVII-1. Gemini Launch Vehicle General Arrangement

XVIII. REFERENCES

1. "Launch Vehicle No. 3 Flight Evaluation," Engineering Report 13227-3, Martin Company, Baltimore, Maryland, May 1965. Confidential

2. "Launch Vehicle No. 2 Flight Evaluation," Engineering Report 13227-2, Martin Company, Baltimore, Maryland, March 1965. Confidential

3. "Launch Vehicle No. 2 Launch Attempt Evaluation," Engineering Report 13227-2X, Martin Company, Baltimore, Maryland, January 1965. Confidential

4. "Launch Vehicle No. 1 Flight Evaluation," Engineering Report 13227-1, Martin Company, Baltimore, Maryland, May 1964. Confidential

5. "Martin-Canaveral Test Procedure," 424-876-ETR, Revision D.

6. "Martin-Canaveral Test Procedure," 424-875-ETR, Revision J.

7. "MOD III Total Uncertainties, Gemini IV," letter from General Electric Company (Mr. E. H. Weldberg) to Martin Company (Mr. W. D. Smith), 11 June 1965, Syracuse, New York. Secret

8. "Master Measurements List," LV-220, Revision J, Martin Company, Baltimore, Maryland, 12 May 1965.

9. "Revised GLV Trajectory Dispersion Analysis," LV-274-4, Martin Company, Baltimore, Maryland, May 1964.

10. "Flight Weight Coordination Report Post-Flight Weight, GT-4," LV-165-4B, Martin Company, Baltimore, Maryland, 24 June 1965.

11. "Gemini Launch Vehicle Performance Specification," MB-1046, SCN-7, Martin Company, Baltimore, Maryland, 24 May 1965.

12. "GT-3 Guidance Equations Accuracy Estimate," Aerospace Technical Memorandum No. ATM-65 (5126-40)-16, Aerospace Corporation, El Segundo, California, 18 February 1965. Confidential

13. "GLV-4 Incentive Catalog," IM-104, Martin Company, Baltimore, Maryland, 1 April 1965.

14. "Mathematical Model for Countdown Availability Study," Engineering Report 13225, Martin Company, Baltimore, Maryland, April 1964.

15. "Gemini Launch Vehicle Acoustic and Vibration Environment," Part 1: Vibration, and Part 2: Acoustics, Engineering Report 12414, Martin Company, Baltimore, Maryland, December 1963.

16. "GLV System Environmental Requirements and Tests," MB-1043, Martin Company, Baltimore, Maryland, September 1963.

17. "Analysis of Gemini Airborne Equipment Temperature Rise," LV-136, Revision A, Martin Company, Baltimore, Maryland, February 1963.

18. "Predicted Heating Rates and Structural Temperatures for the Gemini Launch Vehicle," LV-43, Martin Company, Baltimore, Maryland, September 1963.

19. "GT-4 Pre-flight Report," LV-326-4, Martin Company, Baltimore, Maryland, April 1965. Confidential

20. "Monthly Reliability Report," Engineering Report 12794-27, Martin Company, Baltimore, Maryland, May 1965.

21. "Subsystem Engineering Analysis YLR 87-AJ-5 and YLR 91-AJ-5 Rocket Engines," AGC 521-3.15 Q-15, Aerojet-General Corporation, Sacramento, California, 22 July 1964. Confidential

22. "GLV-2 Tandem Actuator Problem Investigation and Corrective Action," LV-383, Appendix D, Martin Company, Baltimore, Maryland, 15 January 1965.

23. "GLV Martin/Aerojet Interface Specification," SSD Exhibit 62-190A, Space Systems Division, Air Force Systems Command, Los Angeles, California, 1 April 1964.

~~CONFIDENTIAL~~

Summary of Gemini Launches

Mission	Launch Date and Time (hr EST)	Launch Vehicle Payload (lb)	Burning Time Stage I (sec)	Burning Time Stage II (sec)	Inertial Velocity (fps) BECO	Inertial Velocity (fps) SECO	Inertial Velocity (fps) SECO + 20 Sec	Altitude (ft) BECO	Altitude (ft) SECO	Altitude (ft) SECO + 20 Sec	Inertial Flight Path Angle (deg) BECO	Inertial Flight Path Angle (deg) SECO	Inertial Flight Path Angle (deg) SECO + 20 Sec	Time in Orbit ③ (hr) Stage II	Time in Orbit ③ (hr) Spacecraft	Orbit (naut mi) Apogee	Orbit (naut mi) Perigee	Launch Evaluation Report Number
GT-1	4-8-64 1100	7029 ①	157.5	185.3	9752	25,679	25,786	208,262	531,500	528,184	20.00	0.0	-0.03	95.2 ① (64 orbits)	95.2 ① (64 orbits)	173	86.6	ER 13227-1
GT-2	1-19-65 0904	6847 ②	155.1	180.4	9916	25,611	25,738	229,743	546,960	526,380	26.219	-2.4523	-2.3431	N/A ②	N/A ②	N/A ②	N/A ②	ER 13227-2X ④ ER 13227-2
GT-3	3-23-65 0924	7105	155.8	181.3	9981	25,587	25,688	224,777	531,477	532,338	21.79	0.0	0.0323	18 (13 orbits)	4.6 (3 orbits)	121	87	ER 13227-3
GT-4	6-3-65 1016	7868	155.7	181.3	9844	25,670	25,745	214,775	531,522	532,886	18.66	-0.0235	0.059	47.7 (32 orbits)	97.7 (64 orbits)	152.3	87	ER 13227-4

① Spacecraft and Stage II inserted into orbit as a unit.

② Suborbital mission (spacecraft impact 2125 miles downrange).

③ Earth fixed orbit.

④ Launch attempt report.

Summary of Gemini Launches

APPENDIX

SUMMARY OF GEMINI LAUNCHES